PL-NF-90-001

Application of
REACTOR ANALYSIS METHODS
for
BWR Design And Analysis

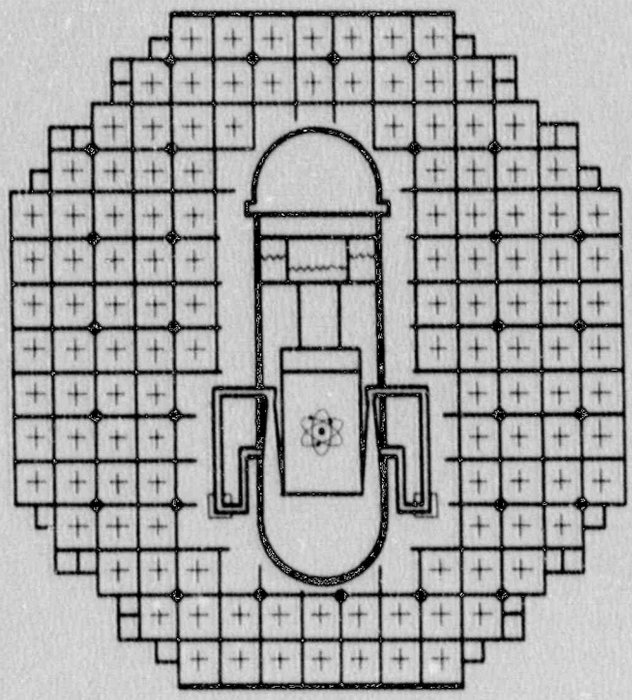

PP&L

Pennsylvania Power & Light Company

APPLICATION OF REACTOR ANALYSIS METHODS FOR BWR DESIGN AND ANALYSIS

PL-NF-90-001

August 1990

Principal Engineers

Cleon E. Dodge
Andrew Dyszel
John J. Geosits
Kenneth C. Knoll
Chester R. Lehmann

Contributing Engineers

John H. Emmett
Kimberley I.R. Knippel
Paul H. Lee
Salvatore A. Somma
Anthony J. Roscioli
William J. Weadon

Approved: _____ Aug. 1, 1990
John M. Kulick — Date
Supervisor-Nuclear Fuels Engineering

_____ Aug 1, 1990
Jerome S. Stefanko — Date
Manager-Nuclear Fuels & Systems Engineering

LEGAL NOTICE

This topical report represents the efforts of Pennsylvania Power & Light Company (PP&L) and reflects the technical capabilities of its nuclear fuel analysis personnel. The information contained herein is completely true and accurate to the best of the Company's knowledge. The sole intended purpose of this report and the information contained herein is to provide a description of PP&L's use of its steady state core physics and transient analysis methods for licensing applications. Any use of this report or the information contained herein by anyone other than PP&L or the U.S. Nuclear Regulatory Commission is unauthorized. With regard to any unauthorized use, Pennsylvania Power & Light Company and its officers, directors, agents, and employees make no warranty, either express or implied, as to the accuracy, completeness, or usefulness of this report or the information, and assume no liability with respect to its use.

ABSTRACT

This topical report describes Pennsylvania Power & Light Company's (PP&L's) use of its core physics and transient analysis methods for licensing applications.

PP&L's steady state core physics and transient analysis methods are based mainly on the computer codes provided by the Electric Power Research Institute (EPRI). The codes used in the steady state core physics methods include: the MICBURN gadolinia fuel pin depletion code; the CPM-2 assembly lattice depletion code; the NORGE-B2 cross section data link code; and the SIMULATE-E three-dimensional core simulation code. The EPRI codes used by PP&L for transient analyses include SIMTRAN-E, ESCORE, and RETRAN02 MOD004. The methodology for thermal margin analysis uses the XN-3 Critical Power correlation developed by the Advanced Nuclear Fuels Corporation (ANF).

Previously published PP&L reports describe PP&L's core physics and transient analysis methods (References 1 and 2). These reports provide benchmarking analyses to demonstrate the validity of these methods and PP&L's ability to use them appropriately. The PP&L models and methods described in those reports comprise a mainly best estimate methodology.

This report describes the adaptation of the steady state core physics and transient analysis methods to perform conservative analyses in support of licensing applications. The analysis methodologies described in this report are planned to be used to establish MCPR operating limits, demonstrate compliance with the ASME overpressure criteria, and provide core physics input to the fuel vendor for use in their accident analyses (e.g., LOCA). Sensitivity studies and evaluations based on first principles are presented and used to identify conservative modelling and input assumptions. Sample analyses are presented for those design basis events which PP&L plans to analyze for a typical reload core: rod

withdrawal error, fuel loading error, loss of feedwater heating, generator load rejection, feedwater controller failure, recirculation flow controller failure, and the closure of all main steam isolation valves. Statistical Combination of Uncertainty (SCU) methodologies for the analysis of pressurization transients and the rod withdrawal error to establish MCPR operating limits are described.

The analysis methodologies described in this report will result in conservative MCPR operating limits. The conservative ASME overpressure analysis methodology described herein will be used to demonstrate that sufficient margin exists in the Susquehanna SES design and operation to comply with the ASME overpressure criteria. The methodologies presented herein will also provide appropriately conservative data to enable the fuel vendor to perform certain of their analyses. In addition, the use of CPM-2 to generate neutronics input to the POWERPLEX plant monitoring system will result in accurate monitoring of thermal limits.

ACKNOWLEDGEMENTS

The authors gratefully acknowledge the expert stenographic work provided by Ms. Evelyn Lugo, Ms. Lisa Walsh, and Ms. Robin Abbott, the clerical support provided by Mr. Francis E. Gria, and the assistance of Mr. Paul Wasson's Systems and Computer Services group whose efforts have contributed to the quality and timely completion of this topical report. The authors also acknowledge the efforts of Mr. Rocco R. Sgarro for his licensing reviews and coordination with the NRC.

The assistance of the Advanced Nuclear Fuels Corporation is gratefully acknowledged. The consulting assistance provided by E. D. Kendrick of Nuclear Engineering Technology Corporation (NETCORP) is greatly appreciated.

The authors also wish to gratefully acknowledge the continuing support of the reload methods development effort by J. S. Stefanko, J. M. Kulick, W. J. Rhoades, and G. D. Miller.

APPLICATION OF REACTOR ANALYSIS METHODS FOR BWR DESIGN AND ANALYSIS

TABLE OF CONTENTS

LIST OF TABLES

LIST OF TABLES (continued)

LIST OF TABLES (continued)

LIST OF FIGURES

LIST OF FIGURES (continued)

LIST OF FIGURES (continued)

LIST OF FIGURES (continued)

1.0 INTRODUCTION

Pennsylvania Power & Light Company (PP&L) operates the two unit Susquehanna Steam Electric Station (SES) near Berwick, Pennsylvania. Both Susquehanna SES units are General Electric Boiling Water Reactor-4 (BWR-4) product line reactor systems; each has a rated thermal power output of 3293 megawatts. The general core design and operating features are given in Table 1-1. Figure 1-1 provides a typical power/flow relation for the Susquehanna SES units.

Reference 1 describes the steady state core physics methods used by PP&L for BWR core analysis and provides qualification of the analytical methodologies which will be used to perform safety related analyses in support of licensing actions. PP&L's steady state core physics methods are based on the Electric Power Research Institute (EPRI) code package (Reference 3), as depicted in the flowchart contained in Figure 1-2. The main computer codes are the CPM-2/PP&L fuel assembly lattice physics depletion code (Reference 4), hereinafter referred to as CPM-2, and the SIMULATE-E/PP&L three-dimensional core simulation code (Reference 5), hereinafter referred to as SIMULATE-E. The MICBURN/PP&L code (Reference 6), hereinafter referred to as MICBURN, provides a detailed representation of the depletion of a single gadolinia (Gd_2O_3) bearing fuel pin; the NORGE-B2/PP&L code (Reference 7), hereinafter referred to as NORGE-B2, provides a nuclear cross section data link from CPM-2 into SIMULATE-E as well as into the POWERPLEX core monitoring system (Reference 8). TIPPLOT provides plotting and statistical analysis capabilities. The RODDK-E/PP&L code (Reference 9), hereinafter referred to as RODDK-E, is used to select the strongest worth control rod locations for shutdown margin analyses and to provide estimates of core shutdown margin.

Reference 2 describes PP&L's transient analysis methods for the analysis of a GE BWR-4 reactor. Qualification analyses are presented to demonstrate the accuracy of the codes, models, and methods and their adequacy for reactor transient analysis. PP&L's transient analysis methods are also based on the Electric Power Research Institute (EPRI) code package as depicted in the flow chart contained in Figure 1-3. The RETRAN-02 MOD004/PP&L coupled neutronic-thermal hydraulic code (Reference 10), hereinafter referred to as RETRAN, is used to model the Nuclear Steam Supply System (NSSS) as a whole, and to model a single fuel assembly for thermal margin evaluations. The SIMTRAN-E/PP&L code (Reference 11), hereinafter referred to as SIMTRAN-E, collapses the three-dimensional neutronics data generated by the steady state core physics codes to the one-dimensional neutronics input required by RETRAN. Thermal margin evaluations are performed using the CPRITER code, which is an automated version of the PP&L developed DELTACPR code described in Reference 2. The CPRITER and DELTACPR codes use the Advanced Nuclear Fuels Corporation (ANF) XN-3 critical power correlation (Reference 12). The ESCORE/PP&L code (Reference 13), hereinafter referred to as ESCORE, is used to calculate gap conductances.

This report describes the application of the steady state core physics and transient analysis methods to licensing analyses, including the assumptions, methods, and application of uncertainties used to calculate conservative results. A portion of the analyses required to support licensing applications will be performed by the fuel vendor, including LOCA, MCPR safety limit, control rod drop, fuel handling accident, and stability analyses. Several of these analyses will utilize input generated using PP&L methods. Therefore, the data generation using PP&L methods to provide input to the fuel vendor methods is also described.

The steady state core physics methods are used to perform explicit analyses which are used directly in determining the Minimum Critical Power Ratio (MCPR) operating limit (e.g., rod withdrawal error), to provide

assurance that the fuel rod Linear Heat Generation Rate (LHGR) does not exceed the Protection Against Fuel Failure (PAFF) limit (Reference 29), and to provide inputs to the fuel vendor for use in their analyses. The RETRAN based transient analyses are used both to perform explicit analyses which are used in determining the MCPR operating limit (e.g., generator load rejection) and to perform reactor vessel ASME overpressure analyses.

Analyses described in this report represent work performed by PP&L. The computer codes, models, and calculations supporting this work are documented, reviewed, and controlled by formal procedures encompassed within PP&L's nuclear quality assurance program.

TABLE 1-1

GENERAL DESIGN AND OPERATING FEATURES OF THE SUSQUEHANNA STEAM ELECTRIC STATION REACTORS

Reactor Type/Configuration:	BWR-4/2 Loop Jet Pump Recirculation System
Rated Core Power:	3293 MW Thermal
Rated Core Flow:	100×10^6 lbm/hr
Reactor Pressure at Rated Conditions:	1020 psia
Number of Fuel Assemblies:	764
Number of Control Rods:	185

FIGURE 1-1
SUSQUEHANNA STEAM ELECTRIC STATION
TYPICAL CORE POWER VS CORE FLOW

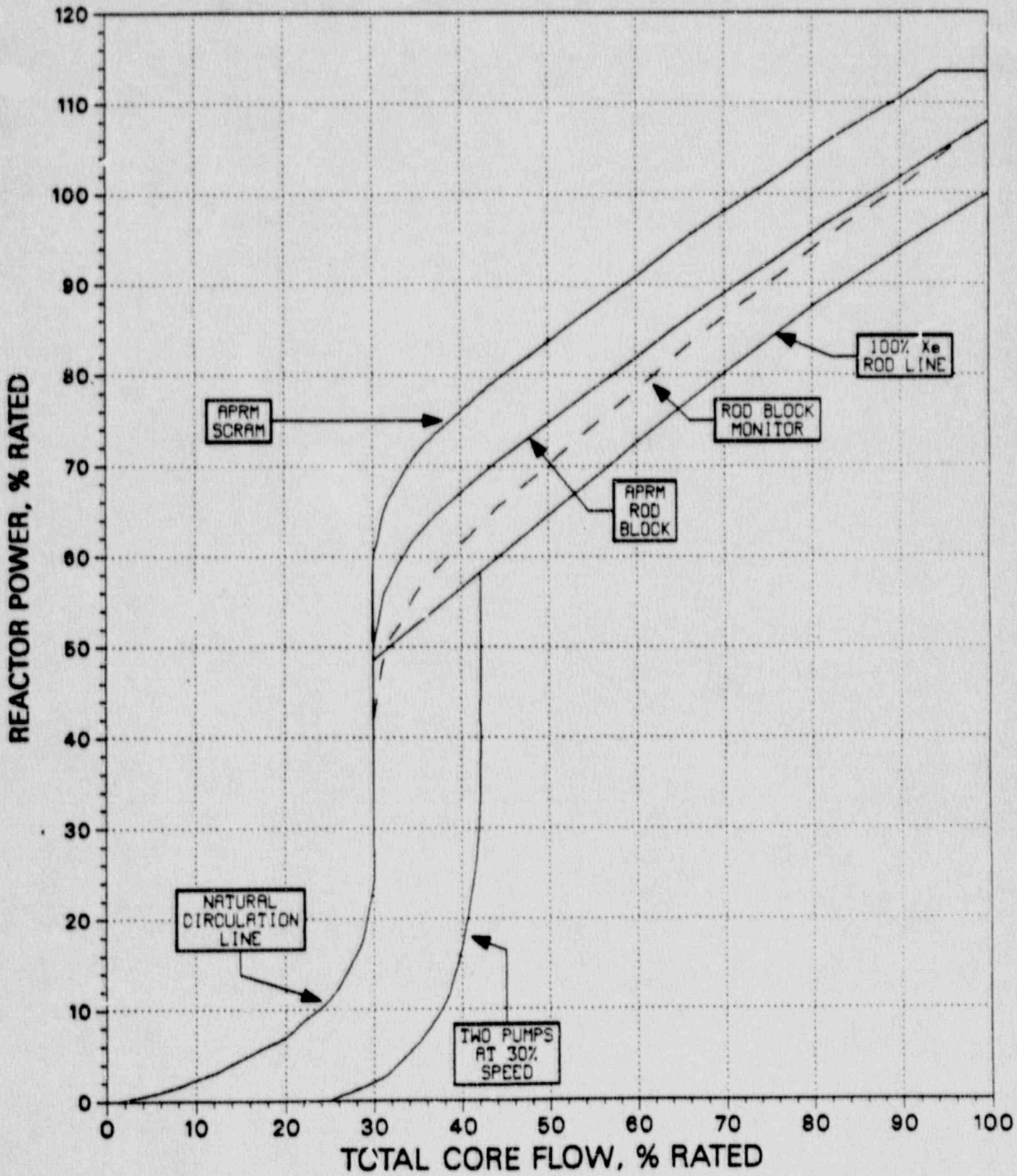

FIGURE 1-2
PP&L STEADY STATE CORE PHYSICS METHODS
COMPUTER CODE FLOWCHART

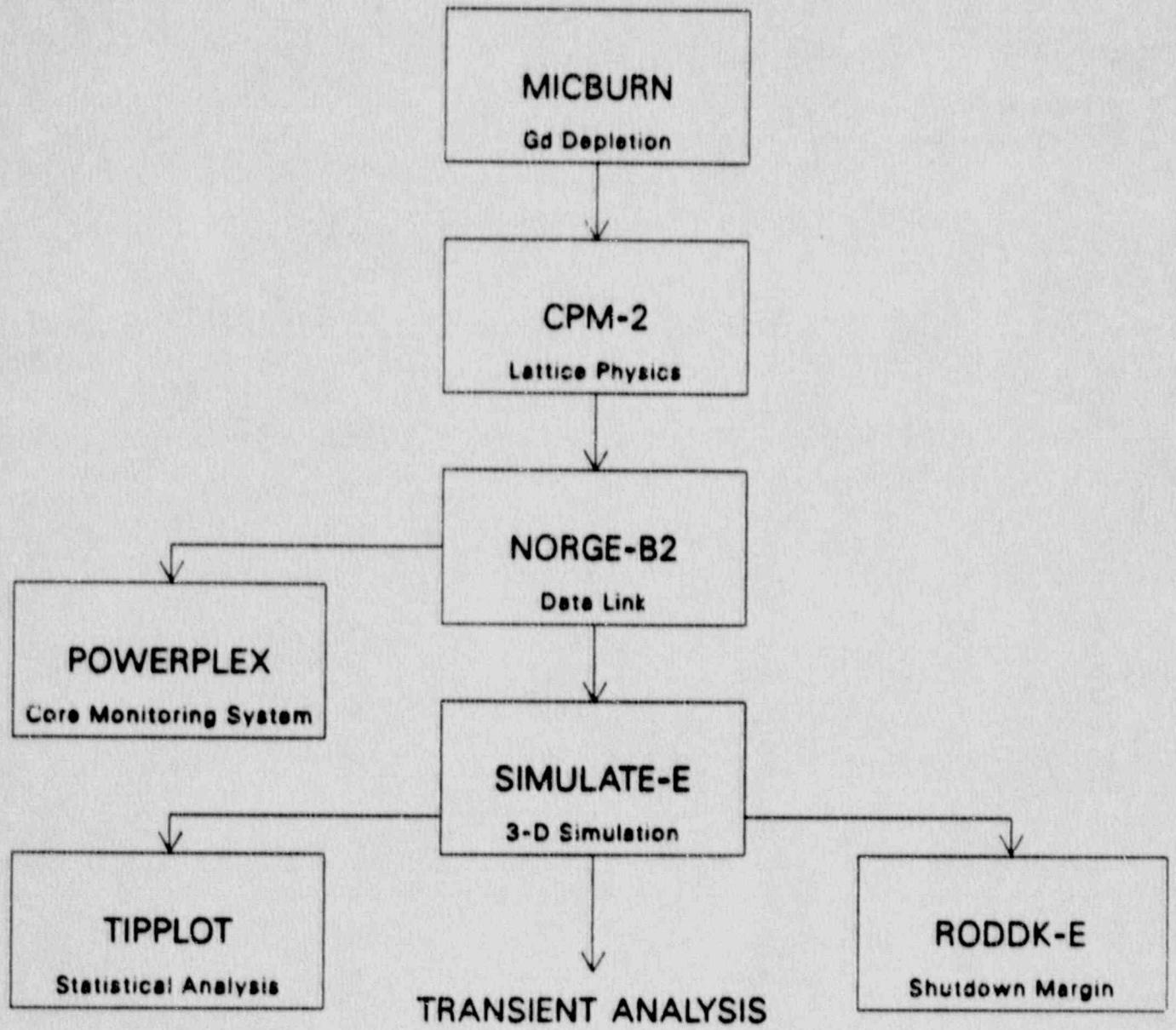

FIGURE 1-3
PP&L REACTOR TRANSIENT ANALYSIS METHODS
COMPUTER CODE FLOWCHART

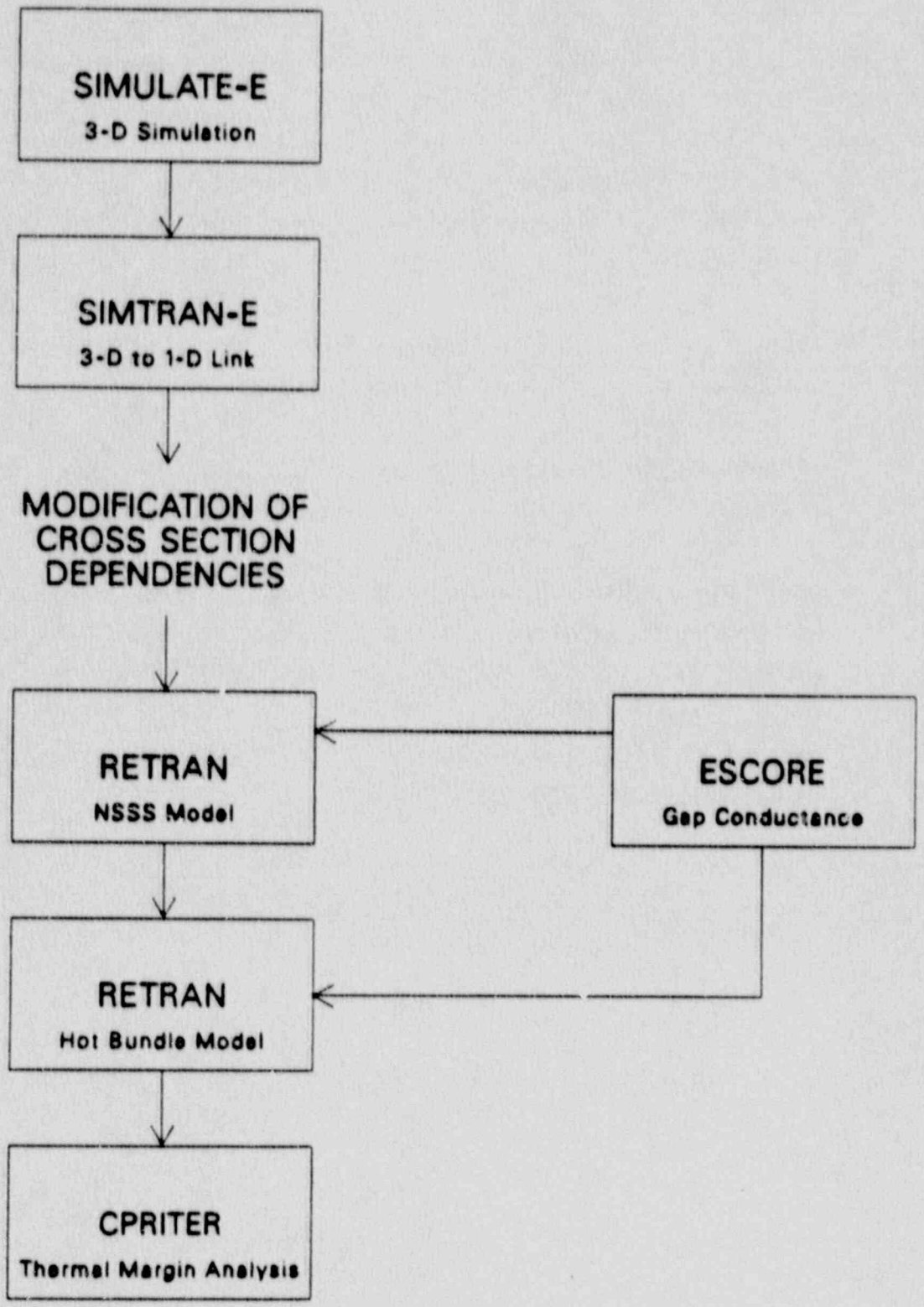

2.0 STEADY STATE CORE PHYSICS METHODS APPLICATIONS

The application of PP&L's steady state core physics methods described in Reference 1 to various licensing analyses is discussed in this section. Also discussed is the preparation of certain of the POWERPLEX core monitoring system inputs using PP&L methodology. The steady state core physics methods are used for four major purposes:

1) To perform explicit event analyses to demonstrate compliance with Technical Specification requirements and to provide Technical Specification input such as MCPR operating limits (Sections 2.1 to 2.5, 2.11). For several of these events, a parameter of interest is defined as the change in Critical Power Ratio (ΔCPR) divided by the initial value of CPR, and is referred to as RCPR.

2) To generate 1-D kinetics data for use by the RETRAN code for analyses of reactor system transients (Section 2.6).

3) To generate physics data which is utilized as input to certain of the fuel vendor analyses such as LOCA, control rod drop accident, and MCPR safety limit analyses (Sections 2.7 to 2.9).

4) To generate lattice physics data for the POWERPLEX core monitoring system (Section 2.10).

2.1 Rod Withdrawal Error

2.1.1 Event Description

The Rod Withdrawal Error (RWE) event is expected to be one of the limiting transient events in establishing the MCPR operating limit. The event is initiated by an operator erroneously selecting and continuously withdrawing a high worth control rod at its maximum withdrawal rate. This control rod withdrawal results in the addition of positive reactivity, and therefore both the local power in the vicinity of the erroneously withdrawn control rod and the core average power increase. The local and core average powers continue to increase as the control rod is withdrawn. The power increases are terminated when the Rod Block Monitor (RBM) response reaches its flow-biased trip setpoint. The RBM system uses inputs from the Local Power Range Monitors (LPRMs) surrounding the erroneously withdrawn rod. As a result of the event, the local bundle powers in the vicinity of the withdrawn control rod and the core average power increase and reach new steady-state conditions. The power distribution in the immediate vicinity of the withdrawn control rod is highly peaked, thus reducing thermal margins in the adjacent fuel bundles. The two primary thermal margins of concern in this event are the Minimum Critical Power Ratio (MCPR) and the maximum Linear Heat Generation Rate (LHGR).

PP&L's Steady-State Core Physics Methods (Reference 1) are used in modelling the RWE event. In the RWE event, the reactor power increases slowly, and the total increase is relatively small. The event may therefore be evaluated using steady-state analysis methods.

2.1.2 Sensitivity Studies

The consequences of the RWE event are primarily driven by the reactor initial conditions, the worth of the control rod, and the RBM response. SIMULATE-E analyses and statistical analyses were performed to determine the sensitivity of calculated RCPR to changes in input assumptions. The parameters of interest examined were:

1) Control rod pattern

2) Error control rod location

3) Xenon concentration

4) RBM setpoint

5) LPRM failure rate

6) Failed LPRM location(s)

7) Failed RBM channel

8) Core average power

9) Total core flow

10) Cycle exposure

The base case values for the analyses are listed in Table 2.1-1.

As previously mentioned, the main output of the RWE analysis is a RCPR for a given RBM Trip Setpoint Setting (typically 108%). The consequences of the RWE event are primarily sensitive to the neutronic coupling of the

limiting CPR bundle with the withdrawn rod and the RBM response. The neutronic coupling is increased as the limiting bundle is moved closer to the location of the rod being withdrawn, referred to as the error rod location. The sensitivity analyses showed that the control rod pattern, error rod location, and the xenon concentration significantly affect the neutronic coupling. Control rod patterns that force the power distribution near the error rod location create large rod worths and large RCPRs during a RWE event. These rod patterns, although technically achievable, will realistically not be used during normal reactor operation due to the excessive power peaking. Therefore, use of this type of rod pattern is a significant conservatism built into the analysis method.

For the fuel management and operational strategies in use at Susquehanna SES (i.e., quarter core symmetry for operational control rod patterns and reload design), the limiting rod locations are in the center of the core as shown in Figure 2.1-1. RWE analyses with the error rod locations outside the area shown in Figure 2.1-1 will not exhibit higher peak powers than the highest peak powers possible in the area shown. The impact of changes to operational and reload strategies on the selection of the error rod location will be evaluated on a cycle by cycle basis.

In addition to rod patterns, the xenon concentration significantly affects the capability of forcing the power distribution toward the error rod location. At full power xenon conditions, a significant amount of rod inventory is withdrawn in order to maintain criticality. Therefore, fewer control rods are available to force the limiting bundle toward the error rod location. RWE cases with equilibrium xenon show that the zero xenon assumption increases the RCPR by as much as 0.08. This assumption produces very conservative results.

In conjunction with MCPR and LHGR operating limits, the RBM system acts to prevent the fuel from exceeding its thermal limits by providing a rod block when the local power has increased to the flow-biased trip setpoint. As the RBM trip setpoint increases the control rod may be withdrawn further. The RBM system is a dual channel system using input from the four LPRM strings surrounding the rod selected for motion. The channel 'A' subsystem uses input from the level 'A' and 'C' LPRMs; the channel 'B' subsystem uses input from the level 'B' and 'D' LPRMs. Either channel must reach the trip setpoint to activate a control rod block.

Operability of the LPRMs directly affects the RBM system response. Because some LPRMs are allowed to be failed during core operation, the number and location of failed LPRMs will strongly influence the RBM response. Technical Specifications allow rod motion with one channel of the RBM system inoperable. Also, the RBM system design allows up to one half of the LPRMs providing input to a given channel to be failed. Figure 2.1-2 shows the minimum RBM response for channel 'A' as a function of a typical rod withdrawal for 0, 1, 2, 3, and 4 failed LPRMs. As expected, the RBM response degrades rapidly as the number of failed LPRMs increase. Typically, two or three LPRM failures may exist in the whole core but are spread out sufficiently so that one RBM channel very rarely uses less than 6 of its 8 LPRM inputs (i.e., 75%).

In addition to the number of failed LPRM's, location of the failed LPRMs can significantly affect the RBM response. A total of 163 failure combinations exist for each RBM channel assuming 0, 1, 2, 3, or 4 failures. A failure combination is defined as a specific set of failed LPRM locations. Table 2.1-2 shows typical channel 'A' and channel 'B' responses as functions of the error rod position for different failure combinations. Figure 2.1-3 shows a typical channel 'A' RBM response as a function of error rod position for four different failure combinations each having four failed LPRMs. Both Table 2.1-2 and Figure 2.1-3 demonstrate the wide variability in the RBM response for different failure

combinations for a given error rod position. This variation in RBM response as a function of rod position is directly related to the location of the operable LPRMs with respect to the error rod tip location. As expected, when an operable LPRM is close to the error rod tip location, the LPRM is more responsive to the error rod movement. As the error rod tip location moves away from an operable LPRM toward an inoperable LPRM, the RBM channel response may in fact be reduced due to the shifting of axial power shape. Failure combination 163 in Figure 2.1-3 shows this effect. Both Table 2.1-2 and Figure 2.1-3 also demonstrate that no one failure combination for either RBM response is the most conservative throughout the whole rod withdrawal. The most conservative LPRM failure combination would be one which would provide the minimum RBM response throughout the entire withdrawal.

The CPR response during the RWE event is very important in establishing the MCPR operating limit. As previously mentioned, the initial conditions of the event place the limiting CPR bundle near the error rod location. This causes the CPR to decrease and RCPR to increase rapidly during the error rod withdrawal. Figure 2.1-4 shows a sample Unit 2 Cycle 2 RCPR response as the error rod is withdrawn. The limiting CPR may be in different bundles during the event, but the limiting bundle is always close to the error rod location. The RCPR response is steadily increasing and flattens out when the error rod is nearly full out.

Figures 2.1-5 and 2.1-6 show the responses of peak LHGR and core thermal power which are also of interest. For the case shown, the conservative initial control rod pattern results in the steady state LHGR limit being exceeded. This would not be allowed by the plant Technical Specifications. For all cases analyzed, including the example shown in the figures, the peak LHGR does not exceed the transient LHGR Protection Against Fuel Failure (PAFF) limit, and the core average power increase is

small. Therefore, the RWE event does not result in LHGRs exceeding the fuel mechanical design limits. The variation in the steady state LHGR and PAFF limits with control rod tip position occurs because these limits are functions of assembly planar exposure.

Initial core power and core flow conditions can also significantly affect the magnitude of the RCPR response during a RWE. RWE cases along the 100% rod line showed that the RCPR is essentially constant with a variation of about 0.01 in RCPR. This variation in RCPR is well within the conservative assumption of zero xenon. At powers below the 100% rod line, however, the Technical Specification flow-biased RBM trip setpoint is farther away from the initial RBM response.

To determine the effect of the RWE at less than the 100% rod line, RWE analyses were performed on the 90%, 80%, 70%, and 60% rod lines to determine initial CPR and RCPR sensitivity. As power decreases, calculated RCPR does increase but the initial CPR increases more rapidly. To place a bundle on MCPR or LHGR limits, the rod patterns had to be adjusted. This adjustment required major rod insertion in the periphery of the core. These adjusted rod patterns had many secondary rods at intermediate and deep positions which are not typical of power operation and caused violation of the MAPLHGR limits used to protect against LOCA. Because no credit is taken for the intermediate and low Rod Block Trip Setpoints, the error rod could be fully withdrawn. All of these assumptions result in excessive conservatism and a RCPR increase of approximately 0.04. To provide a more realistic assessment of RCPR, the zero xenon assumption was removed and equilibrium xenon was assumed. These additional cases showed that the 100% rod line RWE analyses with zero xenon bound the equilibrium xenon cases at lower powers.

The last parameters analyzed for the RWE were the exposure effects due to previous cycle shutdown exposure and current cycle exposure. Beginning of Cycle 2 of Unit 2 RWE analyses were performed for different previous cycle

exposures (11.220 GWD/MTU, 12.050 GWD/MTU, and 13.000 GWD/MTU). The results show a minor effect of previous cycle exposure on the RWE analysis. All the RCPRs were within 0.01 of each other. Typical reload end of cycle exposure windows (i.e., the range of previous cycle exposures on which the current reload cycle analyses are based) are less than the 1.78 GWD/MTU exposure difference analyzed. Therefore, future RWE analysis results should not be dependent on the previous cycle window.

The other exposure effect, cycle exposure of the design cycle, does affect the RCPR for the RWE event. As expected, this effect derives from the critical control rod density required at different cycle exposures. As peak hot excess reactivity is approached, the control rod density reaches its peak. Peak control rod density conditions allow for a greater number of inserted control rods than at BOC to force the limiting bundle location to be closer to the error rod location. This effect is similar to the zero xenon assumption. In addition to the rod pattern effect, the fresh bundles are very close to their peak reactivity. Therefore, neutronic coupling between the limiting CPR bundle and the error rod location may be increased at the cycle exposure corresponding to peak hot excess reactivity. In order to determine the sensitivity of these effects on RCPR, RWE analyses were performed at 5.5 GWD/MTU cycle exposure which corresponds to Unit 2 Cycle 2 peak hot excess reactivity. These analyses showed that the RCPR increased by approximately 0.03 at 5.5 GWD/MTU compared to BOC which demonstrates that a cycle exposure effect on the RCPR for the RWE event exists.

2.1.3 Licensing Analysis Method

The assumptions made in the analysis of the RWE are based on the results and discussions of the sensitivity studies described in Section 2.1.2. Four codes are used to perform the analysis: SIMULATE-E, RBM, RBMSTAT,

and STATOL. The SIMULATE-E code provides the detailed neutronic and thermal hydraulic feedback information during the RWE event. The RBM code uses the SIMULATE-E predicted detector readings and predicted CPR values to generate a RWE response surface of RCPR as a function of RBM trip setpoint, operable RBM channel, and LPRM failure combination. The RWE response surface is used as input to RBMSTAT along with inputs of nominal RBM setpoint, LPRM failure rate, the uncertainty in measured RBM trip setpoint (drift, accuracy, and calibration), the uncertainty in calculated RBM response, and the uncertainty in calculated RCPR. RBMSTAT then statistically combines the input through a Monte Carlo approach as described in Section B.3. This method results in a comprehensive and detailed description of the analyzed RWE event covering all possible failure combinations and RBM responses. The output of RBMSTAT is a RCPR cumulative probability distribution with at least 95% confidence. The RCPR cumulative probability distribution is used to determine the MCPR operating limit using the methods described in Appendix B.

The following assumptions and methods are used for the RWE licensing analysis:

1) Cases are run at 100% power/100% flow.

2) A control rod pattern that forces the limiting core MCPR location to be within one control cell of the error rod and is predicted to be near critical is developed.

3) The error rod location is located in the area shown on Figure 2.1-1.

4) The error rod initial position is full in.

5) Zero xenon is assumed as the xenon concentration for 100% power rod line cases.

6) At least one-half of the LPRM inputs will be assumed operable as enforced by the RBM system design. Every possible failure combination will be considered. A conservatively high LPRM failure probability is assumed.

7) One RBM channel is assumed to be inoperable. Each channel is assumed to have an equal probability of being the inoperable channel.

8) The RBM measured trip setpoint uncertainties, calculated RCPR uncertainty, and the calculated RBM response uncertainty are independent. The 95% probability/95% confidence level uncertainties are used (see Table 2.1-1).

9) Analyses will be performed for both BOC and peak hot excess reactivity.

The Statistical Combination of Uncertainty (SCU) method described in Appendix B can be divided into a number of steps:

1) Create a RWE response surface from SIMULATE-E and RBM calculations that relates calculated RCPR to the variables to be analyzed statistically. The variables are RBM trip setpoint, LPRM failure combination, and RBM channel.

2) Define measured and calculated uncertainty distributions for the parameters used in the response surface.

3) Perform a Monte Carlo analysis with RBMSTAT (as described in Section B.3) to produce a cumulative probability distribution of calculated RCPR.

4) Perform safety limit type analyses to produce cumulative probability distribution functions of fraction of pins in boiling transition for a range of MCPRs. For the sample calculation presented herein, cumulative probability distribution functions were generated by ANF for a core containing all ANF 9x9 fuel, since these distributions will be typical of future licensing applications.

5) Assume a MCPR operating limit and perform STATOL calculations that use Monte Carlo analysis to combine the cumulative probability distribution functions for fraction of pins in boiling transition and the cumulative probability distribution function of transient RCPR, thus producing a combined safety limit and transient analysis.

6) Select the value of number of rods expected to be in boiling transition at the 95% confidence level. If the value is greater than 0.1% of the pins, increase the assumed MCPR operating limit and repeat steps 5 and 6.

2.1.4 Sample Licensing Analysis

This section presents a sample licensing analysis using SIMULATE-E, RBM, RBMSTAT, and STATOL using the previously described methodology.

2.1.4.1 Response Surface

A response surface of calculated RCPR as a function of RBM setpoint, LPRM failure combination, and RBM channel was produced with the SIMULATE-E and RBM codes. The SIMULATE-E calculations produce predicted detector responses and limiting CPR as the error rod is withdrawn beginning at notch 0 (full in) and ending at notch 48 (full out). For this case, the error rod is incrementally withdrawn by 4 notches so a total of 13 sets of

6) At least one-half of the LPRM inputs will be assumed operable as enforced by the RBM system design. Every possible failure combination will be considered. A conservatively high LPRM failure probability is assumed.

7) One RBM channel is assumed to be inoperable. Each channel is assumed to have an equal probability of being the inoperable channel.

8) The RBM measured trip setpoint uncertainties, calculated RCPR uncertainty, and the calculated RBM response uncertainty are independent. The 95% probability/95% confidence level uncertainties are used (see Table 2.1-1).

9) Analyses will be performed for both BOC and peak hot excess reactivity.

The Statistical Combination of Uncertainty (SCU) method described in Appendix B can be divided into a number of steps:

1) Create a RWE response surface from SIMULATE-E and RBM calculations that relates calculated RCPR to the variables to be analyzed statistically. The variables are RBM trip setpoint, LPRM failure combination, and RBM channel.

2) Define measured and calculated uncertainty distributions for the parameters used in the response surface.

3) Perform a Monte Carlo analysis with RBMSTAT (as described in Section B.3) to produce a cumulative probability distribution of calculated RCPR.

4) Perform safety limit type analyses to produce cumulative probability distribution functions of fraction of pins in boiling transition for a range of MCPRs. For the sample calculation presented herein, cumulative probability distribution functions were generated by ANF for a core containing all ANF 9x9 fuel, since these distributions will be typical of future licensing applications.

5) Assume a MCPR operating limit and perform STATOL calculations that use Monte Carlo analysis to combine the cumulative probability distribution functions for fraction of pins in boiling transition and the cumulative probability distribution function of transient RCPR, thus producing a combined safety limit and transient analysis.

6) Select the value of number of rods expected to be in boiling transition at the 95% confidence level. If the value is greater than 0.1% of the pins, increase the assumed MCPR operating limit and repeat steps 5 and 6.

2.1.4 Sample Licensing Analysis

This section presents a sample licensing analysis using SIMULATE-E, RBM, RBMSTAT, and STATOL using the previously described methodology.

2.1.4.1 Response Surface

A response surface of calculated RCPR as a function of RBM setpoint, LPRM failure combination, and RBM channel was produced with the SIMULATE-E and RBM codes. The SIMULATE-E calculations produce predicted detector responses and limiting CPR as the error rod is withdrawn beginning at notch 0 (full in) and ending at notch 48 (full out). For this case, the error rod is incrementally withdrawn by 4 notches so a total of 13 sets of

predicted detector response and CPR result. The RBM code uses this information to calculate the RBM response based on every failure combination for each RBM channel at each axial position. The RBM code then creates the RCPR response surface, an array of RCPR as a function of RBM setpoint, LPRM failure combination, and RBM channel.

2.1.4.2 Treatment of Uncertainties

The uncertainties in measured RBM setpoint, calculated RBM response, and calculated RCPR are included in the RBMSTAT calculations discussed in Section B.3. Table 2.1-1 shows the list of uncertainties and their 95% probability/95% confidence values. The measured RBM setpoint uncertainties are derived from the RBM system performance with respect to instrument drift, accuracy, and calibration. The calculated RBM response is based on the ability of SIMULATE-E to predict the detector response at the location of the LPRMs. The TIP response comparisons presented in Reference 1 and additional comparisons obtained since that time have provided a large data base to derive a cumulative probability distribution of predicted LPRM response error and therefore predicted RBM response error. The calculated RBM response uncertainty is calculated as follows:

$$\sigma_{RBM} = \sigma_{LPRM}/\sqrt{N}$$

where: N = the number of operable LPRMs. N is set to the minimum allowable value of 4 for conservatism.

σ_{LPRM} = the uncertainty in calculated LPRM response.

The calculated RCPR response is based on the ability of SIMULATE-E to predict the radial bundle power response. A linear correlation of RCPR as a function of the change in radial bundle power is first established to

derive the RCPR uncertainty as a function of radial bundle power uncertainty. The radial bundle power uncertainty is discussed in Section 2.2.3. The slope of the correlation, B, is conservatively adjusted to its 95% probability level and used in the following relationship to calculate the RCPR uncertainty for the RWE event.

$$\sigma_{RCPR} = B \sqrt{2}\ \sigma_{RP}$$

where: σ_{RP} = nodal code bundle power uncertainty

For this sample analysis, the 95% probability based value of B is 0.155 MW^{-1}. The correlation coefficient of RCPR as a linear function of radial bundle power based on analyses is 0.999. This correlation coefficient demonstrates that the RCPR is directly related to the radial bundle power during the RWE.

2.1.4.3 Results

The resulting MCPR operating limit for the sample Unit 2 Cycle 2 RWE using the Statistical Combination of Uncertainty (SCU) methodology presented in Appendix B is 1.26 for a 108% rod block trip setpoint at 100% flow. It should be noted that if other events require higher operating limits, then the actual Technical Specification MCPR operating limit would be the higher value.

TABLE 2.1-1

Rod Withdrawal Error Base Case
Input Assumptions

Parameter	Assumption
1. Core Power	100%
2. Core Flow	100%
3. Xenon Concentration	0%
4. RBM Setpoint	108%
5. LPRM Failure Probability	15%
6. RBM Measurement Uncertainties at 95%/95% Probability/Confidence	
a. Drift	3.0%
b. Accuracy	1.6%
c. Calibration	1.6%
7. RBM Calculational Uncertainty at 95%/95% Probability/Confidence	6.4%
8. RCPR Calculational Uncertainty at 95%/95% Probability/Confidence	0.042

TABLE 2.1-2
Rod Block Monitor Response
For a Sample Unit 2 Cycle 2 RWE

CHANNEL A RBM RESPONSE

FAILURE COMBINATION	OPERABLE LPRMS								RBM RESPONSE(%) FOR AXIAL ROD POSITION												
	1A	2A	3A	4A	1C	2C	3C	4C	0	4	8	12	16	20	24	28	32	36	40	44	48
1	X	X	X	X	X	X	X	X	100.0	100.3	100.9	102.1	104.5	108.1	110.4	111.1	111.2	112.3	115.1	119.3	119.9
2	X	X	X	X	X	X	X		100.0	100.3	100.8	101.9	104.2	107.7	109.9	110.6	110.8	112.2	115.5	120.3	120.8
3	X	X	X	X	X	X		X	100.0	100.3	100.8	101.8	103.9	107.1	109.1	109.7	110.0	111.5	114.9	119.8	120.6
4	X	X	X	X	X		X	X	100.0	100.3	100.7	101.6	103.2	105.5	107.0	107.8	108.2	109.9	113.6	118.6	119.6
5	X	X	X	X		X	X	X	100.0	100.2	100.7	101.8	103.9	107.1	109.1	109.8	110.0	111.4	114.9	119.7	120.4
6	X	X	X		X	X	X	X	100.0	100.3	101.0	102.4	105.4	109.7	112.4	113.1	113.0	113.9	116.7	121.2	121.6
7	X	X		X	X	X	X	X	100.0	100.3	101.0	102.4	105.2	109.4	112.0	112.7	112.5	113.3	115.7	119.5	119.8
8	X		X	X	X	X		X	100.0	100.3	101.0	102.4	105.2	109.4	112.0	112.7	112.5	112.9	114.8	115.7	115.7
9		X	X	X	X	X	X	X	100.0	100.3	101.0	102.4	105.3	109.6	112.3	113.0	112.8	113.6	116.0	119.8	120.2
10	X	X	X	X	X	X			100.0	100.2	100.6	101.5	103.5	106.5	108.3	109.0	109.4	111.2	115.3	120.8	121.9
11	X	X	X	X	X		X		100.0	100.2	100.6	101.4	102.7	104.8	106.1	106.8	107.4	109.4	113.8	119.6	120.8
12	X	X	X	X	X			X	100.0	100.2	100.6	101.2	102.3	104.0	105.1	105.8	106.5	108.6	113.2	119.1	120.4
13	X	X	X	X		X	X		100.0	100.2	100.6	101.5	103.5	106.5	108.4	109.1	109.4	111.2	115.3	120.8	121.7
14	X	X	X	X		X		X	100.0	100.2	100.6	101.4	103.2	105.8	107.5	108.1	108.6	110.4	114.6	120.2	121.3
15	X	X	X	X			X	X	100.0	100.2	100.6	101.3	102.4	104.1	105.2	105.9	106.4	108.7	113.1	119.0	120.3
16	X	X	X		X	X	X		100.0	100.3	100.9	102.2	105.1	109.3	112.0	112.7	112.7	113.9	117.4	122.8	123.1
17	X	X	X		X	X		X	100.0	100.3	100.9	102.1	104.7	108.6	111.0	111.7	111.8	113.1	116.7	122.0	122.7
18	X	X	X		X		X	X	100.0	100.3	100.8	101.9	103.8	106.7	108.4	109.2	109.8	111.1	115.0	120.6	121.5
19	X	X	X			X	X	X	100.0	100.3	100.9	102.1	104.8	108.6	111.0	111.7	111.8	113.1	116.6	121.9	122.5
20	X	X		X	X	X	X		100.0	100.3	100.9	102.2	104.9	109.0	111.6	112.3	112.2	113.3	116.2	120.6	121.1
21	X	X		X	X	X		X	100.0	100.3	100.9	102.1	104.5	108.3	110.6	111.3	111.3	112.5	115.5	120.0	120.6
22	X	X		X	X		X	X	100.0	100.3	100.8	101.9	103.7	106.5	108.2	108.9	109.2	110.6	114.0	118.7	119.5
23	X	X		X		X	X	X	100.0	100.3	100.9	102.1	104.6	108.3	110.7	111.3	111.3	112.4	115.5	119.8	120.5
24	X	X			X	X	X	X	100.0	100.4	101.2	102.9	106.4	111.6	114.8	115.5	115.1	115.6	117.0	121.8	121.8
25	X		X	X	X	X	X		100.0	100.3	100.9	102.2	104.9	109.0	111.6	112.3	112.1	112.8	114.1	118.4	118.5
26	X		X	X	X	X		X	100.0	100.3	100.9	102.1	104.5	108.3	110.6	111.3	111.2	112.0	113.4	115.8	116.1
27	X		X	X	X		X	X	100.0	100.3	100.8	101.9	103.7	106.5	108.2	108.9	109.1	110.1	111.8	114.4	114.8
28	X		X	X		X	X	X	100.0	100.3	100.9	102.1	104.6	108.3	110.6	111.3	111.2	112.0	113.4	115.7	116.0
29	X		X		X	X	X	X	100.0	100.4	101.2	102.9	106.4	111.5	114.7	115.5	115.0	115.5	117.0	118.8	118.8
30	X			X	X	X	X	X	100.0	100.4	101.1	102.8	106.2	111.2	114.2	114.9	114.4	114.3	114.3	115.1	114.8
31		X	X	X	X	X	X		100.0	100.3	100.9	102.2	105.1	109.2	111.9	112.6	112.6	113.6	116.8	121.1	121.5
32		X	X	X	X	X	X	X	100.0	100.3	100.9	102.1	104.7	108.5	110.9	111.6	111.6	112.8	115.9	120.5	121.1
33		X	X	X	X		X	X	100.0	100.3	100.8	101.9	103.8	106.6	108.4	109.2	109.4	110.8	114.3	119.1	119.9
34		X	X	X		X	X	X	100.0	100.3	100.8	102.1	104.7	108.5	110.9	111.6	111.6	112.7	115.8	120.4	120.9
35		X	X		X	X	X	X	100.0	100.3	101.2	103.0	106.6	111.9	115.2	116.0	115.5	116.0	118.3	122.3	122.4
36		X		X	X	X	X	X	100.0	100.4	101.2	102.9	106.4	111.5	114.6	115.4	114.9	115.2	117.0	120.1	120.1
37			X	X	X	X	X	X	100.0	100.3	101.1	102.9	106.4	111.5	114.6	115.3	114.8	114.7	114.8	115.4	115.1
38	X	X	X	X	X				100.0	100.2	100.4	100.9	101.6	102.9	103.8	104.5	105.4	108.0	113.4	120.2	121.0
39	X	X	X	X	X		X		100.0	100.2	100.5	101.1	102.6	105.0	106.5	107.1	107.7	110.0	115.0	121.6	122.9
40	X	X	X	X				X	100.0	100.2	100.4	100.9	101.7	103.0	103.9	104.6	105.5	108.0	113.4	120.1	121.7
41	X	X	X	X				X	100.0	100.2	100.4	100.8	101.3	102.2	102.8	103.5	104.5	107.1	112.6	119.5	121.2

TABLE 2.1-2 (continued)

CHANNEL A RBM RESPONSE

FAILURE COMBINATION	OPERABLE LPRMS								RBM RESPONSE(%) FOR AXIAL ROD POSITION															
	1A	2A	3A	4A	1C	2C	3C	4C	0	4	8	12	16	20	24	28	32	36	40	44	48
42	X	X	X		X	X			100.0	100.3	100.7	101.8	104.3	108.0	110.3	111.0	111.3	113.0	117.5	123.8	124.6
43	X	X	X		X		X		100.0	100.2	100.7	101.6	103.3	105.8	107.4	108.2	108.7	110.8	115.6	122.1	123.3
44	X	X	X		X			X	100.0	100.2	100.7	101.5	102.8	104.9	106.2	107.0	107.6	109.8	114.7	121.4	122.8
45	X	X	X			X	X		100.0	100.2	100.7	101.8	104.4	108.0	110.4	111.1	111.3	113.0	117.4	123.6	124.4
46	X	X	X			X		X	100.0	100.2	100.7	101.7	103.9	107.2	109.2	109.9	110.2	112.0	116.5	122.9	123.9
47	X	X	X				X	X	100.0	100.2	100.7	101.5	102.9	105.0	106.3	107.1	107.7	109.8	114.7	121.3	122.6
48	X	X		X	X	X			100.0	100.3	100.7	101.8	104.1	107.7	109.9	110.6	110.8	112.3	116.1	121.4	122.2
49	X	X		X	X		X		100.0	100.3	100.7	101.6	103.2	105.6	107.2	107.9	108.4	110.1	114.3	119.9	120.9
50	X	X		X	X			X	100.0	100.3	100.7	101.4	102.7	104.8	106.0	106.7	107.3	109.2	113.5	119.2	120.4
51	X	X		X		X	X		100.0	100.2	100.7	101.8	104.2	107.8	110.0	110.7	110.8	112.3	116.0	121.3	122.0
52	X	X		X		X		X	100.0	100.2	100.7	101.7	103.8	106.9	108.9	109.5	109.8	111.3	115.2	120.6	121.5
53	X	X		X			X	X	100.0	100.2	100.7	101.5	102.8	104.9	106.1	106.8	107.4	109.2	113.4	119.1	120.2
54	X	X			X	X	X		100.0	100.3	101.1	102.7	106.2	111.4	114.7	115.4	115.1	115.9	118.8	123.6	123.8
55	X	X			X	X		X	100.0	100.3	101.0	102.6	105.8	110.5	113.4	114.1	113.9	114.8	117.9	122.9	123.3
56	X	X			X		X	X	100.0	100.3	101.0	102.4	104.7	108.2	110.3	111.1	111.2	112.4	115.9	121.1	121.8
57	X	X				X	X	X	100.0	100.3	100.7	101.8	104.1	107.7	109.9	110.6	110.7	111.8	113.7	118.6	117.0
58	X		X	X	X	X			100.0	100.2	100.7	101.6	103.2	105.6	107.2	107.9	108.3	109.6	111.9	115.0	118.7
59	X		X	X	X		X		100.0	100.2	100.7	101.5	102.7	104.8	106.0	106.7	107.2	108.7	111.1	114.3	118.2
60	X		X	X	X			X	100.0	100.2	100.7	101.8	104.2	107.8	110.0	110.6	110.7	111.7	113.6	118.5	118.0
61	X		X	X		X	X		100.0	100.2	100.7	101.7	103.8	106.9	108.9	109.5	109.6	110.8	112.3	115.8	118.3
62	X		X	X		X		X	100.0	100.2	100.7	101.5	102.8	104.9	106.1	106.8	107.3	108.7	111.1	114.2	118.1
63	X		X	X			X	X	100.0	100.3	101.1	102.7	106.2	111.4	114.6	115.4	114.9	115.2	118.1	118.1	117.9
64	X		X		X	X	X		100.0	100.3	101.0	102.6	105.8	110.5	113.4	114.1	113.8	114.2	115.2	117.3	117.4
65	X		X		X	X		X	100.0	100.3	101.0	102.4	104.7	108.1	110.2	111.0	111.0	111.8	113.1	115.6	116.0
66	X		X		X		X	X	100.0	100.3	101.0	102.6	105.8	110.5	113.4	114.1	113.7	114.1	115.1	117.2	117.2
67	X		X			X	X	X	100.0	100.3	101.0	102.6	106.0	111.0	114.0	114.7	114.2	114.4	114.7	115.9	118.6
68	X			X	X	X	X		100.0	100.3	101.0	102.5	105.5	110.1	113.5	114.1	113.1	113.4	113.8	115.1	116.0
69	X			X	X	X		X	100.0	100.3	101.0	102.3	104.5	107.8	109.8	110.6	110.5	111.1	111.9	113.4	113.7
70	X			X	X		X	X	100.0	100.3	101.0	102.5	105.6	110.1	112.9	113.5	113.1	113.3	113.8	115.0	114.9
71	X			X		X	X	X	100.0	100.4	101.4	103.6	108.0	114.5	118.4	119.2	118.1	117.4	116.5	116.6	115.8
72	X				X	X	X	X	100.0	100.2	100.7	101.8	104.3	107.9	110.2	110.9	111.1	112.6	116.5	122.0	122.8
73		X	X	X	X	X			100.0	100.2	100.7	101.6	103.3	105.8	107.4	108.1	108.6	110.4	114.7	120.4	121.4
74		X	X	X	X		X		100.0	100.2	100.7	101.5	102.8	104.9	106.2	106.9	107.5	109.4	113.8	119.7	120.9
75		X	X	X	X			X	100.0	100.2	100.7	101.8	104.3	108.0	110.3	111.0	111.1	112.6	116.4	121.9	122.6
76		X	X	X		X	X		100.0	100.2	100.7	101.7	103.9	107.1	109.1	109.8	110.0	111.6	115.6	121.2	122.0
77		X	X	X		X		X	100.0	100.3	101.1	102.8	106.5	111.8	115.2	116.0	115.6	115.4	119.4	124.3	124.5
78		X	X	X			X	X	100.0	100.3	101.0	102.7	106.0	110.8	113.9	114.6	114.4	115.3	118.5	123.8	124.0
79		X	X		X	X	X		100.0	100.3	101.0	102.4	104.8	108.4	110.6	111.5	111.6	112.7	116.4	121.7	122.5
80		X	X		X	X		X	100.0	100.3	101.0	102.7	106.0	110.8	113.9	114.7	114.4	115.2	118.4	123.4	123.7
81		X	X		X		X	X													
82		X	X			X	X	X													

TABLE 2.1-2 (continued)

CHANNEL A RBM RESPONSE

FAILURE COMBINATION	OPERABLE LPRMS								RBM RESPONSE(%) FOR AXIAL ROD POSITION													
	1A	2A	3A	4A	1C	2C	3C	4C	0	4	8	12	16	20	24	28	32	36	40	44	48
83		X		X	X	X	X		100.0	100.3	101.1	102.7	106.2	111.3	114.5	115.3	114.9	115.4	117.0	121.7	121.0
84		X		X	X	X		X	100.0	100.3	101.0	102.6	105.7	110.4	113.3	114.0	113.7	114.4	116.9	121.0	121.2
85		X		X	X		X	X	100.0	100.3	101.0	102.3	104.6	108.1	110.2	111.0	111.0	112.0	114.9	118.2	118.8
86		X		X		X	X	X	100.0	100.3	101.0	102.6	105.0	110.4	113.3	114.0	113.7	114.3	116.9	120.8	121.0
87		X			X	X	X	X	100.0	100.4	101.5	103.0	108.4	115.1	118.2	120.0	119.1	119.7	120.2	123.4	122.9
88			X	X	X	X	X		100.0	100.3	101.1	102.7	106.2	111.3	114.5	115.2	114.7	114.8	116.1	118.3	118.0
89			X	X	X	X		X	100.0	100.3	101.0	102.6	105.7	110.4	113.2	113.9	113.6	113.8	114.2	115.9	115.4
90			X	X	X		X	X	100.0	100.3	101.0	102.3	104.6	108.1	110.1	110.9	110.9	111.4	112.2	113.8	114.0
91			X	X		X	X	X	100.0	100.3	101.0	102.6	105.0	110.4	113.3	114.0	113.6	113.7	114.2	115.4	115.3
92			X		X	X	X	X	100.0	100.4	101.4	103.7	108.4	115.0	119.1	119.9	118.8	118.0	117.0	117.1	116.3
93				X	X	X	X	X	100.0	100.4	101.4	103.6	108.0	114.3	118.2	118.9	117.9	116.8	115.4	114.7	113.7
94	X	X	X	X					100.0	100.1	100.2	100.3	100.3	100.7	101.0	101.6	102.9	105.1	112.7	120.8	120.0
95	X	X	X		X				100.0	100.2	100.5	101.0	102.0	103.6	104.7	105.4	106.3	109.1	115.1	123.4	120.1
96	X	X	X			X			100.0	100.2	100.5	101.3	103.3	106.3	108.2	108.8	109.3	111.7	117.4	125.1	120.4
97	X	X	X				X		100.0	100.2	100.5	101.1	102.1	103.7	104.8	105.6	106.4	109.1	115.2	123.2	124.9
98	X	X	X					X	100.0	100.2	100.4	100.9	101.6	102.7	103.4	104.1	105.1	107.9	114.2	122.4	124.3
99	X	X		X	X				100.0	100.2	100.5	101.0	101.9	103.5	104.5	105.2	106.0	108.4	113.8	120.7	122.2
100	X	X		X		X			100.0	100.2	100.5	101.3	103.1	106.0	107.9	108.5	108.9	110.9	115.8	122.4	123.5
101	X	X		X			X		100.0	100.2	100.5	101.1	102.0	103.6	104.7	105.3	106.1	108.5	113.7	120.6	122.0
102	X	X		X				X	100.0	100.2	100.3	100.9	101.5	102.6	103.3	104.0	104.8	107.3	112.8	119.8	121.4
103	X	X			X	X			100.0	100.3	100.9	102.3	105.4	110.2	113.1	113.8	113.7	115.0	119.2	125.3	120.8
104	X	X			X		X		100.0	100.3	100.9	102.0	104.1	107.3	109.3	110.1	110.4	112.1	118.7	123.2	124.2
105	X	X			X			X	100.0	100.3	100.8	101.8	103.5	106.2	107.8	108.5	109.0	110.8	115.0	122.3	123.5
106	X	X				X	X		100.0	100.3	100.9	102.3	105.5	110.2	113.1	113.8	113.7	114.9	119.0	125.1	120.8
107	X	X				X		X	100.0	100.3	100.9	102.1	104.9	109.1	111.8	112.3	113.7	114.0	118.0	124.2	125.0
108	X	X					X	X	100.0	100.3	100.8	101.9	103.6	106.3	107.8	108.7	109.0	110.9	115.5	122.1	123.9
109	X		X	X	X				100.0	100.2	100.5	101.0	101.9	103.5	104.5	105.2	105.9	107.9	111.0	115.0	116.2
110	X		X	X		X			100.0	100.2	100.5	101.3	103.2	106.2	107.9	108.4	108.8	110.3	113.1	118.7	117.9
111	X		X	X			X		100.0	100.2	100.5	101.1	102.0	103.6	104.7	105.3	106.0	107.8	111.0	114.9	116.0
112	X		X	X				X	100.0	100.2	100.5	100.9	101.5	102.6	103.3	104.0	104.8	106.8	110.9	114.1	115.4
113	X		X		X	X			100.0	100.3	100.9	102.3	105.4	110.1	113.0	113.7	113.5	114.3	115.9	119.7	118.9
114	X		X		X		X		100.0	100.3	100.9	102.0	104.1	107.3	109.3	110.1	110.3	111.4	113.5	116.8	117.2
115	X		X		X			X	100.0	100.3	100.8	101.9	103.5	106.2	107.8	108.5	108.9	110.1	112.4	115.7	116.9
116	X		X			X	X		100.0	100.3	100.9	102.3	105.5	110.1	113.1	113.7	113.5	114.2	118.9	118.8	119.7
117	X		X			X		X	100.0	100.3	100.9	102.1	104.9	109.0	111.6	112.2	112.1	113.0	116.5	117.7	118.0
118	X		X				X	X	100.0	100.3	100.8	101.9	103.6	106.3	107.8	108.6	108.8	110.1	112.3	115.8	116.3
119	X			X	X	X			100.0	100.3	100.9	102.2	105.2	109.7	112.4	113.0	112.8	113.3	116.3	118.1	118.8
120	X			X	X		X		100.0	100.3	100.9	102.0	103.9	107.0	108.9	109.6	109.7	110.6	112.0	114.1	114.9
121	X			X	X			X	100.0	100.3	100.8	101.8	103.4	105.9	107.4	108.1	108.4	108.4	110.9	113.1	113.7
122	X			X		X	X		100.0	100.3	100.9	102.2	105.2	109.7	112.5	113.1	112.8	113.3	116.3	118.0	118.8
123	X			X		X		X	100.0	100.3	100.9	102.1	104.7	108.6	111.0	111.6	111.5	112.1	115.2	115.1	115.2

TABLE 2.1-2 (continued)

CHANNEL A RBM RESPONSE

FAILURE COMBINATION	OPERABLE LPRMS								RBM RESPONSE(%) FOR AXIAL ROD POSITION															
	1A	2A	3A	4A	1C	2C	3C	4C	0	4	8	12	16	20	24	28	32	36	40	44	48			
124	X			X			X	X	100.0	100.3	100.8	101.8	103.5	106.0	107.5	108.2	108.4	109.4	110.9	113.1	113.9			
125	X				X	X	X		100.0	100.4	101.4	103.5	108.1	114.9	119.0	119.8	118.9	118.1	117.5	118.0	117.2			
126	X				X	X		X	100.0	100.4	101.3	103.3	107.5	113.7	117.4	118.1	117.3	116.8	116.3	117.0	116.4			
127	X				X		X	X	100.0	100.4	101.3	103.0	106.7	110.6	113.2	114.1	113.7	113.6	113.6	114.8	114.5			
128	X					X	X	X	100.0	100.4	101.3	103.3	107.6	113.6	117.4	118.1	117.2	116.7	116.2	116.8	116.2			
129		X	X	X	X				100.0	100.2	100.5	101.0	102.0	103.6	104.6	105.4	106.2	108.7	114.2	121.4	122.0			
130		X	X	X		X			100.0	100.2	100.5	101.3	103.3	106.2	108.1	108.7	109.2	111.3	116.3	123.1	124.2			
131		X	X	X			X		100.0	100.2	100.5	101.1	102.1	103.7	104.8	105.5	106.3	108.7	114.2	121.2	122.7			
132		X	X	X				X	100.0	100.2	100.4	100.9	101.6	102.7	103.4	104.1	105.9	107.5	113.2	120.4	122.1			
133		X	X		X	X			100.0	100.3	100.9	102.4	105.7	110.5	113.6	114.3	114.3	115.6	119.9	126.3	126.9			
134		X	X		X		X		100.0	100.3	100.9	102.1	104.3	107.6	109.7	110.5	110.9	112.6	117.3	124.1	125.0			
135		X	X		X			X	100.0	100.3	100.8	101.9	103.7	106.4	108.1	108.9	109.4	111.2	116.2	123.1	124.4			
136		X	X			X	X		100.0	100.3	100.9	102.4	105.8	110.5	113.7	114.4	114.2	115.5	119.7	126.0	126.5			
137		X	X			X		X	100.0	100.3	100.9	102.2	105.2	109.4	112.1	112.8	112.8	114.2	118.6	125.1	125.4			
138		X	X				X	X	100.0	100.2	100.8	101.9	103.8	106.5	108.2	109.0	109.4	111.2	116.1	122.9	124.1			
139		X		X	X	X			100.0	100.3	100.9	102.3	105.4	110.0	112.9	113.6	113.4	114.5	118.0	123.0	123.4			
140		X		X	X		X		100.0	100.3	100.9	102.0	104.1	107.3	109.2	110.0	110.2	111.6	115.5	121.0	121.8			
141		X		X	X			X	100.0	100.3	100.8	101.8	103.5	106.1	107.7	108.8	108.8	110.4	114.5	120.1	121.1			
142		X		X		X	X		100.0	100.3	100.9	102.3	105.5	110.0	113.0	113.7	113.4	114.4	117.8	122.8	123.2			
143		X		X		X		X	100.0	100.3	100.9	102.1	104.9	109.0	111.5	112.1	112.1	113.2	116.8	122.0	122.5			
144		X		X			X	X	100.0	100.3	100.8	101.9	103.6	106.2	107.8	108.6	108.9	110.1	114.4	119.9	120.8			
145		X			X	X	X		100.0	100.4	101.4	103.7	108.6	115.6	120.0	120.8	119.9	119.8	122.1	128.4	129.9			
146		X			X	X		X	100.0	100.4	101.4	103.5	107.9	114.4	118.3	119.1	118.3	118.4	120.9	128.3	129.2			
147		X			X		X	X	100.0	100.4	101.3	103.2	106.4	111.1	113.9	114.8	114.5	115.0	118.0	122.8	123.2			
148		X				X	X	X	100.0	100.4	101.3	103.5	108.0	114.3	118.3	119.1	118.2	118.3	120.7	128.1	124.8			
149			X	X	X	X			100.0	100.3	100.9	102.3	105.4	110.0	112.9	113.5	113.3	113.8	114.7	118.8	119.5			
150			X	X	X		X		100.0	100.3	100.9	102.0	104.1	107.2	109.2	110.0	110.1	110.9	112.3	114.5	114.9			
151			X	X	X			X	100.0	100.3	100.8	101.8	103.5	106.1	107.7	108.4	108.7	109.7	111.3	113.8	114.1			
152			X	X		X	X		100.0	100.3	100.9	102.3	105.5	110.0	112.9	113.6	113.3	113.7	114.6	118.8	119.4			
153			X	X		X		X	100.0	100.3	100.9	102.1	104.9	108.9	111.4	112.1	111.9	112.5	113.6	118.5	118.7			
154			X	X			X	X	100.0	100.3	100.8	101.9	103.8	106.2	107.8	108.6	108.7	109.7	111.2	113.5	114.0			
155			X		X	X	X		100.0	100.4	101.4	103.7	108.5	115.5	119.9	120.7	119.6	119.9	118.2	118.7	117.0			
156			X		X	X		X	100.0	100.4	101.4	103.5	107.9	114.3	118.2	119.0	118.1	117.5	117.0	117.0	116.9			
157			X		X		X	X	100.0	100.4	101.3	103.2	106.4	111.0	113.8	114.7	114.3	114.1	114.2	115.2	115.0			
158			X			X	X	X	100.0	100.4	101.3	103.5	107.9	114.2	118.2	118.9	118.0	117.4	116.9	117.0	116.7			
159				X	X	X	X		100.0	100.4	101.4	103.5	108.0	114.7	118.8	119.5	118.4	117.5	116.2	118.0	116.6			
160				X	X	X		X	100.0	100.4	101.3	103.3	107.4	113.5	117.2	117.9	117.9	116.2	115.1	114.0	113.8			
161				X	X		X	X	100.0	100.4	101.2	103.0	106.0	110.8	113.1	113.9	113.4	113.0	112.4	112.3	111.9			
162				X		X	X	X	100.0	100.4	101.3	103.3	107.5	113.6	117.1	117.9	116.9	116.1	115.0	114.9	113.7			
163					X	X	X	X	100.0	100.5	101.9	105.1	111.4	120.5	126.0	126.9	124.9	122.6	119.1	118.6	116.7			

TABLE 2.1-2 (continued)

CHANNEL B RBM RESPONSE

FAILURE COMBINATION	OPERABLE LPRMS								RBM RESPONSE(%) FOR AXIAL ROD POSITION											
	1B	2B	3B	4B	1D	2D	3D	4D	0	4	8	12	16	20	24	28	32	36	40	44	48
1	X	X	X	X	X	X	X	X	100.0	101.4	104.3	107.3	109.1	110.9	112.2	115.3	119.0	120.8	118.5	115.7	113.6
2	X	X	X	X	X	X	X		100.0	101.3	104.0	106.8	108.4	110.2	111.6	115.1	119.3	121.4	119.0	116.2	113.8
3	X	X	X	X	X	X		X	100.0	101.2	103.7	106.3	107.8	109.5	111.0	114.5	118.8	120.9	118.6	115.8	113.6
4	X	X	X	X	X		X	X	100.0	100.9	102.8	104.8	106.2	108.0	109.6	113.3	117.7	119.9	117.7	115.0	112.8
5	X	X	X	X		X	X	X	100.0	101.2	103.6	106.2	107.8	109.5	111.0	114.5	118.8	120.9	118.6	115.8	113.6
6	X	X	X		X	X	X	X	100.0	101.6	105.1	108.7	110.8	112.6	113.9	117.1	121.1	122.9	120.2	117.2	114.7
7	X	X		X	X	X	X	X	100.0	101.7	105.2	108.8	110.9	112.7	113.8	116.6	119.9	121.4	118.9	116.2	113.9
8	X		X	X	X	X	X	X	100.0	101.7	105.2	108.9	111.0	112.8	113.6	115.2	117.0	117.8	115.9	113.7	112.1
9		X	X	X	X	X	X	X	100.0	101.6	105.0	108.6	110.7	112.4	113.6	116.4	119.8	121.3	118.7	115.9	113.8
10	X	X	X	X	X	X			100.0	101.1	103.3	105.6	107.0	108.7	110.3	114.2	118.1	121.5	119.1	116.2	113.8
11	X	X	X	X	X		X		100.0	100.8	102.3	104.1	105.3	107.0	108.8	112.9	117.9	120.4	118.2	115.4	113.1
12	X	X	X	X	X			X	100.0	100.7	102.0	103.5	104.6	106.4	108.2	112.3	117.3	119.9	117.8	115.0	112.7
13	X	X	X	X		X	X		100.0	101.1	103.2	105.6	106.9	108.6	110.3	114.2	118.1	121.5	119.2	116.3	113.8
14	X	X	X	X		X		X	100.0	101.0	102.9	105.0	106.2	107.9	109.6	113.6	118.6	121.0	118.8	115.9	113.5
15	X	X	X	X			X	X	100.0	100.6	101.9	103.4	104.6	106.3	108.1	112.3	117.4	120.0	117.8	115.0	112.8
16	X	X	X		X	X	X		100.0	101.5	104.8	108.2	110.1	111.9	113.4	117.0	121.6	123.7	121.0	117.9	115.2
17	X	X	X		X	X		X	100.0	101.4	104.4	107.6	109.4	111.1	112.7	116.3	121.0	123.2	120.5	117.4	114.8
18	X	X	X		X		X	X	100.0	101.1	103.4	105.8	107.4	109.3	110.9	114.8	119.6	121.9	119.4	116.5	114.0
19	X	X	X			X	X	X	100.0	101.4	104.4	107.5	109.3	111.1	112.6	116.3	121.0	123.2	120.6	117.5	114.8
20	X	X		X	X	X	X		100.0	101.6	104.9	108.3	110.2	112.0	113.3	118.4	120.4	122.2	119.6	116.7	114.3
21	X	X		X	X	X		X	100.0	101.5	104.5	107.7	109.4	111.2	112.5	115.7	119.7	121.6	119.1	116.2	113.9
22	X	X		X	X		X	X	100.0	101.1	103.4	105.9	107.5	109.3	110.8	114.2	118.4	120.4	118.0	116.3	113.1
23	X	X		X		X	X	X	100.0	101.4	104.5	107.6	109.4	111.2	112.5	115.8	119.6	121.7	119.2	116.3	114.0
24	X	X			X	X	X	X	100.0	102.1	106.5	111.1	113.6	115.5	116.5	119.3	122.8	124.3	121.3	118.2	115.8
25	X		X	X	X	X	X		100.0	101.6	104.9	108.4	110.3	112.1	113.1	115.0	117.1	118.2	116.3	114.1	112.3
26	X		X	X	X	X		X	100.0	101.5	104.5	107.7	109.5	111.3	112.3	114.3	116.5	117.6	115.8	113.8	112.0
27	X		X	X	X		X	X	100.0	101.1	103.4	105.9	107.6	109.4	110.6	112.7	115.1	116.4	114.7	112.6	111.2
28	X		X	X		X	X	X	100.0	101.4	104.5	107.7	109.5	111.2	112.3	114.3	116.5	117.7	115.8	113.7	112.0
29	X		X		X	X	X	X	100.0	102.1	106.6	111.2	113.7	115.6	116.3	117.5	119.1	119.6	117.4	115.2	113.3
30	X			X	X	X	X	X	100.0	102.1	106.7	111.4	113.9	115.8	116.2	116.9	117.8	117.7	115.7	113.7	112.3
31		X	X	X	X	X	X		100.0	101.5	104.8	108.1	110.0	111.7	113.0	116.3	120.2	122.0	119.4	116.5	114.0
32		X	X	X	X	X		X	100.0	101.4	104.4	107.5	109.2	110.9	112.3	115.6	119.8	121.4	118.9	116.0	113.6
33		X	X	X	X		X	X	100.0	101.1	103.3	105.7	107.4	109.1	110.6	114.0	118.2	120.2	117.8	115.1	112.8
34		X	X	X		X	X	X	100.0	101.4	104.3	107.4	109.2	110.9	112.3	115.6	119.8	121.5	119.0	116.1	113.7
35		X	X		X	X	X	X	100.0	102.0	106.3	110.8	113.3	115.0	116.1	119.0	122.8	124.9	121.0	117.9	115.2
36		X		X	X	X	X	X	100.0	102.0	106.4	110.9	113.4	115.2	116.0	118.3	121.2	122.2	119.4	116.5	114.2
37			X	X	X	X	X	X	100.0	102.0	106.5	111.0	113.5	115.3	115.8	116.6	117.5	117.6	115.5	113.8	112.0
38	X	X	X	X	X				100.0	100.5	101.5	102.6	103.4	105.1	107.2	111.8	117.5	120.5	118.3	116.4	113.9
39	X	X	X	X		X			100.0	100.8	102.4	104.2	105.2	106.8	108.8	113.3	118.8	121.7	119.4	116.4	113.8
40	X	X	X	X			X		100.0	100.5	101.4	102.5	103.4	105.0	107.1	111.8	117.5	120.5	118.4	115.8	113.3
41	X	X	X	X				X	100.0	100.4	101.0	101.9	102.6	104.3	106.4	111.1	116.9	120.0	117.9	116.0	112.7

TABLE 2.1-2 (continued)

CHANNEL B RBM RESPONSE

FAILURE COMBINATION	OPERABLE LPRMS								RBM RESPONSE(%) FOR AXIAL ROD POSITION													
	1B	2B	3B	4B	1D	2D	3D	4D	0	4	8	12	16	20	24	28	32	36	40	44	48	
42	X	X	X		X	X			100.0	101.3	104.0	106.9	108.5	110.2	112.0	116.2	121.5	124.1	121.4	118.2	115.3	
43	X	X	X		X		X		100.0	100.9	102.9	104.9	106.4	108.2	110.1	114.5	120.0	122.8	120.3	117.1	114.4	
44	X	X	X		X			X	100.0	100.8	102.4	104.2	105.5	107.3	109.2	113.7	119.4	122.2	119.7	116.6	114.0	
45	X	X	X			X	X		100.0	101.3	104.0	106.8	108.4	110.2	111.9	116.2	121.6	124.2	121.5	118.3	115.4	
46	X	X	X			X		X	100.0	101.2	103.6	106.1	107.6	109.3	111.1	115.4	120.9	123.6	121.0	117.7	114.9	
47	X	X	X				X	X	100.0	100.8	102.4	104.2	105.5	107.2	109.2	113.7	119.4	122.2	119.8	116.7	114.1	
48	X	X		X	X	X			100.0	101.4	104.1	107.0	108.5	110.3	111.8	115.5	120.2	122.4	119.9	116.9	114.4	
49	X	X		X	X		X		100.0	101.0	102.9	105.0	106.4	108.2	109.9	113.8	118.7	121.1	118.7	115.8	113.5	
50	X	X		X	X			X	100.0	100.8	102.5	104.3	105.5	107.4	109.0	113.0	118.0	120.4	118.1	115.3	113.0	
51	X	X		X		X	X		100.0	101.3	104.1	106.9	108.5	110.2	111.8	115.5	120.2	122.5	120.0	117.0	114.4	
52	X	X		X		X		X	100.0	101.2	103.6	106.2	107.6	109.4	110.9	114.8	119.5	121.9	119.4	116.4	114.0	
53	X	X		X			X	X	100.0	100.8	102.4	104.2	105.5	107.3	109.0	113.0	118.0	120.5	118.2	115.4	113.1	
54	X	X			X	X	X		100.0	102.0	106.3	110.7	113.0	114.9	116.1	119.4	123.7	125.6	122.5	119.2	116.3	
55	X	X			X	X		X	100.0	101.9	105.8	109.8	112.0	113.9	115.1	118.5	122.9	124.8	121.8	118.6	116.0	
56	X	X			X		X	X	100.0	101.4	104.4	107.5	109.5	111.4	112.8	116.8	121.1	123.2	120.4	117.3	114.8	
57	X	X				X	X	X	100.0	101.8	105.7	109.8	112.0	113.9	115.1	118.8	123.0	124.9	122.0	118.7	115.9	
58	X		X	X	X	X			100.0	101.4	104.2	107.1	108.6	110.4	111.6	113.9	116.6	118.0	116.2	114.0	112.2	
59	X		X	X	X		X		100.0	101.0	102.9	105.1	106.5	108.3	109.6	112.1	115.1	116.7	115.0	112.9	111.3	
60	X		X	X	X			X	100.0	100.8	102.5	104.4	105.6	107.4	108.8	111.4	114.4	116.0	114.4	112.4	110.9	
61	X		X	X		X	X		100.0	101.3	104.1	107.0	108.6	110.3	111.5	113.9	116.6	118.1	116.3	114.0	112.2	
62	X		X	X		X		X	100.0	101.2	103.7	106.3	107.7	109.4	110.7	113.1	116.0	117.4	115.7	113.5	111.8	
63	X		X	X			X	X	100.0	100.8	102.4	104.3	105.6	107.3	108.7	111.4	114.4	116.1	114.5	112.4	110.9	
64	X		X		X	X	X		100.0	102.0	106.4	110.9	113.2	115.0	115.9	117.5	119.5	120.4	118.2	115.8	113.8	
65	X		X		X	X		X	100.0	101.9	105.8	109.9	112.1	114.0	114.9	116.6	118.7	119.6	117.5	115.1	113.2	
66	X		X		X		X	X	100.0	101.4	104.4	107.6	109.6	111.5	112.6	114.5	116.9	118.0	116.	113.9	112.2	
67	X		X			X	X	X	100.0	101.8	105.8	109.9	112.2	113.9	114.9	116.6	118.7	119.7	117.6	115.2	113.3	
68	X			X	X	X	X		100.0	102.1	106.5	111.0	113.3	115.2	115.8	116.8	117.8	118.2	116.2	114.2	112.6	
69	X			X	X	X		X	100.0	101.9	106.0	110.1	112.3	114.2	114.7	115.8	117.0	117.5	115.5	113.5	112.1	
70	X			X	X		X	X	100.0	101.5	104.5	107.7	109.7	111.6	112.4	113.7	115.2	115.8	114.1	112.2	111.0	
71	X			X		X	X	X	100.0	101.9	105.9	110.1	112.3	114.1	114.7	115.8	117.0	117.5	116.8	113.8	112.1	
72	X				X	X	X	X	100.0	102.9	109.2	115.5	118.9	120.9	120.9	120.8	120.8	120.3	117.8	115.7	114.0	
73		X	X	X	X	X			100.0	101.3	104.0	106.8	108.3	110.0	111.6	115.3	120.0	122.2	119.6	116.6	114.0	
74		X	X	X	X		X		100.0	100.9	102.8	104.9	106.3	108.0	109.7	113.7	118.5	120.9	118.5	115.6	113.2	
75		X	X	X	X			X	100.0	100.8	102.4	104.2	105.4	107.1	108.9	112.8	117.8	120.3	117.9	115.1	112.8	
76		X	X	X		X	X		100.0	101.2	103.9	106.7	108.3	109.9	111.5	115.4	120.0	122.3	119.7	116.7	114.1	
77		X	X	X		X		X	100.0	101.1	103.5	106.0	107.5	109.1	110.7	114.8	119.4	121.7	119.2	116.2	113.7	
78		X	X	X			X	X	100.0	100.7	102.3	104.1	105.4	107.0	108.8	112.9	117.9	120.3	118.0	115.1	112.8	
79		X	X		X	X	X		100.0	101.9	106.1	110.3	112.7	114.4	115.7	119.1	123.4	125.2	122.1	118.8	115.9	
80		X	X		X	X		X	100.0	101.8	105.6	109.5	111.7	113.4	114.8	118.2	122.6	124.5	121.5	118.2	115.4	
81		X	X		X		X	X	100.0	101.3	104.2	107.2	109.2	111.0	112.5	116.2	120.9	122.8	120.1	117.0	114.4	
82		X	X			X	X	X	100.0	101.7	105.5	109.5	111.7	113.4	114.7	118.3	122.7	124.6	121.6	118.3	115.5	

TABLE 2.1-2 (continued)

CHANNEL B RBM RESPONSE

FAILURE COMBINATION	OPERABLE LPRMS								RBM RESPONSE(%) FOR AXIAL ROD POSITION													
	1B	2B	3B	4B	1D	2D	3D	4D	0	4	8	12	16	20	24	28	32	36	40	44	48
83		X		X	X	X	X		100.0	102.0	106.2	110.5	112.8	114.6	115.6	118.4	121.8	123.2	120.3	117.3	114.8
84		X		X	X	X		X	100.0	101.8	105.7	109.8	111.8	113.6	114.6	117.5	121.0	122.5	119.7	116.7	114.3
85		X		X	X	X	X		100.0	101.4	104.3	10..4	109.3	111.1	112.3	115.5	119.3	120.9	118.3	115.5	113.2
86		X		X	X	X		X	100.0	101.8	105.6	109.6	111.8	113.5	114.6	117.5	121.1	122.6	119.8	116.8	114.3
87		X		X	X		X	X	100.0	102.0	106.2	110.6	113.0	114.7	115.4	116.5	117.7	118.1	116.9	113.9	110.6
88		X		X		X	X	X	100.0	101.8	105.7	109.7	111.9	113.6	114.4	115.6	116.9	117.4	115.4	113.3	110.7
89		X			X	X	X	X	100.0	101.4	104.3	107.4	109.4	111.2	112.1	113.6	115.1	115.7	114.0	112.1	110.7
90		X	X	X	X	X	X	X	100.0	101.8	105.7	109.7	112.0	113.6	114.3	115.6	116.9	117.4	115.4	113.4	111.8
91		X	X	X	X	X	X		100.0	102.7	108.8	114.9	118.2	120.0	120.2	120.4	120.8	120.0	117.5	115.3	113.6
92		X	X	X	X	X		X	100.0	102.8	109.0	115.2	118.5	120.3	120.1	119.5	118.4	117.4	115.2	113.4	112.1
93		X	X	X	X		X	X	100.0	100.2	100.3	100.7	101.1	102.8	105.1	110.5	117.1	120.6	118.5	118.5	113.0
94		X	X	X		X	X	X	100.0	100.5	101.6	103.1	104.1	105.8	108.1	113.2	118.8	123.1	120.6	117.3	114.8
95		X	X		X	X	X	X	100.0	101.0	103.0	105.2	106.4	108.1	110.1	115.1	121.6	124.7	122.1	118.8	115.5
96		X		X	X	X	X	X	100.0	100.6	101.7	103.0	104.0	105.7	108.0	113.2	119.8	123.2	120.8	117.5	114.8
97			X	X	X	X	X	X	100.0	100.4	101.2	102.2	103.1	104.8	107.1	112.4	118.1	122.5	120.1	118.0	114.1
98	X	X	X	X	X	X	X	X	100.0	100.6	101.8	103.1	104.1	105.9	107.8	112.5	118.3	121.2	118.9	116.9	113.4
99	X	X	X	X	X	X	X		100.0	101.0	103.1	105.3	106.4	108.1	109.9	114.4	120.0	122.8	120.3	117.2	114.8
100	X	X	X	X	X	X		X	100.0	100.6	101.7	103.1	104.0	105.8	107.7	112.5	118.3	121.3	119.0	116.0	113.8
101	X	X	X	X	X		X	X	100.0	100.5	101.3	102.2	103.1	104.8	106.8	111.6	117.5	120.6	118.3	115.4	113.0
102	X	X	X	X		X	X	X	100.0	101.8	105.5	109.2	111.1	113.0	114.5	118.6	124.0	126.4	123.3	119.8	116.7
103	X	X	X		X	X	X	X	100.0	101.2	103.8	106.5	108.3	110.2	111.9	116.3	121.9	124.5	121.7	118.4	115.5
104	X	X		X	X	X	X	X	100.0	101.1	103.2	105.6	107.1	109.0	110.8	115.2	121.0	123.7	120.9	117.8	114.9
105	X		X	X	X	X	X	X	100.0	101.7	105.4	109.2	111.2	113.0	114.5	118.7	124.1	126.5	123.6	119.9	116.8
106		X	X	X	X	X	X	X	100.0	101.6	104.8	108.2	110.0	111.8	113.3	117.8	123.1	125.7	122.7	119.2	116.2
107	X	X	X	X	X	X	X	X	100.0	101.0	103.1	105.5	107.0	108.9	110.7	115.3	121.0	123.8	121.0	117.8	115.0
108	X	X	X	X	X	X	X		100.0	100.6	101.8	103.2	104.2	105.9	107.6	110.8	114.3	116.3	114.6	112.6	111.0
109	X	X	X	X	X	X		X	100.0	101.0	103.1	105.3	106.5	108.2	109.7	112.6	116.0	117.9	116.2	113.9	112.1
110	X	X	X	X	X		X	X	100.0	100.6	101.8	103.1	104.1	105.8	107.5	110.8	114.3	116.3	114.9	112.7	111.1
111	X	X	X	X		X	X	X	100.0	100.5	101.3	102.3	103.1	104.8	106.5	109.7	113.9	116.4	114.2	112.1	110.6
112	X	X	X		X	X	X	X	100.0	101.8	105.5	109.3	111.3	113.1	114.3	118.4	119.2	120.5	118.3	115.8	113.7
113	X	X		X	X	X	X	X	100.0	101.2	103.9	106.6	108.4	110.3	111.6	114.0	117.1	118.6	116.7	114.4	112.8
114	X		X	X	X	X	X	X	100.0	101.1	103.3	105.6	107.2	109.1	110.5	113.0	116.2	117.7	115.9	113.7	112.0
115		X	X	X	X	X	X	X	100.0	101.7	105.4	109.3	111.3	113.0	114.2	118.4	119.2	120.5	118.4	116.0	113.8
116	X	X	X	X	X	X	X		100.0	101.6	104.8	108.3	110.1	111.9	113.1	115.4	118.3	119.7	117.7	115.2	113.2
117	X	X	X	X	X	X		X	100.0	101.0	103.2	105.6	107.2	109.0	110.4	113.0	116.2	117.8	116.0	113.8	112.0
118	X	X	X	X	X		X	X	100.0	101.8	105.6	109.5	111.5	113.3	114.1	115.5	117.2	118.0	116.1	114.0	112.4
119	X	X	X	X		X	X	X	100.0	101.3	104.0	106.8	108.5	110.4	111.4	113.1	115.1	116.1	114.5	112.5	111.2
120	X	X	X		X	X	X	X	100.0	101.1	103.4	105.8	107.3	109.2	110.2	112.1	114.2	115.3	113.7	111.8	110.6
121	X	X		X	X	X	X	X	100.0	101.8	105.6	109.5	111.5	113.2	114.0	115.5	117.3	118.1	116.2	114.1	112.5
122	X		X	X	X	X	X	X	100.0	101.6	105.0	108.4	110.2	112.0	112.8	114.5	116.3	117.2	115.4	113.3	111.9
123		X	X	X	X	X	X	X													

TABLE 2.1-2 (continued)

CHANNEL B RBM RESPONSE

FAILURE COMBINATION	OPERABLE LPRMS								RBM RESPONSE(%) FOR AXIAL ROD POSITION													
	1B	2B	3B	4B	1D	2D	3D	4D	0	4	8	12	16	20	24	28	32	36	40	44	48
124	x			x			x	x	100.0	101.1	103.3	105.7	107.3	109.1	110.1	112.1	114.2	115.3	113.8	111.9	110.6
125	x				x	x	x		100.0	103.0	109.4	115.8	119.0	121.1	121.2	121.4	121.7	121.5	119.0	116.7	114.8
126	x				x	x		x	100.0	102.8	108.6	114.5	117.5	119.5	119.7	120.0	120.5	120.4	118.0	115.8	114.0
127	x				x		x	x	100.0	102.1	106.4	111.0	113.7	115.8	116.3	116.9	117.8	117.9	115.9	113.9	112.4
128	x					x	x	x	100.0	102.7	108.5	114.5	117.6	119.5	119.7	120.1	120.6	120.5	118.1	115.9	114.1
129		x	x	x	x				100.0	100.6	101.7	103.0	104.0	105.7	107.7	112.4	118.1	121.0	118.6	115.6	113.1
130		x	x	x		x			100.0	101.0	103.0	105.1	106.3	107.8	109.7	114.2	119.8	122.6	120.0	116.9	114.1
131		x	x	x			x		100.0	100.5	101.6	102.9	104.0	105.6	107.6	112.4	118.1	121.1	118.7	115.7	113.2
132		x	x	x				x	100.0	100.4	101.2	102.2	103.0	104.6	106.7	111.5	117.4	120.4	118.1	115.1	112.7
133		x	x		x	x			100.0	101.7	105.2	108.8	110.8	112.5	114.1	118.3	123.6	126.0	122.8	119.3	116.1
134		x	x		x		x		100.0	101.1	103.6	106.3	108.0	109.8	111.6	116.0	121.6	124.2	121.3	117.9	115.0
135		x	x		x			x	100.0	101.0	103.1	105.3	106.9	108.7	110.5	115.0	120.7	123.3	120.5	117.2	114.4
136		x	x			x	x		100.0	101.6	105.1	108.8	110.8	112.4	114.1	118.3	123.7	126.1	123.0	119.5	116.2
137		x	x			x		x	100.0	101.5	104.6	107.8	109.7	111.3	113.0	117.3	122.7	125.3	122.2	118.8	115.7
138		x	x				x	x	100.0	100.9	103.0	105.2	106.9	108.5	110.4	115.0	120.7	123.5	120.7	117.4	114.5
139		x		x	x	x			100.0	101.7	105.3	109.0	110.9	112.7	113.9	117.5	121.8	123.7	120.8	117.6	114.9
140		x		x	x		x		100.0	101.2	103.7	106.4	108.1	109.9	111.4	115.2	119.8	121.9	119.2	116.2	113.7
141		x		x	x			x	100.0	101.0	103.2	105.4	107.0	108.8	110.2	114.1	118.9	121.1	118.5	115.5	113.2
142		x		x		x	x		100.0	101.7	105.3	109.0	110.9	112.6	113.9	117.5	121.9	123.8	120.9	117.7	115.0
143		x		x		x		x	100.0	101.5	104.7	108.0	109.8	111.4	112.8	116.5	121.0	123.0	120.2	117.0	114.4
144		x		x			x	x	100.0	101.0	103.1	105.4	106.9	108.6	110.2	114.1	118.9	121.2	118.6	115.6	113.2
145		x			x	x	x		100.0	102.7	108.8	114.8	118.0	119.8	120.6	123.5	127.3	128.5	124.8	121.1	117.8
146		x			x	x		x	100.0	102.6	108.0	113.6	116.5	118.4	119.2	122.2	126.1	127.5	123.8	120.2	117.1
147		x			x		x	x	100.0	101.9	106.0	110.3	112.9	114.9	116.0	118.3	123.5	125.2	121.8	118.5	115.6
148		x				x	x	x	100.0	102.5	108.0	113.6	116.	.4	119.2	122.3	126.2	127.6	124.0	120.4	117.2
149			x	x	x	x			100.0	101.7	105.4	109.1	111.1	8	113.7	115.3	117.1	117.9	116.9	113.7	112.0
150			x	x	x		x		100.0	101.2	103.8	106.5	108.3	9	111.1	113.0	115.0	116.0	114.3	112.3	110.9
151			x	x	x			x	100.0	101.0	103.2	105.5	107.1	108.8	109.9	111.9	114.1	115.2	113.8	111.6	110.3
152			x	x		x	x		100.0	101.7	105.3	109.1	111.1	112.7	113		117.1	117.9	116.0	113.8	112.1
153			x	x		x		x	100.0	101.5	104.7	108.1	109.9	111.5	11		116.2	117.1	115.2	113.1	111.5
154			x	x			x	x	100.0	101.0	103.1	105.4	107.1	108.7	109	9	114.1	115.2	113.6	111.7	110.3
155			x		x	x	x		100.0	102.8	108.8	115.0	118.2	120.0	120.4		121.3	121.2	118.6	116.3	114.2
156			x		x	x		x	100.0	102.6	108.1	113.8	116.7	118.5	118.		120.2	120.1	117.6	115.4	113.6
157			x		x		x	x	100.0	101.9	106.1	110.4	113.1	115.0	115		117.6	117.8	115.6	113.6	112.0
158			x			x	x	x	100.0	102.5	108.0	113.7	116.8	118.5	118.		120.2	120.2	117.8	116.5	113.8
159				x	x	x	x		100.0	102.9	109.1	115.3	118.6	120.4	120	.8	119.0	118.1	115.9	113.9	112.6
160				x	x	x		x	100.0	102.7	108.3	114.1	117.0	118.9	118	.5	117.8	117.0	114.9	113.0	111.8
161				x	x		x	x	100.0	102.0	106.2	110.7	113.	115.2	115.	115.5	115.1	114.7	112.8	111.2	110.3
162				x		x	x	x	100.0	102.6	108.3	114.1	117.1	118.8	11	8 118.5	117.8	117.1	116.0	113.1	111.9
163					x	x	x	x	100.0	104.5	114.3	124.2	129.3	131.4	130.1	127.4	124.0	121.3	118.3	116.3	114.7

FIGURE 2.1-1

CONTROL ROD LOCATIONS FOR ERROR ROD IN ROD WITHDRAWAL ERROR ANALYSIS

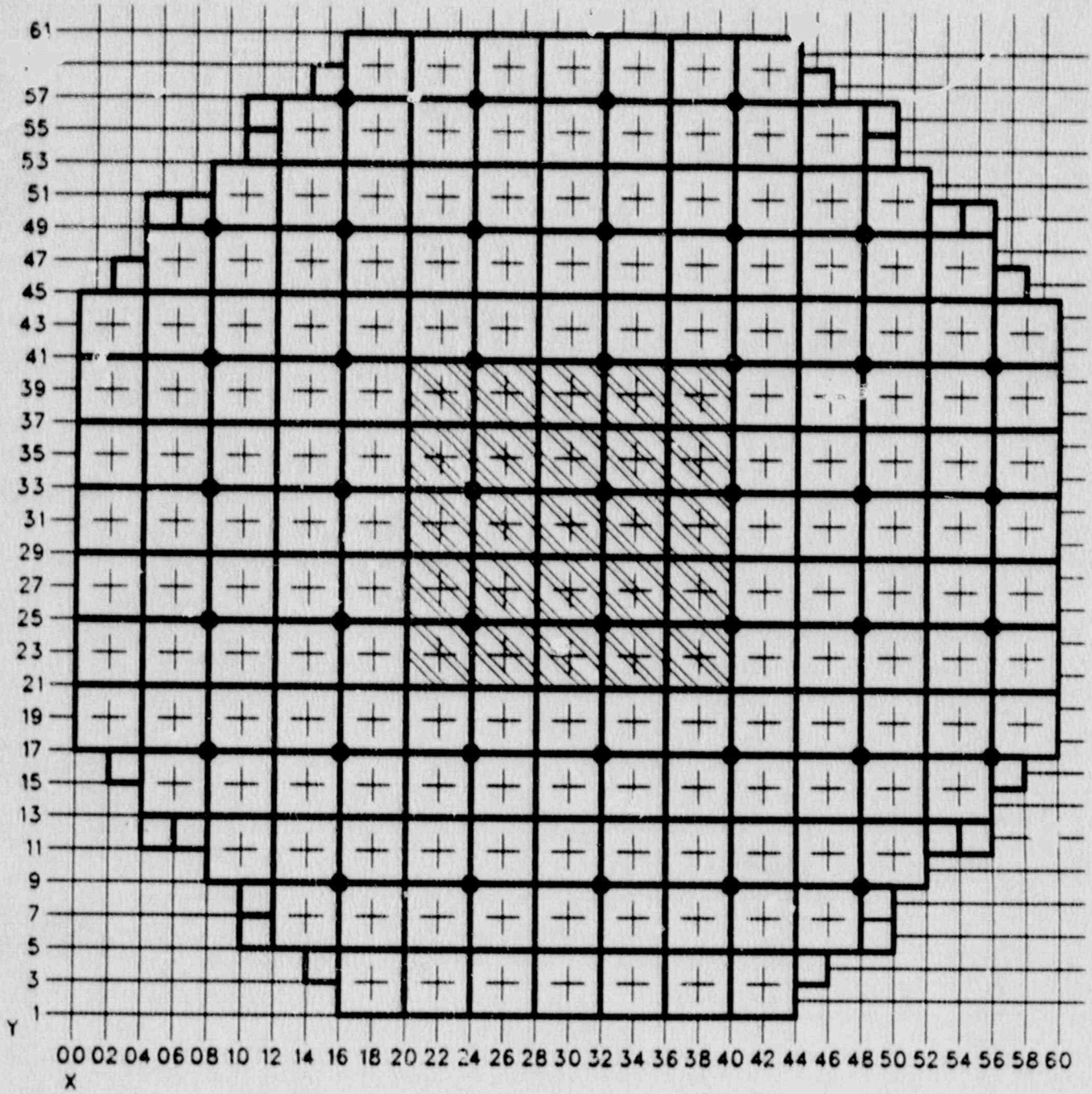

FIGURE 2.1-2
MINIMUM CHANNEL 'A' RBM RESPONSE AS A FUNCTION OF ROD WITHDRAWAL FOR 0, 1, 2, 3, AND 4 LPRM FAILURES

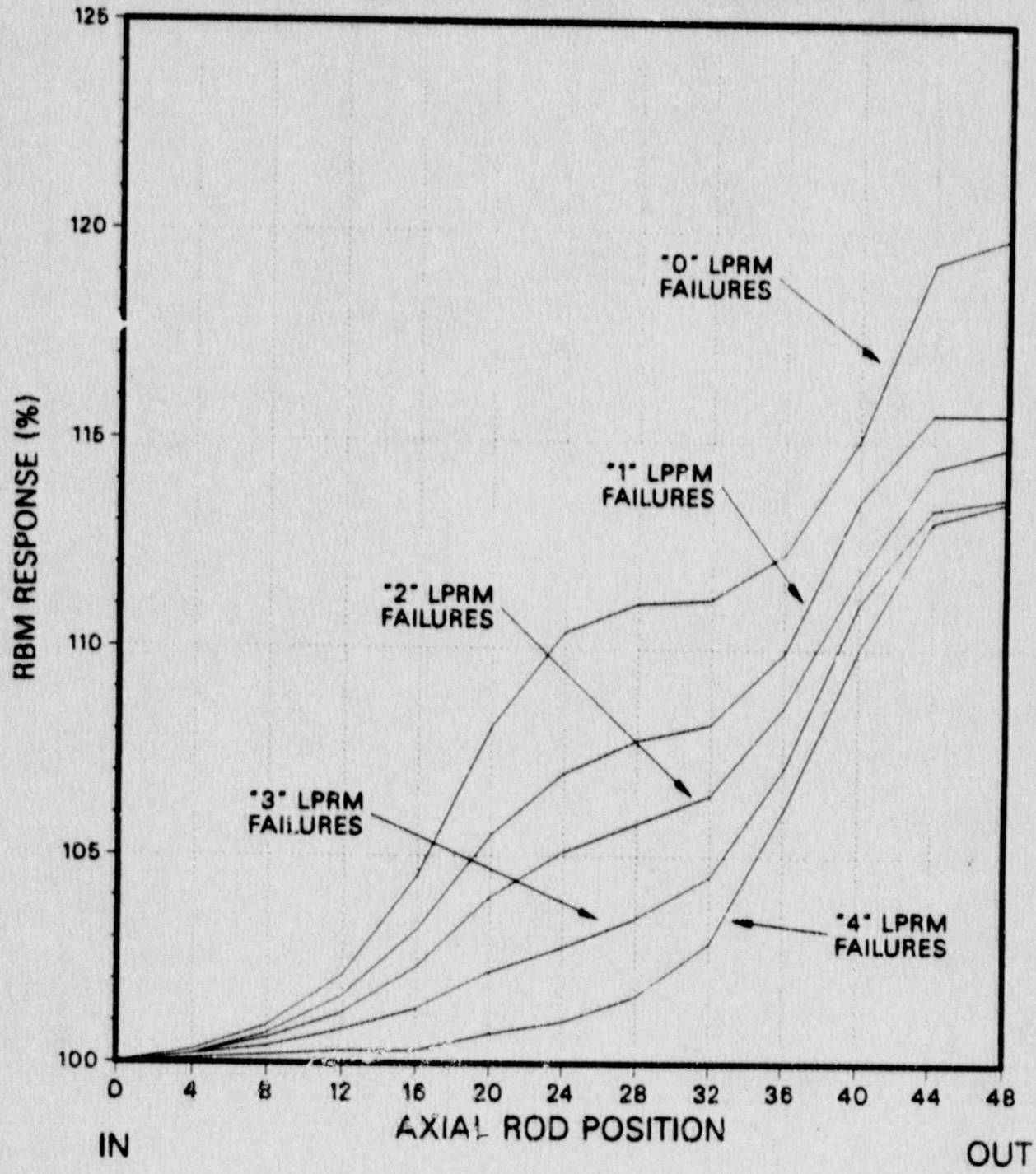

FIGURE 2.1-3
CHANNEL 'A' RBM RESPONSE AS A FUNCTION OF ROD WITHDRAWAL FOR FOUR DIFFERENT FAILURE COMBINATIONS WITH FOUR LPRM FAILURES

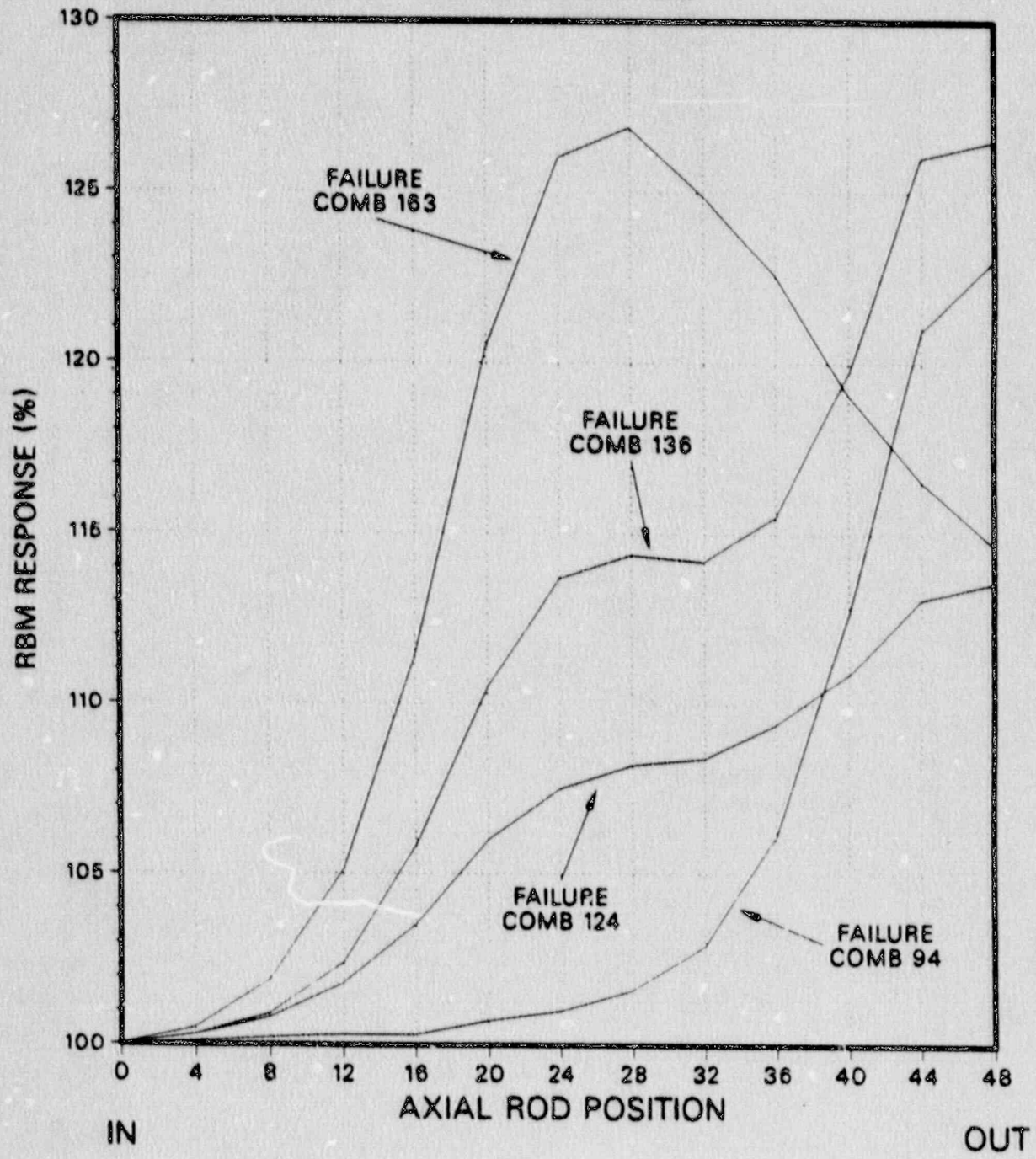

FIGURE 2.1-4
RCPR RESPONSE AS A FUNCTION OF ROD WITHDRAWAL FOR A ROD WITHDRAWAL EVENT

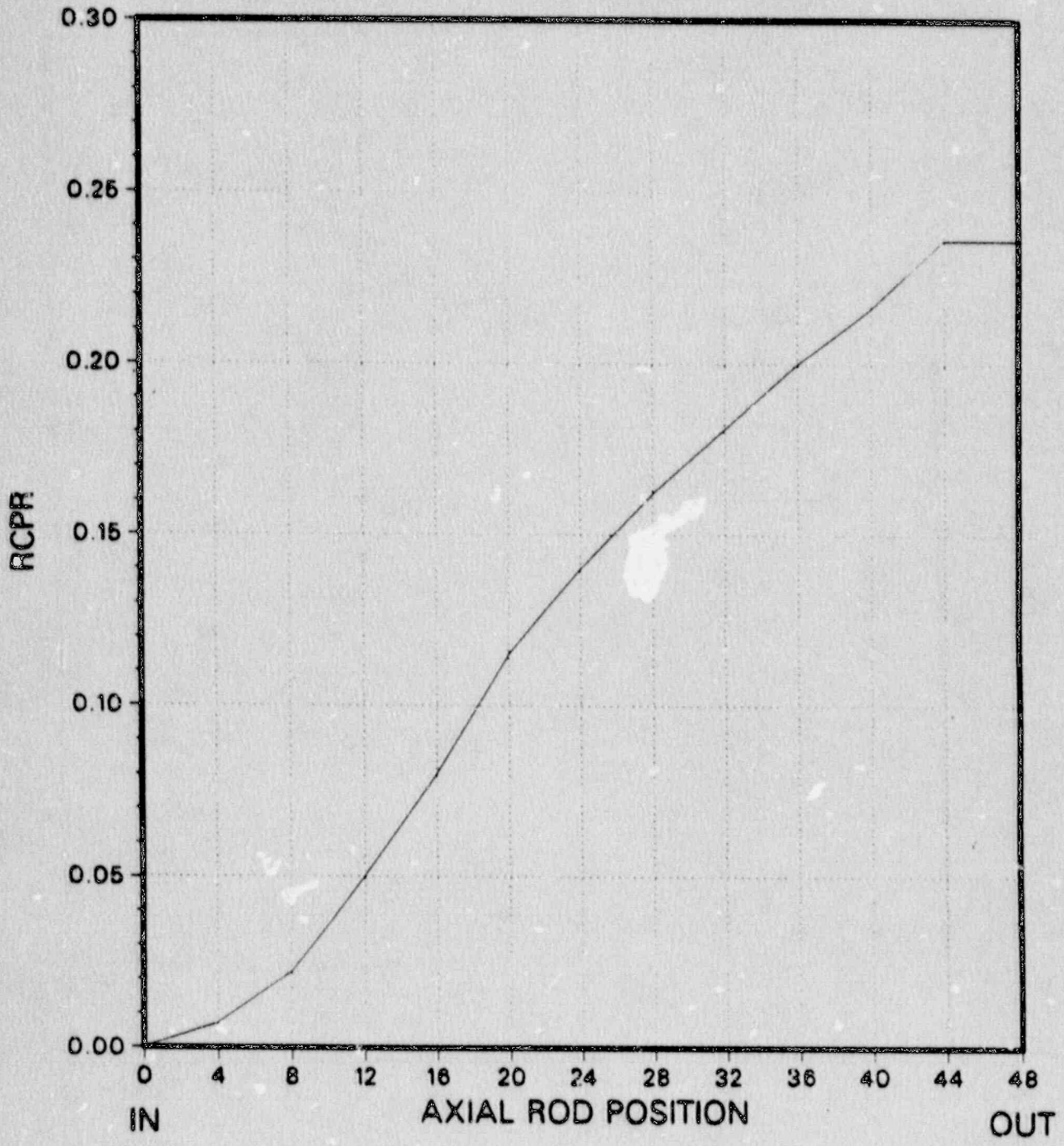

FIGURE 2.1-5
LHGR RESPONSE AS A FUNCTION OF ROD WITHDRAWAL FOR A ROD WITHDRAWAL EVENT

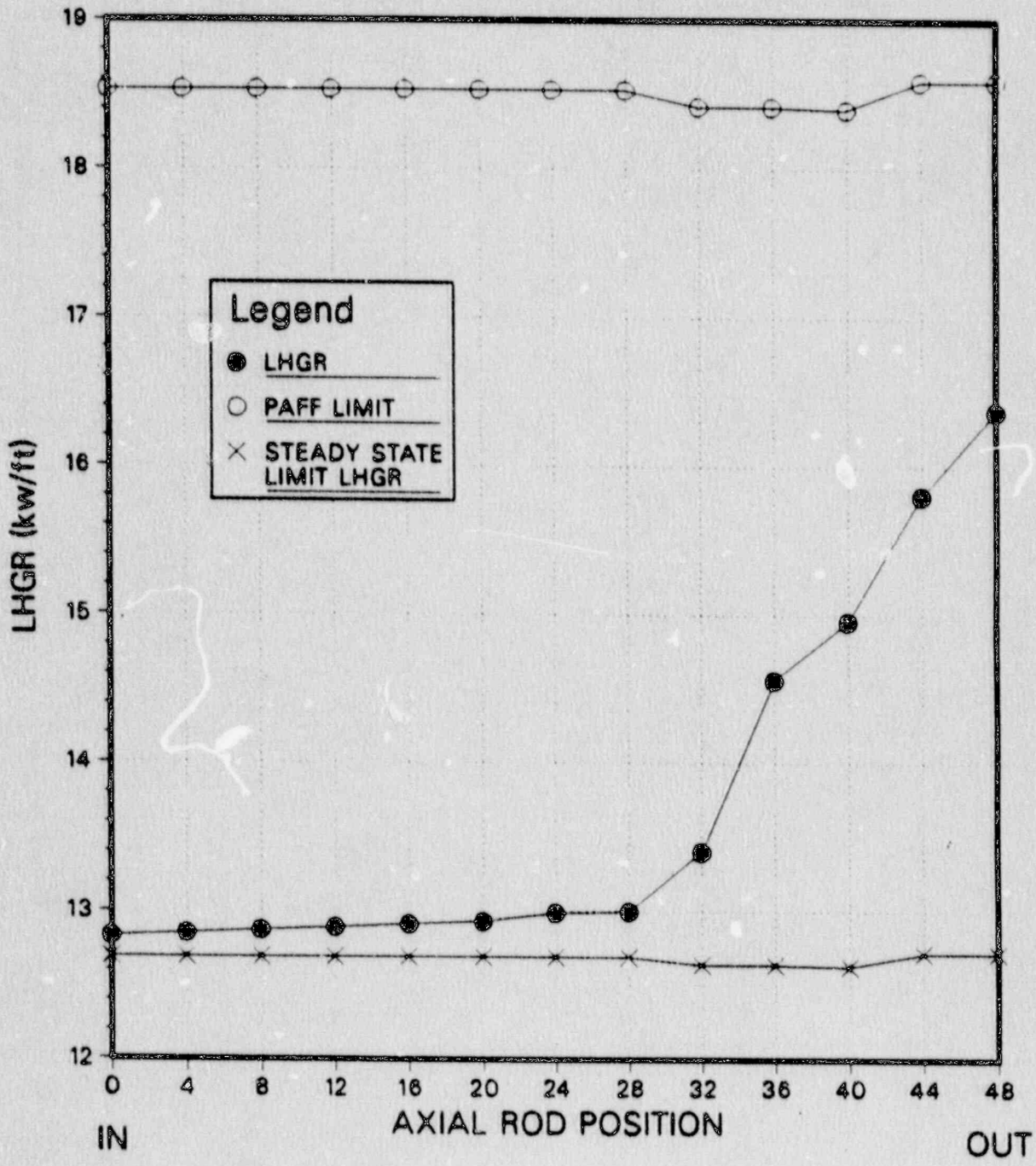

FIGURE 2.1-6
CORE THERMAL POWER RESPONSE AS A FUNCTION OF ROD WITHDRAWAL FOR A ROD WITHDRAWAL EVENT

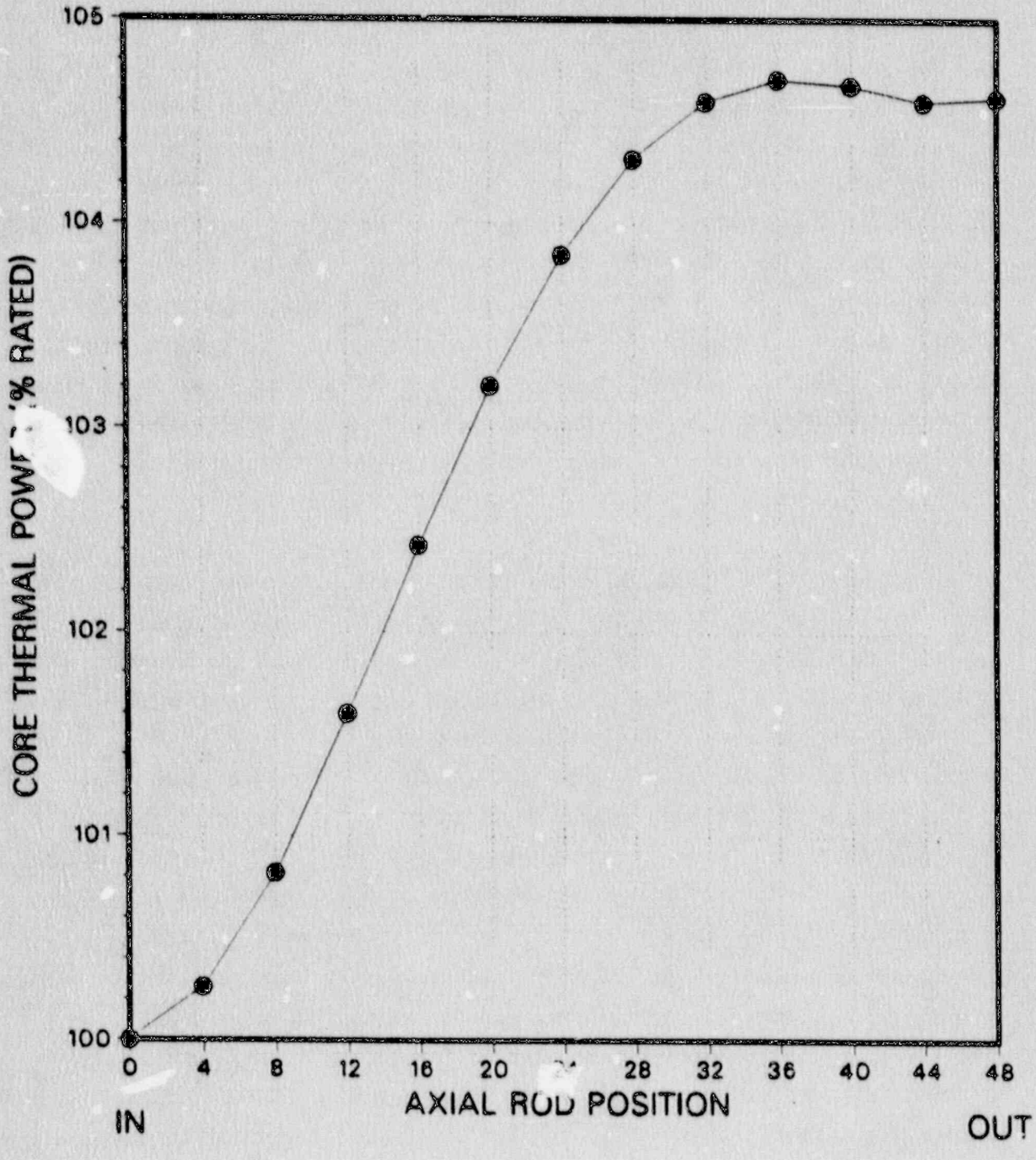

2.2 Fuel Loading Error

2.2.1 Event Description

A fuel loading error can occur during core loading prior to startup of a reload cycle. Two types of loading errors can occur. In the first type, or mislocated bundle error, a fuel assembly is incorrectly loaded into a location in the reactor core causing a discrepancy between the intended reload pattern and the actual core configuration. In the second type, or rotated bundle error, a fuel assembly is loaded into the correct fuel cell but is rotated by 90° or 180° from its correct orientation. For the analysis, it is assumed that the misloading error goes undetected during the final core configuration verification procedure. Core monitoring, however, is based on the intended reload pattern and may thus overestimate the thermal margin. Reactor operation is assumed such that either the misloaded or adjacent fuel assembly is placed on the Technical Specification thermal limits.

The consequences of a fuel mislocation error are highly dependent on the exposure and enrichment of the misloaded and immediately adjacent fuel assemblies. For Susquehanna SES, the most limiting case occurs when a high reactivity fuel assembly is misloaded into a location intended for a low reactivity assembly. At the beginning of cycle, the highest reactivity fuel is usually a once-burned gadolinia bearing assembly which is as close as possible to peak reactivity (i.e., the exposure at which the gadolinium has been reduced to residual levels.) The location for the misloaded assembly will be a location which was intended for a highly exposed twice-burned or thrice-burned assembly or a heavily gadolinia loaded fresh assembly. At the middle of cycle, the high reactivity assembly is usually a fresh assembly which has depleted to peak reactivity. The location of the assumed misloading is the location planned for a depleted assembly which is adjacent to as many high reactivity assemblies as possible. The placement of the additional

(misloaded) high reactivity assembly in a location adjacent to other high reactivity assemblies exacerbates the power peaking in that core location resulting in lower thermal margins. End of cycle is usually not limiting since, by this time, the fresh assemblies are past peak reactivity and the exposed fuel is relatively low in power.

For the rotated bundle event, the fuel assembly is loaded into the correct location but is rotated by 90° or 180° with respect to the intended orientation. As a result, the channel fasteners and spacer pads force the top of the assembly to tilt toward the center of the control cell, changing the size of the water gaps outside of the channel. The water gaps at the lower part of the assembly will not change. Because the Susquehanna units are C-lattice plants (i.e., equal water gaps on all sides of the fuel channel), the consequences of this event are relatively small. The pin enrichment distribution within a fuel assembly is symmetric about the diagonal. Further, enrichments for pins which were intended to be adjacent to the control rod are typically low to help reduce the pin power peaking during control rod motion. Following the assembly rotation, these pins will be adjacent to the larger water gap which causes a corresponding change in the pin power distribution. This change will affect the actual CPR. Since the rotation was assumed to be undetected during core verification, the core monitoring system will monitor the core as if the core had been loaded correctly and, consequently, the calculated thermal margin will not reflect the effect of the rotation.

The intent of the fuel loading error analyses is to demonstrate that the CPR and LHGR safety limits are not violated during normal operation. For both the mislocated and rotated bundle analyses, the critical parameter is the change in the CPR. For Susquehanna, the CPR is determined via the XN-3 correlation developed by ANF (Reference 12). A measure of the event

severity is determined by calculating the maximum RCPR which could be expected from all credible operating scenarios. The RCPR is defined as:

$$RCPR = \frac{MCPR_{CLC} - MCPR_{MLC}}{MCPR_{CLC}}$$

where: $MCPR_{CLC}$ = the minimum CPR for the correctly loaded core, and

$MCPR_{MLC}$ = the minimum CPR for the misloaded core (i.e., either mislocated or rotated bundle)

For the mislocated bundle analysis on a given reload, the worst credible mislocation is identified and analyzed. All applicable code uncertainties are factored into the analysis to assure a conservative estimate of the RCPR. For the rotated bundle analysis on a given reload, maximum changes in local peaking and S-factors are determined. These changes are compared to the changes assumed for a bounding rotated bundle calculation to assure that the bounding analysis is still valid.

2.2.2 Sensitivity Studies

2.2.2.1 Mislocated Bundle Analyses

The mislocated bundle analysis is performed using the SIMULATE-E computer program (Reference 5). The same models which have been benchmarked against data and approved by the NRC (Reference 1) are used for the evaluation. To assure that the worst credible mislocations could be identified, the effects of several key parameters were investigated to

determine their impact on the analysis. From these studies, an analysis approach was developed to assure a conservative estimate of the RCPR from the event. The items investigated included:

1) Assembly type/Core location
2) Core/cycle exposure
3) Control rod pattern
4) Core monitoring system

The most important input assumption affecting the RCPR for the mislocated bundle analysis is the selection of the assembly and the location of the misloaded assembly. As mentioned earlier, the event RCPR will be maximized by replacing a low reactivity assembly with a high reactivity assembly. At beginning of cycle, this is done by misloading a once-burned assembly which is close to peak reactivity into a location intended for a heavily gadolinia loaded fresh or a highly exposed fuel assembly. By middle of cycle, the gadolinium in the fresh fuel assemblies in the highest power location will have depleted to residual levels and the assembly will therefore be at peak reactivity. Thus at middle of cycle, the worst case mislocation error results from replacing a highly exposed fuel assembly with a fresh assembly. In all cases, the mislocation must be at least one control cell away from the core periphery. Otherwise, the neutron leakage prevents the assembly power from becoming excessive.

For most reload analyses, the most severe mislocation occurs at the middle of cycle. For beginning of cycle cases, the once burned assemblies have exceeded their peak reactivity exposures. The fresh assemblies are heavily loaded with gadolinia to reduce the overall core reactivity. This reduces the consequences of the mislocation. If the reactivities of the once-burned assemblies are at or before peak reactivity, then beginning of cycle cases can be limiting and will be evaluated. At middle of cycle,

the worst mislocation occurs when a fresh assembly was misloaded in place of an exposed assembly which was to be surrounded by other fresh assemblies. The mislocation then places several fresh assemblies face adjacent to one another. The higher power in this region will accelerate the gadolinium depletion rate resulting in higher assembly reactivities earlier in cycle. This effect, combined with the higher core average reactivity, increases the power peaking which reduces the CPR. The lower CPR for the misloaded core will increase the RCPR.

The end of the previous cycle exposure also affects the results from the mislocated assembly analysis. Higher cycle exposures from the previous cycle will reduce the assembly reactivities of the exposed fuel. The reduced reactivity in the exposed fuel shifts more power generation to the fresh assemblies. When a fresh assembly is misloaded adjacent to other fresh assemblies, the power peaking is even higher. This results in reduced CPR and, hence, increased RCPR values.

The presence of control rods can also has a significant effect on the severity of the mislocation analysis. If a control rod is inserted in the control cell or adjacent control cell to the misloaded assembly, the RCPR will be dramatically minimized or completely eliminated. For reload licensing applications, no credit is taken for the presence of control rods. Many control rod pattern sensitivity analyses were performed to identify the control rod pattern which would maximize the RCPR for the event. Most of these rod patterns intentionally shifted the power into the region of the mislocation. Based on these calculations, it was determined that an all-rods-out calculation provides a consistently conservative RCPR. As a result, an all-rods-out rod pattern will be used to evaluate the mislocated assemblies analysis for reload licensing applications.

The core monitoring system will also influence the degree to which the effects of the fuel assembly mislocation will be factored into the thermal

limits evaluation. For the Susquehanna SES units, the core monitoring system in use is the ANF POWERPLEX system (Reference 8). In POWERPLEX, a nodal reactor code is used to calculate a three-dimensional power distribution consistent with the current state of the reactor core (i.e., core exposure, power, flow, control rod pattern, etc.). This power distribution is then adjusted based on the core LPRM readings. During this adjustment, which is performed in the UPDATE algorithm of POWERPLEX, no credit is taken for core symmetry and each fuel assembly power distribution is adjusted based on measurements from its closest LPRM strings. Even though the calculated nodal power distribution is based on a correctly loaded core, the LPRM readings will be influenced by the effects of the mislocated assemblies. The UPDATE algorithm will increase the calculated assembly powers in the area of the mislocation. This would result in a lower RCPR relative to the case when the monitoring system is not considered. Typically, the monitoring system is not credited in the event analysis.

2.2.2.2 Rotated Bundle Analyses

The rotation of a fuel assembly in the reactor core causes a significant shift in the pin power distribution. This is caused by the change in the size of the water gap surrounding the fuel channel. The change in power distribution is determined by using the CPM-2 computer code (Reference 4). This computer program has already been reviewed and approved by the NRC for use in licensing applications for Susquehanna SES (Reference 1). As a result of the power distribution change, the assembly secondary local peaking factors (S-factors) will also change. These changes in local peaking factor and S-factors will affect the XN-3 calculation of CPR.

Sensitivity studies were performed with both CPM-2 and SIMULATE-E to determine the effect of water gap size, assembly exposure, assembly axial

power distribution, and fuel assembly design. CPM-2 was used to determine the effect of each parameter on the calculated peaking factors while SIMULATE-E was used to determine the impact on the calculated thermal margins.

Each parameter was varied to determine its impact on the calculated peaking factors. These calculations were then used to determine a set of local peaking factor and S-factor changes which would conservatively bound all anticipated future designs. The magnitude of the conservatism was determined by comparing CPR calculations using these bounding peaking factor changes with calculations using a best estimate change in peaking factors. The bounding peaking factor changes used in the analysis are listed in Table 2.2-1. The use of these peaking factor changes results in a maximum event RCPR of 0.17, as discussed in Section 2.2.4.

The calculation of the bounding peaking factor changes has several significant conservatisms. The most significant conservatism is the assumption that the maximum possible fuel assembly displacement as determined at the top of the fuel is the same throughout the entire axial length. Second, the bounding peaking factor changes were selected to provide significant margin to the expected peaking factor changes for actual assembly designs. Third, the rotation of the fuel assembly results in a decrease in fuel assembly reactivity of up to 0.01 Δk. Although the decrease in reactivity will provide a decrease in the assembly power and a corresponding increase in the assembly CPR, the effect is not credited. Finally, the rod-patterns used to estimate the RCPR were designed to shift the axial power distribution to the top of the core and into the rotated assembly. Since the peaking factor changes are largest at the 70% void levels, this further exacerbates the calculated RCPR.

To determine the magnitude of the conservatism in the bounding analysis, several calculations were performed using best estimate peaking factors. The axial tilt of the assembly was also considered such that no assembly

displacement was assumed at the bottom of the core while maximum assembly displacement was assumed at the top of the core. The rod patterns used for the analysis were typical of operationally acceptable patterns. The assembly chosen for the rotation was the fuel assembly closest to the CPR limit. The maximum RCPR from these cases was 0.07 which illustrates the large amount of conservatism provided by the use of bounding peaking factor changes. As a result, no additional conservatism or uncertainties need to be applied to the analysis.

If the rotated bundle analysis should ever become the limiting event, some relaxation could be made to the bounding peaking factor changes presented in Table 2.2-1. If any relaxation is made, thorough analyses will be performed to ensure that the new set of peaking factor changes continues to provide conservative results for this event.

2.2.3 Licensing Analysis Methods

2.2.3.1 Mislocated Bundle Analysis

The mislocated bundle analysis is typically performed at the middle of cycle for the reload being analyzed. If fuel assemblies from the previous cycle are at or before peak reactivity exposure, then beginning of cycle cases will also be examined. Typically, cycle step-out analyses for the correctly loaded core using anticipated operational control rod patterns will be performed from the upper end of the expected exposure range of the previous cycle. Restart calculations are made from the cycle step-out in which all control rods are withdrawn. These calculations are typically done at cycle exposure intervals of 1.0 GWD/MTU. The exposure points around peak core reactivity are of most interest as they usually provide the limiting values for RCPR. The radial power distribution from the all-rods-out calculation can then be used to select the worst location for

the misloaded assembly which will occur at the location which has the highest assembly power for a non-fresh assembly. If multiple batches are present for the exposed fuel, several locations may require analysis. If several batches are present for fresh fuel, only the most reactive type need be considered (i.e., lowest gadolinia content and/or highest enrichment.)

A cycle step-out depletion calculation is performed for the misloaded core with the same rod patterns which were used for the correctly loaded core analysis. Thermal margin is evaluated for all rods out restart calculations. Comparisons to the thermal margin calculated for the correctly loaded core are needed to generate RCPR values for the specific misload. The largest RCPR from all mislocation evaluations at all exposure points becomes the event RCPR.

Although the analysis uses inputs which generate conservative RCPR's (i.e., assembly location, control rod pattern), the SIMULATE-E calculation provides a best estimate calculation of the MCPR. As a result, it is necessary to add appropriate calculational uncertainty into the result to assure conservatism. For the mislocated bundle event, the RCPR can be conservatively estimated as:

$$RCPR = C\ (RP_2 - RP_1)$$

where: RP_2 = Relative assembly power in MCPR location for the misloaded core,

RP_1 = Relative assembly power in MCPR location for the correctly loaded core,

RCPR = Event RCPR, and

C = Constant from regression analysis, including appropriate uncertainty factor

Note that this correlation is used only for the purpose of developing the RCPR uncertainty. Actual SIMULATE-E calculations using the XN-3 correlation will be used to evaluate the event RCPR. The RCPR standard deviation can then be derived as:

$$\sigma_{RCPR} = C \sqrt{2}\ \sigma_{RP}$$

where: σ_{RP} = nodal code assembly power uncertainty

The assembly power uncertainty can be conservatively estimated by using the integral TIP comparisons which are available from Susquehanna SES operation. The database includes all steady-state TIP sets taken for Units 1 and 2 through April 15, 1990. Each TIP set for Susquehanna SES consists of measurements for each of 43 individual strings. Only TIP strings with known measurement problems or excessively large errors (i.e., errors greater than five standard deviations) were eliminated. This resulted in a total of 6976 integral TIP string comparisons. The assembly power uncertainty (based on assembly relative power) is:

$$\sigma_{RP} = 0.0277$$

This produces an RCPR standard deviation for the mislocated bundle analysis of:

$$\sigma_{RCPR} = 0.0320$$

A tolerance factor on the event RCPR was calculated by statistically combining the RCPR uncertainty calculated above with the actual RCPR

distribution from the mislocated bundle analysis. The RCPR code error is assumed to be normally distributed which, based on data, is conservative since data from the assembly power uncertainty indicates that the distribution is actually more peaked than a normal distribution. The resulting tolerance factor bounding 95% of all RCPR values is:

$$K\sigma_{RCPR\ 95\%} = 0.037$$

2.2.3.2 Rotated Bundle Analysis

The CPM-2 code is used to evaluate the pin power distributions for all fresh assemblies being loaded into the new reload cycles using the maximum possible assembly displacement resulting from a 180° rotation. The changes in the peaking factors (i.e., local peaking factor, interior S-factor, and peripheral S-factor) are calculated by comparing the rotated assembly calculations to the non-rotated assembly calculations at various exposures and void levels. The maximum change in each peaking factor is compared to the bounding value provided in Table 2.2-1. If the changes in peaking factors are less than the values presented in that table, the bounding analysis can be used and the resultant RCPR for the event will be less than 0.17. If the changes in peaking factors are greater than the values given in Table 2.2-1, explicit SIMULATE-E calculations will be performed using the calculated peaking factor changes. Due to the large conservatism in the bounding analysis described in Section 2.2.2, no additional uncertainties are applied.

2.2.4 Sample Licensing Analysis

A sample reload analysis was performed for the Unit 2 Cycle 2 reload core. For the mislocated bundle analysis, the effects of depletion were modelled using a cycle step-out approach. The maximum RCPR including code uncertainty for this event was:

$$RCPR_{MBA} = 0.144$$

Assuming a safety limit of 1.06, the event ΔCPR becomes:

$$\Delta CPR_{MBA} = 0.18$$

For the rotated bundle analysis, the maximum peaking factor changes were computed for the fresh fuel assemblies. The maximum changes in peaking factors are given in Table 2.2-2. Comparing these values to the bounding values in Table 2.2-1 demonstrates that the bounding analysis is valid and the RCPR for this event will be:

$$RCPR_{RBA} < 0.17$$

Assuming a safety limit of 1.06, the event ΔCPR becomes:

$$\Delta CPR_{RBA} < 0.22$$

The large magnitude of this value is caused by the significant conservatism in the bounding analysis as discussed in Section 2.2.2.2.

TABLE 2.2-1

Maximum Changes In Local Peaking Factor and S-Factors For The Rotated Bundle Analysis

Void Level (%)	Local Peaking Factor	Maximum Change Interior S-Factor	Peripheral S-Factor
0	0.20	0.040	0.050
40	0.25	0.050	0.080
70	0.30	0.080	0.100

TABLE 2.2-2

Rotated Bundle Sample Reload Analysis
Maximum Calculated Changes in Local Peaking Factors and S-Factors

Void Level (%)	Local Peaking Factor	Interior S-Factor	Peripheral S-Factor
0	0.164	0.0103	0.0455
40	0.225	0.0295	0.0692
70	0.285	0.0514	0.0959

2.3 Loss of Feedwater Heating

2.3.1 Event Description

The loss of feedwater heating transient at Susquehanna SES can be caused by either of the following system malfunctions:

1) the closure of a steam extraction line to one of the feedwater heaters, or

2) the bypass of one or more of the feedwater heaters.

The result from either malfunction is a decrease in the feedwater enthalpy as it enters the reactor vessel. The reduction in feedwater enthalpy will cause a corresponding decrease in the core inlet enthalpy. As a result, the neutron flux and corresponding core thermal power increase due to the additional moderation at the bottom of the core. This change in thermal power is accompanied by an increase in steam flow. The increase in steam flow results in an increase in the steam line pressure drop and a corresponding increase in the core pressure. If the increase in power level does not cause a scram, the core thermal power and core pressure will reach a new steady state level with a small shift in the axial power distribution toward the bottom of the core.

At Susquehanna SES, there are three feedwater heater trains in each unit. Each train is composed of five separate feedwater heaters. The as-built system was analyzed to identify the worst single failure of equipment or single operator error which would cause the largest possible change in feedwater temperature. The two most severe failures were:

1) failure of the relay coil closing the extraction steam lines to feedwater heaters 3, 4 and 5 on a single train. This would

result in an approximately 50°F decrease in feedwater temperature.

2) drain failures resulting from the loss of control air to four feedwater heaters in all three strings and moisture separators. This would result in an approximately 46°F decrease in the feedwater temperature.

The assumption used for the licensing analysis is a 100°F decrease in the feedwater temperature. This provides additional conservatism in the analysis.

The consequences of a loss of feedwater heating are an increase in the core thermal power and a corresponding decrease in the limiting bundle CPR. The operating limit CPR must be sufficiently high such that the core MCPR after the transient is greater than or equal to the safety limit MCPR.

2.3.2 Sensitivity Studies

The loss of feedwater heating analysis is performed using the SIMULATE-E computer program (Reference 5). The same model development process benchmarked by PP&L and approved by the NRC in Reference 1 is used for the evaluation. To develop a conservative analysis approach, several key parameters were investigated to determine their impact on the results. These included core pressure, control rod patterns, assembly reactivity, and core exposure.

The first effect investigated was the change in CPR due to a change in core pressure. As noted in the previous section, the core pressure will increase as a result of the increase in core power. The amount of the

change will be dependent on the change in steam flow which is in turn dependent on the change in core thermal power. This increase in core pressure has the effect of decreasing the calculated post-transient CPR resulting in a larger ΔCPR. Typical changes in the core pressure are relatively small. A conservative increase of 5 psi will be assumed in the licensing application of this analysis.

The goal of the licensing analysis is to produce a conservatively large ΔCPR starting at any possible initial core state such that the final core state MCPR will be at the safety limit. The resulting operating limit MCPR must be greater than or equal to this ΔCPR plus the safety limit. Because of the small change in CPR associated with this transient, it is difficult if not impossible to define a set of operationally realistic initial conditions which will provide a post-transient MCPR equal to the safety limit

Two mechanisms were used to study the effect on ΔCPR as the final state MCPR approached the safety limit. The first method used control rods to shift the power distribution into a localized area in the core. Although many of these control rod patterns were operationally unacceptable (i.e., violating control rod sequences, excessive power peaking, etc.), the trends observed in these calculations were consistent with the results obtained from more realistic control rod patterns. The second method which was used to reduce the post-transient MCPR was to increase the reactivity of the limiting assembly. Gradual increases in the assembly reactivity were made until the post-transient MCPR was at the safety limit. The results from these cases showed trends consistent with the rod pattern study. Finally, the calculations were reproduced at a variety of cycle exposures. Both proposed control rod patterns as well as Haling calculations were used to provide the cycle depletions.

The results from all of the calculations showed that the post-transient core MCPR was strongly dependent on the pre-transient core MCPR and

insensitive to cycle exposure or control rod pattern. The results from these calculations are shown graphically in Figure 2.3-1. Due to the high degree of correlation between the post-transient core MCPR and the pre-transient core MCPR, a regression analysis was performed using the two variables. The resulting regression line is:

$$MCPR_i = 1.108 * MCPR_f - 0.051 \qquad \text{Eq. 2.3.1}$$

where: $MCPR_i$ = pre-transient core MCPR

$MCPR_f$ = post-transient core MCPR

The largest deviation from the regression line for all cases analyzed was less than 2%. The mean square error from the analysis was 0.000096, indicating a high degree of accuracy in the fit.

Tolerance limits on the regression analysis were generated such that, with 95% confidence, 95% of the residuals will be bounded by these limits. The tolerance limits were evaluated for the regression line and are plotted with the data in Figure 2.3-2. Note that all of the data is bounded by the tolerance limits. Throughout the range of interest, this tolerance interval is bounded by a constant adder of 0.024. For simplicity of application, a constant of 0.024 will be added to the resulting pre-transient core MCPR to adequately cover analysis uncertainty. Thus, Equation 2.3.1 becomes:

$$MCPR_i = 1.108\ MCPR_f - 0.027 \qquad \text{Eq. 2.3-2}$$

The RCPR for the transient is defined as:

$$RCPR = \frac{MCPR_i - MCPR_f}{MCPR_i}$$

Substituting Equation 2.3-2 into this definition gives:

$$RCPR = \frac{0.108\ MCPR_f - 0.027}{1.108\ MCPR_f - 0.027} \qquad \text{Eq. 2.3-3}$$

Although this equation has been adjusted to account for analysis approach uncertainty via the evaluated tolerance limits, the regression analysis is based on calculations from SIMULATE-E. As a result, a SIMULATE-E RCPR code uncertainty for this transient must be applied to the results from Equation 2.3-3. A conservative adder has been developed based on SIMULATE-E's ability to predict a change in core thermal power. This bounding value applicable to the loss of feedwater heating analysis is:

$$K\sigma_{RCPR,bound} = 0.015 \qquad \text{Eq. 2.3-4}$$

The RCPR of interest is the value given a post-transient core MCPR equal to the safety limit. Substituting this into Equation 2.3-3 and adding the bounding RCPR uncertainty, the loss of feedwater heating licensing RCPR can be calculated as:

$$RCPR_{LOFWH} = \frac{0.108\ SLMCPR - 0.027}{1.108\ SLMCPR - 0.027} + 0.015 \qquad \text{Eq. 2.3-5}$$

where: SLMCPR = safety limit for the reload being licensed

2.3.3 Licensing Analysis Method

The analysis described in the previous section is generic to Susquehanna SES, provided significant changes to the operating strategy are not made which would affect the regression line in Equation 2.3-1. To assure continued applicability of the generic analysis, specific SIMULATE-E analyses will be performed for each reload licensing application at BOC, MOC and EOC using the anticipated operational control rod patterns. If new data indicates that the regression coefficients are no longer applicable, a new set will be generated to maintain a conservative evaluation of the loss of feedwater heating event.

2.3.4 Sample Licensing Analysis

To demonstrate the results of a loss of feedwater heating evaluation, a sample reload analysis was performed for Susquehanna SES Unit 1 Cycle 3. Table 2.3-1 shows the BOC, MOC, and EOC, SIMULATE-E calculated initial and final MCPR values and the corresponding initial MCPR values using the regression line. Since the calculated values are within the 95/95 tolerance limits, the generic regression analysis is applicable to Unit 1 Cycle 3. For this unit and cycle, the safety limit MCPR was 1.06. Using this in Equation 2.3-5 provides the maximum RCPR for this transient (including all applicable uncertainties):

$$RCPR_{LOFWH} = 0.091$$

Converting to a ΔCPR yields:

$$\Delta CPR = 0.106$$

TABLE 2.3-1

Loss of Feedwater Heating Sample Analysis
Compliance with Generic Regression Analysis

Cycle Exposure (GWD/MT)	SIMULATE-E Calculation $MCPR_f$ [1]	$MCPR_i$ [1]	Regression Analysis Bounds on $MCPR_i$ [2] Lower	Upper
BOC(0.0)	1.570	1.689	1.665	1.713
MOC(5.0)	1.469	1.585	1.553	1.601
EOC(10.35)	1.439	1.529	1.519	1.567

Notes:

1) $MCPR_i$ = initial (pre-transient) MCPR
$MCPR_f$ = final (post-transient) MCPR

2) Values of $MCPR_i$ based on the calculated SIMULATE-E $MCPR_f$ and the 95/95 tolerance limits to Equation 2.3.1.

FIGURE 2.3-1
LOSS OF FEEDWATER HEATING EVENT
CHANGE IN MINIMUM CRITICAL POWER RATIO

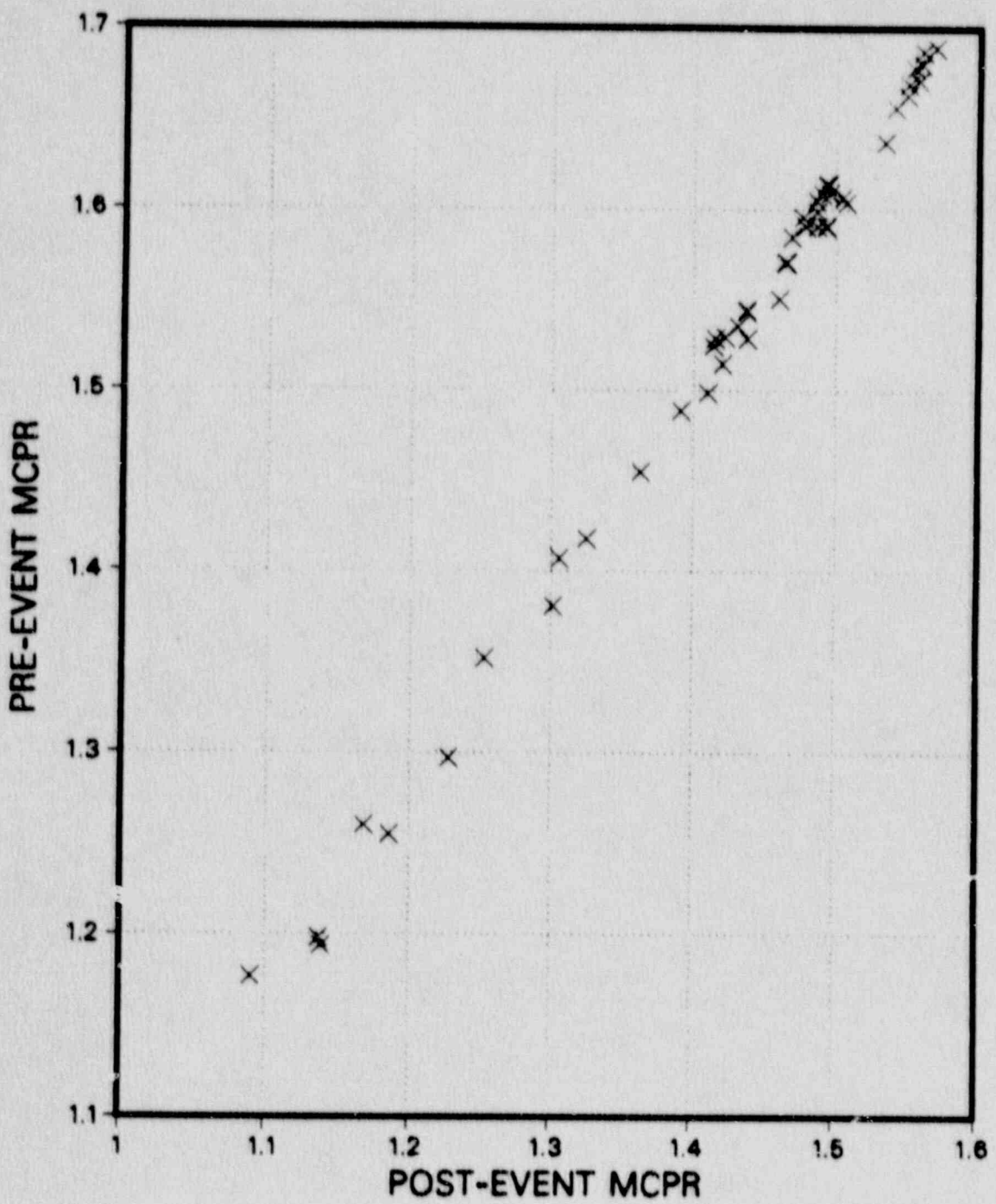

FIGURE 2.3-2
LOSS OF FEEDWATER HEATING EVENT
95/95 TOLERANCE LIMITS ON
REGRESSION ANALYSIS

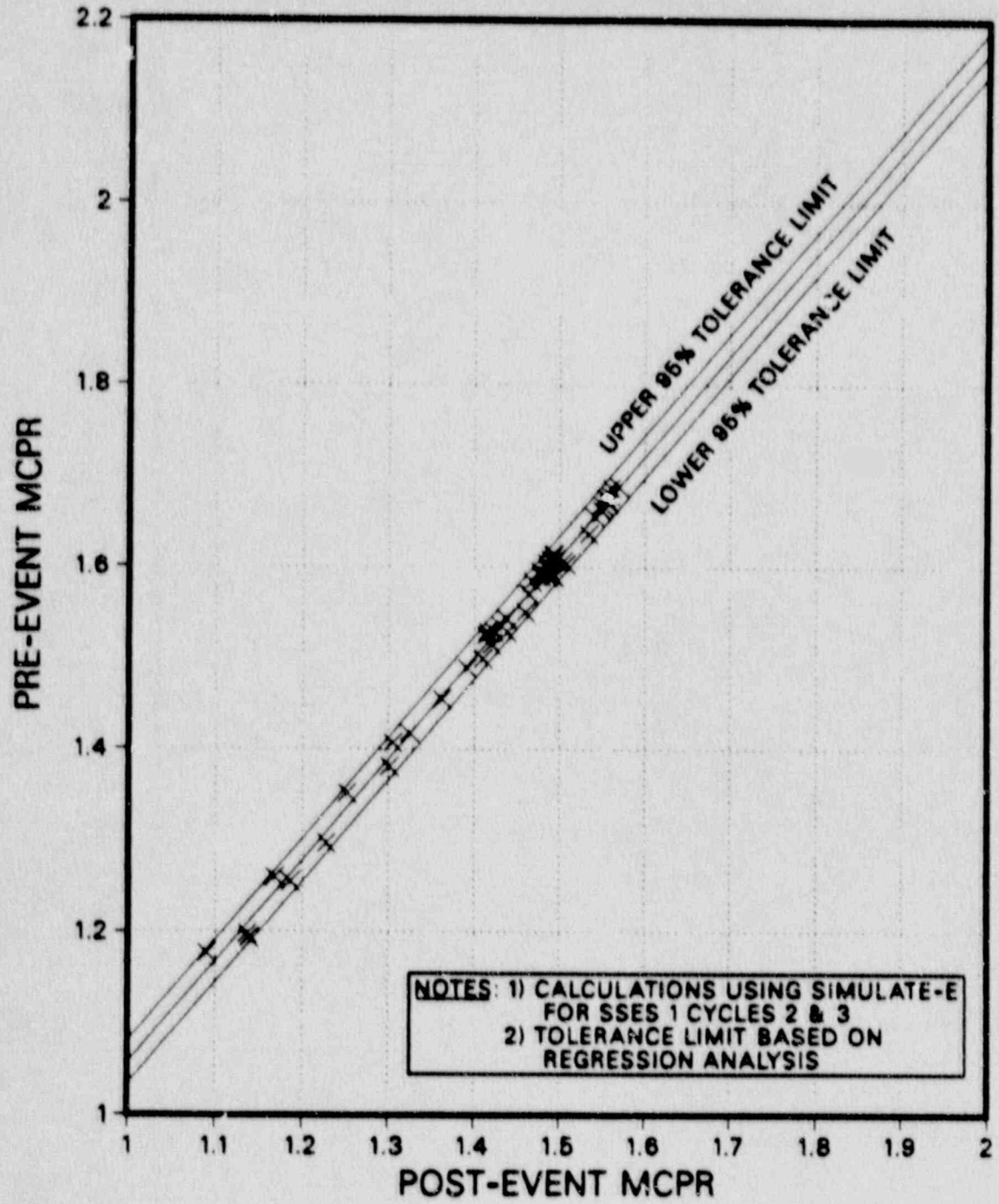

2.4 Shutdown Margin Determination

2.4.1 Event Description

Core Shutdown Margin (SDM) is defined as the amount of negative core reactivity at 68 degrees F and 0% xenon with all the control rods fully inserted except for the strongest reactivity worth control rod, which is fully withdrawn. The SDM analysis is performed using SIMULATE-E and RODDK-E as a part of the reload analyses and to demonstrate compliance with plant Technical Specifications. The SDM evaluation is not considered to be related to an accident or abnormal operating occurrence. The SDM analysis demonstrates that the core will be subcritical in the most reactive (i.e., cold) condition with sufficient margin using only control rods. The Technical Specification required margin assures that under the specified conditions, the core will not be critical considering the uncertainties associated with manufacturing tolerances and calculational method. As a result of these uncertainties, the minimum required demonstrated SDM is 0.38% $\Delta k/k$. For predictive calculations typically performed during the reload design process, an additional uncertainty is added to the 0.38% $\Delta k/k$ value to cover uncertainties in predicting the critical k-effective bias for SIMULATE-E. This prediction uncertainty is evaluated prior to finalizing the reload design and updated if appropriate. This evaluation considers all past critical calculational comparisons and the current fuel and core design. The limiting SDM (i.e., the smallest SDM) for the operating cycle occurs near the peak cold reactivity core condition with the most reactive control rod fully withdrawn. The core and local fuel exposure and void history significantly affect the reactivity worth of the strongest rod and the core SDM. Therefore, the core SDM analysis is performed as a function of cycle exposure and uses conservative values for the previous cycle fuel exposures.

2.4.2 Sensitivity Studies

SIMULATE-E and RODDK-E calculations were performed for Unit 2 Cycle 4 to determine the sensitivity of calculated SDM to changes in input assumptions. The parameters considered were:

1) Previous cycle exposure, and
2) Cycle exposure for the design cycle.

The results of these various sensitivities are graphically represented in Figure 2.4-1. As the figure depicts, a lower previous cycle exposure assumption results in less SDM. This is expected since the core is in a more reactive state due to the irradiated fuel being less exposed and, hence, more reactive.

Cycle exposure for the design cycle also affects the SDM. Figure 2.4-1 shows that SDM varies significantly as a function of cycle exposure. For typical reloads, the limiting SDM occurs either at BOC or near EOC. The limiting SDM occurs near the time when the fresh fuel reaches its peak reactivity (near [illegible]) or when the once-burned fuel is at its peak reactivity (BOC or near BOC).

2.4.3 Licensing Analysis Method

For each reload design, the 0.38% Δk/k SDM Technical Specification Limit and the related predictive uncertainties are verified to be applicable considering the most recent data, and if necessary, the uncertainties are reevaluated. Core SDM is then evaluated using the RODDK-E code and the SIMULATE-E core simulation code. The strongest worth rod location is determined by selecting a number of rod locations ranked by RODDK-E as potential strongest worth rod locations at the specific exposure point of interest. The exposure point of interest will be based on a control rod step-out depletion using the lowest expected energy production of the

previous cycle. The strongest worth rod candidates will be used as input in the SIMULATE-E evaluations to determine the analytically determined strongest worth rod at the exposure points (within at least 1.0 GWD/MTU of each other) throughout the entire design cycle. Core SDM is evaluated using the equation below:

$$SDM(E) = \frac{1 - (K\text{-}eff(E) - Bias(E))}{(K\text{-}eff(E) - Bias(E))} \times 100\%$$

where: SDM(E) = the core SDM at cycle exposure, E;

K-eff(E) = the SIMULATE-E core k-effective with the strongest worth control rod fully withdrawn at 68°F and xenon-free conditions at cycle exposure, E; and

Bias(E) = the SIMULATE-E cold critical k-effective bias at cycle exposure, E. The bias equals the expected SIMULATE-E critical k-effective minus 1.0.

The minimum core SDM of all the SDM(E) values shall be greater than the SDM design limit which includes allowances for manufacturing tolerances and calculational uncertainty. This value is then used to establish the R value which is defined as the difference between the BOC SDM value and the minimum SDM value. The R value and other calculated parameters (e.g., control rod worths) are utilized in the Shutdown Margin Technical Specification test performed at BOC.

2.4.4 Sample Licensing Analysis

This section presents a sample core SDM analysis for Unit 2 Cycle 4. The sample SDM design criterion of 0.8% Δk/k was used which includes the 0.38% Δk/k Technical Specification value and the 0.42% Δk/k prediction uncertainty. From Figure 2.4-1 the minimum core SDM value is 1.28% Δk/k. The BOC SDM value is 1.29% Δk/k and the R value is 0.01% Δk/k. The minimum core SDM value exceeds the 0.8% Δk/k design criterion, and therefore sufficient SDM has been assured for the Unit 2 Cycle 4 core.

FIGURE 2.4-1
EXPOSURE EFFECTS ON CORE SHUTDOWN MARGIN

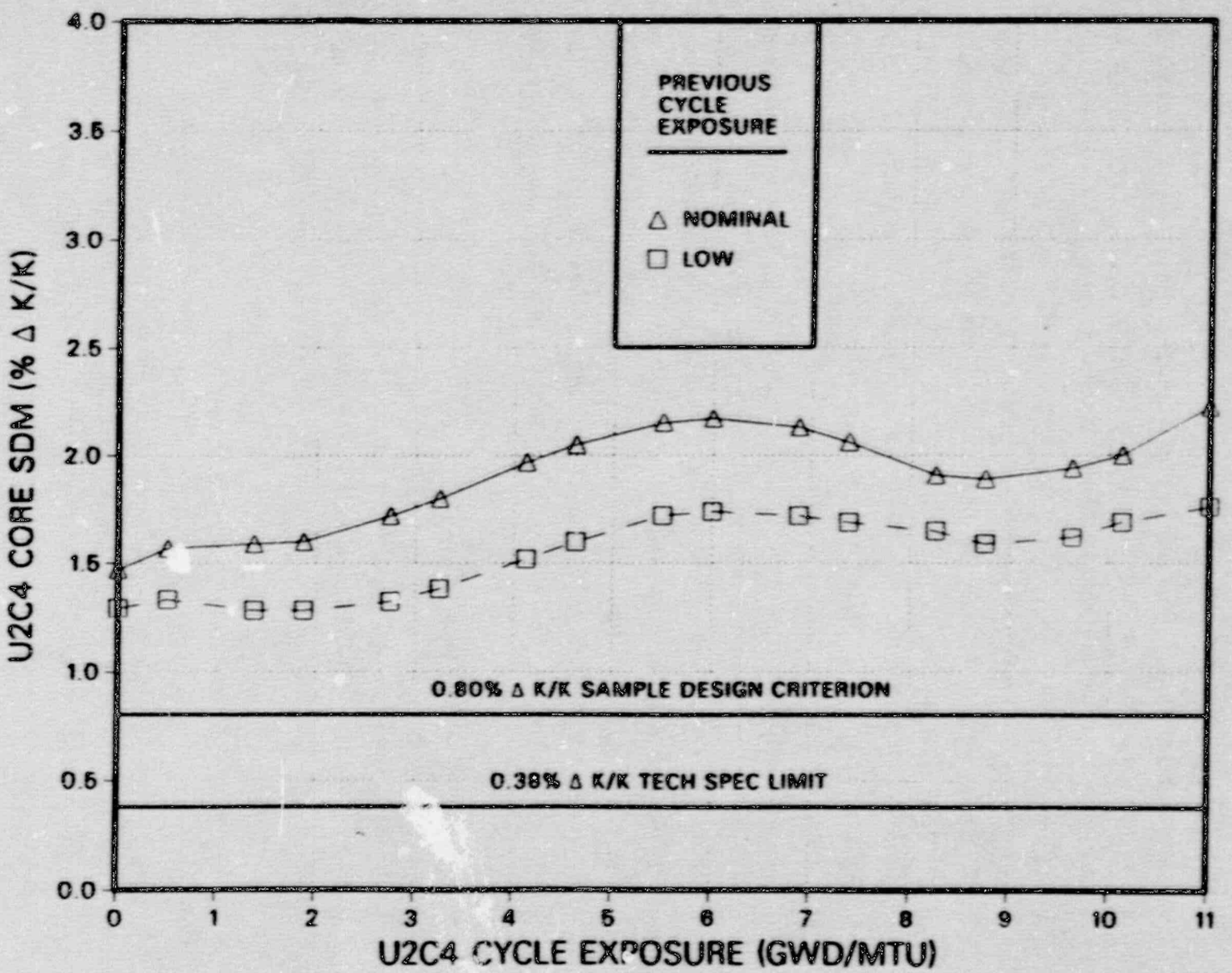

2.5 Standby Liquid Control System Capability

2.5.1 Event Description

The Standby Liquid Control System (SLCS) is designed to provide an alternate method of bringing the reactor from full power operation to a cold (68°F), xenon-free shutdown condition without reliance on control rods. At Susquehanna SES, this emergency shutdown capability is provided by injection of a sodium pentaborate solution through the standby liquid control sparger located in the lower plenum of the reactor core. The minimum boron concentration in the reactor after injection is 825 ppm. However, the analysis of the SLCS is intended to demonstrate that the reactor will be at least .01 ΔK shutdown with only 660 ppm boron present.

The SLCS will only be used in the event that the control rod drive system fails to insert sufficient rod inventory to bring the reactor to a cold xenon-free shutdown. Due to the undesirable consequences of inadvertent system operation, there are no automatic initiations. The SLCS is manually initiated by the operators in accordance with the Susquehanna SES emergency operating procedures. The analysis assumes that the control rods remain at their hot operating positions with no additional insertion.

2.5.2 Sensitivity Studies

The SLCS analysis is most dependent on the concentration of boron assumed in the reactor coolant. Although the system is designed to insert at least 825 ppm boron, only 660 ppm boron will be credited in the analysis. The reduced value is to account for imperfect mixing of the sodium pentaborate solution.

The effect of a given concentration of boron will be dependent on the water to fuel ratio of the fuel assembly. A higher ratio means more boron atoms will be present in the core, thus increasing the boron reactivity

worth per ppm. Fuel design parameters which affect the water to fuel ratio will consequently affect the boron worth. The analysis developed here is for application to the current fuel designs which are in use at Susquehanna SES (ANF 8x8 and ANF 9x9-2). If significant changes are made to the fuel assembly design parameters that would alter the boron worth characteristics, new boron worth parameters will be developed.

Two methods can be used to evaluate the effectiveness of SLCS. The first method applies a conservatively low boron reactivity worth to a non-borated nodal core k-effective calculation. The second method modifies the thermal absorption cross section in the nodal calculation to directly model the boron in the reactor coolant. For both methods, the nodal evaluation is performed with the SIMULATE-E computer code (Reference 5).

To determine a conservative boron worth, numerous lattice physics calculations using the CPM-2 computer program (Reference 4) were made to determine the reactivity worth of 660 ppm boron. The reactivity worth of the boron was evaluated for numerous fuel designs at various lattice exposures as:

$$\Delta\rho'_{boron} = \frac{K_{660ppm} - K_{0ppm}}{K_{660ppm} * K_{0ppm}} / 660 \text{ ppm}$$

where: $K_{660\ ppm}$ = lattice K_∞ with 660 ppm boron at cold xenon-free conditions,

$K_{0\ ppm}$ = lattice K_∞ with 0 ppm boron at cold xenon-free conditions, and

$\Delta\rho'_{boron}$ = boron reactivity worth per ppm boron

A conservatively low boron reactivity worth was developed to bound all anticipated fuel designs and lattice exposures. The value selected based on the CPM-2 evaluations was -20×10^{-5} $\Delta\rho$/ppm. This provides at least 5×10^{-5} $\Delta\rho$/ppm margin to the minimum calculated boron worth. If the fuel design changes such that the bounding reactivity worth is no longer applicable, the value will be updated accordingly.

The CPM-2 computer program was also used to determine the change in the thermal absorption cross section at various lattice exposures for different fuel designs. For a constant boron concentration, the change in the thermal absorption cross section is relatively insensitive to exposure for a given lattice design. Therefore, a beginning of life calculation can be used to determine the necessary adjustment to the cross section. Recalculating the lattice reactivity with the modified thermal absorption cross section shows that this approach conservatively estimates the lattice reactivity until well past the exposure of peak assembly reactivity. At high exposures, these modified cross sections may underestimate the lattice reactivity by as much as 0.006 ΔK. Although fuel assemblies at these exposures are generally on the core periphery and contribute little to the overall core reactivity, the calculated core eigenvalue with 660 ppm boron in the reactor coolant will be conservatively increased by 0.01 ΔK when using this approach.

2.5.3 Licensing Analysis Method

The purpose of the SLCS licensing analysis is to show that for the reload being analyzed, the SLCS will provide adequate shutdown margin assuming cold xenon-free reactor core conditions. The core eigenvalue calculation is performed with the SIMULATE-E computer code. At least 0.01 ΔK shutdown margin will be demonstrated for each reload cycle to assure shutdown capability and to account for code uncertainty. The SLCS analysis can be performed using either of the two methods described in Section 2.5.2. The first uses a conservative boron reactivity worth. If this method fails to

demonstrate the required shutdown margin, the cross section modification process will be used to more accurately account for the effects of the boron worth.

The boron reactivity worth used in the first method was developed to bound all anticipated ANF 8x8 or 9x9-2 fuel assembly designs. If the fuel mechanical design changes in such a fasnion as to alter this value, new conservative boron worths will be developed and applied. The analysis assumes that the control rods remain at their hot operating positions. Cold, xenon free SIMULATE-E calculations are performed at various points in the cycle. The cold k-effective from these calculations are adjusted for bias and boron worth. The amount of shutdown margin is calculated as:

$$SD = K_{eff}^{crit} - K_{eff}^{boron}$$

where: K_{eff}^{crit} = critical eigenvalue after adjustment for bias

K_{eff}^{boron} = eigenvalue after adjustment for bias and boron worth

SD = amount of shutdown in units of ΔK

If the conservative boron worth approach does not demonstrate the required 0.01 ΔK shutdown margin, a more accurate approach is used. In the more accurate method, the effect of the 660 ppm boron concentration is accounted for by a change in the thermal absorption cross section. This change is based on beginning of life lattice calculations for each fuel type in the core. The change in thermal absorption cross section based on

beginning of life calculations is made in the SIMULATE-E calculation. The resulting eigenvalue is adjusted for model bias plus a conservative adder of 0.01 ΔK before, at least 0.01 ΔK shutdown must be demonstrated.

2.5.4 Sample Analysis

A sample SLCS licensing evaluation is provided using both approaches for Unit 1 Cycle 2. Using the conservative boron reactivity worth method, 660 ppm boron provides 0.047 ΔK shutdown margin. Using the cross section modification approach, 660 ppm boron provides 0.070 ΔK shutdown margin. The difference in the results can be attributed to the conservative value of boron reactivity worth used in the first method in which the boron reactivity worth was intentionally reduced to assure a conservative evaluation of the SLCS capability. Therefore, both analysis methods demonstrate greater than 0.01 ΔK shutdown margin.

2.6 RETRAN Transient Analysis Inputs

This section describes the generation of core physics data required for RETRAN transient analyses. The initial conditions for the reactor must be defined to begin a transient analysis. RETRAN transient analyses to develop MCPR operating limits and perform the ASME overpressure analyses are performed for a range of initial conditions. The parameters required to define the initial reactor state are system pressure, core power, core flow, core inlet subcooling, and fuel exposures (i.e., time in cycle). Core physics data is generated once the necessary parameters are defined. The process to develop one-dimensional kinetics input to RETRAN is described in detail in Appendix A of Reference 2. The process consists of three major steps.

First, using SIMULATE-E (Reference 5), an initial core state is calculated in three dimensions. This case is referred to as the base case. If modelling a scram is required during the transient, additional SIMULATE-E cases are run with intermediate and all-rods-in control states. The information from these cases must be collapsed to one dimension to be used by RETRAN. This collapsing is performed by SIMTRAN-E (Reference 11).

Second, SIMTRAN-E performs perturbations on the three-dimensional moderator density and fuel temperature arrays from SIMULATE-E to determine the dependence of the cross sections on these parameters. The perturbed three-dimensional data is then collapsed to one dimension in the axial direction. All of the collapsed cross sections and their associated one dimensional density and temperature distributions are used to produce polynomials that represent the cross sections as functions of the change in density and fuel temperature from the initial values. These polynomials are used as input to RETRAN.

The dependence of cross section change on moderator density change is extremely important for transients with large void changes (i.e., severe pressurization transients). Since RETRAN models the core as a single channel and SIMULATE-E models the core as individual bundles, the SIMTRAN-E generated cross sections must be modified to account for this difference. The axial moderator density change in a three dimensional array of fuel bundles and in an average one dimensional model of a fuel bundle may be quite different for a given pressure change. Thus, the cross section polynomials are recorrelated to minimize this effect of collapsing from three to one dimensions. This recorrelation assures that the change in cross sections predicted by RETRAN for a given instantaneous pressure change is the same as that predicted by SIMULATE-E. This modification procedure is described further in Reference 2. Use of this cross section modification procedure is not required for transients in which a small change in the void fraction occurs.

2.7 Loss of Coolant Accident Inputs

The Loss of Coolant Accident (LOCA) analyses that support the Susquehanna SES units were performed by Advanced Nuclear Fuels Corporation and are contained in References 30 and 31. PP&L's design and analysis methods (References 1 and 2) will be used to provide fuel and core design information for input to the cycle specific heatup calculations performed by ANF and to confirm that the core neutronics parameters are bounded by the assumptions used in the Susquehanna SES blowdown and reflood calculations. The LOCA inputs calculated by PP&L are (1) local power distributions for each lattice type, (2) fuel rod power history, (3) core scram reactivity versus time, (4) moderator density reactivity (i.e., reactivity as a function of moderator density), and (5) Doppler reactivity (i.e., reactivity as a function of fuel temperature).

The local power distributions are calculated as a function of void history and exposure using the CPM-2 computer code for each reload fuel assembly. These are provided to ANF for use in the heatup calculation. ANF selects the limiting local power distribution to analyze using their NRC approved LOCA methods. The peak cladding temperature is calculated and verified to be less than 2200°F.

The fuel rod gap conductance and, hence, initial stored energy are dependent on the fuel rod power history. Rod power histories are generated by combining the CPM-2 local power distribution with the SIMULATE-E cycle depletion calculations. ANF reviews this data to assure that the initial fuel rod stored energy for the reload fuel is within the bounds of that assumed in the LOCA analysis.

ANF used a conservative scram reactivity insertion rate, moderator density reactivity, and Doppler reactivity in the LOCA blowdown calculations of

References 30 and 31 to help ensure that cycle specific variations of these parameters would not require a new LOCA blowdown calculation. PP&L methods will be used to determine cycle specific scram, Doppler, and moderator density reactivities to demonstrate that the ANF blowdown calculations are conservative. All rods out (end of cycle) conditions will be evaluated because the scram reactivity insertion rate is worse when control rods are initially at their full out position. At other points in the cycle, the more adverse moderator density reactivity coefficient and Doppler reactivity coefficient are less significant than the higher scram reactivity insertion rate. Therefore, PP&L will calculate scram, moderator density, and Doppler reactivities for end of cycle conditions and compare them to the reactivities assumed in the ANF LOCA calculations.

RETRAN will be used to calculate the scram reactivity as a function of rod position. First, SIMULATE-E and SIMTRAN-E cases are run for end of cycle conditions. Then, the RETRAN base model inputs are modified so that moderator density and fuel temperature feedback is eliminated from the neutronics calculation. With this revised model, the RETRAN one-dimensional kinetics calculation is performed to simulate a reactor scram. Total calculated reactivity from RETRAN is converted to units of dollars using the core average delayed neutron fraction (from the SIMTRAN-E calculation) and compared to the values used in the ANF LOCA analysis.

The reactivity as a function of moderator density is obtained from SIMULATE-E calculations. The SIMULATE-E base case used for the scram curve calculation is also used as the base case for the moderator density reactivity calculations. Additional SIMULATE-E cases with no temperature feedback are run using various pressures, holding inlet enthalpy constant. The resulting SIMULATE-E calculated core average moderator densities and core k-effectives are used to calculate a reactivity table. Normalized

densities are calculated relative to the base case and the corresponding reactivity is calculated using the following equation:

$$\rho_i = \left[1.0 - \frac{1.0}{1.0-(\lambda_b-\lambda_i)}\right]\frac{1}{\beta}$$

where: ρ_i = reactivity in dollars,
λ_b = core k-effective from the base case,
λ_i = core k-effective from perturbed pressure case i,
β = core average delayed neutron fraction from SIMTRAN-E.

During the initial few seconds of the LOCA, the cycle specific moderator density reactivities must be demonstrated to be more negative than the values used by ANF in order to validate the conservatism of the LOCA analyses. After the first few seconds, the negative scram reactivity shuts down the reactor.

The fuel temperature (Doppler) reactivities are calculated by SIMULATE-E. The SIMULATE-E base case used for the scram calculation is also used as the base case for the Doppler reactivity calculations. Additional SIMULATE-E cases with no moderator density feedback are run using various core average fuel temperatures. The reactivities for each perturbed case are calculated using the same equation shown above for the moderator density reactivity table, except with λ_i defined as the core k-effective from the temperature perturbed case i. During the initial few seconds of the LOCA, the cycle specific fuel temperature reactivities must be less than the reactivities used by ANF in order to validate the conservatism of the LOCA blowdown calculations.

In summary, the data described above is generated using PP&L's analysis methods and used by PP&L and ANF to assure the validity of the reported LOCA results and the Technical Specification MAPLHGR limits.

2.8 Control Rod Drop Accident Inputs

The generic parametric based methodology used by Advanced Nuclear Fuels Corporation (Reference 28) to calculate the peak deposited fuel rod enthalpy will be used by PP&L in order to calculate the consequences of the Control Rod Drop Accident (CRDA). The CRDA has been shown to be the bounding reactivity insertion event (Reference 14).

The CRDA is the postulated dropping of a fully inserted and decoupled control rod of maximum worth. The control rod is assumed to fall at its maximum velocity and the worth of the control rod is assumed to have the maximum incremental worth consistent with the withdrawal constraints of the Banked Position Withdrawal Sequence (Reference 33). The initial plant response of a CRDA is a prompt power burst which is initially terminated by Doppler feedback from the fuel temperature increase. Void reactivity also assists in terminating the power burst, but this effect is not considered in the analysis. The prompt power burst can lead to significant fuel cladding failures and an increase in reactor pressure. The final shutdown via control rod insertion is achieved by the high neutron flux scram.

The specific criteria used to assess the cycle specific CRDA are to verify the following:

1. The radially averaged fuel rod enthalpy is less than 280 cal/gm at any axial location in any fuel rod.

2. The maximum reactor pressure shall be less than the pressure that will cause stresses to exceed the ASME "Service Limit C" stresses. Past evaluations (References 14 and 28) have shown that the CRDA is not a concern for reaching the ASME "Service

Limit C" values, and that the transient evaluations for the ASME overpressurization event bound those of a CRDA.

3. The radiological consequences based on the assumed failures of all rods that exceed 170 cal/gm shall be less than the General Electric evaluation for the initial core (i.e., the radiological consequences of 770 GE 8x8 fuel rods failing) (Reference 14). Otherwise, new radiological releases will be determined and results submitted with the reload application.

The important parameters used in the analysis are the worth of the dropped control rod, local power peaking factors, delayed neutron fraction, Doppler reactivity, and the scram reactivity. These values are used in ANF's generic parametric analysis where the radially averaged fuel rod enthalpy deposition is determined as a function of control rod worth, four bundle peaking factor, delayed neutron fraction, and Doppler coefficient of reactivity. The ANF generic parametric analysis used both a conservative scram curve and a conservative positive reactivity insertion rate for the dropped rod.

To assure consistency with the ANF CRDA methods as well as consistency with Technical Specification requirements, the following assumptions are used for the initial core conditions:

1) Hot zero power

2) Zero void fraction

3) Zero xenon concentration

4) Equal moderator and fuel temperature

5) Inoperable Rod Worth Minimizer

6) Operable Rod Sequence Control System

7) Eight inoperable rods may exist and are fully inserted.

8) Inoperable rods are separated by at least two control rods in all directions.

9) One or two inoperable control rods may only exist in a Rod Sequence Control System rod group.

The maximum control rod worth and the four bundle peaking factor at the limiting time in the cycle will be determined by CPM-2 and SIMULATE-E calculations. The Doppler coefficient of reactivity and the delayed neutron fraction are core wide best estimate values which are evaluated at the limiting times in the cycle.

Results for a sample Unit 2 Cycle 2 CRDA analysis are shown below which will be applied to the ANF generic parametric analysis:

1) Maximum rod worth (mk) = 12.2

2) Doppler coefficient ($\Delta k/k/deg\ F$) = -11.0×10^{-6}

3) Delayed neutron fraction (β) = 0.00571

4) Four bundle local peaking factor (P4BL) = 1.47

Based on items 1) through 4) above and the generic parametric analysis (Reference 28), the peak radial average fuel rod enthalpy is 209 cal/gm. This enthalpy is less than the 280 cal/gm limit. In addition, less than 395 fuel rods exceed the 170 cal/gm limit, and the radiological

consequences are less than the initial core evaluation. Therefore, the consequences of the Unit 2 Cycle 2 CRDA fall within the acceptance criteria.

2.9 MCPR Safety Limit Inputs

The methodology used by ANF to perform MCPR safety limit calculations is described in References 17 and 18. As part of PP&L's reload licensing effort, data generated with PP&L's codes and methods will be used by the fuel vendor to perform MCPR safety limit analyses. The data will be used in both the conventional safety limit analysis and the "safety limit type" analyses performed as part of the Statistical Combination of Uncertainty (SCU) methods described in Appendix B.

The codes and analysis techniques utilized by the fuel vendor are not changed from those described in References 17 and 18. The only difference is that some of the inputs are supplied based on PP&L's methodology. The data calculated to support the analyses using the fuel vendor's methodology consists of two major parts. The first part contains data generated by PP&L's NRC approved core physics methods (Reference 1). The second part consists of the system and fuel related uncertainties (See Table 2.9-1).

2.9.1 Core Physics Inputs

PP&L's NRC approved core physics methods (Reference 1) will be used to generate three sets of data as input to the safety limit analyses: rod relative power distributions, secondary local peaking factors, and core wide radial peaking factor histograms.

For the purposes of a safety limit calculation, a "flat" local power distribution in a fuel assembly is conservative. This fact is evident since, when an assembly is operated at the Safety Limit MCPR, a flat distribution contains more pins at higher powers. Thus, a flat

distribution has more pins close to transition boiling than a strongly peaked distribution.

The local power distributions which will be used in the analyses using the fuel vendor's methodology to perform the safety limit analyses are generated using PP&L's NRC approved steady state core physics methods (Reference 1). This data is generated by the CPM-2 code for a range of void levels and lattice exposures which span the range of expected values for the specific reload cycle. From this data, the most conservative local power distribution(s) will be selected (i.e., lowest maximum local peaking factor for the exposure range expected during the cycle). For peripheral assemblies, a maximum local peaking factor equal to 1.0 is assumed (i.e., all fuel pins at the same power). The use of these local peaking factor distributions is consistent with current ANF methodology; only the lattice physics code used to generate the local power distributions is different.

In addition to the local power distributions, the fuel vendor's methodology also requires the limiting peripheral and interior secondary local peaking factors (S-factors) for each of the lattice types in the reload core. As with the local power distributions, the S-factors are generated for a range of void levels as a function of lattice exposure. This data is generated using the CPM-2 lattice physics code.

The third important core physics input to the safety limit calculation is a histogram of the number of fuel bundles having a given radial peaking factor versus radial peaking factor. PP&L will perform a cycle step-out analysis with the nodal physics code SIMULATE-E and generate bundle power histograms at each exposure point. The criteria used by ANF to select the "bounding" histogram(s) are:

1) Histogram from the exposure point which has the largest bundle radial peaking factor.

2) Histogram having the largest number of bundles with powers close to the maximum bundle power.

To comply with the fuel vendor's methodology in selecting the bounding histogram, PP&L will generate the information necessary to produce these histograms at each exposure point.

2.9.2 Uncertainties

Both the conventional safety limit and the "safety limit type" analyses utilize a Monte Carlo procedure to combine various uncertainties in order to demonstrate that 99.9% of the fuel rods in the core are not expected to experience boiling transition, in conformance with Standard Review Plan 4.4 (Reference 19). The uncertainties considered are listed in Table 2.9-1. The "system uncertainties" listed in Table 2.9-1 concern measurement uncertainties of system parameters. The values used are the same as those listed in References 17 and 18.

As described in Section 2.10, the CPM-2 lattice physics code will be used to generate inputs to the POWERPLEX core monitoring system. Of the "fuel related uncertainties" listed in Table 2.9-1, the only ones which are potentially affected by PP&L's methodology are: 1) radial bundle power, 2) local power, and 3) axial power. Evaluations by PP&L were performed that demonstrate that the uncertainties on those three parameters used by the fuel vendor (Reference 17) bound the uncertainties obtained using CPM-2 input in the core monitoring system. Thus, for conservatism, the Reference 17 uncertainties for all the fuel related uncertainties are used. If other values of these uncertainties are used, further justification will be provided.

TABLE 2.9-1

Uncertainties Used To Generate MCPR Safety Limit

System Uncertainties

Feedwater Flow Rate

Feedwater Temperature

Core Pressure

Core Flow Rate

Core Inlet Temperature

Fuel Related Uncertainties

XN-3 Correlation

Assembly Flow Rate

Radial Bundle Power

Local Power

Axial Power

2.10 Core Monitoring System Inputs

PP&L utilizes the POWERPLEX® Core Monitoring Software System (Reference 8) to perform the on-line thermal margin calculations for Susquehanna SES. ANF is the developer of POWERPLEX, and the original application of POWERPLEX at Susquehanna SES was based on input from ANF's lattice physics code XFYRE (Reference 28). POWERPLEX input decks are fuel cycle specific and contain nuclear physics data, peaking factors, and thermal limits information. PP&L developed, validated, and will use an input deck generation methodology based on results from the CPM-2 lattice physics code (References 1 and 4). PP&L has developed modifications to the NORGE-B2 code (Reference 7) to create the lattice physics input data needed by the POWERPLEX core monitoring system (e.g., cross sections, peaking factors, etc.). The calculation flow path is shown in Figure 1-2. CPM-2 performs lattice physics calculations for specific fuel designs; NORGE-B2 formats the CPM-2 results into the POWERPLEX input deck format; and then the NORGE-B2 output and other POWERPLEX inputs (i.e., thermal hydraulic data, core geometry, calculation options, neutron detector response data, etc.) are combined to complete the POWERPLEX input deck for a specific cycle.

Benchmarking was performed using this process for Susquehanna SES Unit 1, Cycles 1, 2, and 3 and Unit 2 Cycles 1, 2, and 3. The results were evaluated against measured data, SIMULATE-E results, and POWERPLEX results using ANF generated input. The use of PP&L's input deck generation methodology for POWERPLEX produced better comparisons to measured Traversing Incore Probe (TIP) data than the ANF generated input decks, and results which are approximately equivalent to the SIMULATE-E TIP response comparisons (Figures 2.10-1 through 2.10-6). The k-effective calculated by POWERPLEX using PP&L's input decks is very predictable and is compared to the SIMULATE-E calculated k-effective in Figures 2.10-7 through

2.10-12. These results and statistical evaluations of the results lead to the conclusions that for Susquehanna SES, POWERPLEX using PP&L generated CPM-2 input data generates results better than those obtained from POWERPLEX using ANF generated inputs, and similar to the SIMULATE-E results. Because of this, PP&L's use of the ANF power distribution uncertainties in the Safety Limit MCPR calculations is conservative and justified (See Section 2.9 of this report).

FIGURE 2.10-1
SUSQUEHANNA SES UNIT 1 CYCLE 1
RELATIVE NODAL RMS OF
TIP RESPONSE COMPARISONS

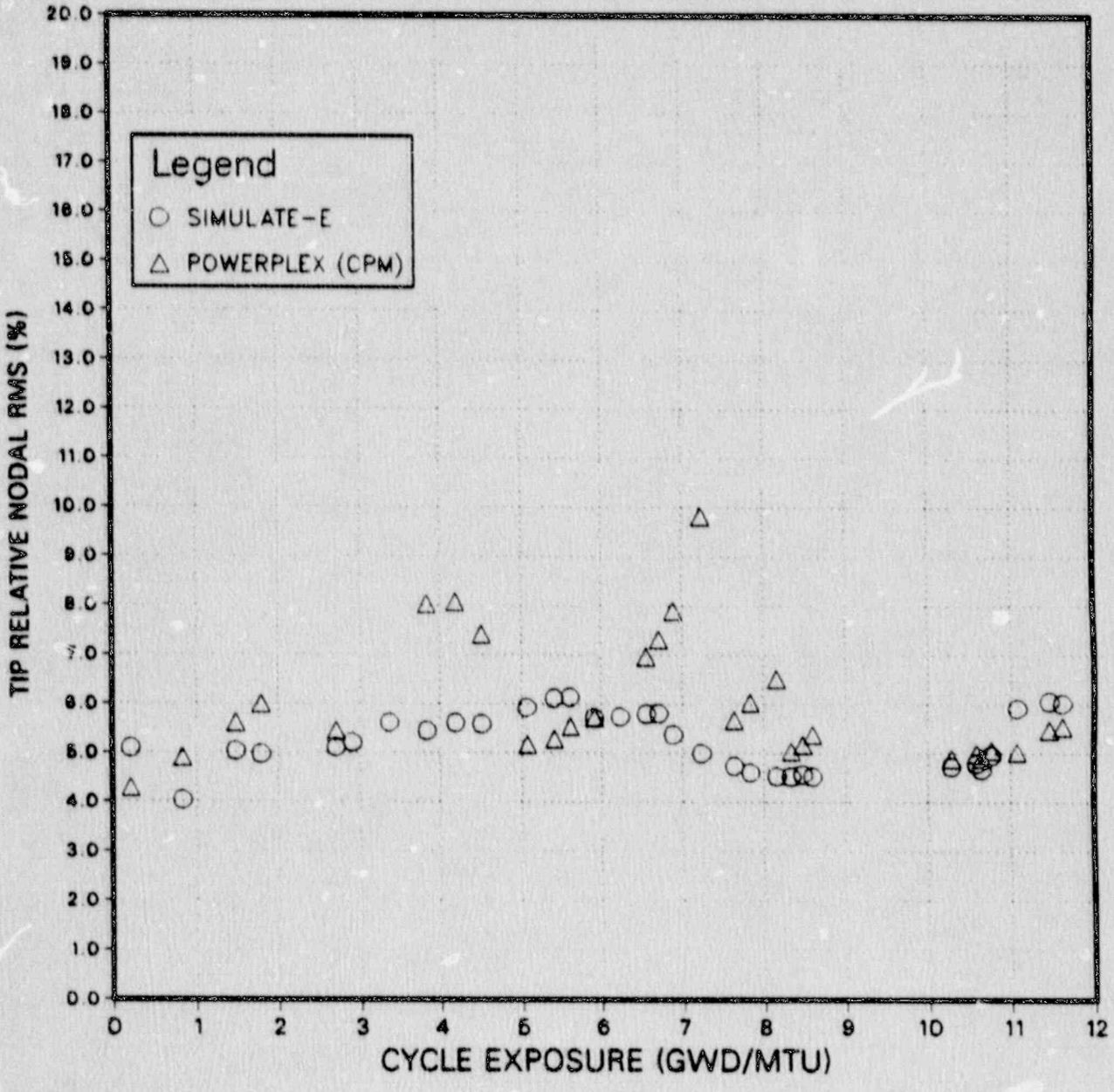

FIGURE 2.10-2
SUSQUEHANNA SES UNIT 1 CYCLE 2
RELATIVE NODAL RMS OF
TIP RESPONSE COMPARISONS

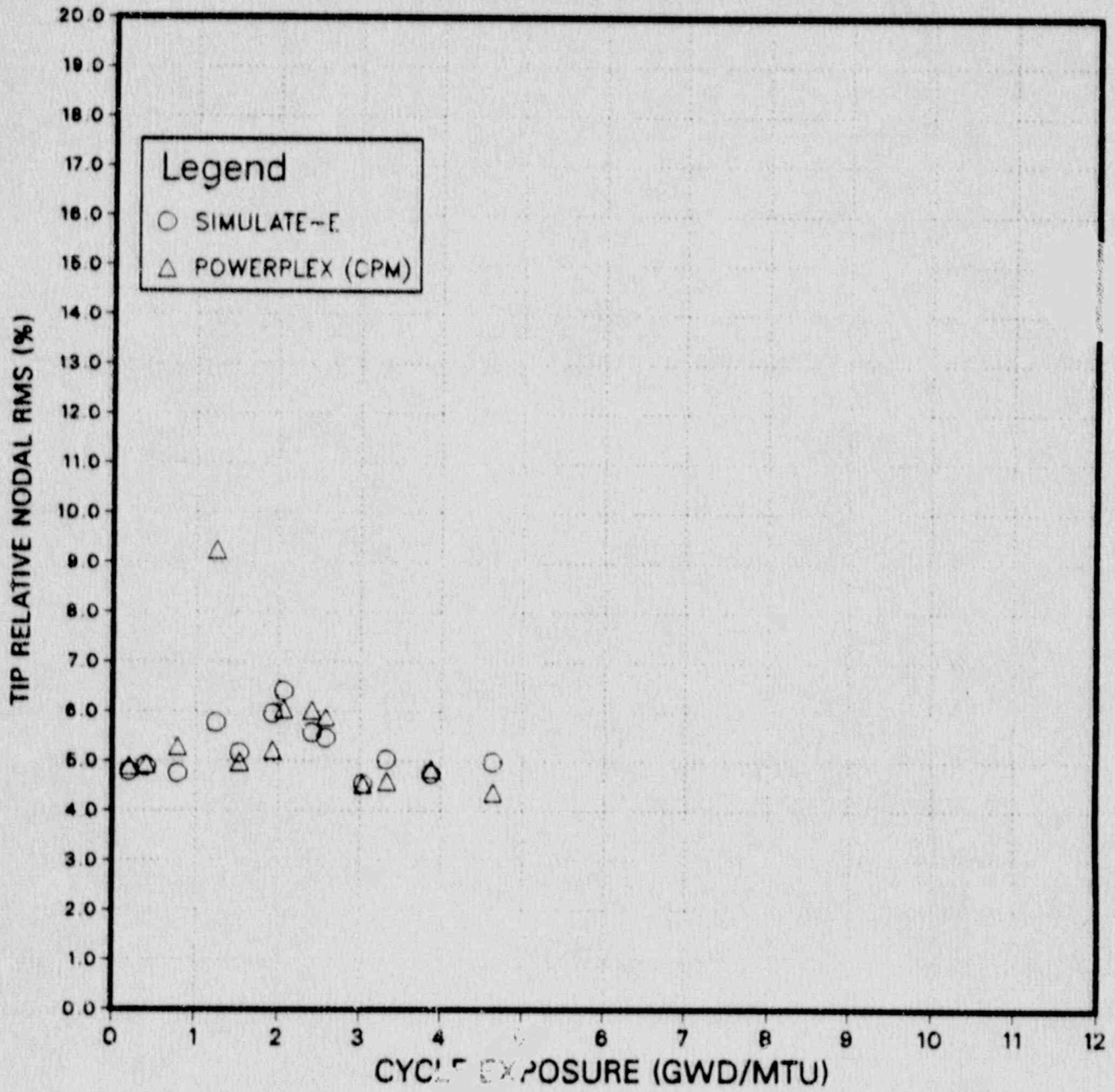

FIGURE 2.10-3
SUSQUEHANNA SES UNIT 1 CYCLE 3
RELATIVE NODAL RMS OF
TIP RESPONSE COMPARISONS

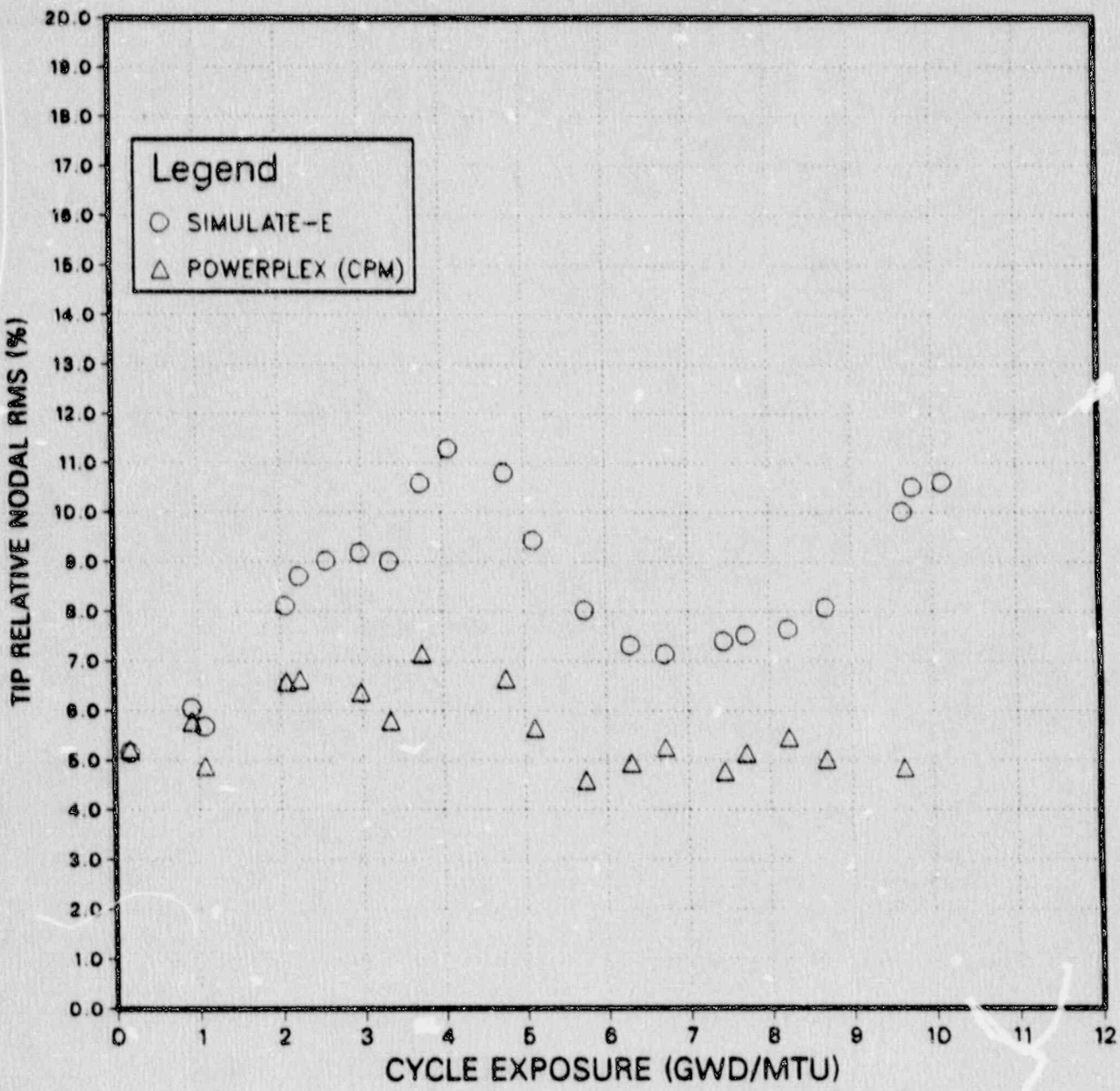

FIGURE 2.10-4
SUSQUEHANNA SES UNIT 2 CYCLE 1
RELATIVE NODAL RMS OF
TIP RESPONSE COMPARISONS

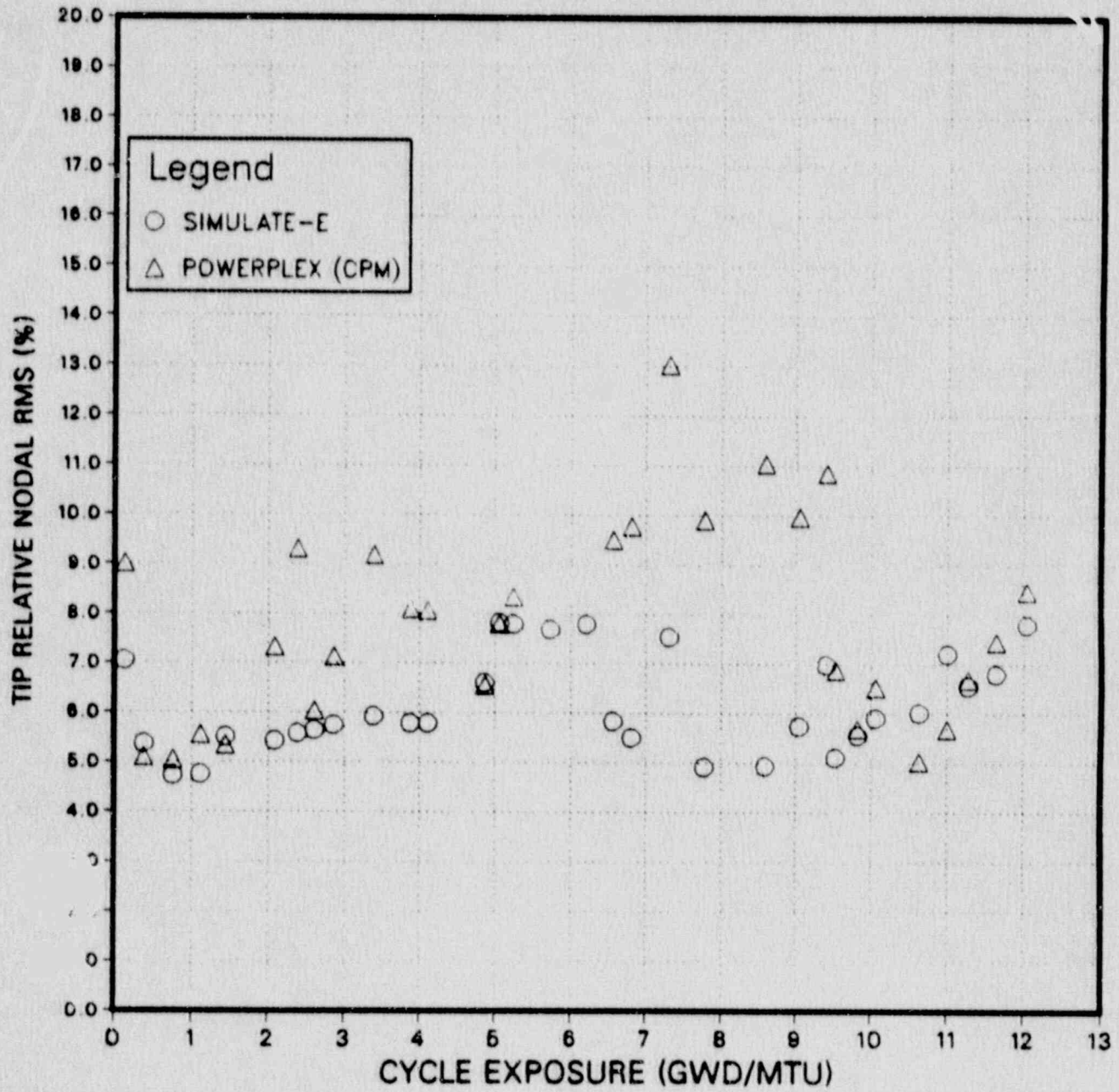

FIGURE 2.10-5
SUSQUEHANNA SES UNIT 2 CYCLE 2
RELATIVE NODAL RMS OF
TIP RESPONSE COMPARISONS

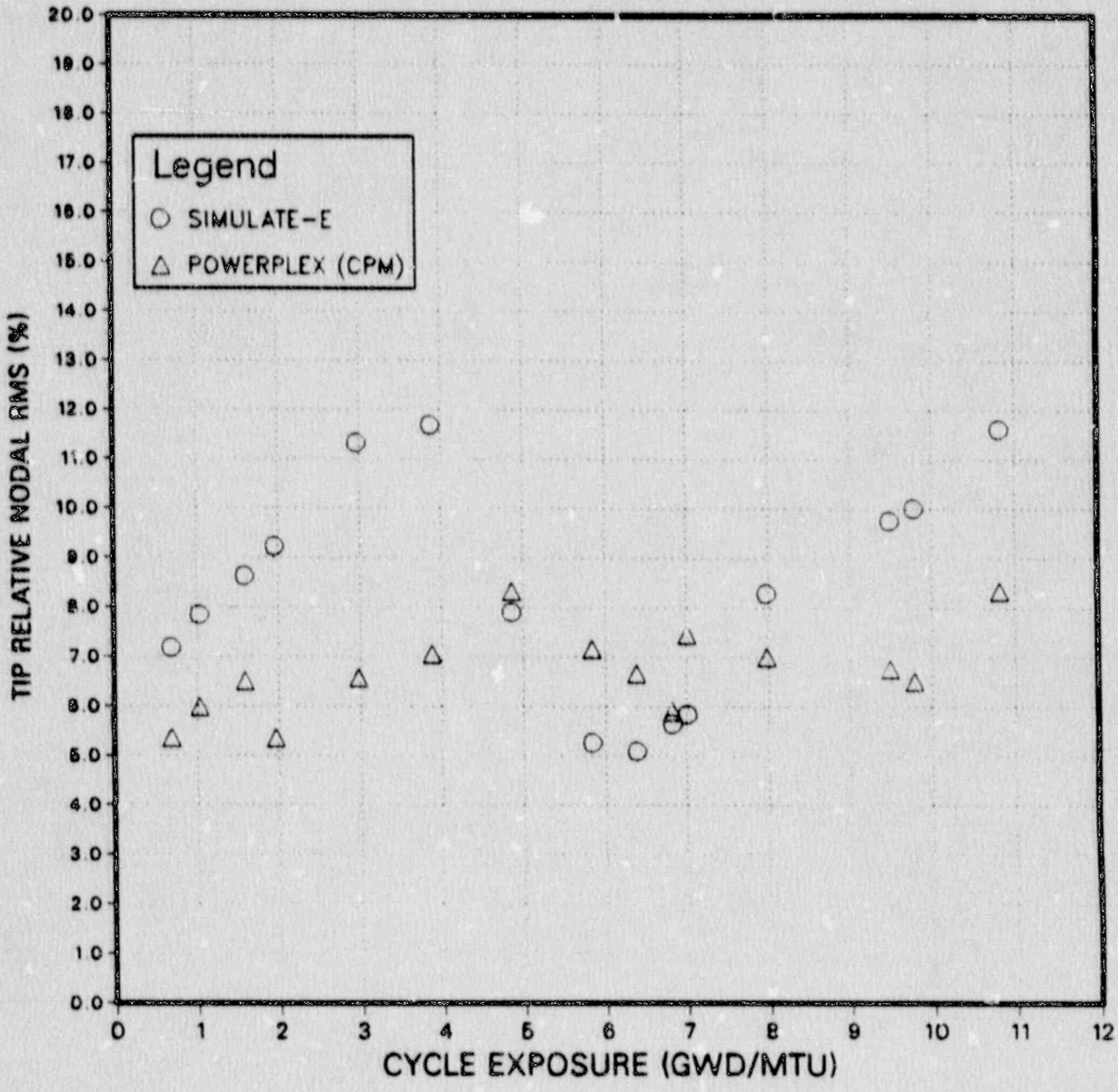

FIGURE 2.10-6
SUSQUEHANNA SES UNIT 2 CYCLE 3
RELATIVE NODAL RMS OF
TIP RESPONSE COMPARISONS

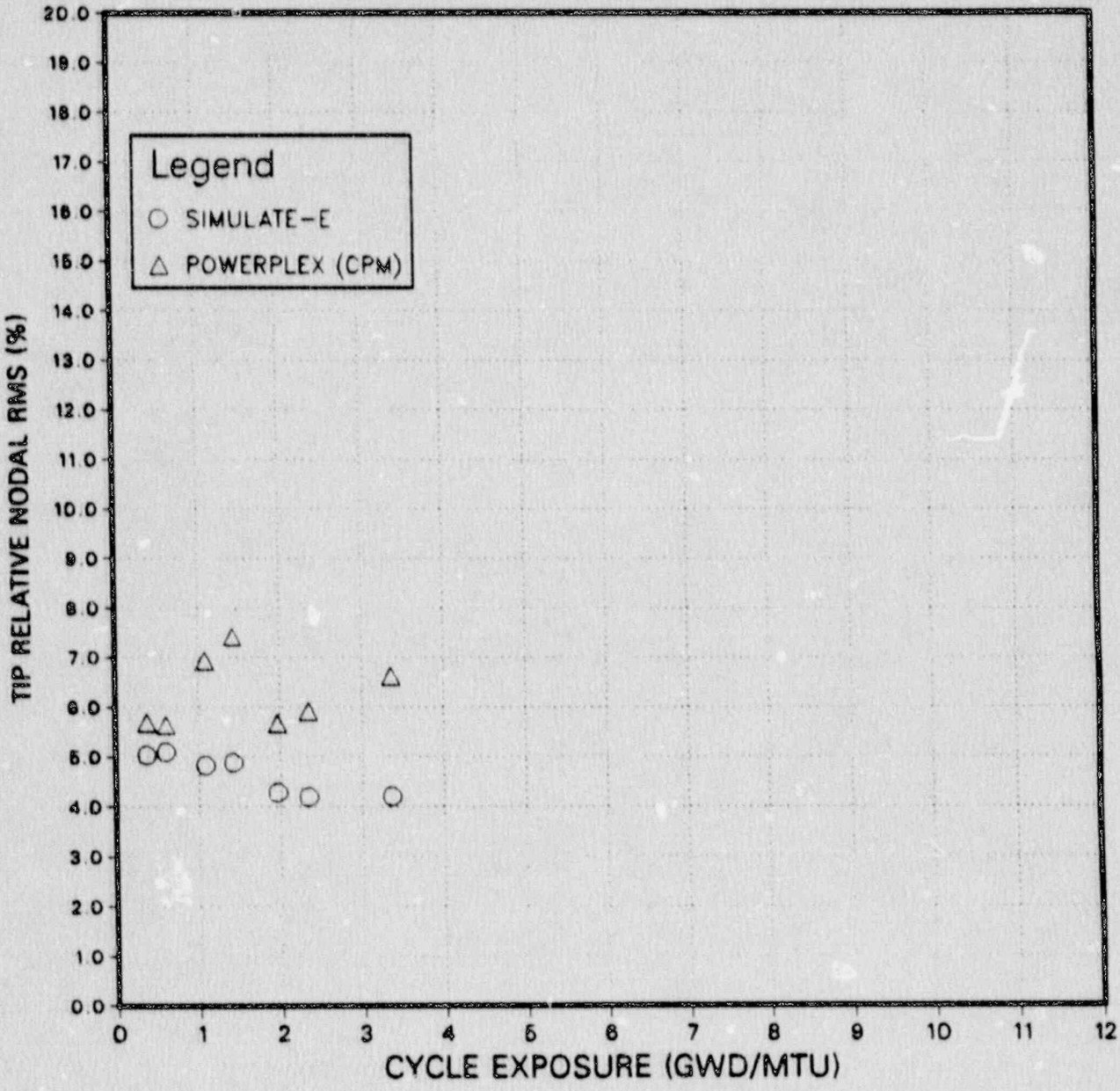

FIGURE 2.10-7
SUSQUEHANNA SES UNIT 1 CYCLE 1
HOT CALCULATED K-EFFECTIVES

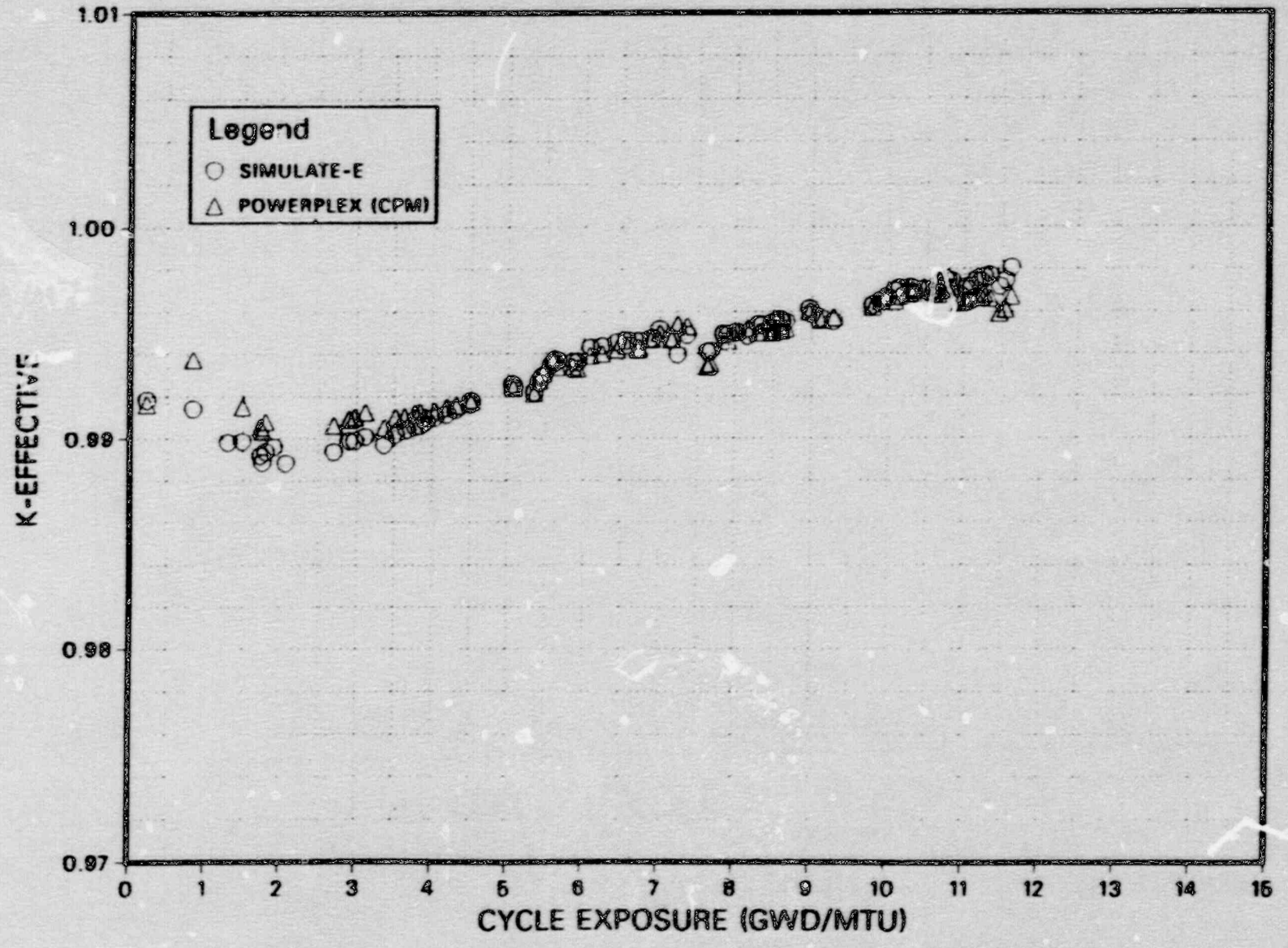

FIGURE 2.10-8
SUSQUEHANNA SES UNIT 1 CYCLE 2
HOT CALCULATED K-EFFECTIVES

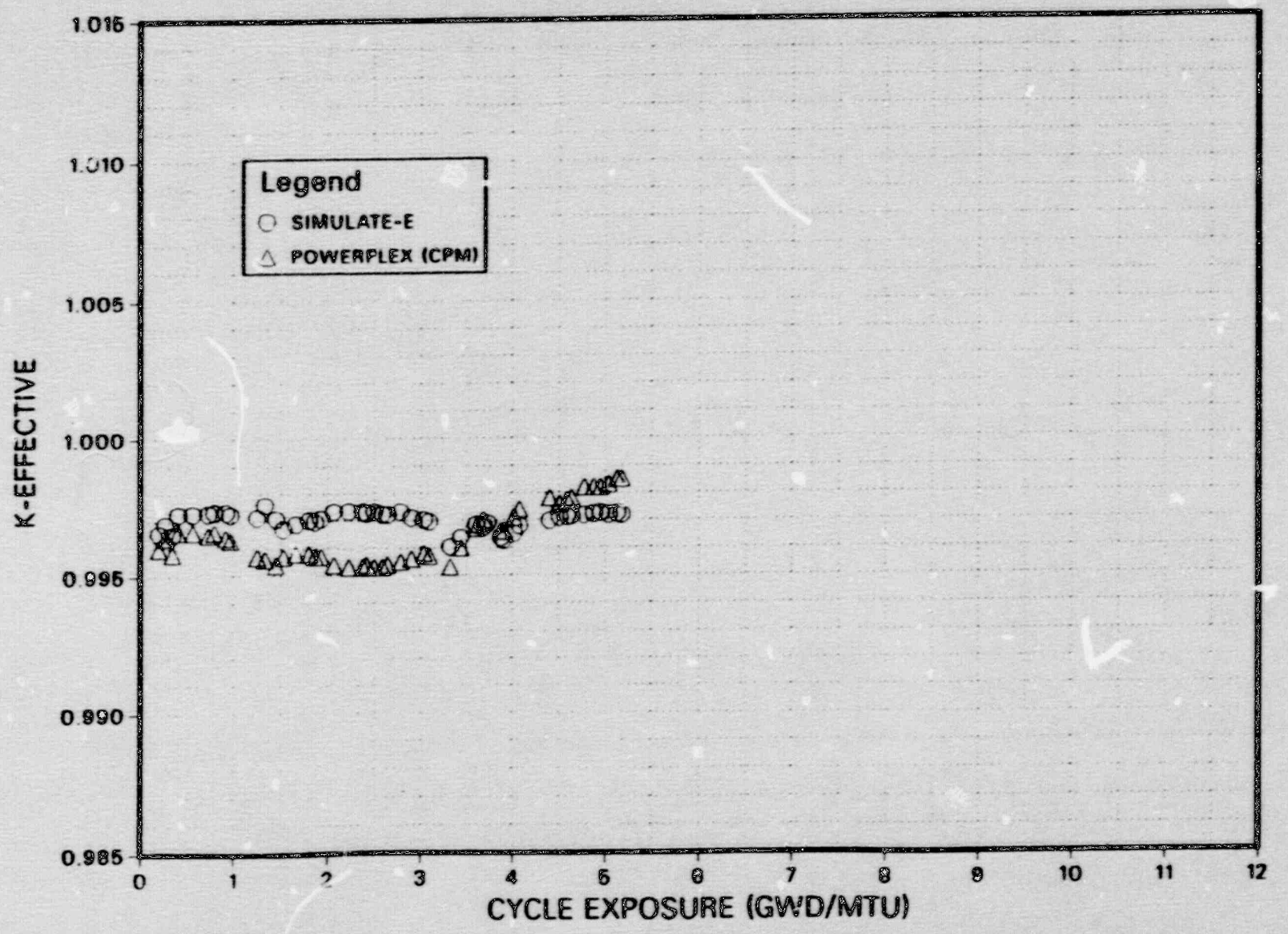

FIGURE 2.10-9
SUSQUEHANNA SES UNIT 1 CYCLE 3
HOT CALCULATED K-EFFECTIVES

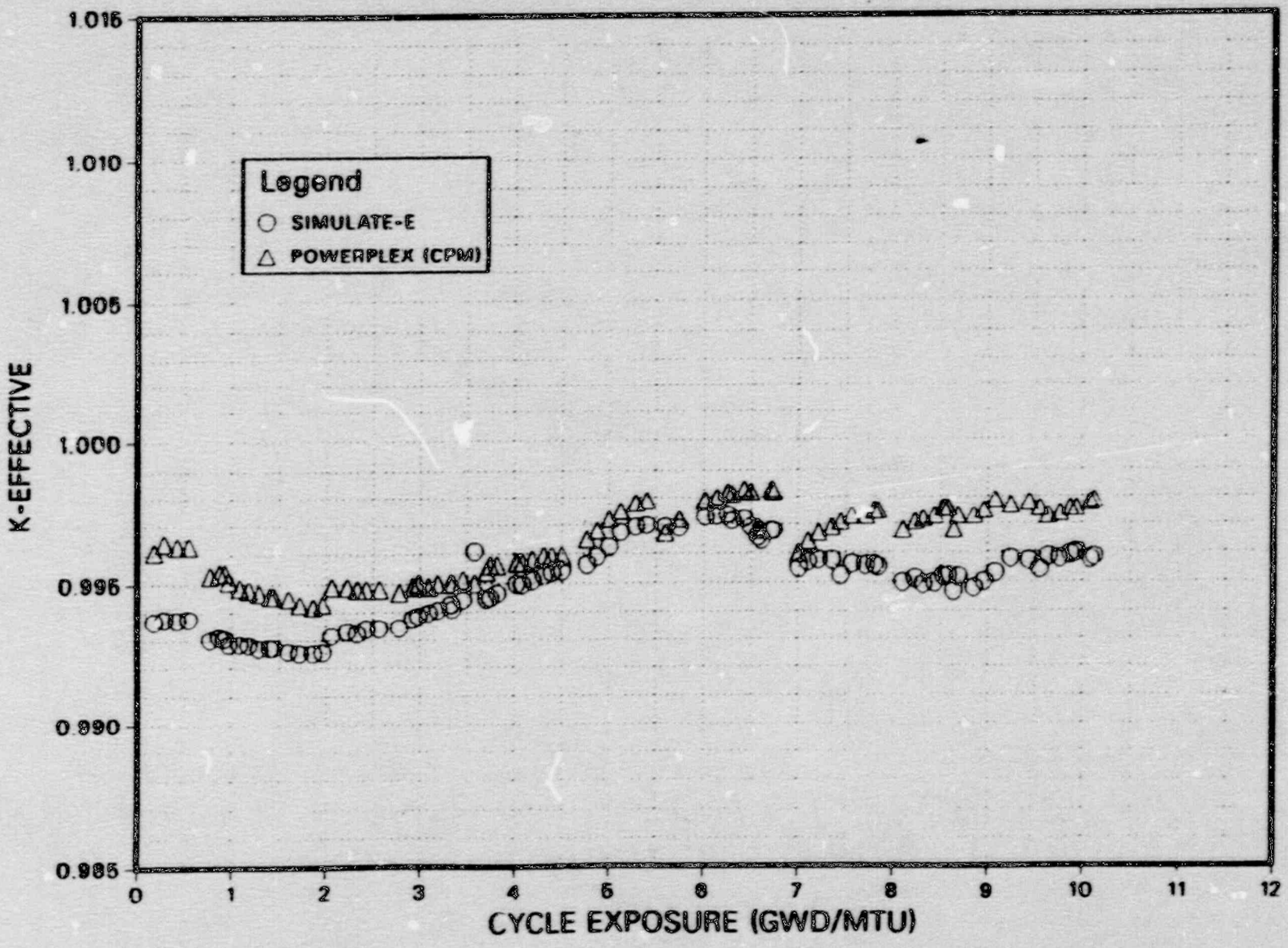

FIGURE 2.10-10
SUSQUEHANNA SES UNIT 2 CYCLE 1
HOT CALCULATED K-EFFECTIVES

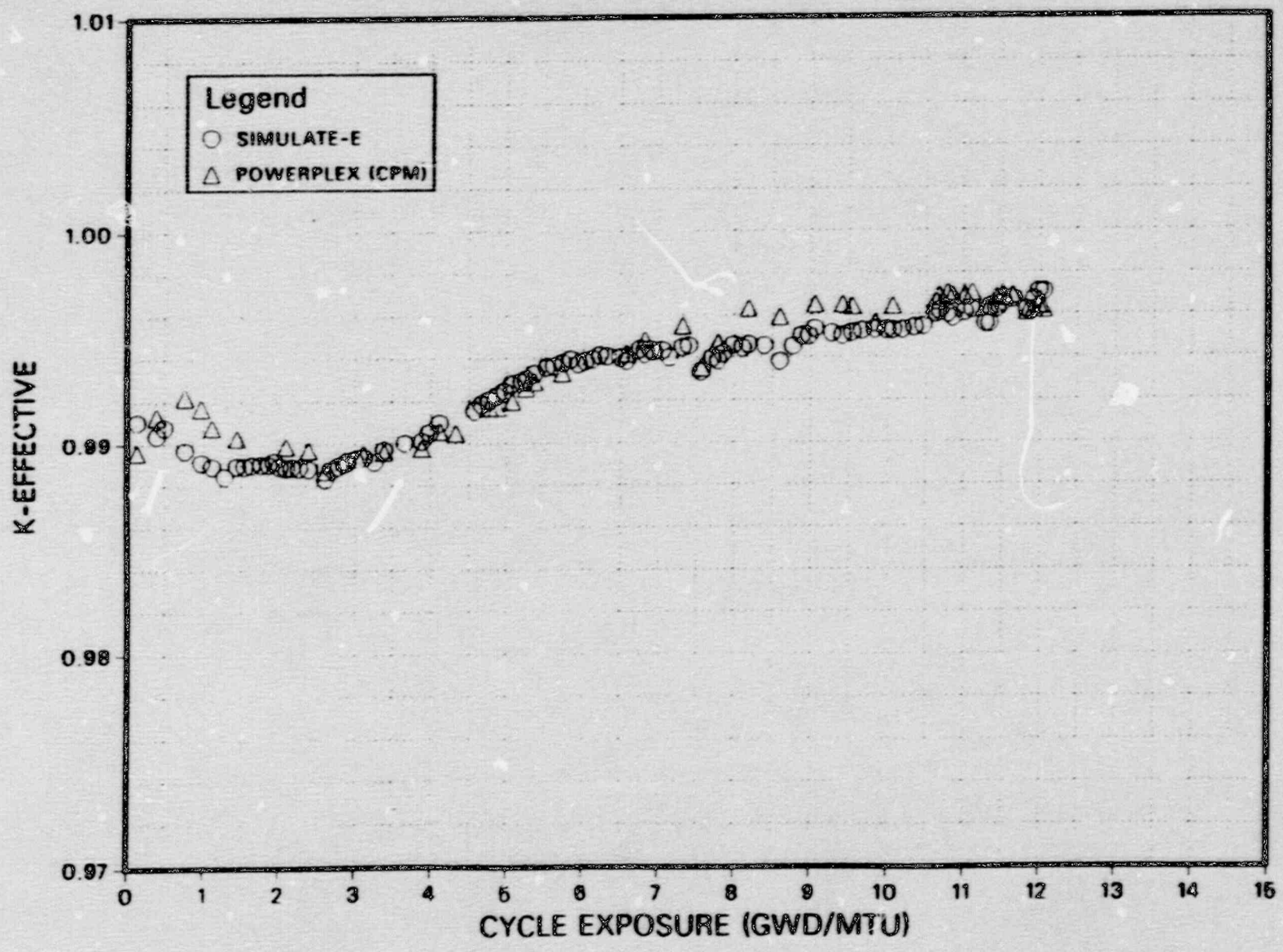

FIGURE 2.10-11
SUSQUEHANNA SES UNIT 2 CYCLE 2
HOT CALCULATED K-EFFECTIVES

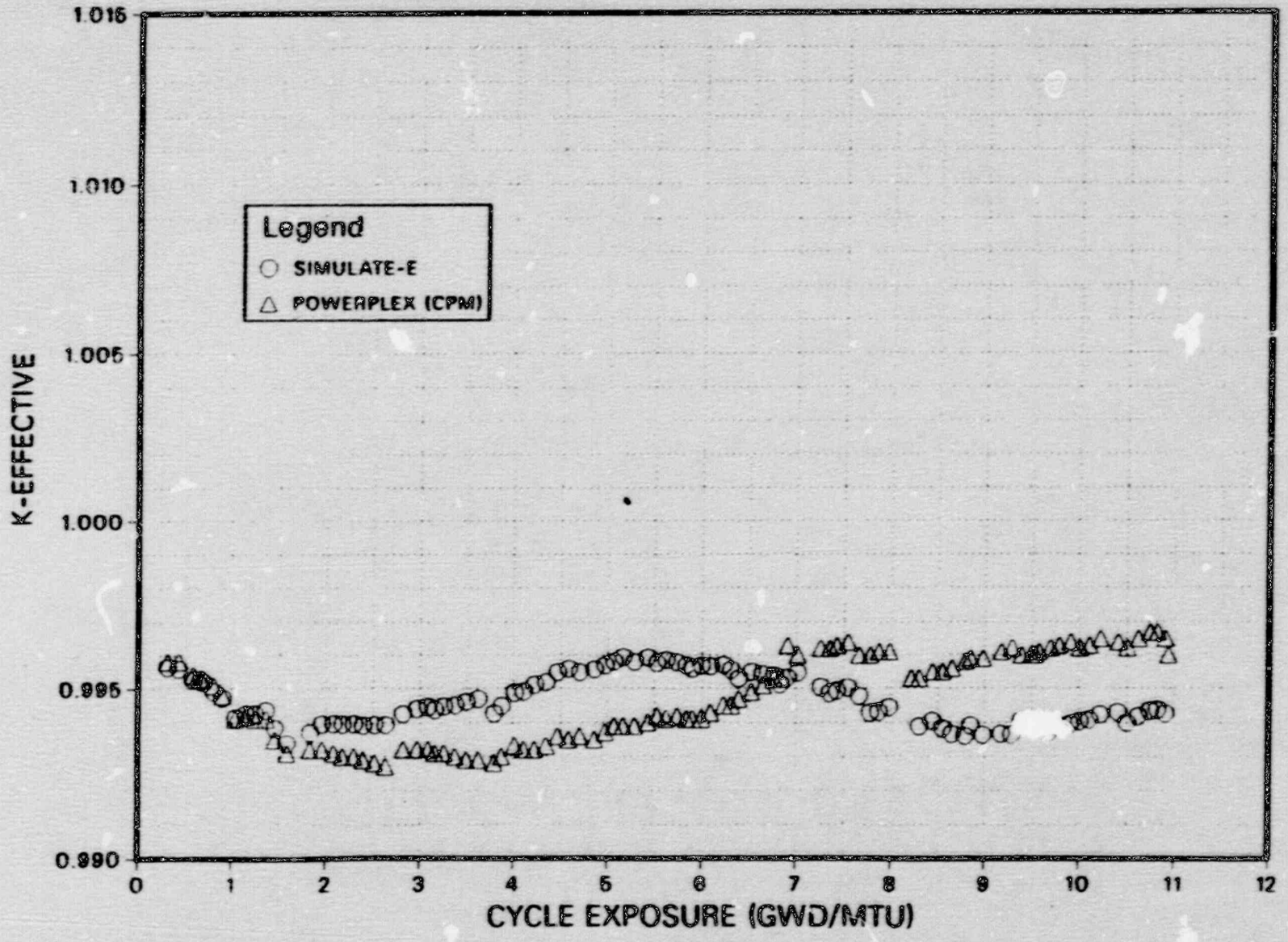

FIGURE 2.10-12
SUSQUEHANNA SES UNIT 2 CYCLE 3
HOT CALCULATED K-EFFECTIVES

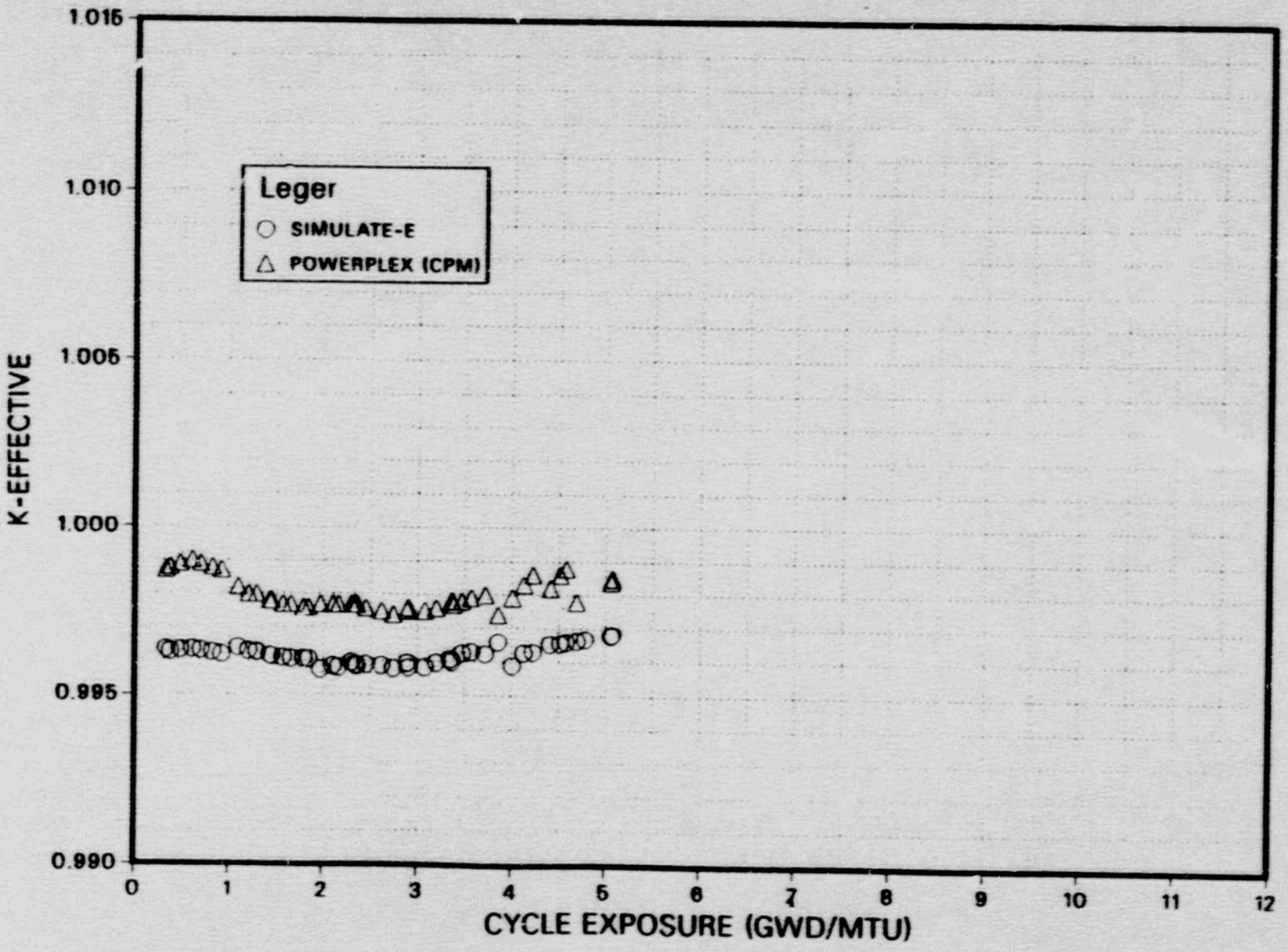

2.11 Fuel Storage Criticality Compliance

Fuel storage criticality analyses have been performed by ANF for both the new fuel vault (Reference 26) and the spent fuel pool (Reference 27). Both of these analyses are used to assure that the vault or pool k-effective is less than 0.95 under normal conditions and less than 0.98 under all credible accident scenarios. All appropriate calculational and geometric uncertainties have been accounted for in these analyses.

Continued compliance with these analyses is performed for each new fuel design as part of the reload licensing analysis. For both the new fuel vault and the spent fuel pool, the ANF analyses remain valid provided the reload fuel is an ANF 9x9-2 design with a lattice nominal enrichment plus enrichment tolerance less than 4.00 wt% U-235. For axially zoned assemblies, this applies to the maximum enrichment zone. For the new fuel vault, an additional criterion is placed on the maximum enrichment zone reactivity. The beginning of life k-infinity evaluated using in-core geometry shall not exceed 1.388 for the maximum reactivity zone of the reload fuel assembly. This criterion is verified using the CPM-2 computer program (Reference 4) using the PP&L analysis methods previously approved by the NRC (Reference 1).

3.0 TRANSIENT ANALYSIS METHODS APPLICATIONS

The application of PP&L's transient analysis models and methodologies to licensing analyses is discussed in this section. Reference 2 describes PP&L's transient analysis models and methods. The Susquehanna SES system and hot bundle RETRAN base models are described in Sections 3.0 and 4.0 of Reference 2, respectively. Since the publication of Reference 2, a minor modification was made to the DELTACPR code used to compute Critical Power Ratios (CPRs) and Critical Heat Flux Ratios (CHFRs). The modification implemented a means of automatically iterating on hot bundle power until a minimum CHFR equal to 1.0 is achieved. The thermal limits calculations in the modified code, referred to as the CPRITER code, remain unchanged. An outline of PP&L's RETRAN/CPRITER analysis methodology is provided below and illustrated in Figure 3.0-1.

The RETRAN system model (see Figure 3.0-2 and 3.0-3) simulates the core and system response to an event. The system model calculates normalized core power, core inlet temperature, upper plenum pressure, and lower plenum pressure as functions of time. These time dependent parameters are input as boundary conditions to the RETRAN hot bundle model. The hot bundle model output is used by the CPRITER code for thermal margin calculations.

In a manner similar to Advanced Nuclear Fuels Corporation's methodology (References 17 and 18), the system model calculated initial core average Axial Power Distribution (APD) and the calculated normalized power versus time are used as input to the RETRAN hot bundle model. The all-rods-out axial power distributions for MCPR limiting assemblies at end of cycle tend to be more bottom peaked than the core average. These assemblies are actually affected by scram control rod insertion sooner than the use of the core average APD would predict. Therefore using the core average normalized power versus time curve in the hot bundle model is conservative for licensing basis pressurization events.

The RETRAN hot bundle model calculates the following parameters as functions of time and axial location: heat flux, enthalpy, flow rate, and pressure. The CPRITER code uses these hot bundle calculated parameters to calculate CHFR versus time and the initial value of CPR. The CPRITER code iterates on initial hot bundle power and performs successive RETRAN hot bundle model calculations until the transient minimum CHFR equals 1.0. The transient ΔCPR is then equal to the initial CPR minus 1.0.

For the events whose results factor into the MCPR operating limits, the parameter of interest is defined as the change in Critical Power Ratio (ΔCPR) divided by the initial value of CPR, and is referred to as RCPR. Results of the sensitivity studies presented in Sections 3.1 to 3.3 are expressed in terms of RCPR.

With the exception of the ASME overpressure analysis described in Section 3.5, all analyses in this section are considered as Anticipated Operational Occurrences (AOOs) for the purpose of establishing MCPR operating limits. The AOOs presented in Chapter 15 of the FSAR (Reference 14) were evaluated and the potentially limiting events were analyzed. A subset of the FSAR events was evaluated and determined to be non-limiting as described in Section 3.4.

The three potentially limiting MCPR events which use the RETRAN/CPRITER methodology are: Generator Load Rejection Without Bypass (GLRWOB), Feedwater Controller Failure (FWCF), and Recirculation Flow Controller Failure (RFCF). These events will be analyzed for each reload core. The conservative method of analysis, along with sensitivity studies and sample licensing analyses are presented for these events (Sections 3.1 to 3.3).

The sample licensing analyses were performed for Susquehanna SES Unit 2 Cycle 2. The Unit 2 Cycle 2 core consisted of 324 ANF 9x9 fuel assemblies

and 440 GE 8x8R fuel assemblies. As discussed in Reference 2, the RETRAN system model used GE 8x8 fuel pin geometry to represent the core, since it was the "dominant" (i.e., most prevalent) fuel type. The hot bundle model represented an ANF 9x9 fuel bundle for the sample analyses, since this fuel type is expected to produce higher calculated ΔCPRs. An actual reload licensing analysis would include hot bundle/ΔCPR analyses for each potentially limiting fuel type.

The RETRAN system model and hot bundle model gap conductances were generated with ESCORE using the methodology described in Appendix A.

FIGURE 3.0-1

RETRAN/CPRITER CODE RELATIONSHIPS

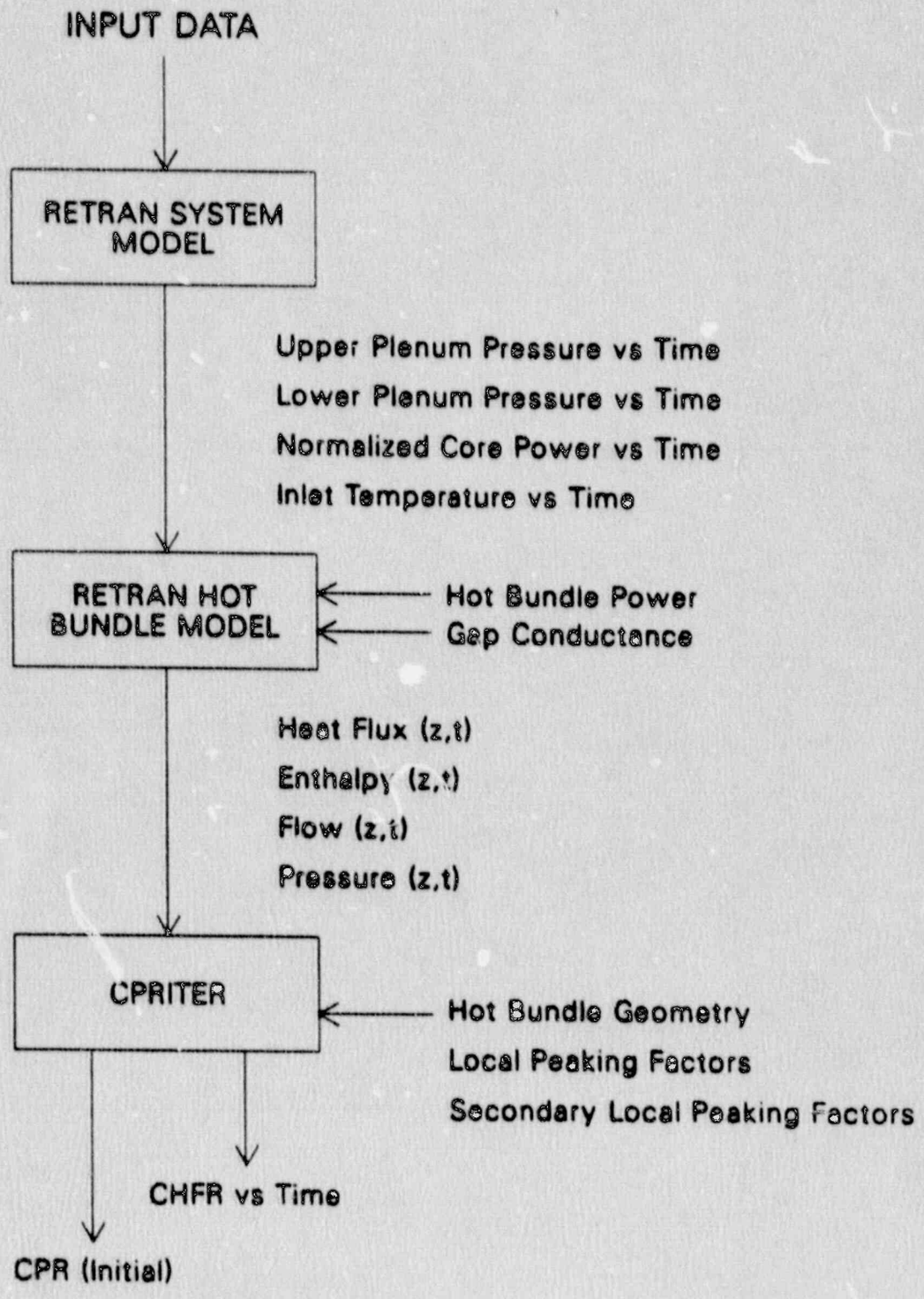

FIGURE 3.0-2
SUSQUEHANNA SES RETRAN MODEL
(VESSEL)

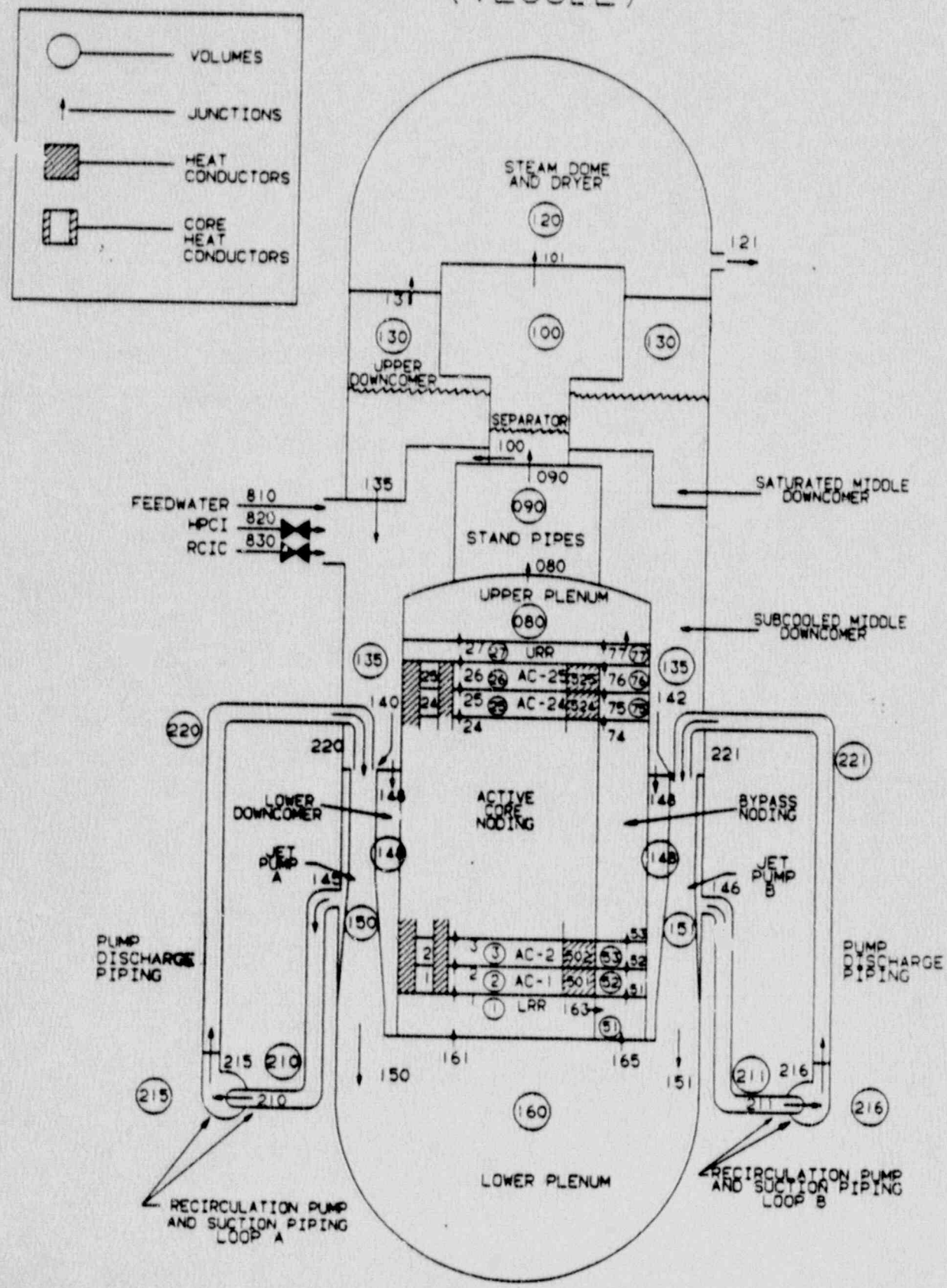

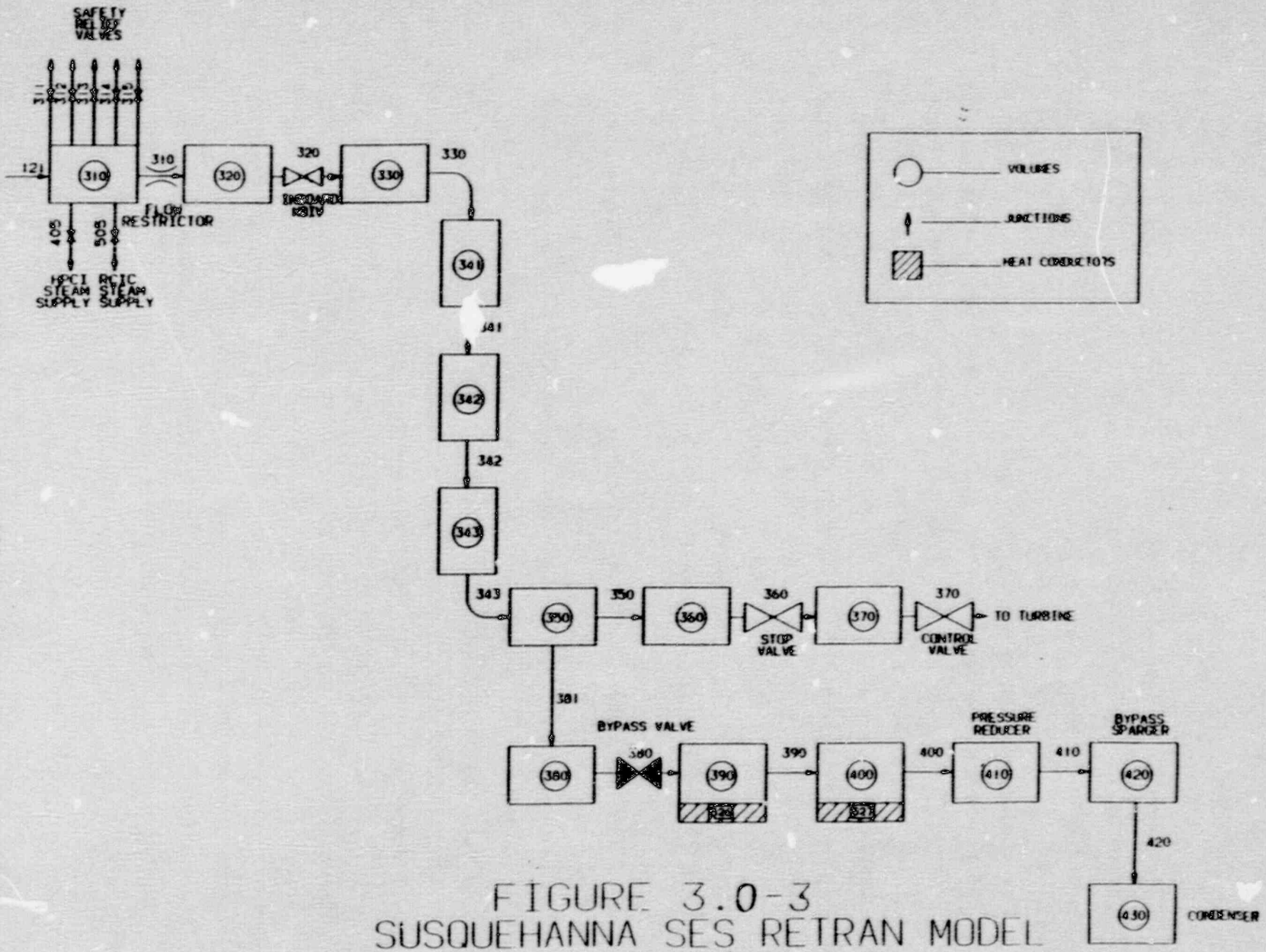

FIGURE 3.0-3
SUSQUEHANNA SES RETRAN MODEL
(STEAM LINE AND BYPASS)

3.1 Generator Load Rejection without Bypass

3.1.1 Event Description

The Generator Load Rejection Without Bypass (GLRWOB) event is expected to be one of the limiting pressurization events in establishing the MCPR operating limits.

For the Susquehanna SES units, there are two events that are considered. One is initiated by a power load imbalance signal which initiates fast closure of the Turbine Control Valves (TCVs). The second event can be caused by a number of other generator conditions and actuates the generator primary lockout relay, thus causing closure of both the TCVs and Turbine Stop Valves (TSVs). Both of these events were analyzed (Section 3.1.2) and calculated ΔCPR results were virtually identical, since at most power levels, the TCVs close more rapidly than the TSVs in the full arc mode of pressure regulation. As changes are made to the mode of TCV operation, this conclusion will be reviewed for accuracy.

The GLRWOB produces a fast closure signal to the TCVs. Closure of the TCVs causes a rapid increase in reactor pressure. A reactor scram and an End of Cycle-Recirculation Pump Trip (EOC-RPT) occur as a result of low TCV oil pressure. Control rods begin moving into the core and the recirculation pumps begin coasting down, thus reducing core flow. The system pressurization causes a rapid decrease in core void fraction and a subsequent void reactivity induced power increase. The increase in core power causes a degradation in thermal margin (i.e., a reduction in CPR). The event is typically analyzed at end of cycle, since the core is unrodded, and the void reactivity coefficient is more negative.

The Susquehanna SES Technical Specifications allow operation with the EOC-RPT inoperable. Analyses of the GLRWOB to produce MCPR operating limits for this mode of operation will be performed using the methodology

described in this section with the exception that the EOC-RPT will not be credited.

3.1.2 Sensitivity Studies

RETRAN/CPRITER analyses were performed to determine the sensitivity of calculated RCPR to changes in input assumptions. The parameters considered were:

1) Control rod insertion rate
2) Recirculation Pump Trip (RPT)
3) Turbine Control Valve (TCV) closure time
4) Safety Relief Valve (SRV) opening setpoints and flow capacity
5) Feedwater temperature
6) Pressure regulator setpoint
7) Core power
8) Core flow
9) Steam line inertia
10) Steam line volume
11) Steam line pressure drop

In addition, two extra analyses were performed: 1) a Turbine Trip Without Bypass (TTWOB) which, for the Susquehanna SES Units, closes both the TSVs and the TCVs, and 2) a GLRWOB which occurs due to a power load imbalance signal and closes the TCVs only.

The base case values of the above mentioned parameters are listed in Table 3.1-1. Fast closure of the TCV in the RETRAN model is accomplished by a manual trip on elapsed time. Results of the study are shown in Table 3.1-2. Conclusions and observations from these analyses are discussed below.

A faster control rod insertion (scram curve) clearly produces a significant reduction in peak core power and, hence, RCPR. A reduction in RPT delay results in a faster reduction in core flow, which produces a reduction in peak core power and RCPR. Use of the Technical Specification maximum RPT delay (currently 0.175 seconds) is, thus, conservative. A faster TCV closure produces a more severe pressurization and results in a higher calculated RCPR.

For the Susquehanna SES units, there are two modes of operation for the Safety Relief Valves (SRVs), referred to as the safety mode and the relief mode. In the safety mode, the valves are opened mechanically when system pressure overcomes the force of a spring. The number of operable valves required and the pressure setpoints are specified in the Susquehanna SES units' Technical Specifications (References 15 and 16). In the relief mode, the valve opening is initiated by electrical signals when measured dome pressure exceeds the specified setpoints. The relief mode pressure setpoints are lower than the safety mode pressure setpoints.

The difference in assumed SRV operation between the Technical Specification safety mode (6 valves out of service) and the nominal relief mode (all valves operable) produces only a small change in RCPR. However, the Technical Specification safety mode assumption produced a more severe pressurization, and gave a slightly higher calculated RCPR.

The effect of decreased feedwater temperature on the GLRWOB is an increase in peak core power due to a more top peaked Axial Power Distribution (APD). However, the effect on calculated RCPR is negligible. An increase in pressure regulator setpoint, which increases dome pressure approximately the same amount, results in a decrease in calculated RCPR. The effects of decreased feedwater temperature and increased pressure regulator setpoint on peak power and calculated RCPR are complex. Both cases show slightly more top peaked APDs than the base case, which accounts for the slight increase in peak core power. However, the changes

in hot bundle enthalpies produced by the pressure, flow, and heat flux transients are difficult to predict for the different cases. In any case, for changes of 10°F in feedwater temperature and 32 psi in pressure regulator setpoint, the impact on RCPR is very small, as shown in Table 3.1-2.

Increased initial core power and increased initial core flow produce a higher calculated RCPR. At increased power, the initial steam flow and, hence, vessel pressurization rates are higher. At increased flow, the core APD is more top peaked causing a significantly higher peak core power and, hence, a larger calculated RCPR.

The steam line parameters (inertia, volume, and pressure drop) all affect the pressure wave in the steam line. Higher inertia creates a higher pressure peak at the TCV and a higher pressurization rate in the steam dome. This adverse pressurization produces a higher and broader power versus time curve, which produces a larger calculated RCPR. A larger steam line volume reduces the vessel pressurization and RCPR, since more mass and energy are required to pressurize the larger volume. A larger steam line pressure drop means a higher resistance to flow (i.e., larger loss coefficients). The larger loss coefficients will attenuate the pressure wave more as it travels from TCVs to the vessel, producing a lower peak power and a lower RCPR.

3.1.3 Licensing Analysis Method

The GLRWOB analysis method is based on the results of the sensitivity studies discussed in the previous section. The analysis approach may use the Statistical Combination of Uncertainties (SCU) methodology described in Appendix B. Unless treated statistically with the SCU methodology, the following input assumptions are used:

1) Technical Specification scram curve.

2) Technical Specification (maximum) scram and EOC-RPT delay times.

3) Technical Specification safety mode for the SRVs (6 valves inoperable).

4) Analysis is performed at end of cycle/all-rods-out. If cycle exposure dependent thermal limits are to be specified, additional cycle exposure conditions will be analyzed.

5) Analysis is performed at the most limiting condition from 0% to 104.4% of rated core power and 100% core flow.

6) Code uncertainty is applied as specified in Section 8 of Reference 2.

7) Use nominal feedwater temperature.

8) The uncertainties on steam line ΔP, steam line inertia, steam line volume, TCV closure time, and pressure regulator setpoint are statistically combined with the Reference 2 code uncertainty.

Results of an analysis for Unit 2 Cycle 2 using the above assumptions, with the exception that initial core power was 100%, are presented in Figures 3.1-1 to 3.1-7.

3.1.3.1 Treatment of Steam Line Uncertainties

The RETRAN code uncertainty derived in Reference 2 excludes the steam line parameter uncertainties. The steam line parameters of importance are:

1) Steam line ΔP
2) Steam line inertia
3) Steam line volume
4) TCV closure time
5) Pressure regulator setpoint

These uncertainties were combined with the Reference 2 code uncertainty to produce a total model uncertainty by the root sum square method. Table 3.1-5 illustrates the calculation. The total model uncertainty was used in the SCU analyses described in this Section. It is clear from Table 3.1-5 that the steam line parameter uncertainties, when combined with the code uncertainty generated in Reference 2, will have only a small effect on calculated RCPR. The larger uncertainty, which includes the steam line uncertainties, will be used in the analysis.

3.1.3.2 SCU Method

As previously stated, several of the assumptions listed above may be modified if a Statistical Combination of Uncertainties (SCU) approach is used. The SCU methodology described in Section B.2 consists of the following steps:

1) Create a response surface from RETRAN/CPRITER calculations that relates calculated RCPR to the variables to be analyzed statistically. The variables chosen for the sample GLRWOB are core power and scram insertion speed.

2) Define uncertainty distributions for the parameters used in the response surface.

3) Perform Monte Carlo analysis to produce a cumulative probability distribution of calculated RCPR.

4) Perform safety limit type analyses to produce cumulative probability distribution functions of fraction of pins in boiling transition for a range of MCPRs. For the sample calculation presented in Section 3.1.4, cumulative probability distribution functions were generated by the ANF methodology for a core co ining all ANF 9x9 fuel. These distributions are used since they are typical for future licensing applications.

5) Assume a MCPR operating limit.

6) Perform Monte Carlo analysis to combine the cumulative probability distribution functions for fraction of pins in boiling transition and the cumulative probability distribution function of transient RCPR, thus producing a combined safety limit and transient analysis.

7) Select the value of number of rods expected to be in boiling transition at the 95% confidence level. If the value is greater than 0.1% of the pins, increase the assumed MCPR operating limit and repeat steps 5, 6, and 7.

3.1.4 Sample Licensing Analysis

To demonstrate the application of the SCU methodology for the GLRWOB, a sample analysis was performed for Susquehanna SES Unit 2 Cycle 2. This is the method PP&L plans to use for reload licensing applications. The variables treated statistically were core power and control rod scram insertion speed.

A response surface of calculated RCPR as a function of core power and average scram speed was produced with CPRITER. The choice of scram speed was based on statistical analyses of over 3800 individual Susquehanna SES control rod scram time measurements. These analyses demonstrated that average scram speed can be treated as a normally distributed variable. The nine RETRAN cases run to produce the response surface are shown in Table 3.1-3. The response surface is of the form:

$$RCPR = A_o + A_1X_1 + A_2X_2 + A_{12}X_1X_2 + A_{11}X_1^2 + A_{22}X_2^2,$$

where: X_1 = change in core power from 100% power (% rated)

X_2 = change in scram speed from 4.167 ft/sec (ft/sec)

The coefficients of the response surface for the U2C2 sample GLRWOB analysis are given in Table 3.1-4.

The mean and standard deviation of the core power error were assumed to be 0.0 and 2%, respectively. The mean and standard deviation of average scram speed were chosen, based on a conservative evaluation of plant data, to be 4.167 ft/second and 0.2 ft/second, respectively.

The core power uncertainty is common to both the safety limit type and transient RCPR analyses for the GLRWOB. A higher core power adversely affects both analyses (i.e., higher number of rods in boiling transition and larger calculated RCPR). As stated in Section B.2.3, Item 7, the safety limit type and RCPR analyses are not strictly statistically independent, and an additional conservatism is required. The maximum variation in calculated RCPR over the core power range of 96% to 104.4% was only .007. Thus, as an additional conservatism to cover the

assumption of statistical independence of the safety limit and RCPR analyses, a value of .007 was added to the transient calculated RCPRs, and the operating limit was recalculated. Another valid approach would be to select the core power level which produces the maximum calculated RCPR within two standard deviations (96-104% power) and use that power level for all response surface analyses (i.e., conservatively treat power uncertainty and exclude it from the response surface).

The calculated MCPR operating limit for the sample U2C2 GLRWOB, using the SCU methodology described in Appendix B was 1.30. It should be noted that if other events require higher operating limits, then the actual Technical Specification MCPR operating limits would be the highest value obtained for any of the events.

TABLE 3.1-1

Generator Load Rejection Without Bypass
Base Case Input Assumptions

Parameter	Assumption
1. Control Rod Insertion	Technical Specification insertion rate (slowest allowed)
2. Recirculation Pump Trip Delay Time (sec.)	Technical Specification value (maximum allowed)
3. Turbine Control Valve Closure Time (sec.)	85% of the best estimate value based on plant data
4. Safety/Relief Valve Operation	Technical Specification required safety valve mode of SRVs with six SRVs out of service
5. Feedwater Temperature	Best estimate value based on plant data
6. Pressure Regulator Setpoint	Best estimate value based on plant data
7. Core Power	3293 Mwt (100%)
8. Core Flow	100 Mlb/hr
9. Steam Line Inertia	Best estimate values (Reference 2)
10. Steam Line Volume	Best estimate values (Reference 2)
11. Steam Line Pressure Drop	Best estimate values (Reference 2)

TABLE 3.1-2

Generator Load Rejection Without Bypass
Results of Sensitivity Analyses

Parameter	Change from base value	Change in Peak Core Power (% rated)	Change in RCPR
1. Control Rod Insertion	Best estimate curve based on plant data	-71.3	-.080
2. RPT Delay (sec.)	-.05 seconds	-25.0	-.008
3. TCV Closure Time (sec.)	+.01 seconds	-2.9	-.002
4. SRV Operation	Relief mode/all valves operable	0.0	-.002
5. Feedwater Temperature	-10 °F	+10.1	+.000
6. Pressure Regulator Setpoint	+32 psi	+2.3	-.007
7. Core Power	+4.4% (104.4/100) -35% (65/100)	- -	+.002 -.024
8. Core Flow	-1.% (100/87)	-45.2	-.027
9. Steam Line Inertia	+2[illegible]%	+64.8	+.015
10. Steam Line Volume	+5%	-2.6	-.004
11. Steam Line Pressure Drop	+29.5 psi	-58.6	-.028
12. TSV Closure (yes/no)	no	+14.4	+.001
13. Event	TTWOB	-1.0	-.002

TABLE 3.1-3

Cases Analyzed for GLRWOB
Response Surface

	Scram Speed (ft/sec)		
Core Power Error	4.902	4.167	3.623
+4.4%	X	X	X
+0.0%	X	X	X
-4.0%	X	X	X

NOTE: X - means case was used in response surface generation.

TABLE 3.1-4

Coefficients for GLRWOB Response Surface

A_0 = +.174109

A_1 = -.0005875

A_2 = -.066197

A_{12} = -.0002802

A_{11} = +.0002237

A_{22} = -.0079919

Response Surface Standard Deviation = .0002

TABLE 3.1-5

Steam Line Parameters:
Contribution to Code Uncertainty
for GLRWOB

Parameter	Uncertainties[1]	dRCPR/dx[2]	S_x^{RCPR}
Steam Line ΔP(psi)	5	-.0009/psi	.0045
Steam Line Inertia (%)	5	+.0006/%	.0030
Steam Line Volume (%)	5	-.0008/%	.0040
Turbine Control Valve Closure Time (% of best estimate)	10	-.0002/%	.0020
Pressure Regulator Setpoint (psia)	5	-.0002/psi	.0010

(1) S_x; based on an engineering assessment of the parameters.

(2) $S_x^{RCPR} = S_x \left| \frac{dRCPR}{dx} \right|$

(3) Steam Line Parameters' Contribution to Code Uncertainty ($S_{steamline}^{RCPR}$)

$$S_{steamline}^{RCPR} = \left[\sum \left(S_x^{RCPR} \right)^2 \right]^{1/2} = .007$$

FIGURE 3.1-1 : GLRWOB CORE POWER

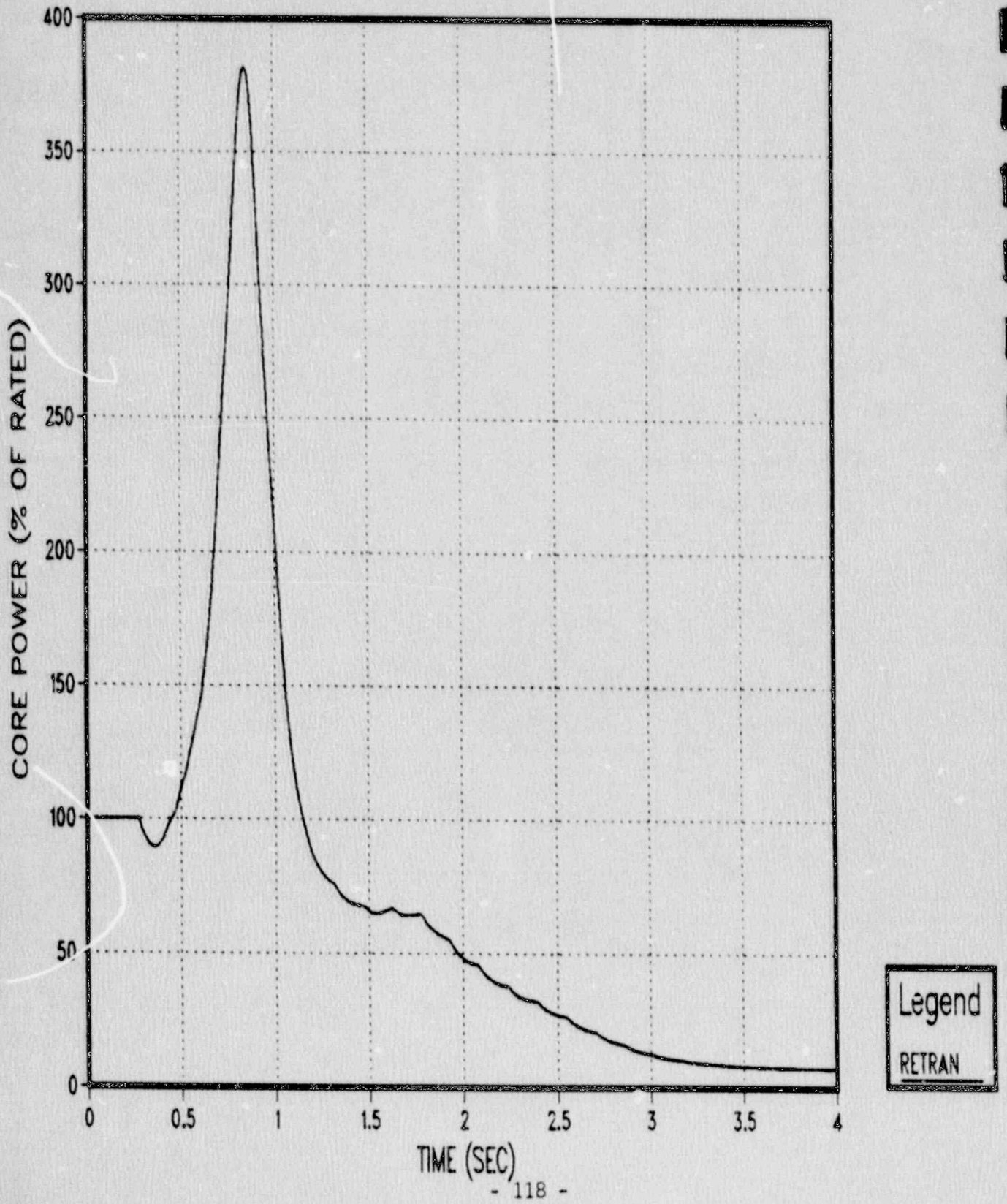

FIGURE 3.1-2 : GLRWOB CORE FLOW

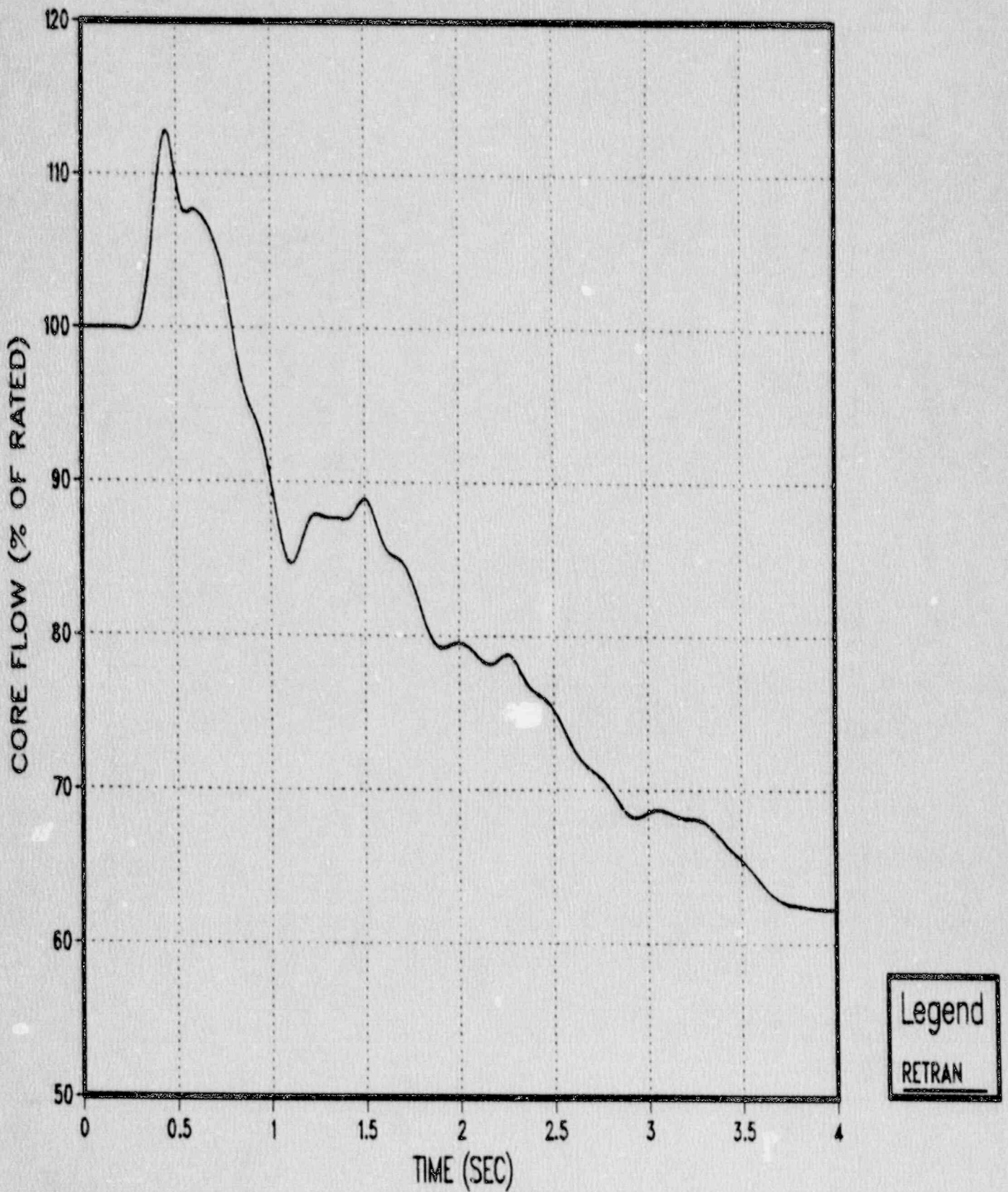

FIGURE 3.1-3 : GLRWOB DOME PRESSURE

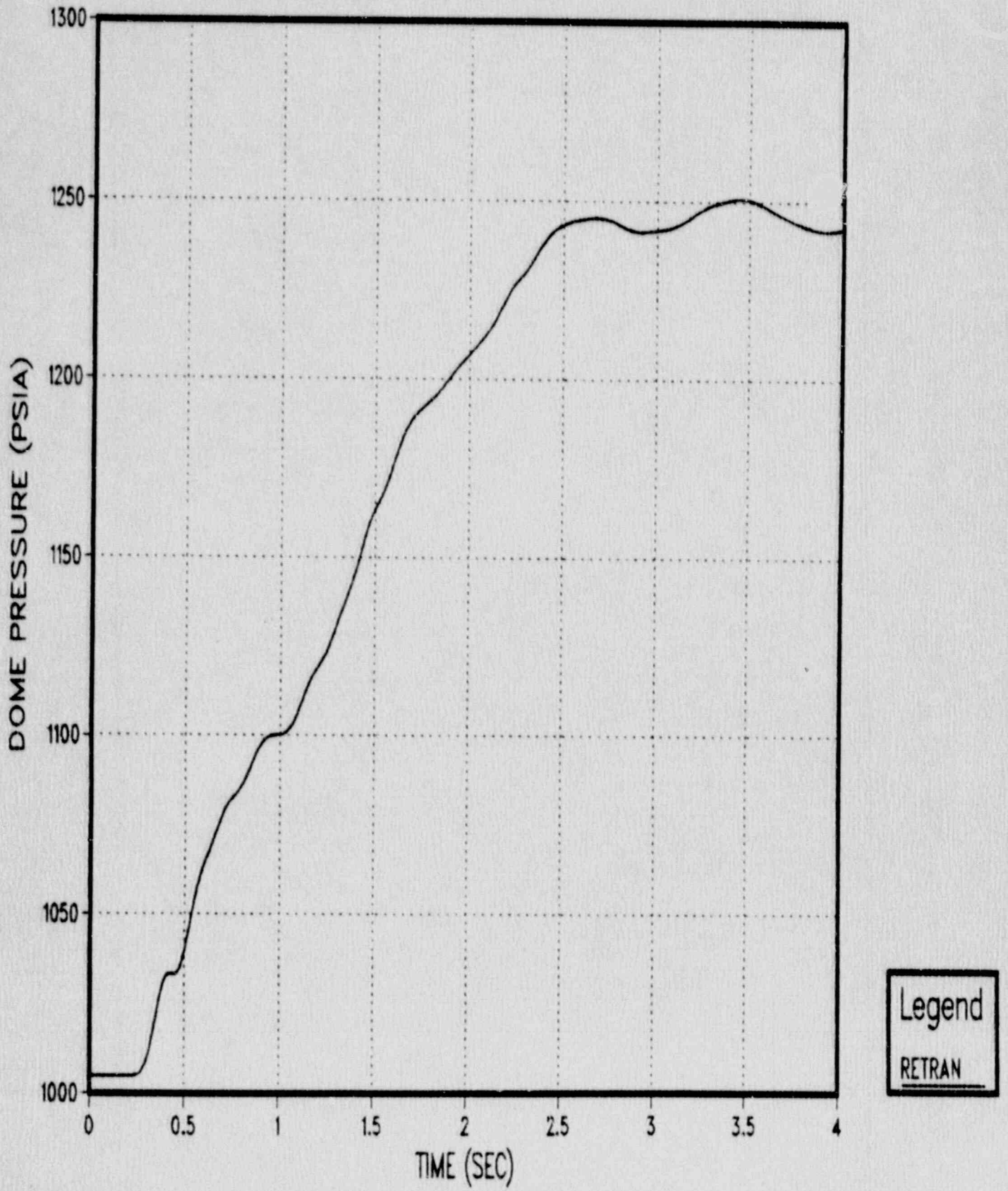

FIGURE 3.1-4 GLRWOB VESSEL STEAM FLOW

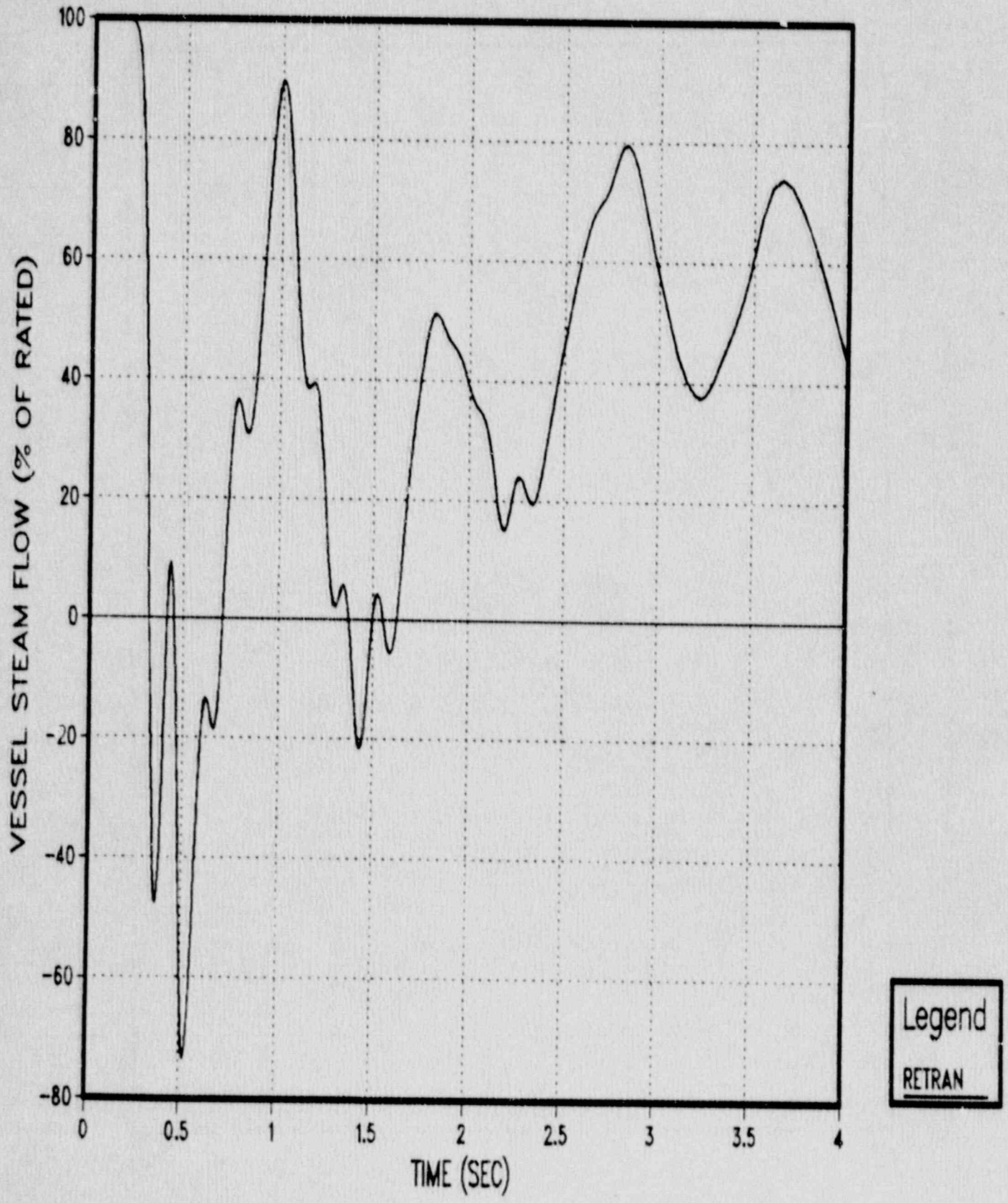

FIGURE 3.1-5 GLRWOB NARROW RANGE LEVEL

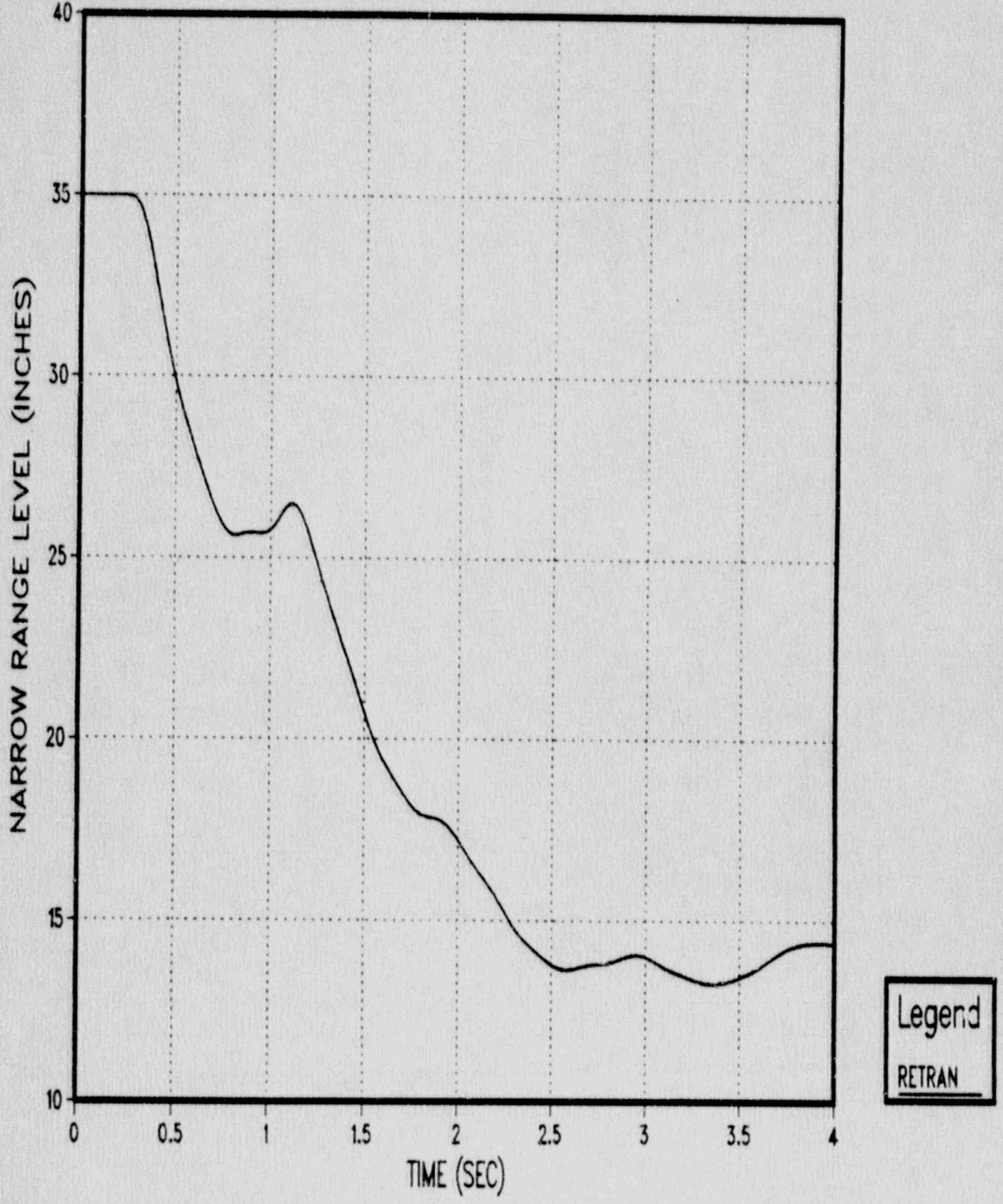

FIGURE 3.1-6 GLRWOB FEEDWATER FLOW

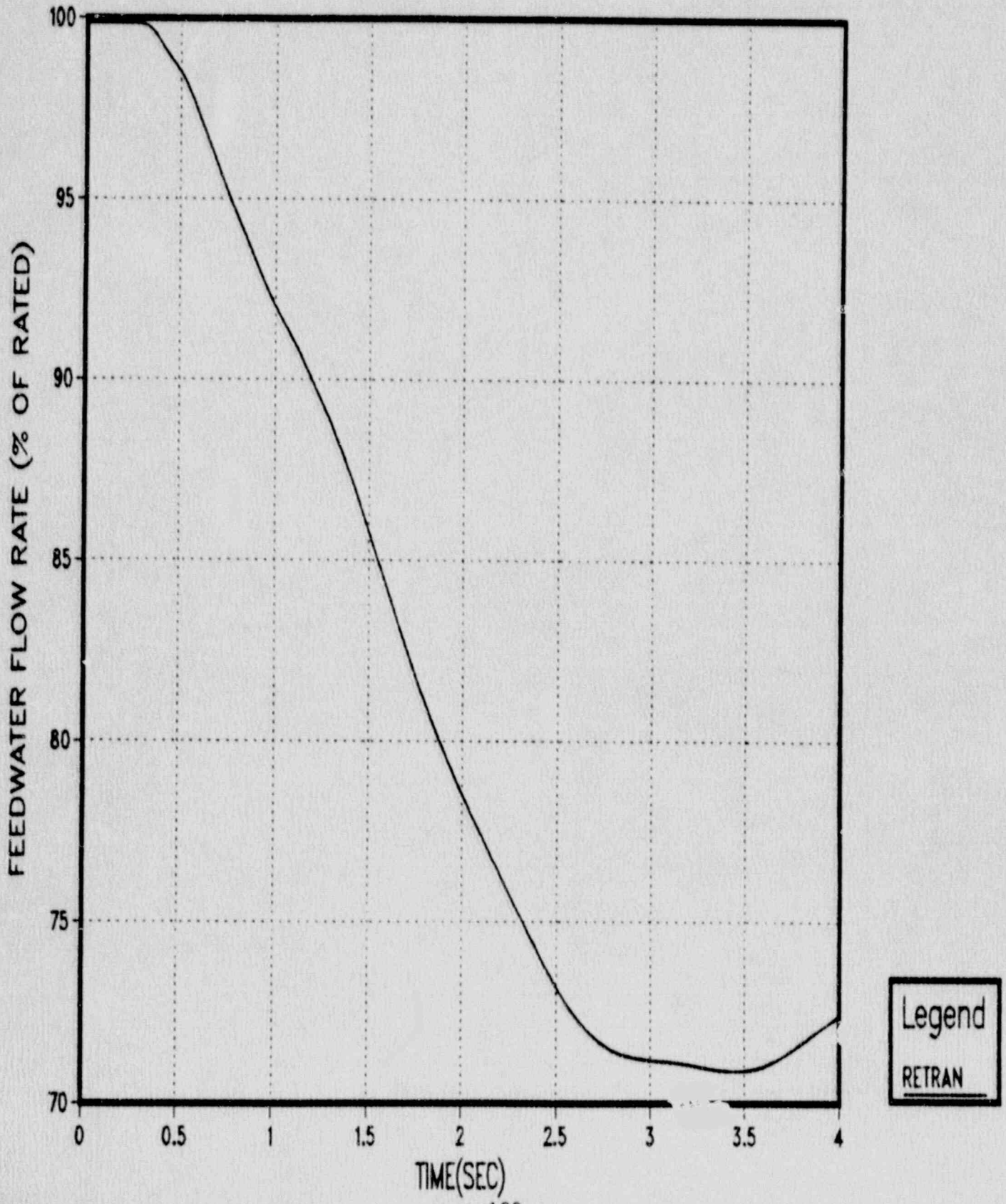

FIGURE 3.1-7 GLRWOB AVERAGE HEAT FLUX

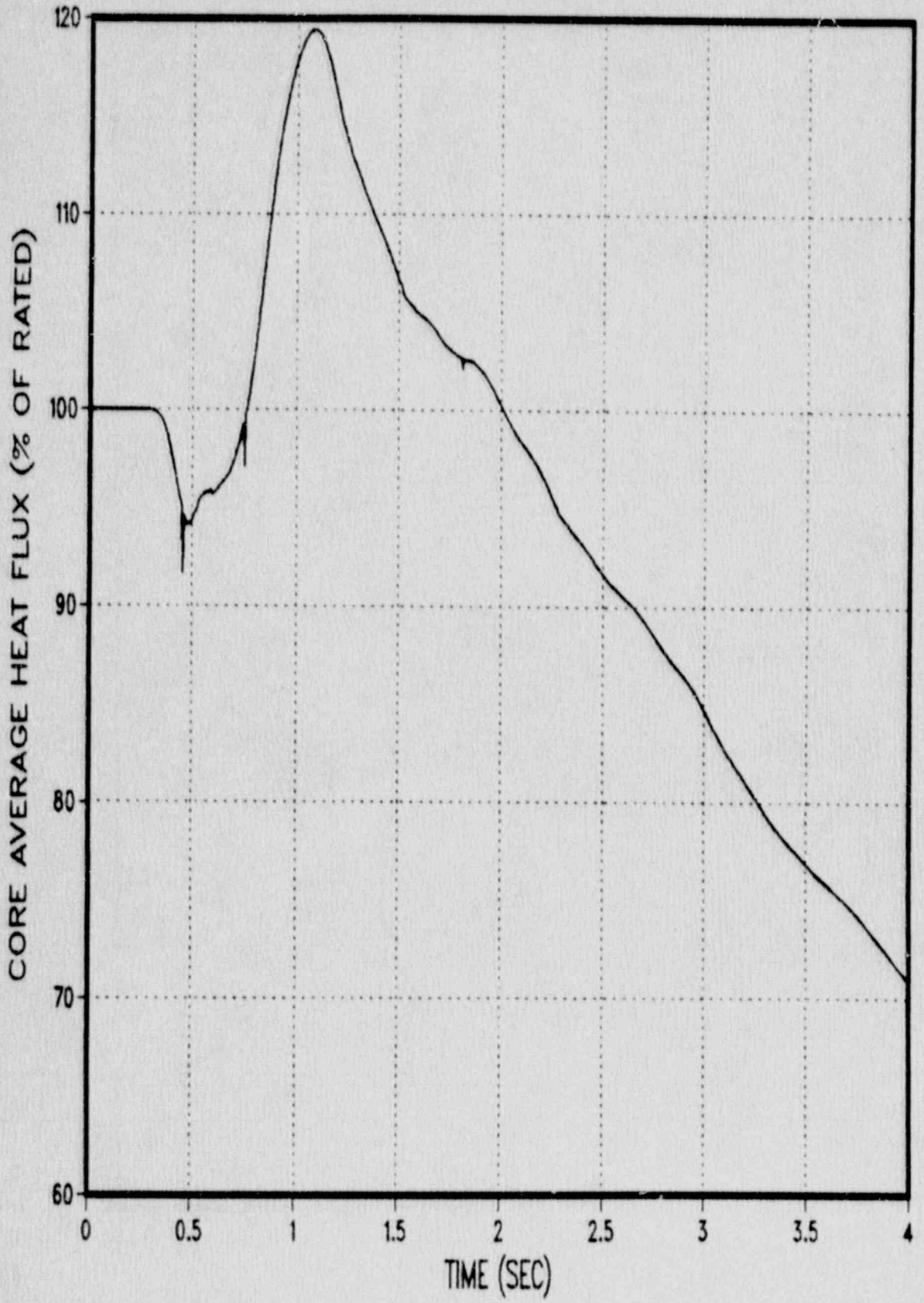

3.2 Feedwater Controller Failure

3.2.1 Event Description

The Feedwater Controller Failure (FWCF) event is expected to be one of the limiting events in establishing the MCPR operating limits. As demonstrated by the analyses presented in Section 3.2.2, the event produces larger calculated ΔCPRs at lower power levels.

The FWCF event is assumed to result in an increase in the feedwater demand signal to its maximum value. The failure causes the feedwater control system to increase feedwater flow to its maximum flow rate. This produces a cooldown of the middle and lower downcomer fluid and a reduction in core inlet temperature. The decrease in core inlet temperature causes a slow increase in core power due to a reduction in the core void fraction. The water level in the downcomer increases until a turbine trip signal is generated on high narrow range vessel level.

As a result of the turbine trip signal, both the TSVs and TCVs begin to close, causing an increase in reactor pressure. The rapidly increasing pressure causes a rapid core power increase due to void reactivity feedback. Closure of the TSVs and TCVs generates reactor trip and EOC-RPT signals. The turbine trip produces a fast opening signal for the main turbine bypass valves. Thus, the portion of the FWCF following turbine trip is similar to the Generator Load Rejection event presented in Section 3.1, except that the pressurization is mitigated by steam relief through the main turbine bypass valves. After a small power decrease due to initial scram rod insertion, the rapid pressurization produces a core power increase due to positive void reactivity feedback. The increase in core power causes a degradation in thermal margin (i.e., a reduction in

CPR). The event is typically analyzed at end of cycle, since the core is unrodded (i.e., worst case scram response) and the void coefficient is at its most negative value at this point in the cycle.

The Susquehanna SES Technical Specifications also allow operation with either the turbine bypass system or the EOC-RPT inoperable. Analyses of the FWCF to generate MCPR operating limits for these modes of operation will be performed using the methodology described in this section, with the exception that either the bypass system or EOC-RPT will be assumed to be inoperable, respectively.

3.2.2 Sensitivity Studies

RETRAN/CPRITER analyses were performed to determine the sensitivity of calculated RCPR to changes in input assumptions for the FWCF. The parameters analyzed were:

1) Control rod insertion rate
2) Recirculation Pump Trip (RPT) delay time
3) Turbine Control Valve (TCV) closure time
4) Safety Relief Valve (SRV) pressure setpoints and flow capacity
5) Feedwater temperature
6) Pressure regulator setpoint
7) Core power
8) Core flow
9) Steam line inertia
10) Steam line volume
11) Steam line pressure drop
12) Bypass valve capacity
13) Turbine trip high level setpoint
14) Maximum feedwater flow

The base case values for the sensitivity analyses are listed in Table 3.2-1. The FWCF is initiated in the RETRAN model by a manual trip on elapsed time. Results of the sensitivity analyses are shown in Table 3.2-2. Conclusions and observations from these analyses are discussed below.

A faster control rod insertion (scram curve) clearly produces a significant reduction in peak core power and, hence, RCPR. A reduction in RPT delay results in a faster reduction in core flow, which produces a reduction in peak core power and RCPR. Thus, use of the Technical Specification maximum RPT delay (currently 0.175 seconds) is conservative. A faster TCV closure produces a more severe vessel pressurization and results in a higher calculated RCPR.

The effects of using the relief mode of the SRVs (as opposed to the safety mode) are complex, because the pressure and core flow transients are different. A separate set of cases was run without bypass valve operation. The effect of assuming the relief valve mode of SRV operation for the case without bypass operation was to make the event less severe as it did for the GLRWOB event (see Section 3.1.2). Analysis results show that use of the relief mode for the FWCF (bypass available) and safety mode for the FWCF (bypass unavailable) is conservative.

A lower initial feedwater temperature causes a higher power rise before turbine trip. Although the effect is small, the lower initial feedwater temperature case produces a slightly higher peak power and calculated RCPR. An increase in pressure regulator setpoint, which raises dome pressure approximately the same amount, produces a small increase in RCPR. The effects of decreased feedwater temperature and increased pressure regulator setpoint on peak power and calculated RCPR are complex. Both cases show slightly more top peaked APDs than the base case, which

accounts for the slight increase in peak core power. However, the relative effects of changes in hot bundle enthalpies produced by the different pressure, flow, and heat flux transients are difficult to evaluate. The impact on RCPR is very small, as shown in Table 3.2-2 for changes of 10°F and 32 psi in feedwater temperature and pressure regulator setpoint, respectively.

The FWCF event is more adverse (i.e., higher calculated RCPR) at lower initial core power. This is due to the fact that the initial feedwater flow is lower. Thus, an increase of feedwater flow to its maximum value has a larger effect on the core inlet temperature reduction and core power increase prior to turbine trip. Therefore, licensing analyses must consider the FWCF at different power levels. At 100% core flow compared to 87% core flow, with all other factors the same, the core axial power distribution is more top peaked. The more top peaked axial power distribution produces a higher peak core power due to scram effects and, hence, a higher calculated RCPR.

The steam line parameters (inertia, volume, and pressure drop) all affect the pressure wave in the steam line. Higher inertia creates a higher pressure peak at the TCV and a higher pressurization rate in the steam dome. This adverse pressurization produces a higher and broader power versus time curve, which produces a larger calculated RCPR. A larger steam line volume reduces the vessel pressurization and RCPR, since more mass and energy are required to pressurize the larger volume. A larger steam line pressure drop means a higher resistance to flow (i.e., larger loss coefficients). The larger loss coefficients will attenuate the pressure wave more as it travels from the TCVs to the vessel, producing a lower peak power and a lower RCPR.

The capacity of the bypass valves has a significant effect on the pressurization portion of the FWCF and, hence, the peak core power and RCPR. A higher turbine trip water level setpoint allows a longer cooldown

and power increase prior to turbine trip and produces a higher calculated RCPR. The FWCF to maximum demand is more adverse than the FWCF to a smaller than maximum demand, since the FWCF to maximum demand produces a more severe cooldown and power rise prior to turbine trip.

3.2.3 Licensing Analysis Method

The FWCF event will be analyzed at 100% core flow and various power levels, since calculated RCPR increases as initial power level decreases. Additional assumptions made in the analysis are based on the sensitivity analyses described in Section 3.2.2. These assumptions include:

1) Technical Specification scram curve.

2) Technical Specification maximum scram and EOC-RPT delays.

3) Conservative bypass valve opening times based on startup test acceptance criteria.

4) High water level turbine trip setpoint is equal to the Technical Specification allowable value, plus accuracy and calibration uncertainty, plus 5.0 inches for initial level variations (= 63.7 inches).

5) Conservative turbine stop valve closure time (= 0.1 seconds).

6) Failure is assumed to the maximum flow rate.

7) Analysis performed at the maximum allowed cycle exposure with all rods out. If cycle exposure dependent MCPR operating limits

are to be specified, additional cycle exposure points will be analyzed.

8) Code uncertainty is applied to calculated RCPR as specified in Section 8 of Reference 2. The Reference 2 code uncertainty is increased to include steam line uncertainties using the root sum square technique in the same manner that was used for the GLRWOB. The uncertainty in feedwater temperature was included along with the steam line parameter uncertainties, and Table 3.2-3 illustrates the calculation. The effect of the steam line uncertainties on the FWCF event is less than their effect on the GLRWOB, as can be seen by comparing Tables 3.1-5 and 3.2-3. This is expected since the pressurization effect for the FWCF is less severe than it is for the GLRWOB, due to operation of the turbine bypass valves. Also, the effect of these uncertainties on the total code uncertainty is small.

The sample licensing event presented in Section 3.2.4 uses the above assumptions. However, the Statistical Combination of Uncertainties (SCU) methodology described in Appendix B may also be used for the FWCF event.

3.2.4 Sample Licensing Analysis

This section presents a sample licensing analysis for a Unit 2 Cycle 2 FWCF at 100% power/100% flow using the conservative assumptions described in Section 3.2.3. The transient behavior of key system parameters is presented in Figures 3.2-1 through 3.2-8. As shown in Figure 3.2-6, the FWCF causes a rapid increase in feedwater flow. The immediate effect of the flow increase is to increase the downcomer level and elevation head which produces an increase in core flow at about 2 seconds. As shown in Figure 3.2-8, the core inlet enthalpy begins to decrease rapidly around 6 seconds into the event, which causes a rapid power increase. A second "wave" of cold water comes by way of the recirculation loop piping. After

transitting the recirculation loops, additional colder water enters the jet pumps as drive flow at around 21 seconds. At approximately 25 seconds, the turbine trip causes a scram and rapid pressurization as shown in Figure 3.2-1. Due to the operation of the bypass valves, the resulting power peak is significantly less severe than the GLRWOB described in Section 3.1. The calculated ΔCPR for the event, including RETRAN code uncertainty is 0.20.

TABLE 3.2-1

Feedwater Controller Failure
Base Case Input Assumptions

	Parameter	Assumption
1.	Control Rod Insertion	Technical Specification minimum insertion rate
2.	Recirculation Pump Trip Delay Time (sec)	Technical Specification value
3.	Turbine Control Valve Closure Time (sec)	Best estimate value based on plant data
4.	Safety/Relief Valve Operation	Technical Specification required safety valve mode of SRVs with six SRVs out of service.
5.	Feedwater Temperature	Best estimate value based on plant data
6.	Pressure Regulator Setpoint	Best estimate value based on plant data
7.	Core Power	100%
8.	Core Flow	100%
9.	Steam Line Inertia	Best estimate values (Reference 2)
10.	Steam Line Volume	Best estimate values (Reference 2)
11.	Steam Line Pressure Drop	Best estimate values (Reference 2)
12.	Bypass Valves Capacity	Best estimate values based on plant measurements
13.	Turbine Trip Level Setpoint	Technical Specification allowable value, plus accuracy and calibration uncertainty plus 5 inches for initial level variations (= 63.7 inches)
14.	Maximum Feedwater Flow	135% rated

TABLE 3.2-2

Feedwater Controller Failure
Results of Sensitivity Analyses

Parameter	Change from Base Value	Change in Peak Core Power (% rated)	Change in RCPR
1. Control Rod Insertion	Best estimate curve based on plant data	-31.9	-.053
2. RPT Delay (sec)	-.025 seconds	-5.2	-.003
3. TCV Closure Time (sec)	-.008 seconds (-10%)	+2.8	+.002
4. SRV Operation	Relief mode/all valves operable	0.0	+.006
5. Feedwater Temperature	-10°F	+13.4	+.003
6. Pressure Regulator Setpoint	+32 psi	+7.9	+.003
7. Core Power	-35% (65% power/100% flow)	-	+.072
8. Core Flow	-13% (100% power/87% flow)	-25.1	-.031
9. Steam Line Inertia	+25%	+12.0	+.006
10. Steam Line Volume	+5%	-3.2	-.003
11. Steam Line Pressure Drop	+29.5 psi	-22.8	-.015
12. Bypass Capacity	-10% -100%	+24.7 +232.1	+.016 +.120
13. Turbine Trip Level Setpoint	-5 inches	-5.6	-.006
14. Maximum Feedwater	-10% rated	-5.7	-.004

TABLE 3.2-3

Steam Line Parameters: Contribution to Code Uncertainty for FWCF

Parameter	Uncertainties[1]	dRCPR/dx[2]	S_x^{RCPR}
Steam Line ΔP(psi)	5	-.0005/psi	.0025
Steam Line Inertia (%)	5	+.00032/%	.0016
Steam Line Volume (%)	5	-.0006/%	.0030
Turbine Control Valve Closure Time (% of best estimate)	10	-.0002/%	.0020
Pressure Regulator Setpoint (psia)	5	+.0001/psi	.0005
Feedwater Temperature (°F)	5	-.0003	.0015

(1) S_x; based on an engineering assessment of the parameters.

(2) $$S_x^{RCPR} = S_x \left| \frac{dRCPR}{dx} \right|$$

(3) Steam Line Parameters' Contribution to Code Uncertainty ($S_{steamline}^{RCPR}$)

$$S_{steamline}^{RCPR} = \left[\sum (S_x^{RCPR})^2 \right]^{1/2} = .005$$

FIGURE 3.2-1 : FWCF CORE POWER

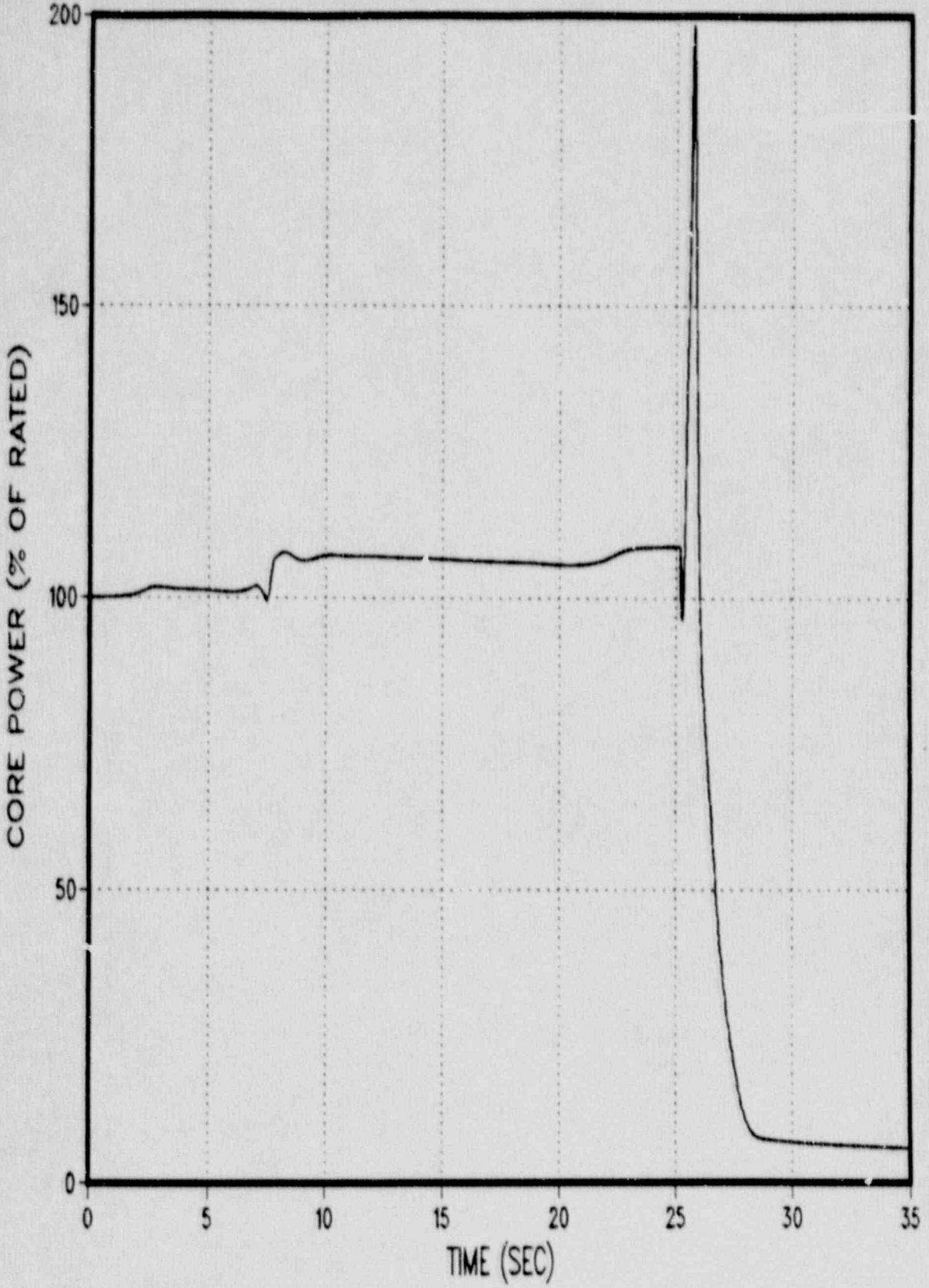

FIGURE 3.2-2 : FWCF CORE FLOW

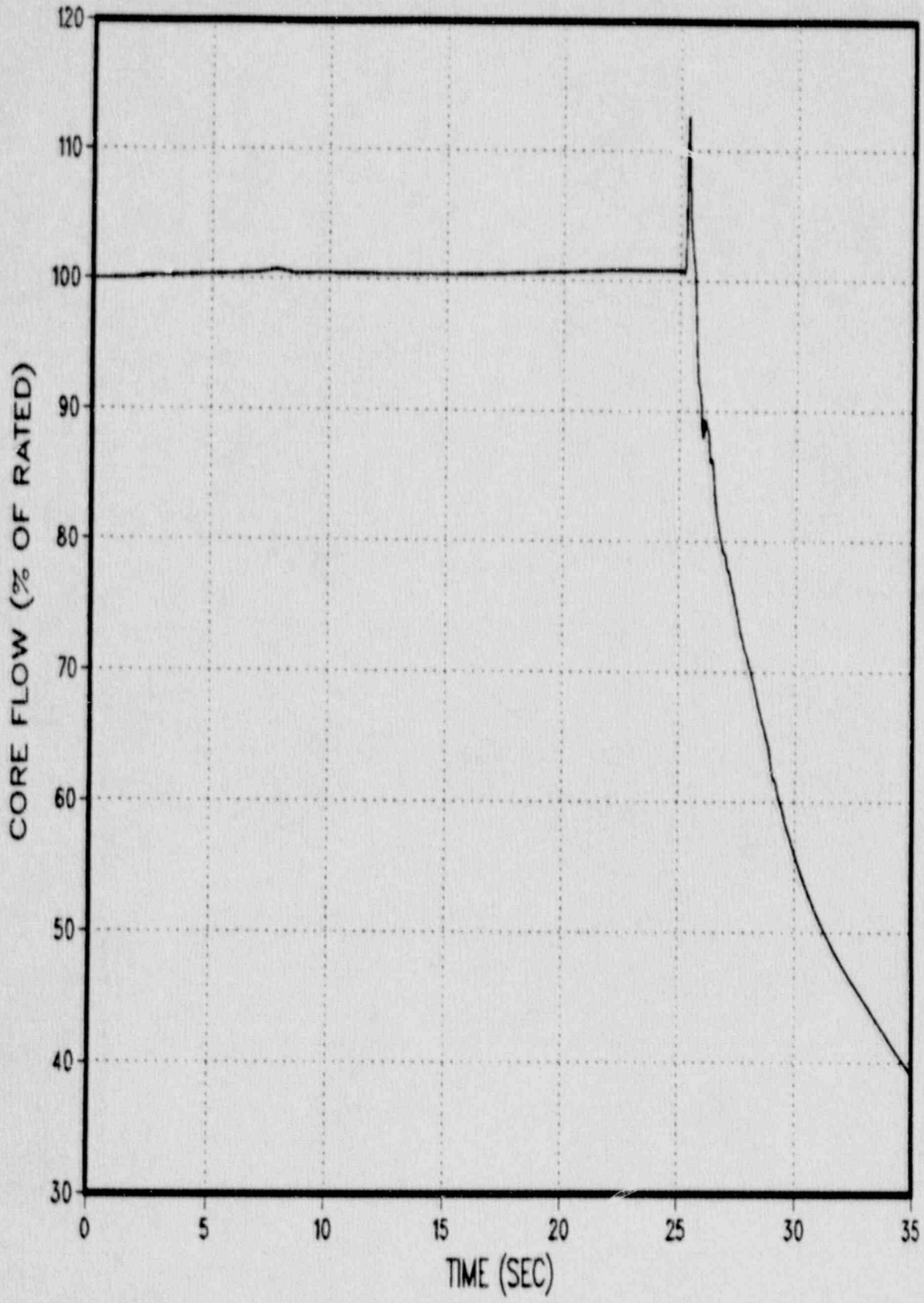

FIGURE 3.2-3 : FWCF DOME PRESSURE

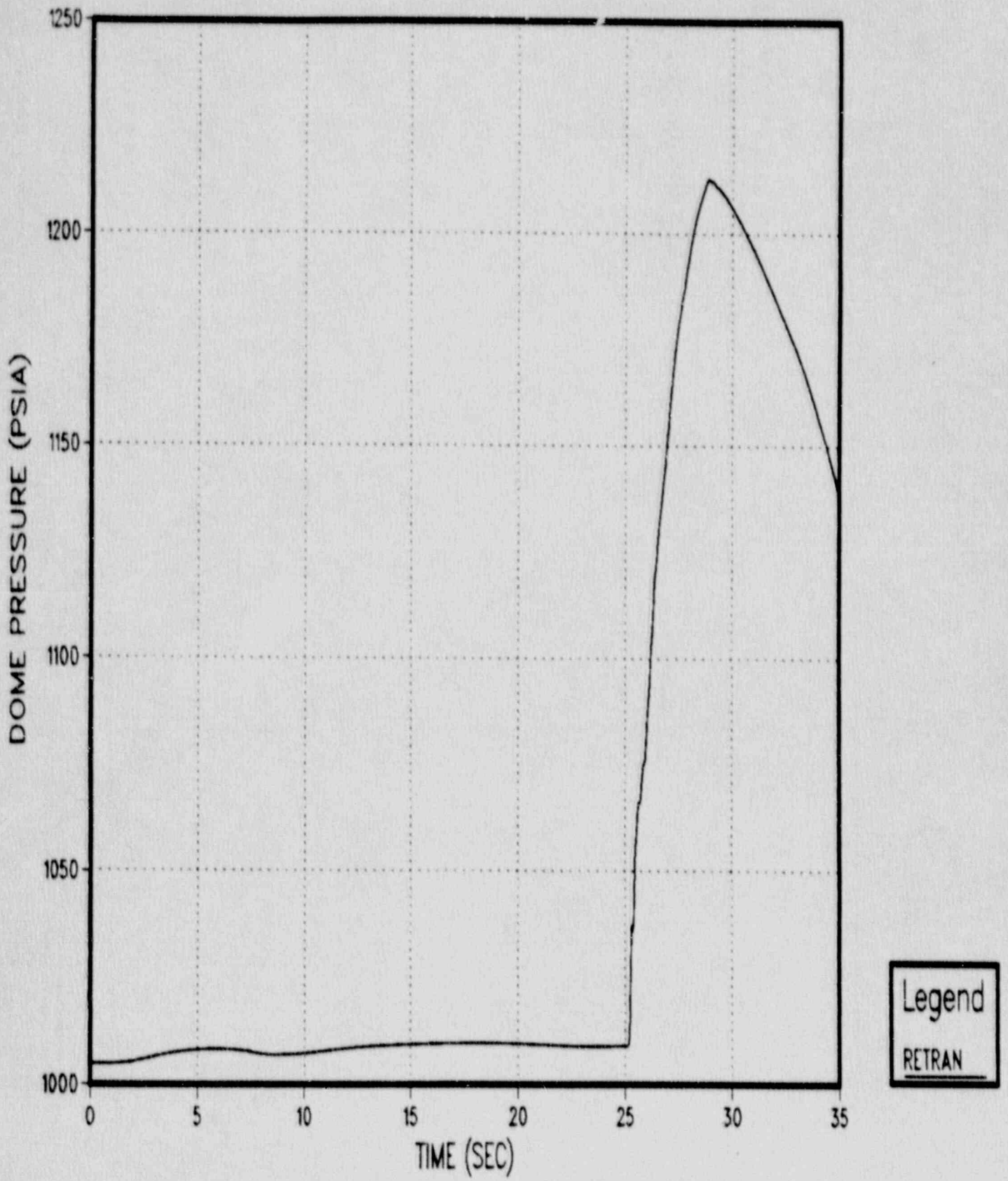

FIGURE 3.2-4 FWCF VESSEL STEAM FLOW

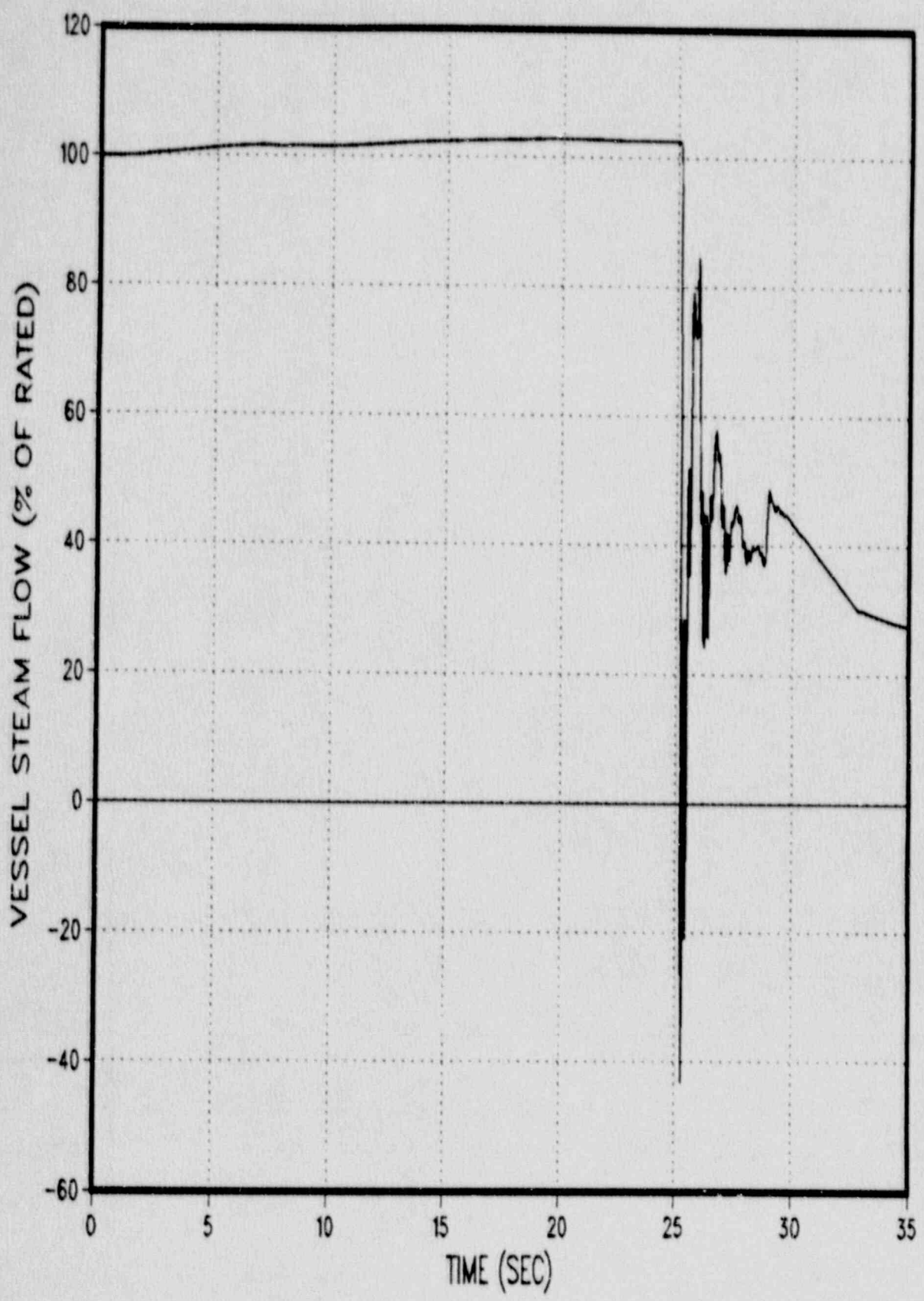

FIGURE 3.2-5 FWCF NARROW RANGE LEVEL

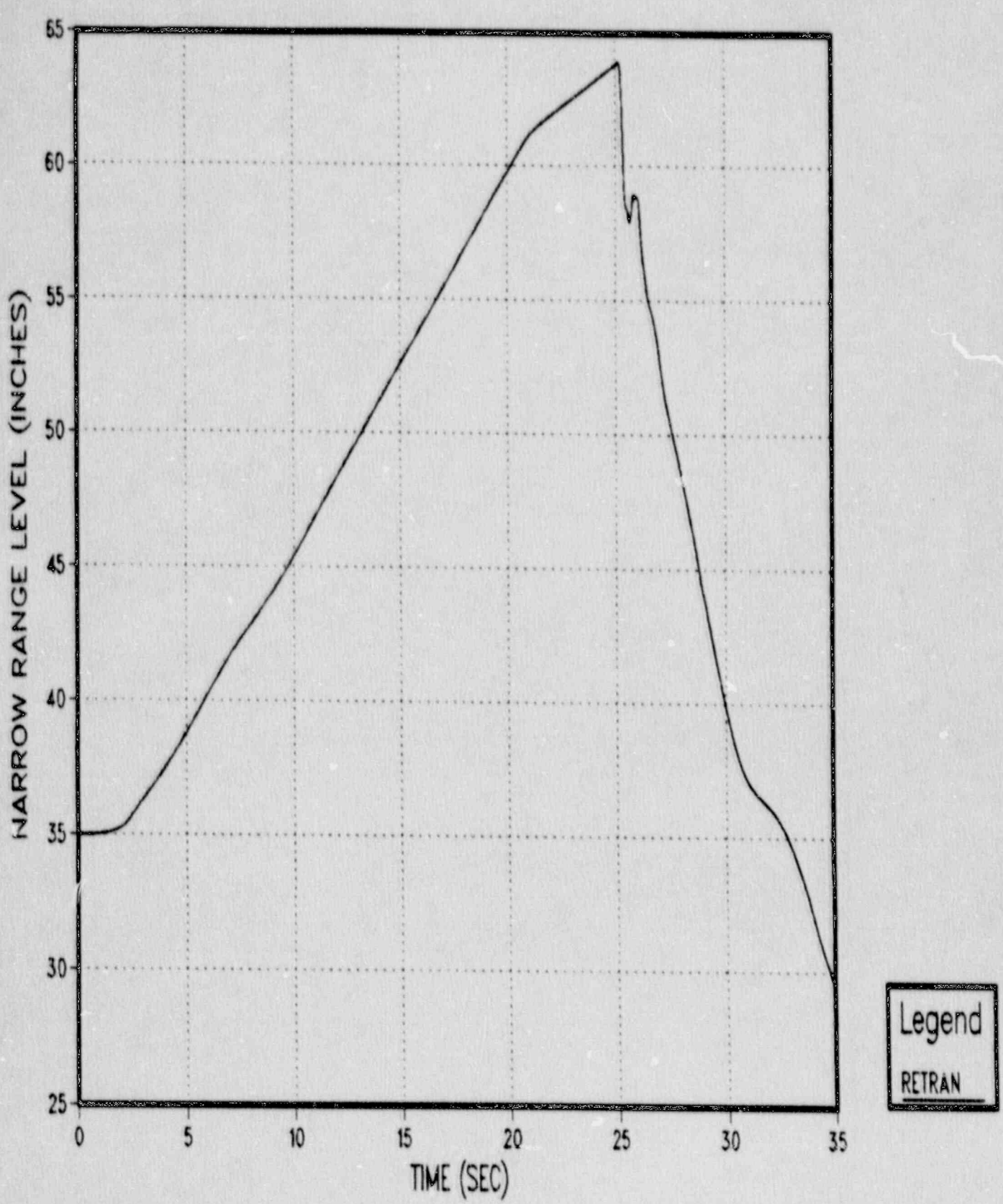

FIGURE 3.2-6 FWCF FEEDWATER FLOW

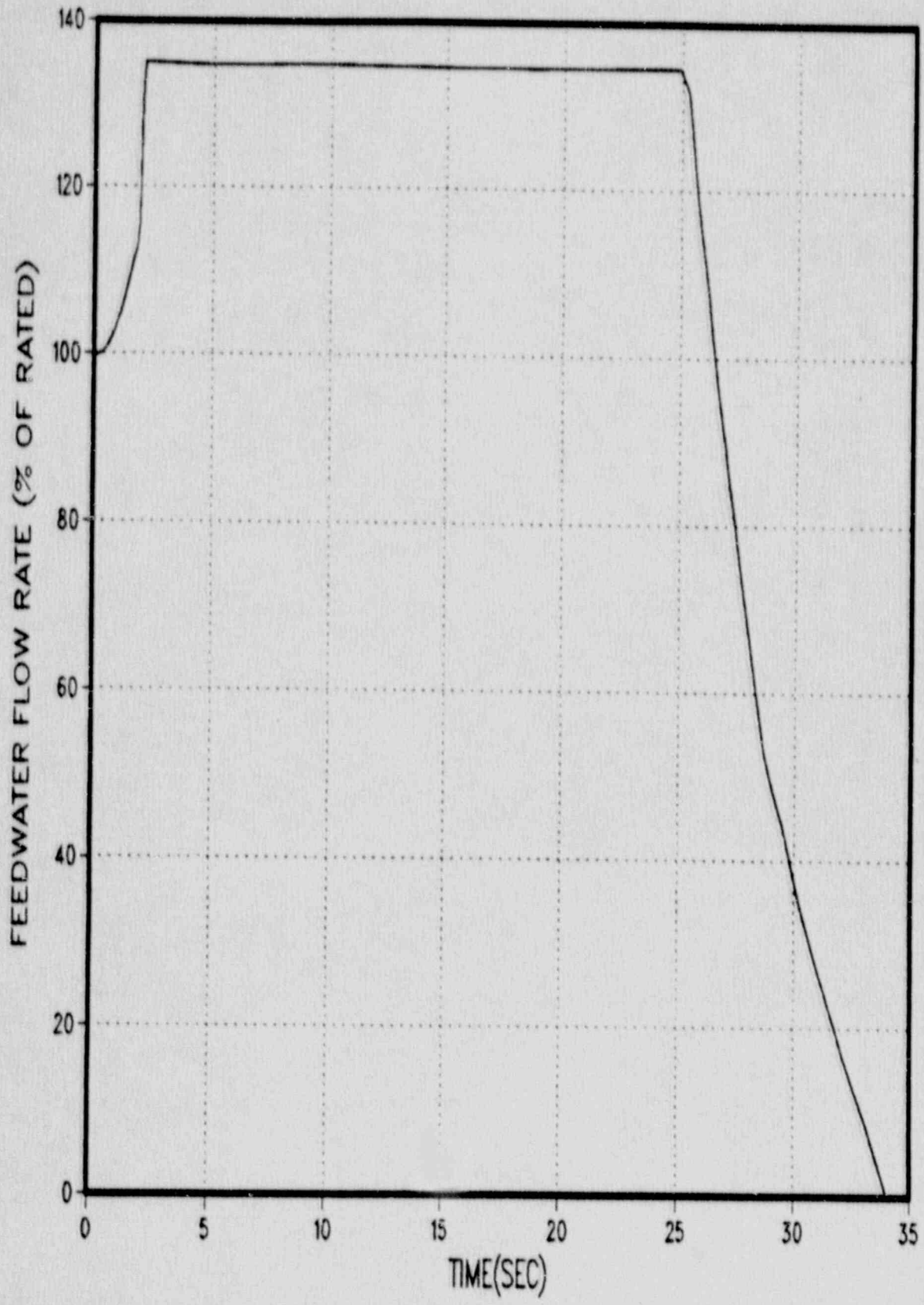

FIGURE 3.2-7 FWCF AVERAGE HEAT FLUX

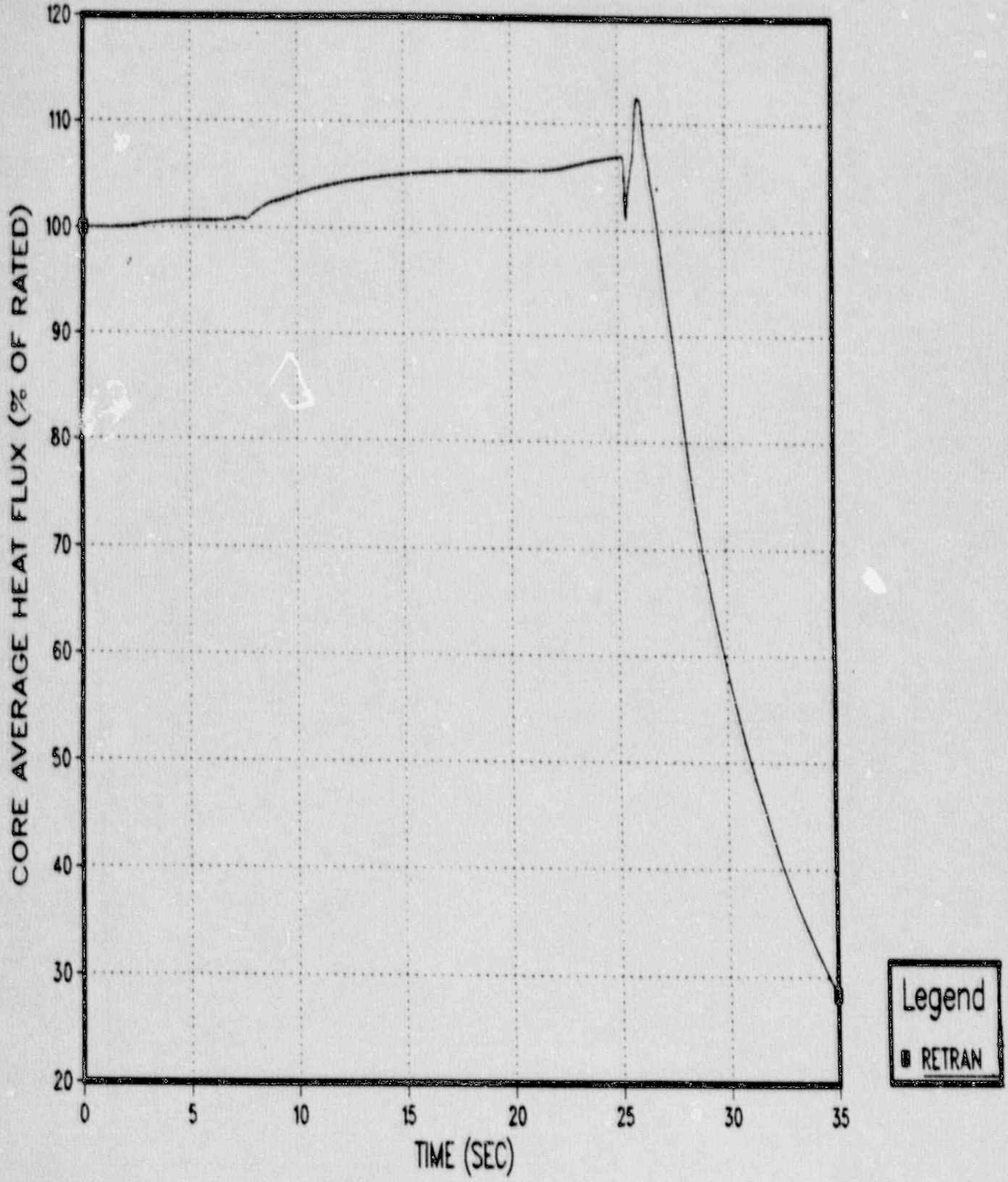

FIGURE 3.2-8 CORE INLET ENTHALPY

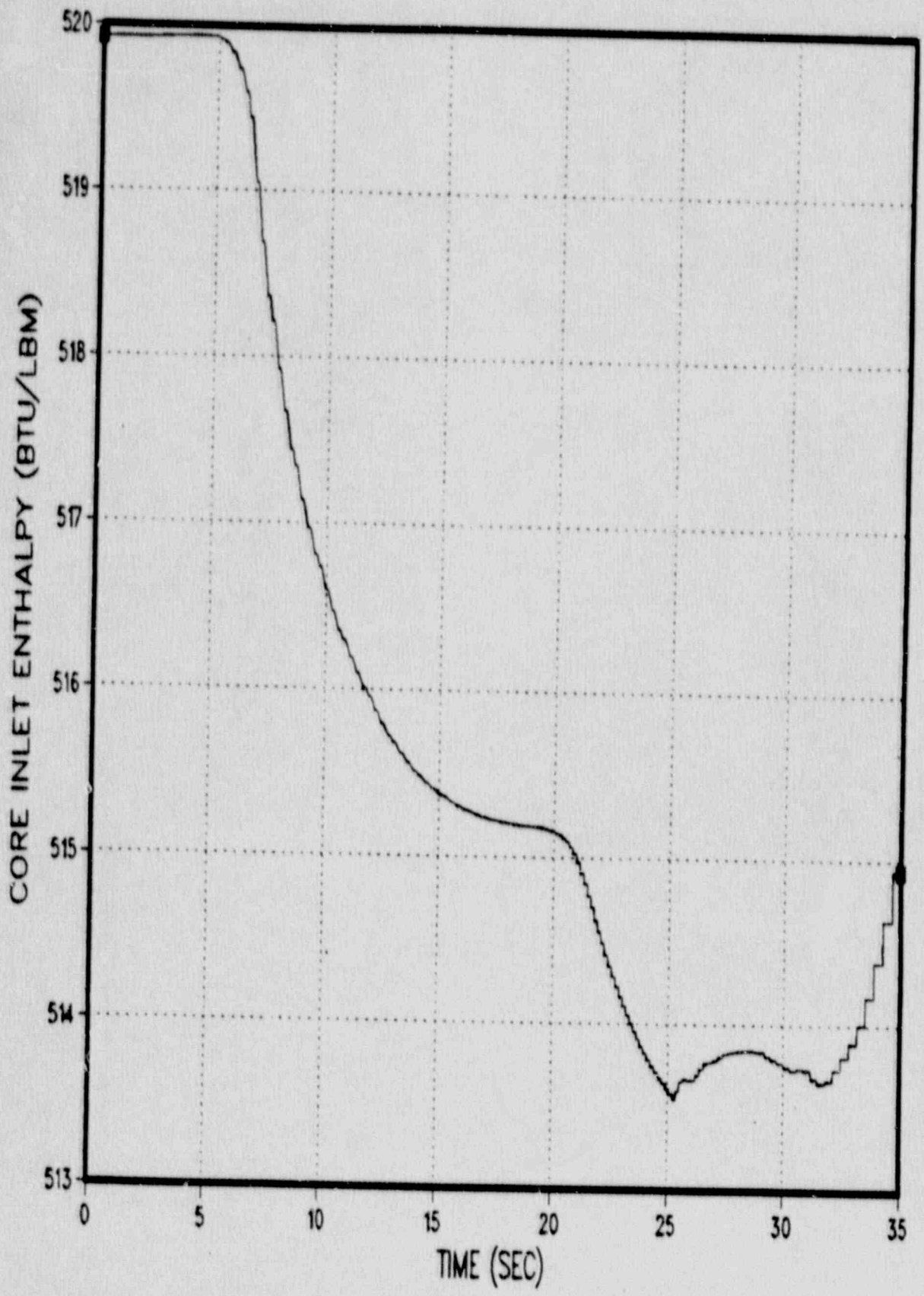

3.3 Recirculation Flow Controller Failure

3.3.1 Event Description

The Recirculation Flow Controller Failure (RFCF) event with increasing flow is expected to be one of the limiting events in establishing the Minimum Critical Power Ratio (MCPR) operating limits at low reactor core flow conditions. A RFCF event can result in either an increase or a decrease in core flow. The RFCF event with decreasing flow is not analyzed for each reload, because the power decreases during the event. The decrease in power for the RFCF event with decreasing flow makes it non-limiting from a MCPR standpoint.

The RFCF event is initiated when either the master controller or a single individual loop controller fails. The failure of the master controller causes the individual loop controller input demands to increase. This causes both reactor recirculation pumps to increase core flow thereby increasing reactor power. The maximum rate at which the individual controller inputs can change is limited electronically to prevent rapid core flow increases while still providing adequate operating maneuverability. Failure of an individual loop controller causes the demand input to the MG-set scoop tube positioner to increase. The rate of increase of the positioner is limited by the physical size of the system. Since there is no mechanical or electrical limiting of the positioner demand input, an individual controller failure can cause a faster recirculation loop flow increase than a master controller failure. In either case, the events are either terminated by a reactor scram on high neutron flux or when a new steady state is reached.

3.3.2 Sensitivity Studies

3.3.2.1 Initial Studies

Sensitivity studies were performed to determine the most limiting master controller failure event and individual loop controller failure event. These events were analyzed from the three different power/flow conditions shown in Table 3.3-1. This range of conditions was chosen to determine the sensitivity of RCPR to core power and flow.

Analyses demonstrated that the RFCF event in which an individual loop controller fails is less limiting than the event in which the master controller fails. To determine this, the most limiting controller demand increase rate (hereinafter referred to as run-up rate) for both types of failures was determined. The RFCF event with an individual loop controller failure is more adverse when the run-up rate is high. This is also true for the master controller failure provided the high neutron flux trip setpoint is not reached. The slow rates are more adverse for the master controller failure if the high flux trip setpoint is reached. Each event is described below to explain this behavior.

The RFCF event in which the individual loop controller fails is terminated either by the high neutron flux scram trip or when the reactor reaches a new steady state, depending on the run-up rate that is used and the rod line from which the event is initiated. The slow run-up rate case has a peak core power and therefore a peak heat flux that is lower than the fast run-up rate case. Thus, a slower run-up rate produces a smaller change in CPR. This behavior was observed for all analyzed power/flow conditions with or without a reactor scram.

The RFCF event in which the master controller fails either is terminated by the high neutron flux reactor trip or reaches a new steady state, depending on the run-up rate that is used and the rod line from which the

event is initiated. If the event is initiated with a fast run-up rate at a high enough rod line to cause a scram on high neutron flux, then there exists a slower run-up rate which is limiting. A slower run-up rate will be limiting because the heat flux follows power more closely than it does for a faster run-up rate, thus producing a higher heat flux at the time of scram. The flow is also higher at the time of scram but this is not enough to compensate for the effect on CPR of the increase in heat flux. Therefore, the ΔCPR is greater for the slower run-up rate case. However, the ΔCPR will decrease if the run-up rate is too slow to cause a scram on high neutron flux. Results from a run-up rate study are presented in Table 3.3-2. The decrease in RCPR occurs for the slowest run-up case because the run-up rate is not fast enough to offset the effect that the increasing feedwater temperature has on the core power. This causes the core power to peak below the high neutron flux reactor trip setpoint. A smaller RCPR is calculated for this case because the power and heat flux peaks are lower than the peaks calculated for the faster run-up cases.

If the rod line that is chosen is too low to cause a scram on high neutron flux with the fastest allowable run-up rate, then the fastest rate will be limiting. This is because the power peak from the fast rate case is not limited by scram and will therefore be higher than the power peak from any case with a slower rate.

3.3.2.2 Limiting Case Studies

The most limiting RFCF event was determined by the RETRAN analyses discussed in Section 3.3.2.1 to occur when the master controller fails. The change in calculated CPR for this event is a strong function of the initial core power and flow condition. As the initial power level is lowered at a given core flow rate for this event, the ΔCPR increases. Even though the ΔCPR becomes greater for events initiated from lower

initial rod lines, the event will be analyzed along the 100% rod line. This is justified by the fact that as the core is operated on a lower rod line, the actual operating MCPR increases more than the calculated ΔCPR. Thus, the master controller failure from points along the 100% rod line is selected as the limiting event. Since this event will result in a high flux scram, the slow run-up rate will be limiting.

Analyses of the master controller slow run-up failure were performed for the 65% core power, 38% core flow initial condition. Sensitivities for this event are expected to be similar to those obtained from the low flow point of the 100% rod line. Two important parameters examined were the system model fuel pin gap conductance and the Maximum Combined Flow Limit (MCFL) setting. The effect of the cross section modification on the RFCF results was also investigated.

As gap conductance increases, the change in CPR increases. However, the increase in the ΔCPR was small. A larger value of gap conductance produces conservative results.

The MCFL setting determines the maximum amount of steam flow that is allowed to pass through the main steam line control valves and bypass valves. Once the steam flow reaches the MCFL setpoint, the valves are not allowed to open further. This prevents the valves from regulating vessel pressure. Once pressure regulation is lost, the vessel pressurizes rapidly causing an equally rapid power increase. The power increases until the high neutron flux scram setpoint is reached. The additional pressurization that occurs makes the event more severe. The amount of pressurization, if any, depends on the amount of steam flow generated during the event. Slow run-ups that are initiated from high power rod lines could produce steam flows high enough to cause a loss of pressure control depending on the MCFL setting. The effect of the MCFL setting on this event will be evaluated on a cycle by cycle basis.

Modification of the SIMTRAN-E cross sections is required for events with rapid and/or large amounts of core void change. Since the limiting RFCF event is not rapid and the amount of void change is small, the cross section modification process is not required for this event. The sensitivity study performed determined that using unmodified SIMTRAN-E cross sections produces conservative results for the RFCF event.

Additional sensitivity studies were performed to account for uncertainties in calculating the RCPR for the most limiting RFCF event. The code uncertainty in Section 8 of Reference 2 can not be applied to this transient, since it was generated for an event that is not similar to the RFCF event. A separate uncertainty was generated specifically for this event. The uncertainty was derived based on the uncertainties associated with calculating void and Doppler coefficients of reactivity for the event. The uncertainties for the calculated void and Doppler coefficients are estimated to be 25 and 10 percent, respectively. The sensitivities of RCPR to changes in Doppler and void coefficient were determined and multiplied by their respective uncertainties to calculate the uncertainties in terms of RCPR. The uncertainties in RCPR due to Doppler and void coefficients are combined by the Root Sum Square (RSS) method into a net uncertainty. This net uncertainty is doubled for conservatism (i.e., 2-sigma value), and expressed as a multiplier on the calculated RCPR for the event. The calculated multiplier for this event is 1.04. This multiplier can then be applied to the calculated RCPR to produce a conservative value of RCPR. This multiplier is applied to the RFCF event described in Section 3.3.4.

3.3.3 Licensing Analysis Method

The RFCF event will be analyzed on the 100% rod line for various core flows, since calculated RCPR increases as core flow is decreased along the

rod line. Additional assumptions made in the analysis are based on the sensitivity analyses described in Section 3.3.2. These assumptions include:

1) The Technical Specification scram curve is used.

2) The Technical Specification maximum scram delay is assumed.

3) The Simulated Thermal Power Monitor scram trip is not credited.

4) The High Neutron Flux Trip setpoint is at least equal to the allowable Technical Specification limit, plus calibration and accuracy uncertainties.

5) The limiting run-up rate will be determined for the event.

6) The RCPR uncertainty generated in Section 3.3.2 is applied to the calculated RCPR for this event. This multiplier is applied to the RFCF event described in Section 3.3.4.

The sample licensing analysis presented in Section 3.3.4 used the above assumptions.

3.3.4 Sample Licensing Analysis

This section presents a sample licensing analysis for a Unit 2 Cycle 2 RFCF from 65% power/38% flow using the conservative assumptions described in Section 3.3.3. The transient behavior of key system parameters is presented in Figures 3.3-1 through 3.3-7. The calculated change in CPR for the event, including the RFCF event specific uncertainties is 0.44. For an actual reload application, several RFCF analyses will be performed

from points on the 100% rod line to generate the MCPR operating limit as a function of core flow.

TABLE 3.3-1

Single and Two Loop RFCF Events
Initial Power/Flow Conditions

Core Power (% rated)	Approximate Core Flow (% rated)	Rod Line (%)
65	38	118
40	38	73
40	65	52

TABLE 3.3-2

Change in RCPR as a Function of Master Controller Run-up Rate for the 65/38 Power/Flow RFCF

Run-up Rate (%/Sec)	Change in RCPR
0.3	-.006*
0.4	0.0
0.5	-.002
2.0	-.007
10.0	-.032

* Did not result in reactor scram

FIGURE 3.3-1 : RFCF CORE POWER

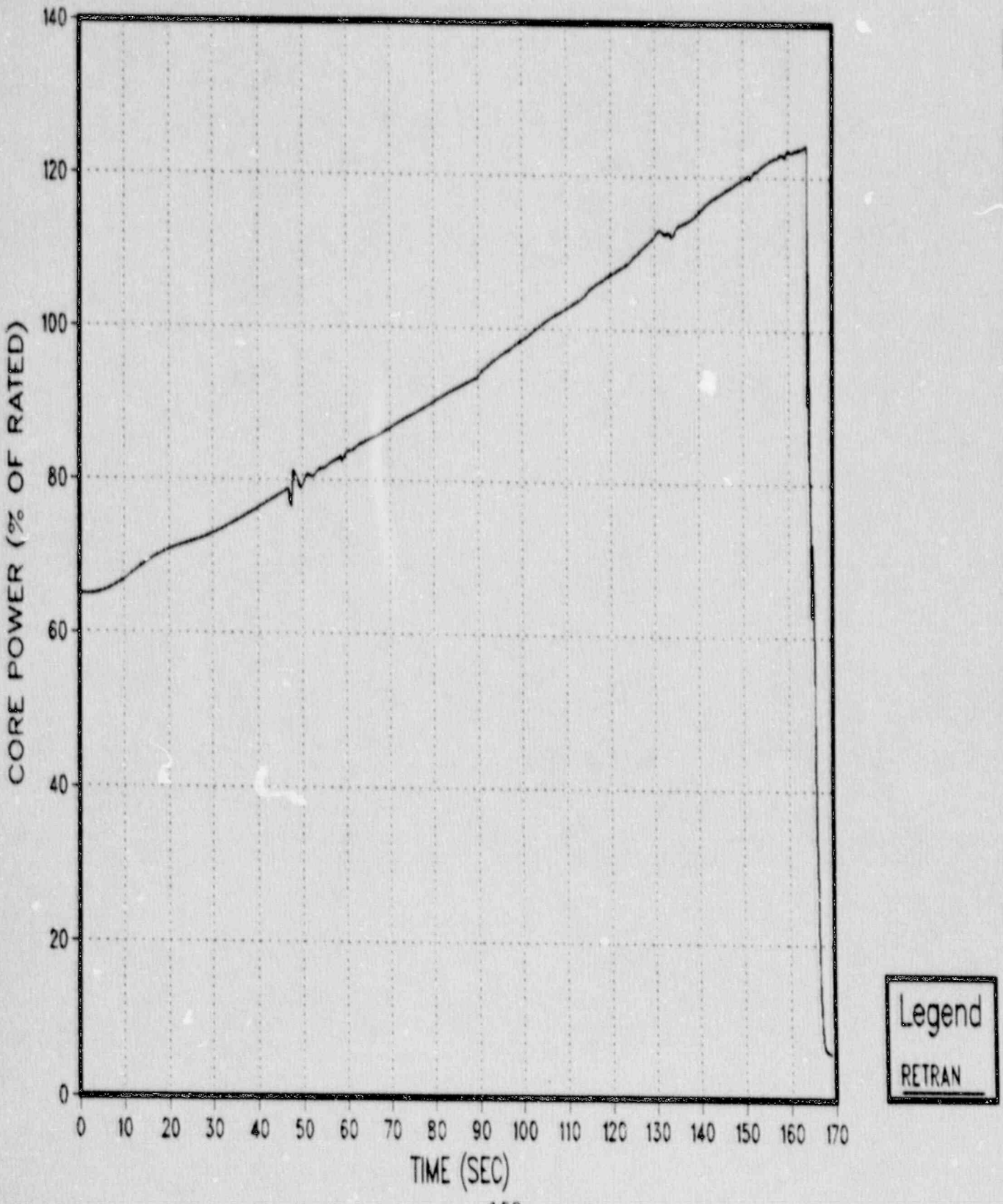

FIGURE 3.3-2 : RFCF CORE FLOW

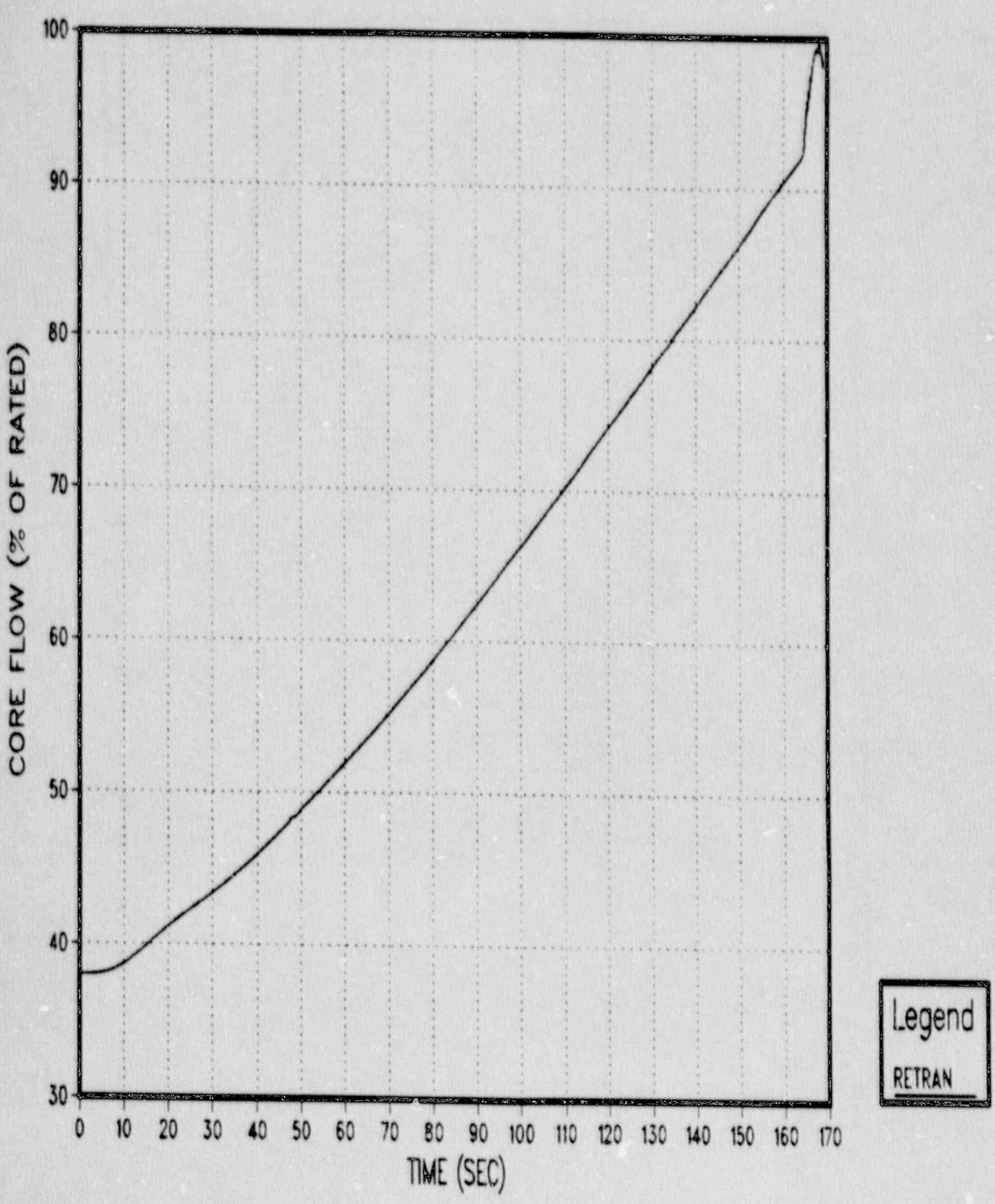

FIGURE 3.3-3 : RFCF DOME PRESSURE

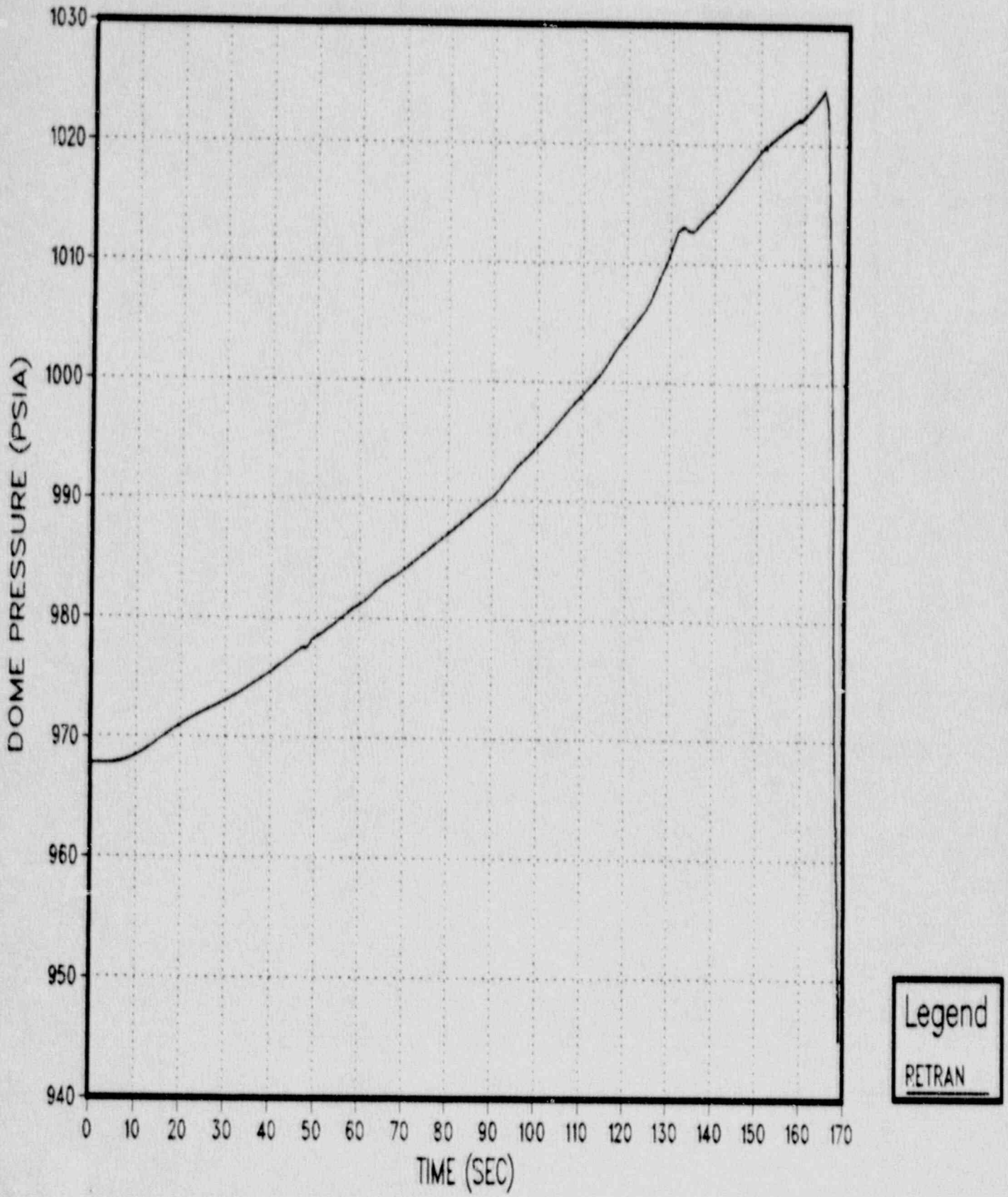

FIGURE 3.3-4 RFCF VESSEL STEAM FLOW

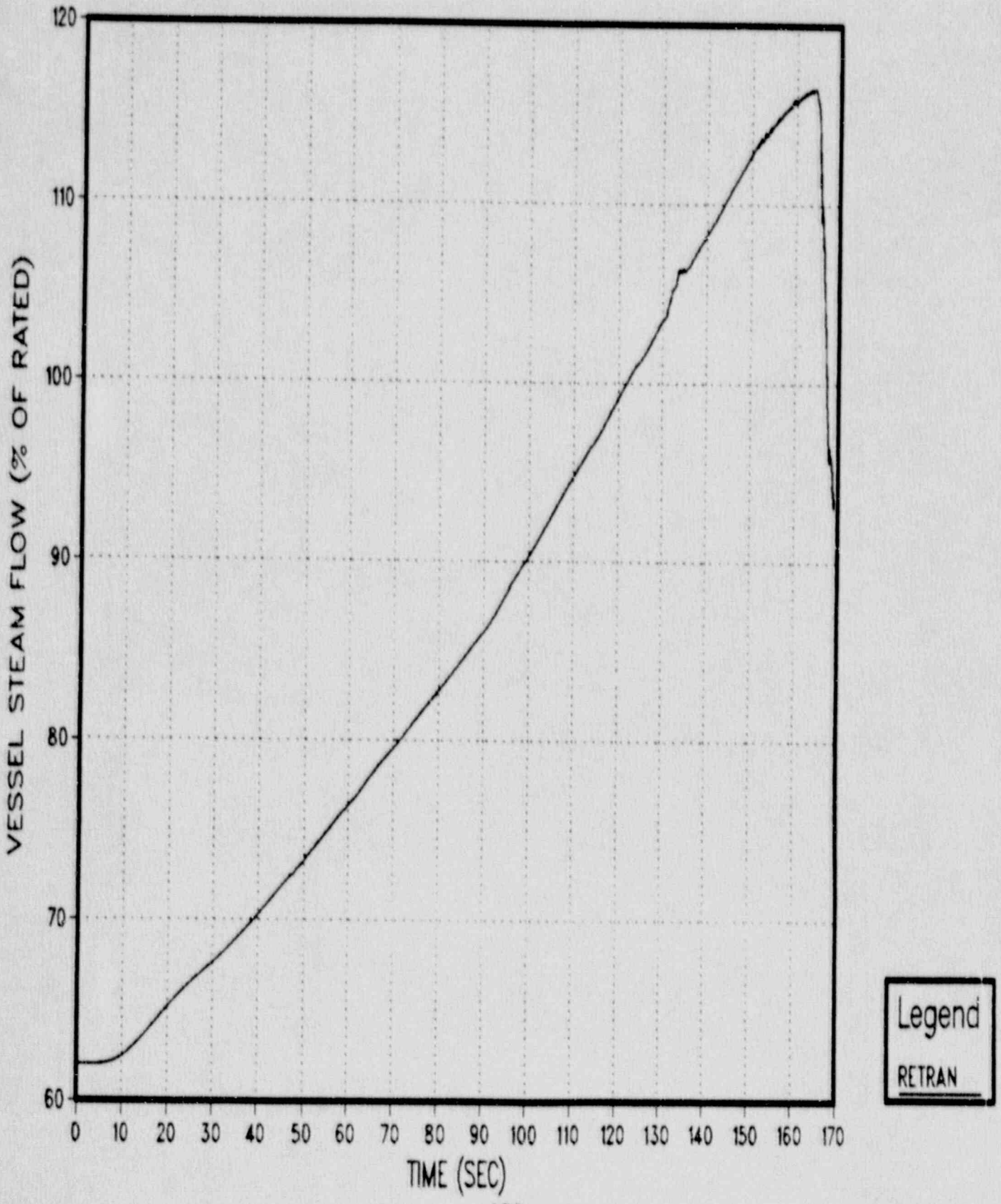

FIGURE 3.3-5 RFCF NARROW RANGE LEVEL

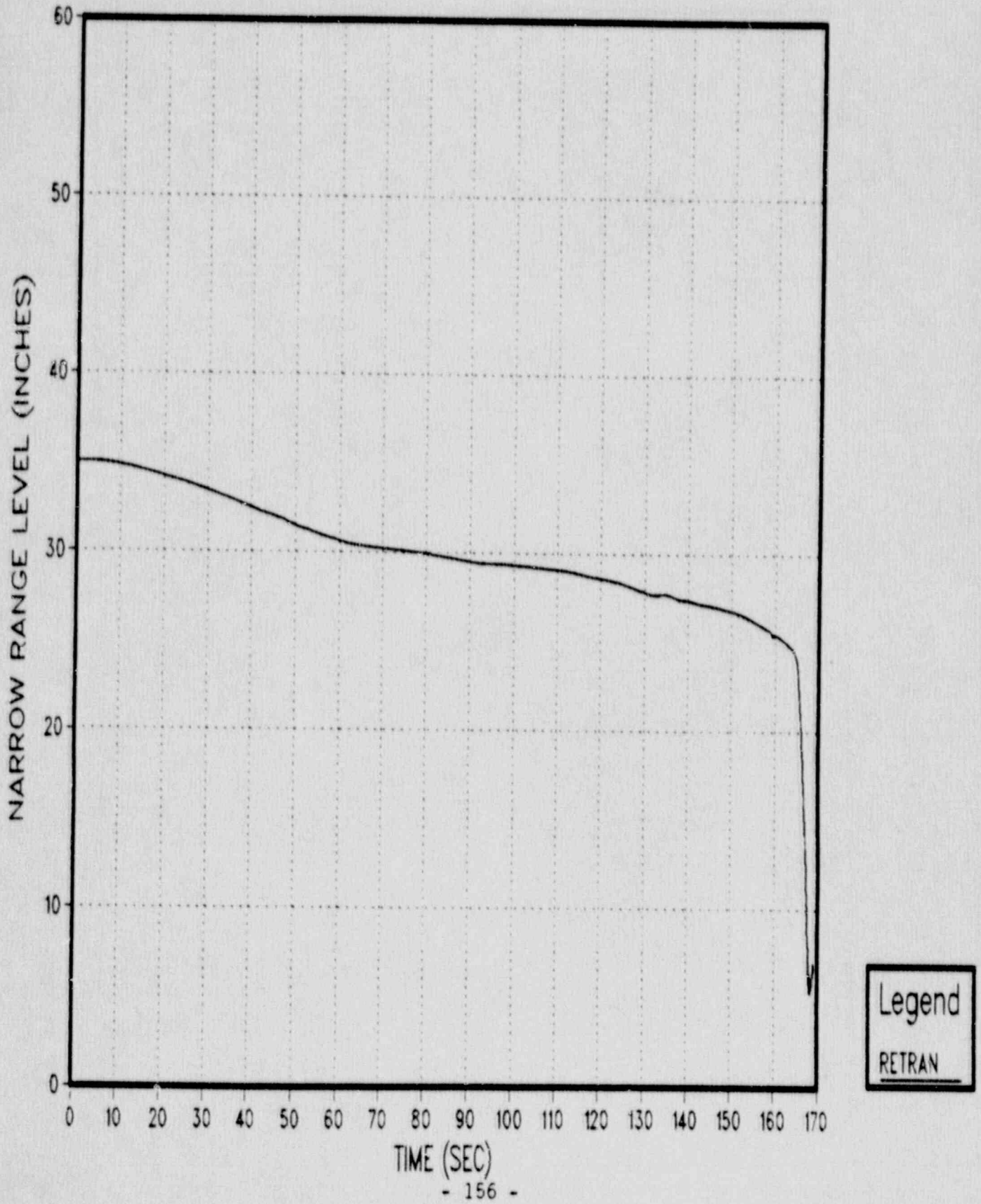

FIGURE 3.3-6 RFCF FEEDWATER FLOW

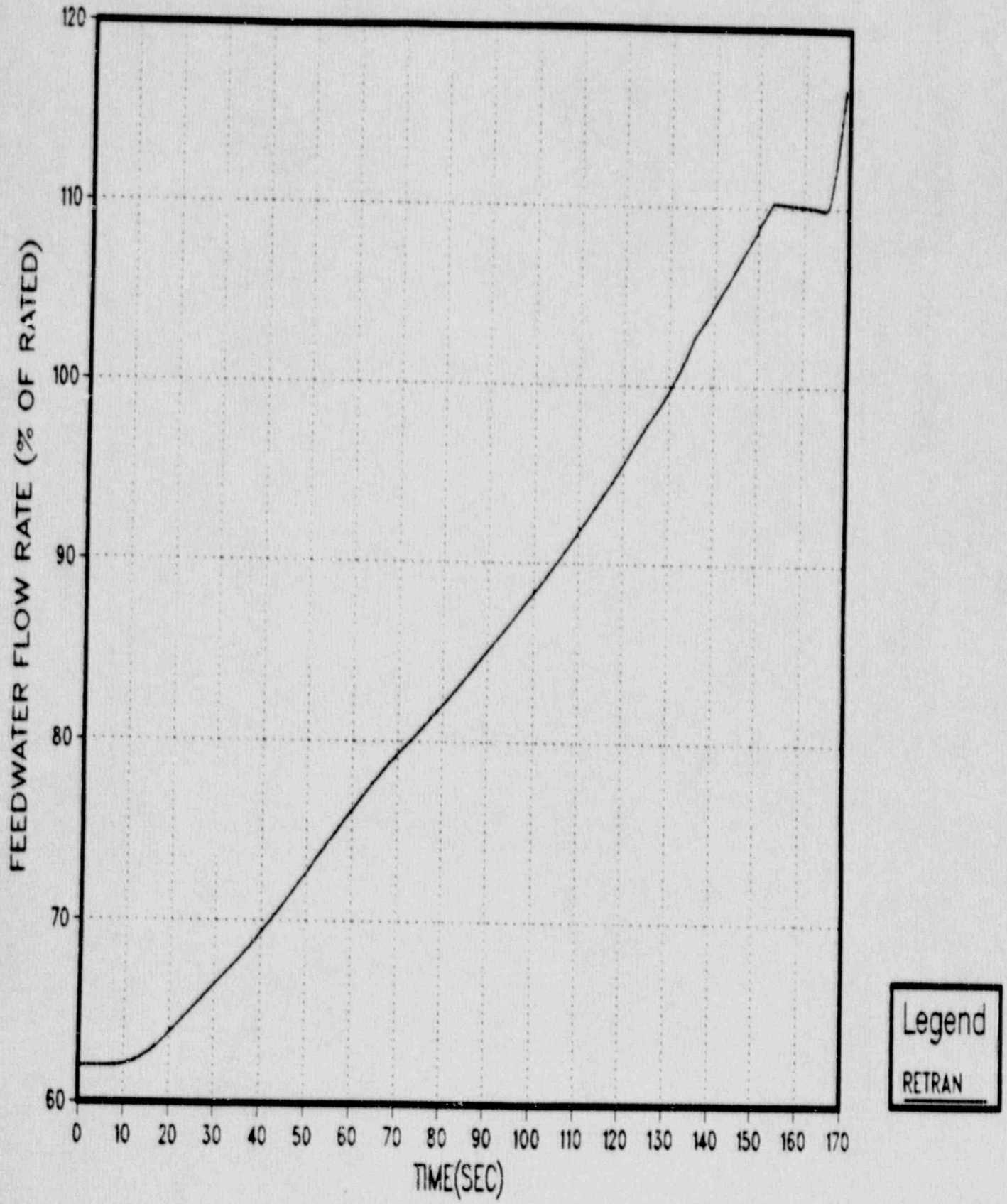

FIGURE 3.3-7 RFCF AVERAGE HEAT FLUX

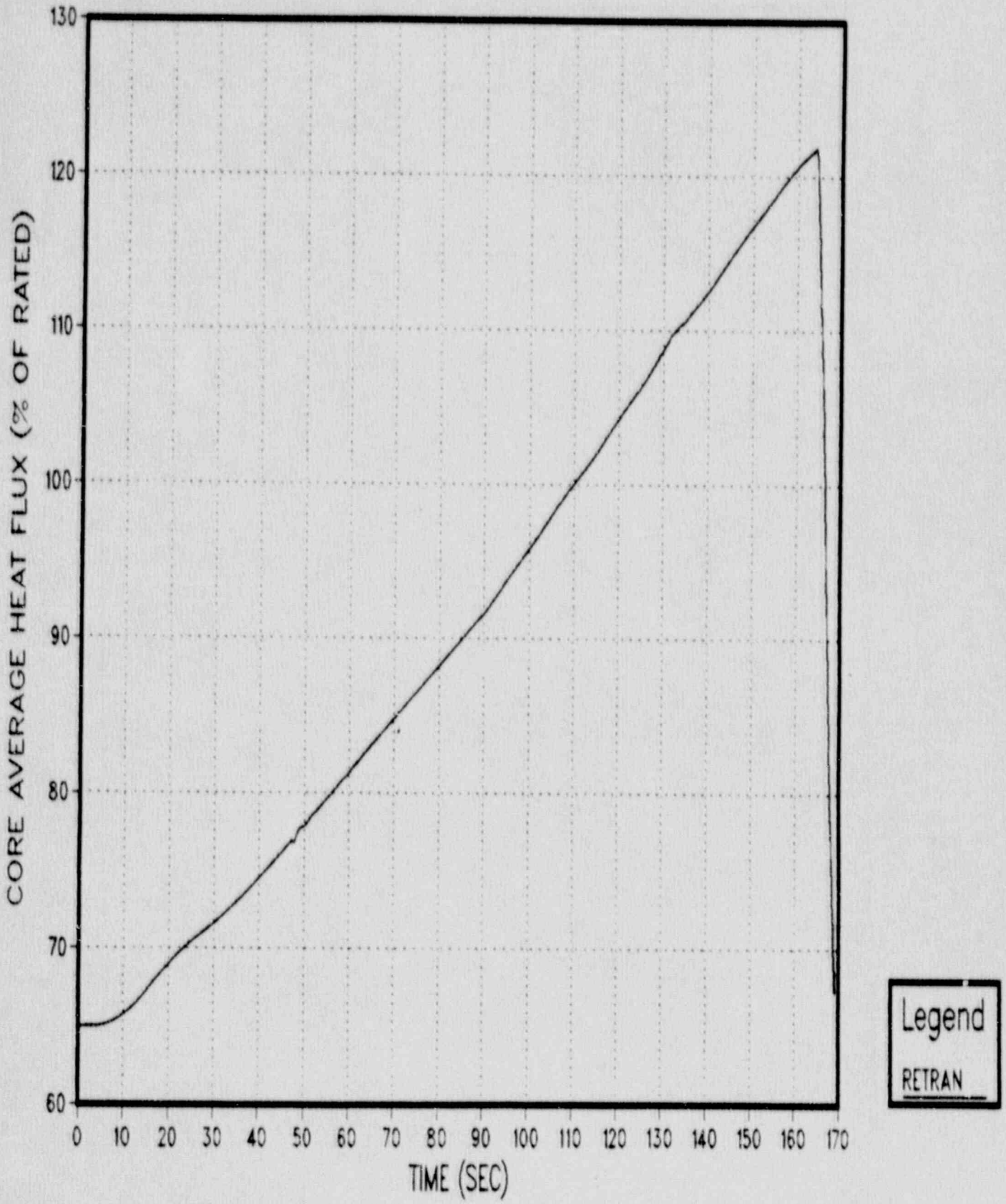

3.4 Non-Limiting Events

This section describes an evaluation of the Susquehanna SES FSAR (Reference 14) Chapter 15 transient events (i.e., anticipated operational occurrences) to determine which events need to be evaluated in establishing the MCPR operating limits for each reload licensing submittal. The detailed analysis methods for the events selected for analysis on a typical reload are described in Sections 2.1 to 2.3 and 3.1 to 3.3 of this report. This section describes the evaluations performed to establish that the other Chapter 15 events are non-limiting and, hence, that they will not be analyzed for each reload.

The FSAR Chapter 15 transient events for which calculated ΔCPR is of importance are divided into 5 main categories:

1) Decrease in Coolant Temperature (15.1)
2) Increase in Reactor Pressure (15.2)
3) Decrease in Reactor Coolant System Flow Rate (15.3)
4) Reactivity and Power Distribution Anomalies (15.4)
5) Increase in Reactor Coolant System Inventory (15.5)

Calculated values of ΔCPR for Cycle 1 are given in Table 15.0-1 of the FSAR (Reference 14). Events which show a calculated ΔCPR greater than zero in FSAR Table 15.0-1 and potentially limiting events in each category were evaluated. The events selected on this basis for evaluation are listed in Table 3.4-1. Evaluations of specific events identified as non-limiting in Table 3.4-1 are provided in the following sections.

3.4.1 Turbine Trip

A Turbine Trip Without Bypass (TTWOB) was analyzed and compared to the GLRWOB as described in Section 3.1 of this report. The events are nearly identical with only small differences in the times for the start of TCV motion. The results presented in Table 3.1-2 show the TTWOB to be slightly less limiting than the GLRWOB, due to the fact that the TCVs start to close slightly later with respect to time of reactor trip for the TTWOB. Thus, the TTWOB need not be analyzed as it is less limiting than the GLRWOB.

3.4.2 MSIV Closure (Position Scram)

The MSIV closure from 100% power/100% flow with reactor trip on valve position (85% open) was analyzed. The calculated ΔCPR was equal to 0.0. Because of the rapid post-trip power reduction, which occurs prior to the pressurization induced power increase, the core average heat flux never exceeds its initial value. As indicated by these results, the MSIV closure with valve position reactor trip is less limiting than the GLRWOB for calculated ΔCPR.

3.4.3 Loss of Condenser Vacuum

The Loss of Condenser Vacuum event is described in Section 15.2.5 of the Susquehanna SES FSAR (Reference 14). The Loss of Condenser Vacuum consists of a turbine trip with partial bypass capacity. Reactor scram occurs as the result of the turbine trip. Because of steam release through the bypass valves, the pressurization and, hence, the calculated ΔCPR for this event would be less than those calculated for the TTWOB and GLRWOB events.

3.4.4 Recirculation Pump Trip

An analysis was performed of the simultaneous trip of both recirculation pumps. The rapid decrease in flow produces increased voiding in the core and causes a rapid decrease in core power. The calculated ΔCPR was approximately 0.02, which is an order of magnitude less than typical limiting events. Thus, this event is judged to be non-limiting.

3.4.5 Inadvertent HPCI Startup

A RETRAN analysis of the inadvertent startup of the High Pressure Coolant Injection (HPCI) system was performed at 100% power/100% flow. Plant test data was used to produce a table of HPCI flow versus time. The condensate storage tank supplies the initial HPCI flow to the reactor vessel. Plant data indicates that the actual HPCI injection flow temperature is usually greater than 100°F. Thus, the analysis conservatively assumed that the HPCI system delivered 40°F water to the reactor vessel. Also, the high neutron flux and high thermal power reactor trips were disabled to allow the event to reach a new steady state. The calculated ΔCPR for the HPCI startup was less than 0.10. Since the event is expected to be relatively independent of unit and cycle, and more limiting events will produce significantly higher calculated ΔCPRs, the event is considered to be non-limiting.

TABLE 3.4-1

Potentially Limiting Events in Establishing MCPR Operating Limits

	Event	Classification*
1.	Loss of Feedwater Heating	R
2.	Feedwater Controller Failure	R
3.	Generator Load Rejection	R
4.	Turbine Trip	N/L
5.	MSIV Closure (position scram)	N/L
6.	Loss of Condenser Vacuum	N/L
7.	Recirculation Pump Trip	N/L
8.	Rod Withdrawal Error	R
9.	Recirculation Flow Controller Failure (increasing)	R
10.	Fuel Loading Error	R
11.	Inadvertent HPCI Startup	N/L

* R = Analysis performed for each reload
N/L = Not limiting but demonstrated by analysis or evaluation; do not analyze for each reload

3.5 ASME Overpressure Analysis

3.5.1 Criteria

The Susquehanna SES nuclear pressure relief system has been designed to prevent overpressurization which could lead to failure of the reactor coolant pressure boundary. The ASME Boiler and Pressure Vessel Code, Section III (Reference 24) requires that the peak pressure be maintained less than or equal to 110% of the vessel design pressure under upset conditions.

The combination of the Reactor Protection System and the Safety/Relief Valves (SRVs) must ensure that this criterion is met. Analyses of the limiting overpressure event for each reload will be performed to demonstrate that the peak calculated pressures are within 110% of the design pressures of the reactor coolant pressure boundary components. As specified in Standard Review Plan 5.2.2 (Reference 19), credit can be taken for the spring loaded safety valves and the second safety grade reactor protection signal.

The components which comprise the reactor coolant pressure boundary have been designed with several different design pressures, as detailed in FSAR Table 5.2-3 (Reference 14). The criteria used for overpressure analyses on the Susquehanna SES units are given in Table 3.5-1.

The criteria specified in Table 3.5-1, which represent 110% of the pressure boundary component design pressures, must be met for the most adverse pressurization transient. The two potentially limiting pressurization events are the closure of all Main Steam Isolation Valves (MSIVs) and the Generator Load Rejection Without Bypass (GLRWOB). Both

these events were evaluated by PP&L using the RETRAN models and methods described in this section and assuming that the first safety grade reactor trip does not function. Thus, both events produce a reactor scram on high neutron flux. Results of the RETRAN analyses demonstrate that the MSIV closure event with high neutron flux scram produces higher vessel pressures than the GLRWOB with high neutron flux scram.

3.5.2 Event Description

In the Susquehanna SES, MSIV closure is initiated by any one of a number of trips (e.g., by low reactor water level, high radiation, low condenser vacuum, operator action, etc). The MSIVs are large valves (two in each of the four steam lines) which have a range of allowable closing times specified in the Technical Specifications. The maximum allowable closure time is established to contain fission products and to ensure the core is not uncovered following steam line breaks. The minimum allowable closure time is limited by vessel component overpressure criteria.

The analyses presented in this section assumed an inadvertent simultaneous closure of all MSIVs. As the MSIVs close, valve position limit switches activate the Reactor Protection System (RPS), which produces a reactor scram. For overpressure analyses, however, this trip is not credited, and reactor scram occurs on high neutron flux.

The decrease in steam flow caused by the MSIV closure produces an increase in vessel pressure. The pressure rise continues and some or all of the Safety Relief Valves (SRVs) open. Normally, the SRVs will open as the result of a vessel pressure signal in the relief mode. However, for the overpressure analyses, the relief mode is assumed to be unavailable, and spring pressure safety mode operation is assumed.

As the pressure increase collapses voids in the core, neutron power rises and downcomer water level decreases. The decreasing level will generate a reactor recirculation pump runback signal.

System pressure typically increases further until the Anticipated Transient Without Scram Recirculation Pump Trip (ATWS-RPT) high pressure setpoint is reached. This occurrence does not have a pronounced effect on overall vessel pressure, but it does affect the overpressure margin locally in the external recirculation loop discharge piping.

Feedwater response to the MSIV closure event is assumed to provide a constant flow. Although the steam driven feedwater turbines are isolated from the reactor steam supply, the feedwater pumps continue to inject feedwater into the vessel for approximately 30 seconds utilizing steam from the steam line piping downstream of the closed MSIVs. The additional mass and energy of the feedwater flow added to the subcooled downcomer fluid effectively reduces the steam space in the vessel and results in an increased system pressure rise. The decreased power level following scram and steam release through the SRVs limit the vessel peak pressures.

3.5.3 RETRAN Modelling

The base RETRAN system model used for the overpressure analysis of the MSIV closure is described in Section 3 of Reference 2. In order to conservatively model the MSIV closure event, three changes were made to the models described in Reference 2:

1) A conservative model of the safety mode of the SRVs was developed, since the Reference 2 "best estimate" model represents the relief mode of the SRVs.

2) An improved MSIV model was developed to better represent the transient flow rate during valve closure. This model, which is based on data from the valve manufacturer, was then conservatively biased to reduce steam flow more rapidly than would be expected.

3) A trip and control system was added that automatically calculates the pressure boundary pressures and compares them to their respective peak pressure criteria. This control system is for information only, and it has no effect on the calculated system response.

3.5.3.1 Safety/Relief Valve Model

Susquehanna SES Technical Specification 3.4.2 (Reference 16) specifies that 10 of the 16 SRVs must be operable and specifies the valve setpoints and tolerances. The model developed for the overpressure analysis assumes the 6 SRVs with the lowest pressure setpoints are inoperable and that the valve setpoints are at the high pressure end of the tolerance band specified in the Technical Specification (i.e., +1%). The SRV vendor specified maximum opening times were used to minimize the pressure relief through the SRVs. The assumed SRV opening characteristics are shown in Figure 3.5-1. Table 3.5-2 supplies the valve capacities used in the analyses.

The RETRAN system model was modified to incorporate the assumptions described above. Valve openings are initiated by means of RETRAN trips, and the mass flux through the SRVs is calculated via the control system illustrated in Figure 3.5-2.

3.5.3.2 MSIV Model

Since the publication of Reference 2, PP&L obtained detailed loss coefficient data on the Atwood & Morrill MSIVs. This data, which consists of loss coefficient versus valve position, was used to produced more accurate modelling of the reduction in steam flow caused by closure of the MSIVs. The Reference 2 MSIV model was replaced by the one described herein. Since none of the Reference 2 benchmarking analyses involved closure of the MSIVs, those analyses remain valid. The reduction in steam flow during MSIV closure is modelled as an increase in loss coefficient for a constant junction area (i.e., valve area assumed constant). The control system to vary the valve loss coefficient as a function of valve position (i.e., time) is illustrated in Figure 3.5-3. The ratio of loss coefficient to full open loss coefficient as a function of stem position was increased by 25% to produce a conservatively rapid reduction in steam flow as the MSIVs close. The effect of closing both inboard and outboard MSIVs is modelled.

3.5.3.3 Trip and Control System

Two RETRAN control systems were set up to track peak vessel pressures for comparison to the relevant ASME criteria. These two control systems provide edits for analyst convenience, and they do not affect the transient being analyzed. The first control system calculates pressures for components which have a 1250 psig design pressure (Figure 3.5-4). The RETRAN volumes whose pressures are tracked with this control system are:

1) Steam Dome (Volume 120)
2) Upper Downcomer (Volume 130)
3) Lower Downcomer (Volume 148)
4) Steam Line Inside Containment (Volumes 320 & 330)

The pressure at the bottom of the reactor vessel is taken to be the RETRAN lower plenum (Volume 160) pressure plus the elevation head associated with one-half the volume height, since RETRAN pressures are calculated at the middle of a volume. Based on GE design data, the pressure in the feedwater lines is less than or equal to 28 psi higher than the dome pressure. Thus, the RETRAN dome pressure (Volume 120) is increased by 28 psi for comparison with the limit. The control system illustrated in Figure 3.5-4 calculates the maximum of the above defined pressures for comparison with the pressure criterion.

The control system that calculates pressures for the vessel components whose design pressure is 1500 psig is illustrated in Figure 3.5-5. The pressure in the recirculation pump discharge piping (Volume 220) and the pump discharge pressure (based on the RETRAN junction pressure plus the contribution of the recirculation pump minus the local frictional loss) are tracked. This control system assumes that the event is symmetric with respect to the vessel and should not be used for asymmetric events. It should be noted that results of MSIV closure analyses clearly indicate that the components having a 1500 psig design pressure will not be the limiting components.

3.5.4 Sensitivity Studies

RETRAN system model analyses were performed to determine the sensitivity of peak power and vessel pressures to changes in input assumptions for the MSIV closure event. The parameters analyzed were:

1) Core power
2) Feedwater temperature
3) Pressure regulator setpoint
4) Steam line pressure drop
5) Control rod insertion rate
6) Gap conductance

7) MSIV closure time
8) Neutronics input/Cross section modification
9) Feedwater flow transient behavior
10) ATWS recirculation pump trip setpoint
11) Steam dome volume

The base case values of the above mentioned parameters are listed in Table 3.5-3. Closure of the MSIVs was initiated at time zero by activating the MSIV manual trip logic in the RETRAN model (Reference 2). The study results demonstrated that the components whose design pressure is 1250 psig had the closest approach to their ASME overpressure limit. The components whose design pressures are 1230 and 1240 psig were slightly less limiting, and the components whose design pressure is 1500 psig showed at least 200 psi margin to the applicable ASME overpressure limit. The study results are presented in Table 3.5-4. The peak pressure changes are presented for the 1250 psig design pressure category only, since this category exhibited the closest approach to the applicable ASME overpressure limit. Conclusions and observations drawn from the analysis results are discussed below.

The results given in Table 3.5-4 indicate that the peak pressure is most strongly affected by: core power, core flow, feedwater temperature, pressure regulator setpoint, scram curve, and MSIV closure time. The other parameters investigated produced a less than 2 psi change in calculated peak pressure.

A higher initial core power implies a higher steam flow (all other things being unchanged), which produces a larger pressurization of the vessel on MSIV closure. The higher pressurization rate also increases the peak core power due to positive void reactivity feedback, which increases the energy

input to the vessel and, hence, the pressure. Thus, higher initial core power is conservative for MSIV closure overpressure analysis.

A higher initial core flow has two main effects on the MSIV closure events. First, higher core flow means less voids in the core, which makes the vessel water less compressible and increases the pressurization. Second, the higher core flow produces a more top peaked core axial power distribution. The more top peaked power distribution results in a higher peak power due to scram effects, which increases the energy deposited to the vessel and increases the pressurization. Therefore, higher core flow is conservative for MSIV closure overpressure analysis. Based on the sensitivity study results (cases 1 and 2), however, the effect of a change in flow on the order of the flow uncertainty (2.5%, Reference 17) is only about 1 psi.

A lower feedwater temperature at a given power/flow condition has the effect of reducing the initial vessel steam flow. A lower initial steam flow makes the vessel pressurization less severe for the MSIV closure, resulting in lower peak power and pressure. The effect is relatively minor for changes on the order of the temperature measurement uncertainty (0.76%, Reference 17).

The main effect of a higher pressure regulator setpoint is to raise the initial dome pressure. While this places the initial pressures closer to the ASME criteria, it also places the steam line and vessel pressures closer to the SRV setpoints and ATWS RPT setpoint, respectively. Thus, the net effect is only a 6 psi increase in peak pressure for a 32 psi increase in pressure regulator setpoint (Table 3.5.4, Case 4).

Since the larger part of the steam line is downstream of the MSIVs, the steam line pressure drop has negligible impact on the MSIV closure event.

A faster reactor scram control rod insertion reduces the peak core power and the integrated heat added to the vessel, which reduces the peak vessel pressures. The effect of using the Technical Specification scram curve versus a best estimate scram curve is substantial (increase in peak pressure of 33 psi, Cases 1 and 6).

The gap conductance has little effect on peak vessel pressure (Case 7). However, use of a lower value results in a slightly higher peak pressure. Thus, the same conservatively low value generated for ΔCPR calculations (See Appendix A) will be used for the MSIV closure overpressure analyses.

A shorter MSIV closure time creates a more significant vessel pressurization since less energy is removed from the system.

The modification of cross sections as described in Section 2.6 has a negligible effect on peak vessel pressure. This is due to the fact that a MSIV closure is a less rapid event than a GLRWOB, resulting in smaller changes in core nodal water densities prior to the insertion of significant scram reactivity. Since the cross section modification process is performed to account for differences between RETRAN and SIMULATE-E calculated moderator density changes for rapid pressurization events, the effect is much less than it is for the GLRWOB. Also, small changes in peak core power have only a small effect on peak pressure, although they may have a big effect on ΔCPR. Therefore, use of the cross section modification process is not necessary.

The impact of feedwater flow differences during the MSIV closure event is extremely small (Cases 1 and 10), mainly due to the fact that peak pressure is attained in about 5 seconds, and the feedwater flow differences have not had sufficient time to significantly influence vessel conditions.

The Anticipated Transient Without Scram (ATWS) Recirculation Pump Trip (RPT) setpoint has a negligible effect on peak vessel pressure and power since it occurs after peak power and not long before peak pressure. Small changes in steam volume in the vessel, such as could be caused by a different vessel water level, will have a negligible impact on peak vessel pressure for the MSIV closure event, due largely to the very large steam space upstream of the MSIVs.

3.5.5 Licensing Analysis Method

The ASME overpressure analysis will be based on the event defined by a simultaneous closure of all MSIVs. The following conservative assumptions will be used to perform the analysis for a licensing application:

1) The event will be analyzed at 104.4% of rated core power (105% steam flow) and 100% rated core flow.

2) The pressure regulator setpoint is assumed equal to 966 psia, which corresponds to a dome pressure of approximately 1040 psia.

3) The Technical Specification (maximum) average scram times will be assumed.

4) A value of MSIV closure time which is less than or equal to the Technical Specification minimum closure time will be assumed.

5) Feedwater Flow will be held constant at its initial value.

6) A conservatively low value of gap conductance will be used (see Appendix A).

7) The maximum value of the ATWS-RPT pressure setpoint including uncertainties will be used.

8) The conservative MSIV model described in Section 3.5.3.2 will be used.

The results of the RETRAN system model benchmarking analyses presented in Reference 2 show that the PP&L best estimate methodology can accurately predict vessel pressurization (Reference 2, Sections 5 and 6). Therefore, the conservative assumptions outlined above introduce significant conservatism into the calculated peak vessel pressures. The cross section modification process will not be used for MSIV closure overpressure analyses.

3.5.6 Sample Licensing Analysis

This section presents a sample licensing analysis for a Unit 2 Cycle 2 MSIV closure event. The analysis was performed using the set of assumptions described in Section 3.5.5, with the exception that the nominal pressure regulator setpoint was used. However, on an actual reload licensing application, the higher pressure regulator setpoint will be used.

The transient behavior of selected system parameters is presented in Figures 3.5-6 to 3.5-13. The calculated peak pressures for the event and their locations are given in Table 3.5-5. Adequate margin to the ASME overpressure criteria was demonstrated.

TABLE 3.5-1

ASME Overpressure Analysis Criteria

Component	Design Pressure (psig)	Criterion (psig)
Reactor Vessel	1250	1375
Recirculation Suction Piping	1250	1375
Main Steam Piping	1250	1375
Recirculation Discharge Piping	1500	1650
Recirculation Pump	1500	1650
HPCI and RCIC Steam Piping	1230	1353
Core Spray System	1240	1364

TABLE 3.5-2

Safety/Relief Valve
Flow Rates

Number of Valves	Nominal Spring Set Pressure(psig)	Flow Rate at 103% Spring Set Pressure (lb/hr valve)**
2	*	-
4	*	-
4	1185	891,380
3	1195	898,800
3	1205	906,250

*These valves were assumed to be inoperable.
**Flow rate from the Susquehanna SES FSAR (Reference 14).

TABLE 3.5-3

MSIV Closure/ASME Overpressure Analysis
Base Case Input Assumptions

Parameter		Assumption
1.	Core Power	3293 Mwt (100% rated)
2.	Core Flow	100 Mlbm/hr (100% rated)
3.	Feedwater Temperature	Best estimate value based on plant data
4.	Pressure Regulator Setpoint	Best estimate value based on plant data
5.	Steam Line Pressure Drop	Best estimate values (Reference 2)
6.	Control Rod Insertion	Technical Specification insertion rate
7.	Gap Conductance	Value calculated using Appendix A methodology (855 BTU/hr $ft^{2o}F$)
8.	MSIV Closure Time	2.0 seconds
9.	Cross Section Modification	Cross section dependencies modified (see Section 2.6)
10.	Feedwater Flow Transient Behavior	Determined by the feedwater controller (Reference 2)
11.	ATWS Recirculation Pump Trip Setpoint	Analytical setpoint (1184.7 psia)
12.	Steam Dome Volume	Best estimate value (Reference 2)

TABLE 3.5-4

MSIV Closure/ASME Overpressure Analysis
Results of Sensitivity Study

Parameter	Change from Base Value	Change in Peak Core Power (% rated)	Change in Peak Pressure (psi)
1. Core Power	+4.4% rated	+76%	+7.
2. Core Flow	-13% rated	-31%	-6.
3. Feedwater Temperature	-10°F	-9%	-7.
4. Pressure Regulator Setpoint	+32 psi	-9%	+0.
5. Steam Line Pressure Drop	+8.65 psi	+5%	+0.
6. Control Rod Insertion Rate	Best estimate based on plant data	-23%	-33.
7. Gap Conductance	Increase to 1000 (BTU/hrft^{2}F)	-14%	-2.
8. MSIV Closure Time	Increased to 3 sec.	-31%	-16.
9. Cross Section Modification	Not Modified	+10%	-1.
10. Feedwater Flow Behavior	Held constant at 100%	+1%	+2.
11. ATWS RPT Setpoint	Decreased to 1149.7 psia (nominal)	+0%	+0.
12. Steam Dome Volume	-138 ft^3	+4%	+0.

TABLE 3.5-5

MSIV Closure Sample Licensing Analysis
Peak Calculated Pressures

Design Pressure Category	Criterion (psia)	Maximum Pressure (psia)	Time of Peak Pressure (sec)
1230 psig	1367.7	1301	5.3
1240 psig	1378.7	1308	5.1
1250 psig	1389.7	1331	5.2
1500 psig	1664.7	1412	3.5

FIGURE 3.5-1
ASSUMED SRV FLOW CHARACTERISTICS

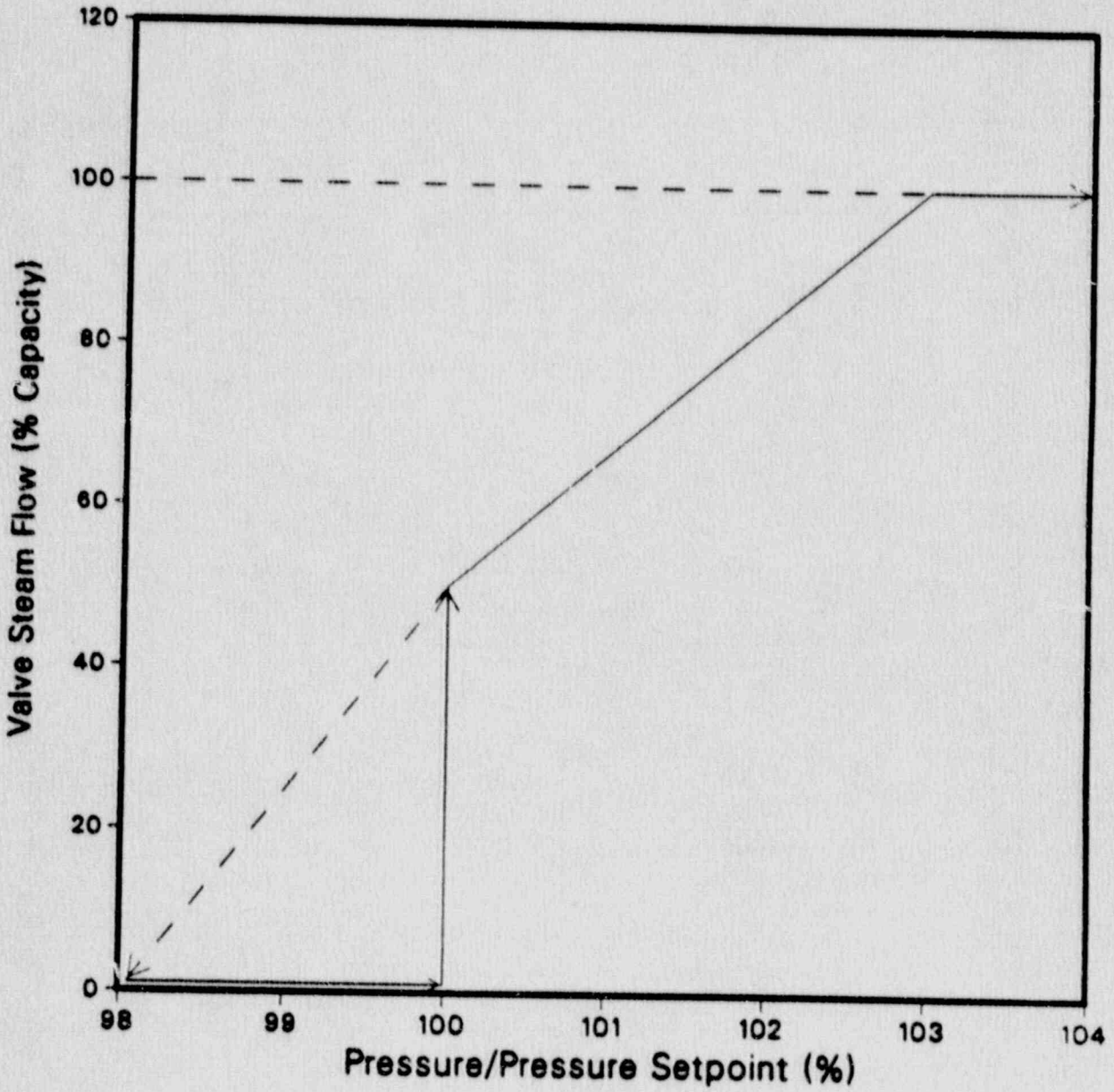

FIGURE 3.5-2 : CONSERVATIVE SRV FLOW MODEL

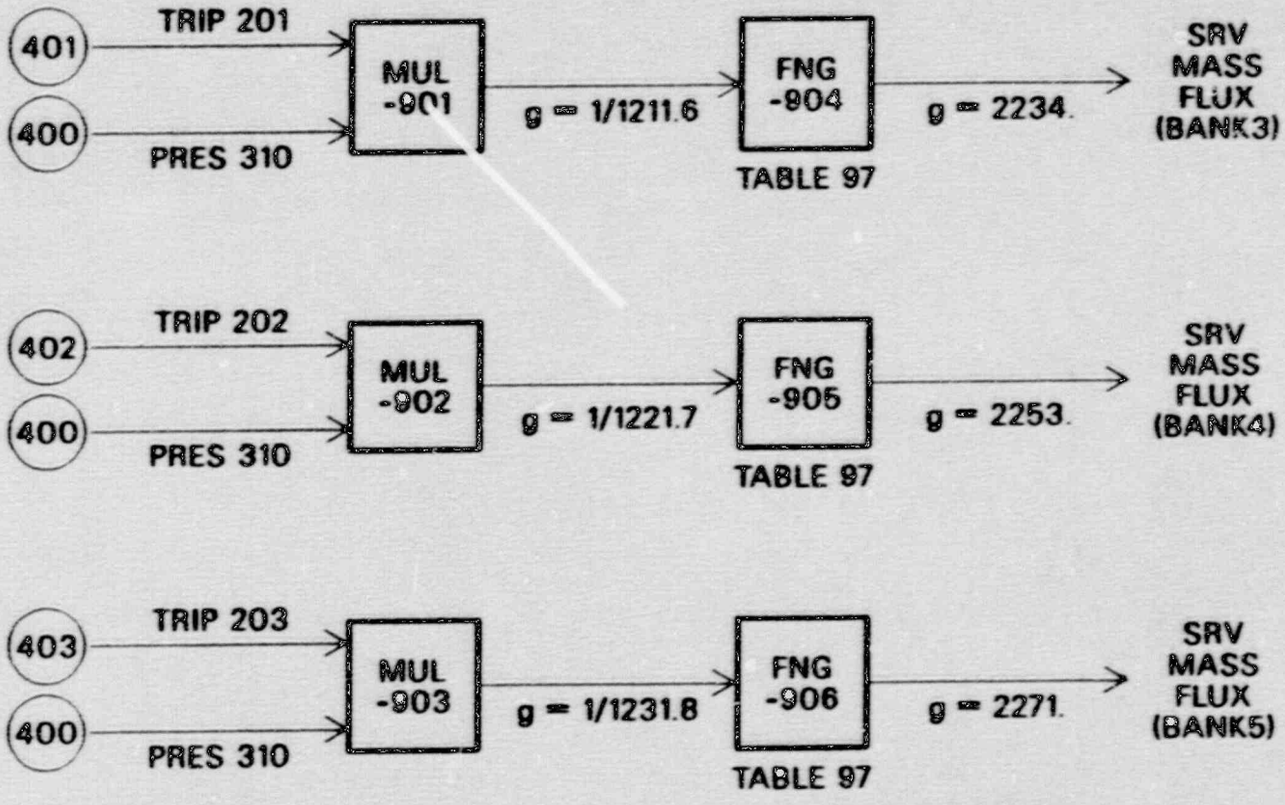

NOTE: Banks 1 and 2 (6 values) are assumed out of service

FIGURE 3.5-3 : MSIV LOSS COEFFICIENT

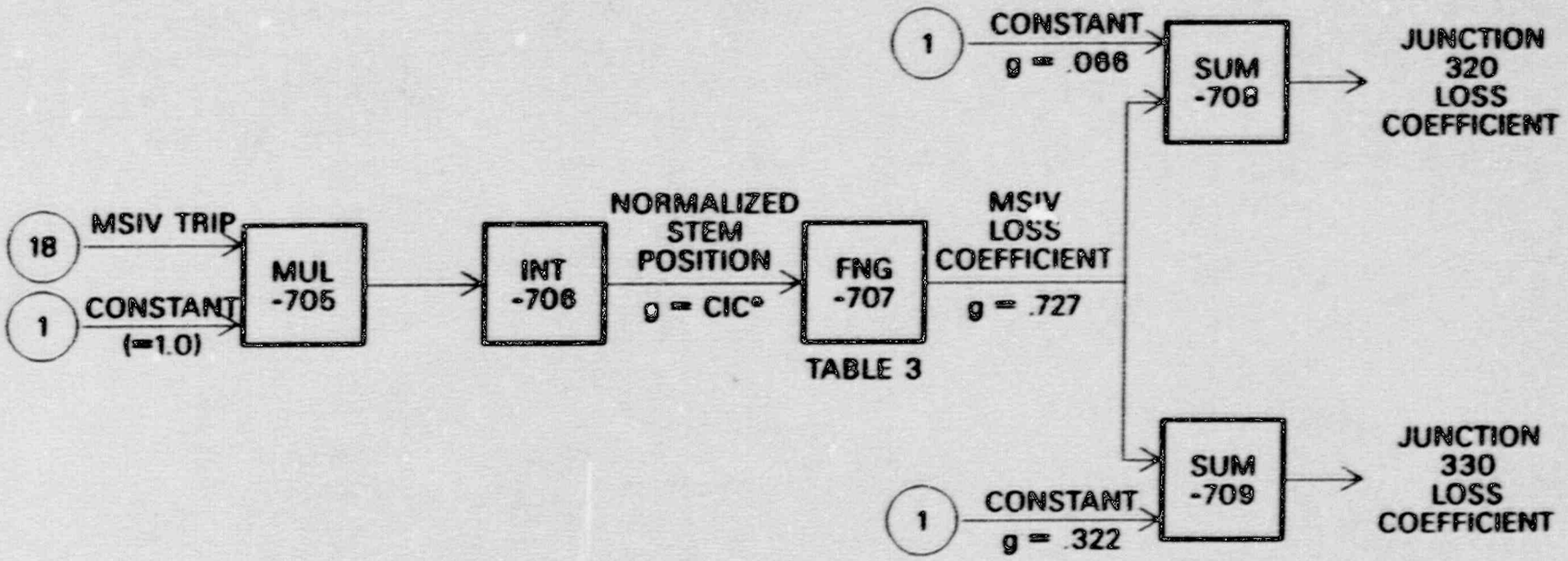

* gain = -(1 / MSIV closure time); SEC^{-1}

FIGURE 3.5-4 : OVERPRESSURE MARGIN (1250 PSIG DESIGN PRESSURE)

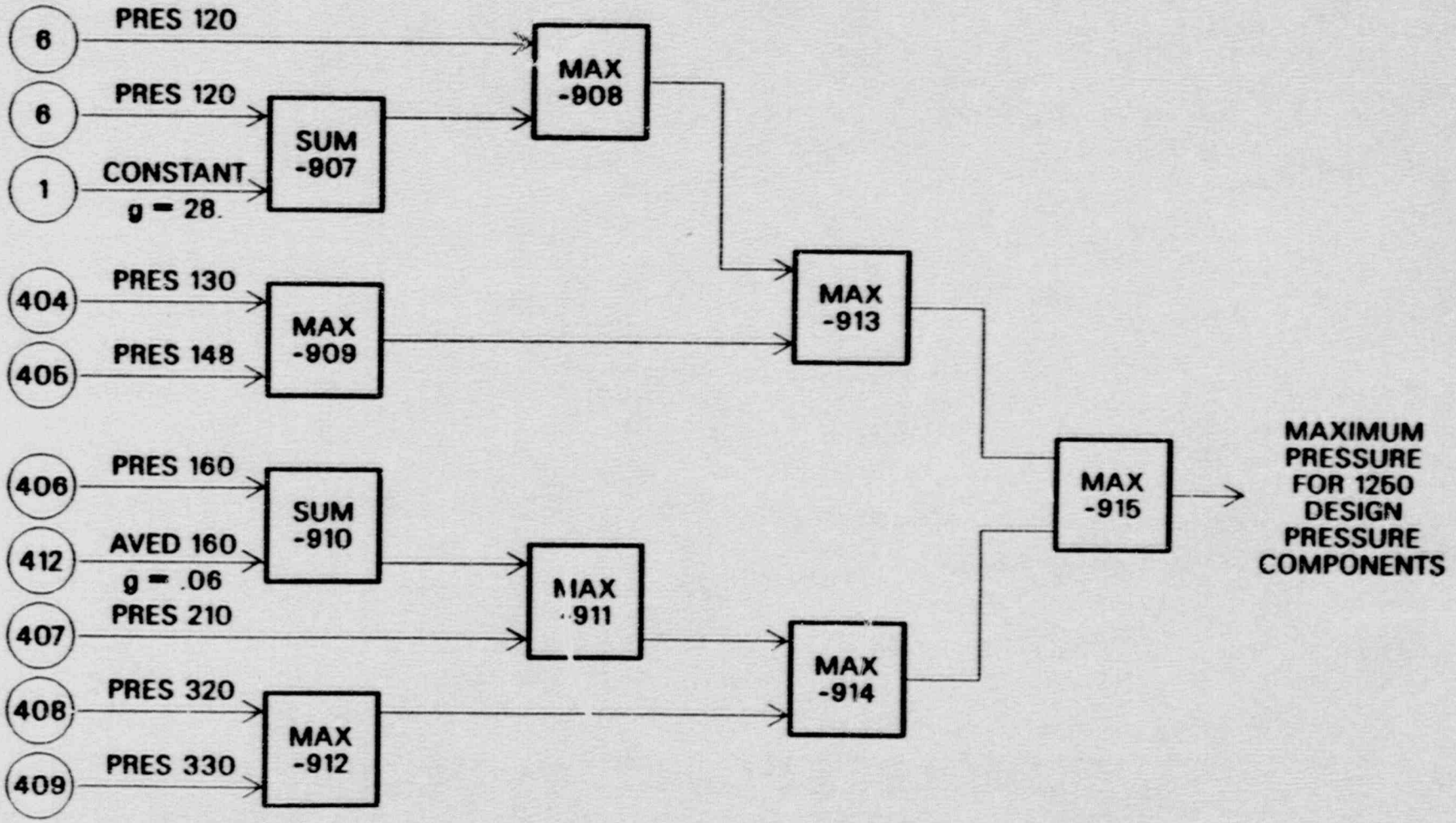

FIGURE 3.5-5 : OVERPRESSURE MARGIN (1500 PSIG DESIGN PRESSURE)

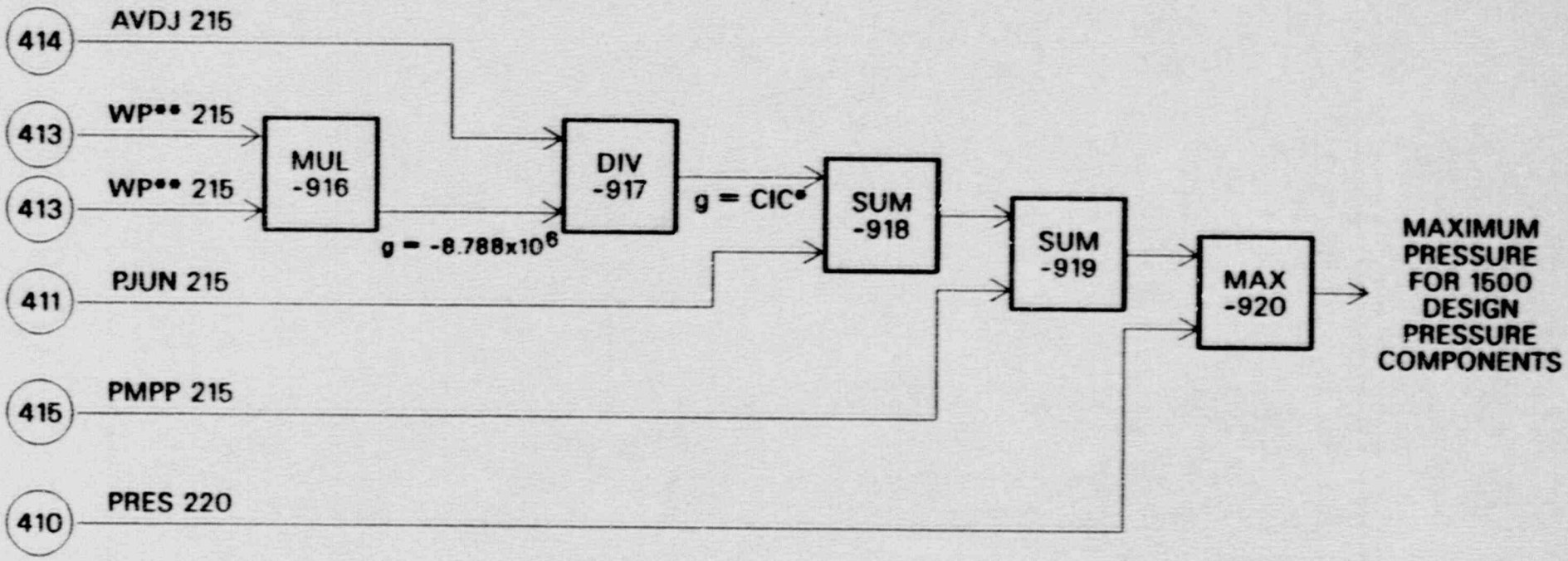

* gain = Initial values of loss coefficient in Junction 215 from the RETRAN initialization run

FIGURE 3.5-6 : MSIVC CORE POWER

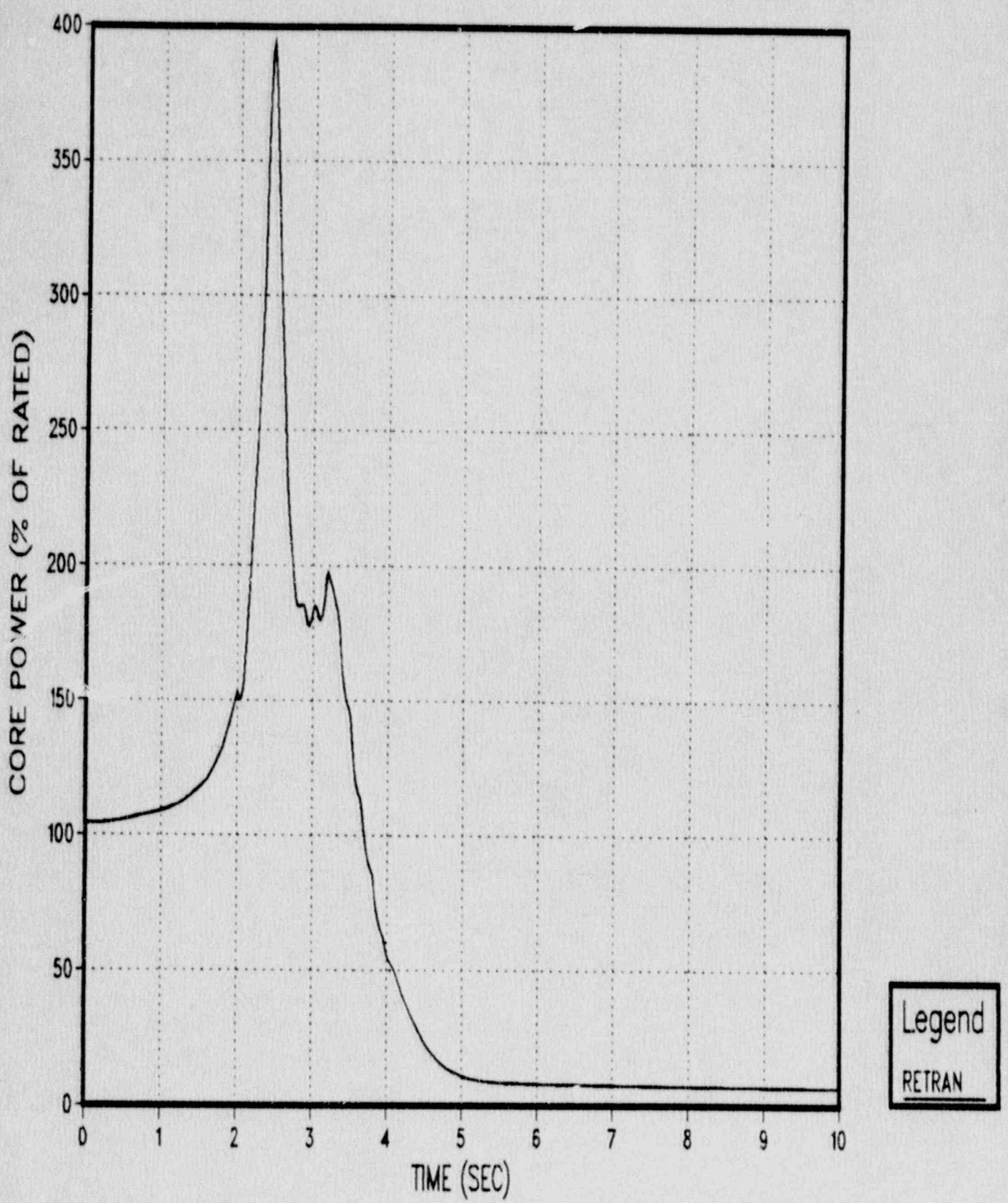

FIGURE 3.5-7 : MSIVC CORE FLOW

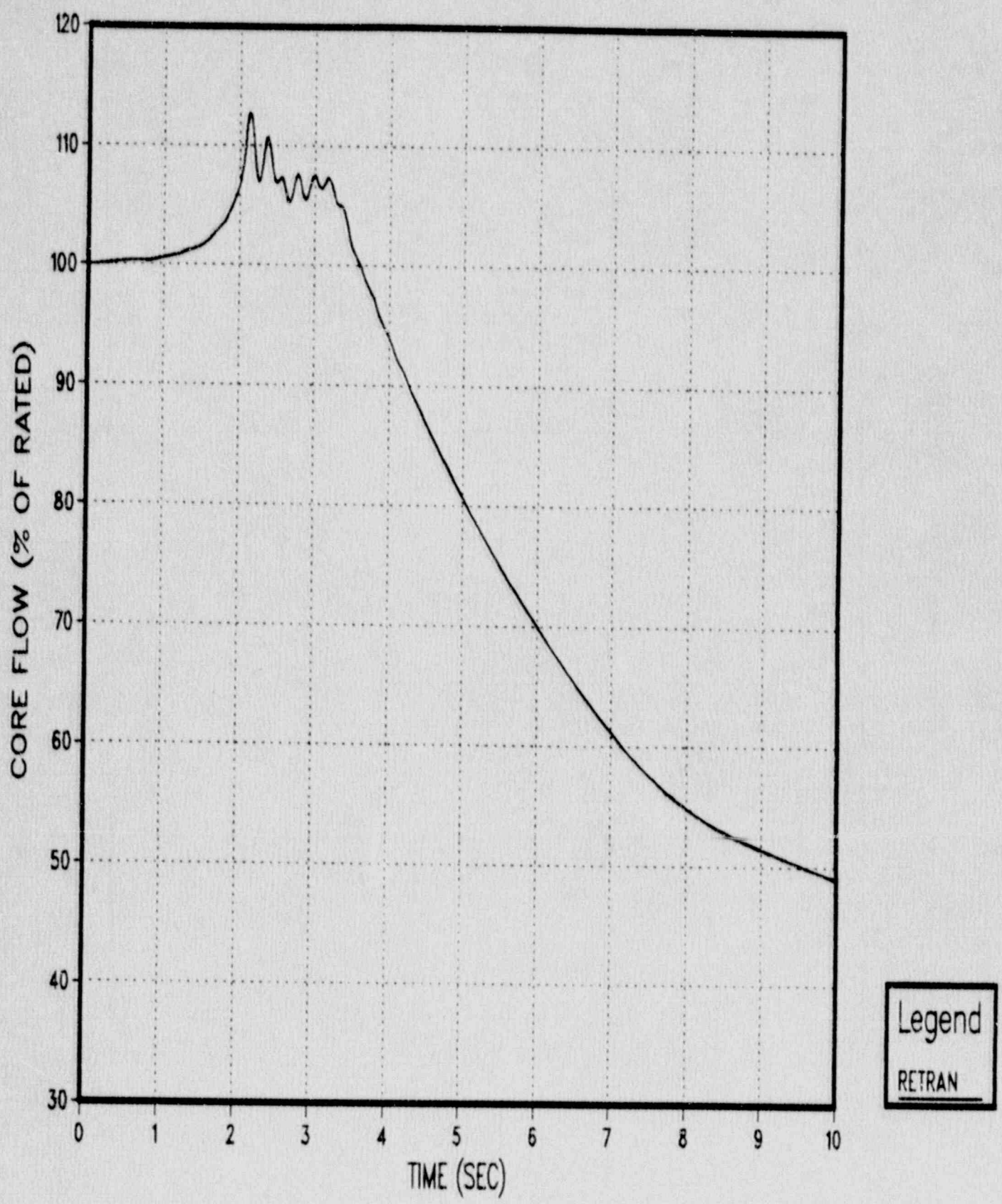

FIGURE 3.5-8 : MSIVC DOME PRESSURE

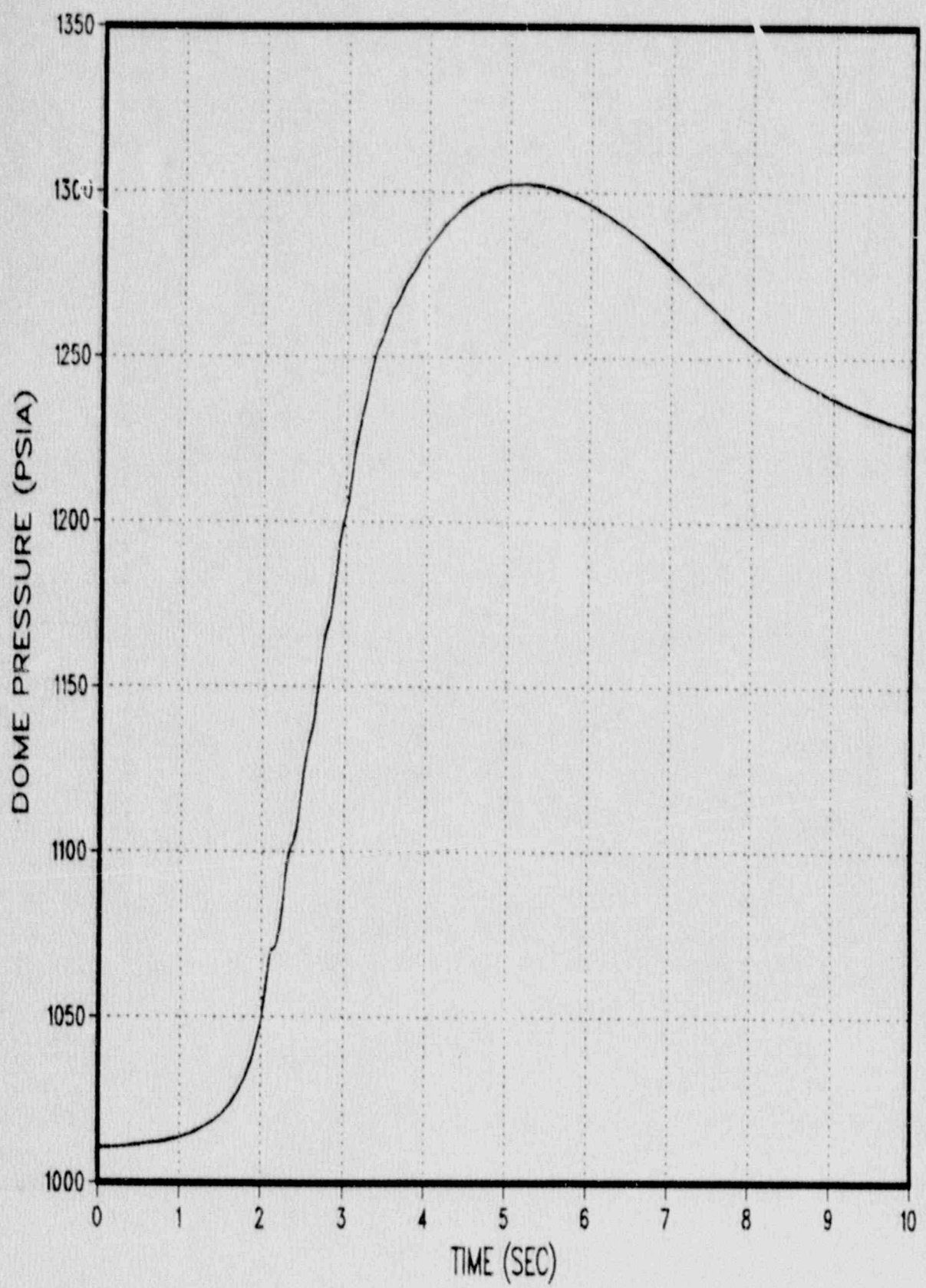

FIGURE 3.5-9 : MSIVC VESSEL STEAM FLOW

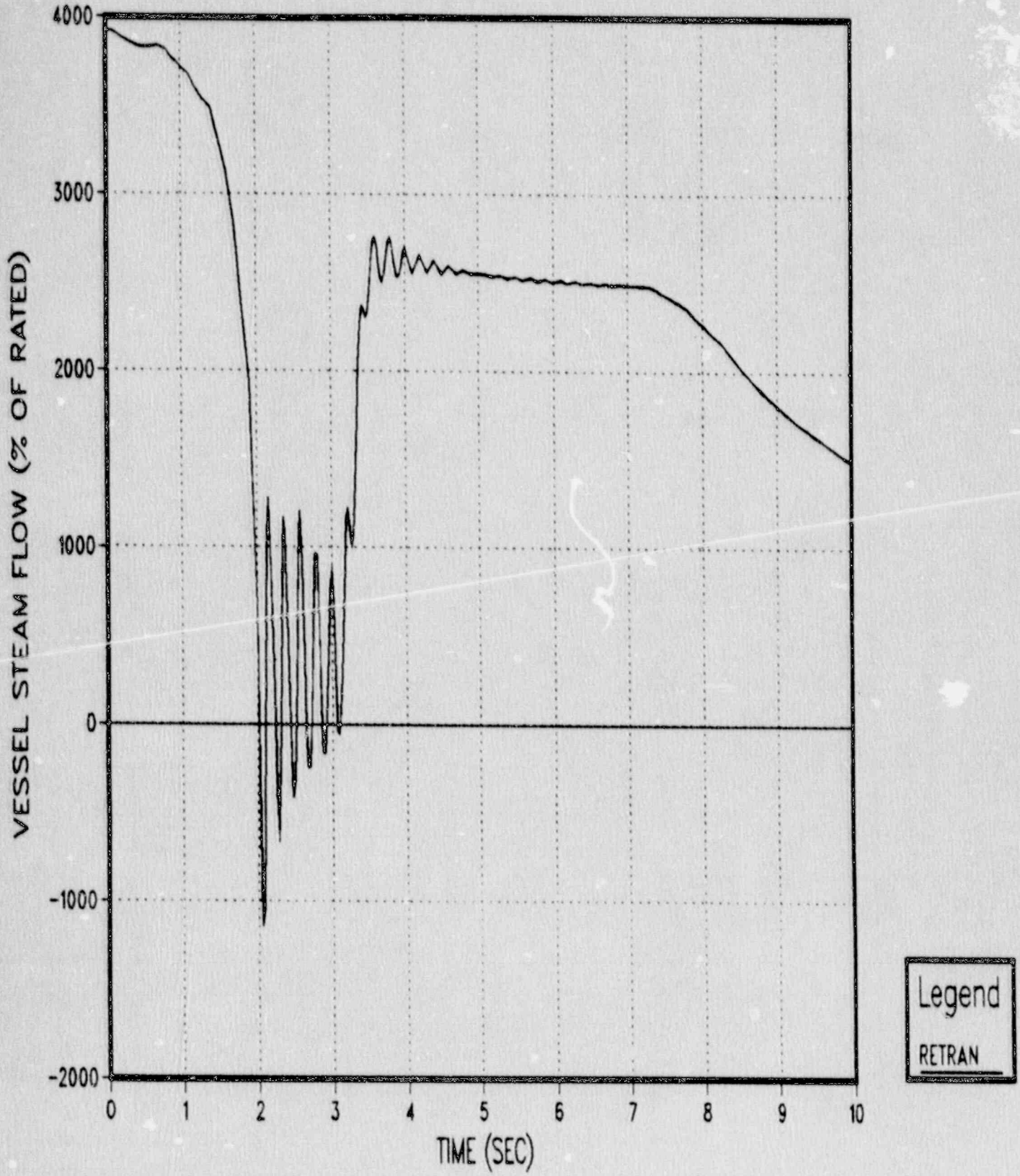

FIGURE 3.5–10 : MSIVC NARROW RANGE LEVEL

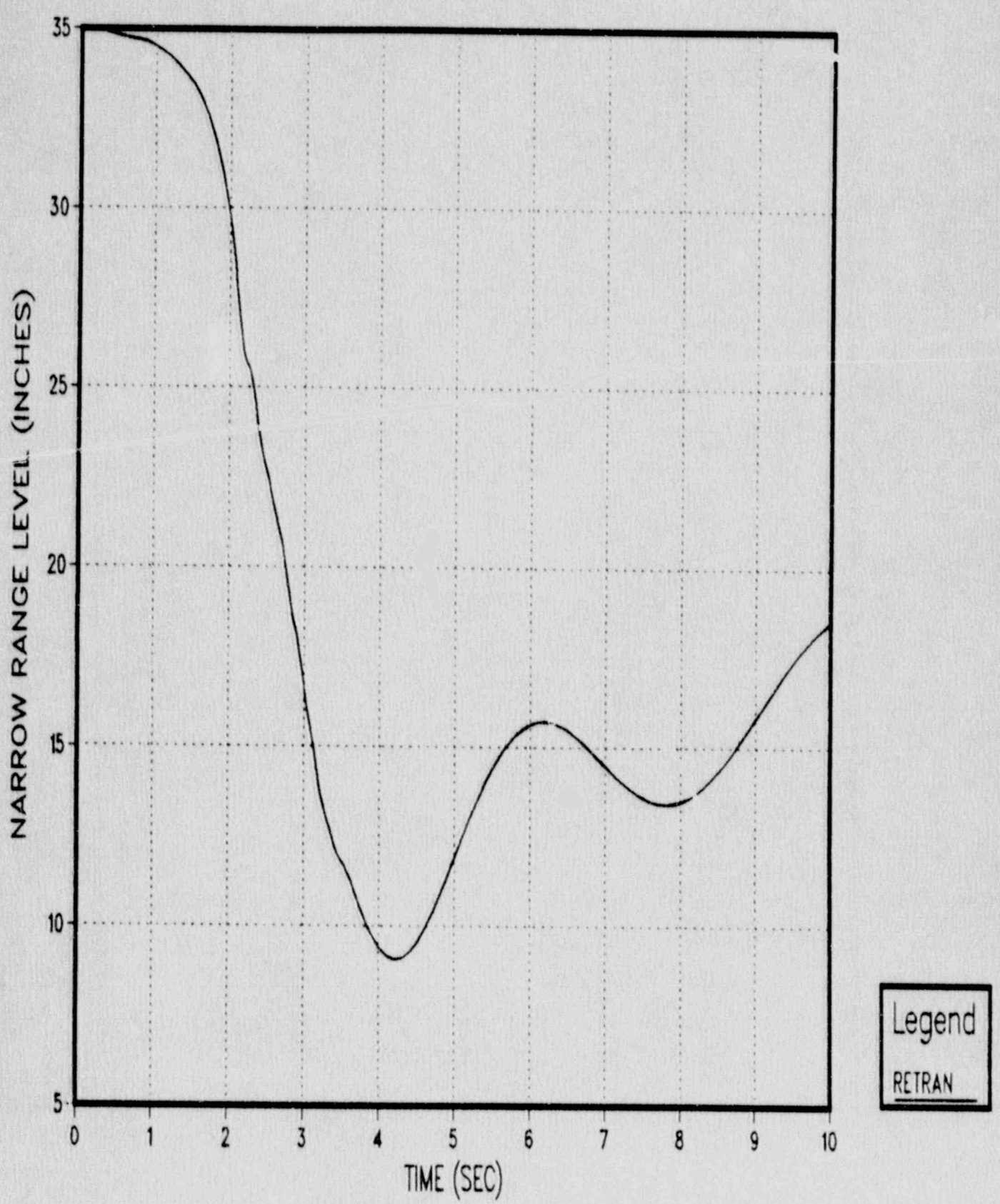

FIGURE 3.5-11 : MSIVC FEEDWATER FLOW

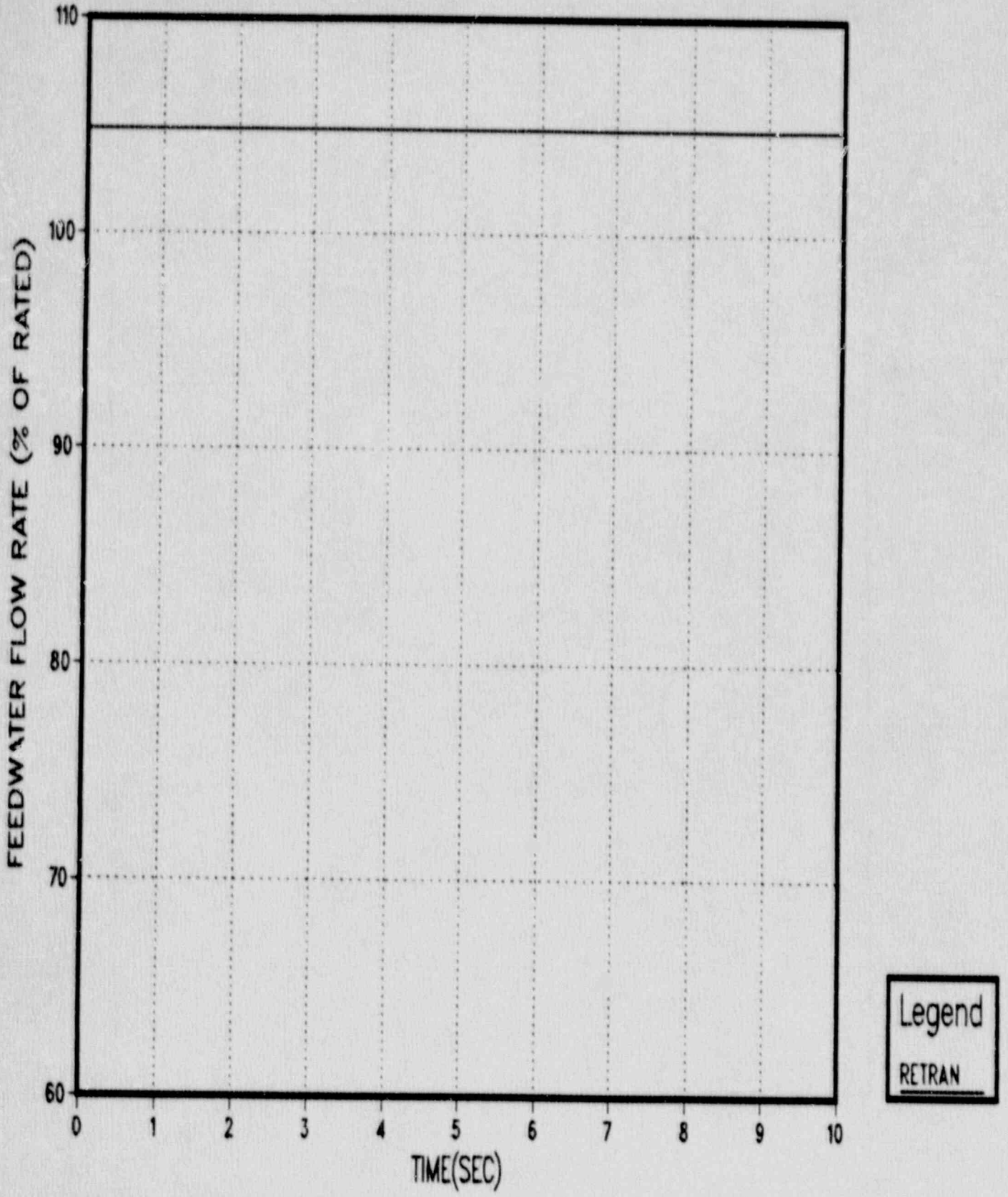

FIGURE 3.5-12 : MSIVC AVERAGE HEAT FLUX

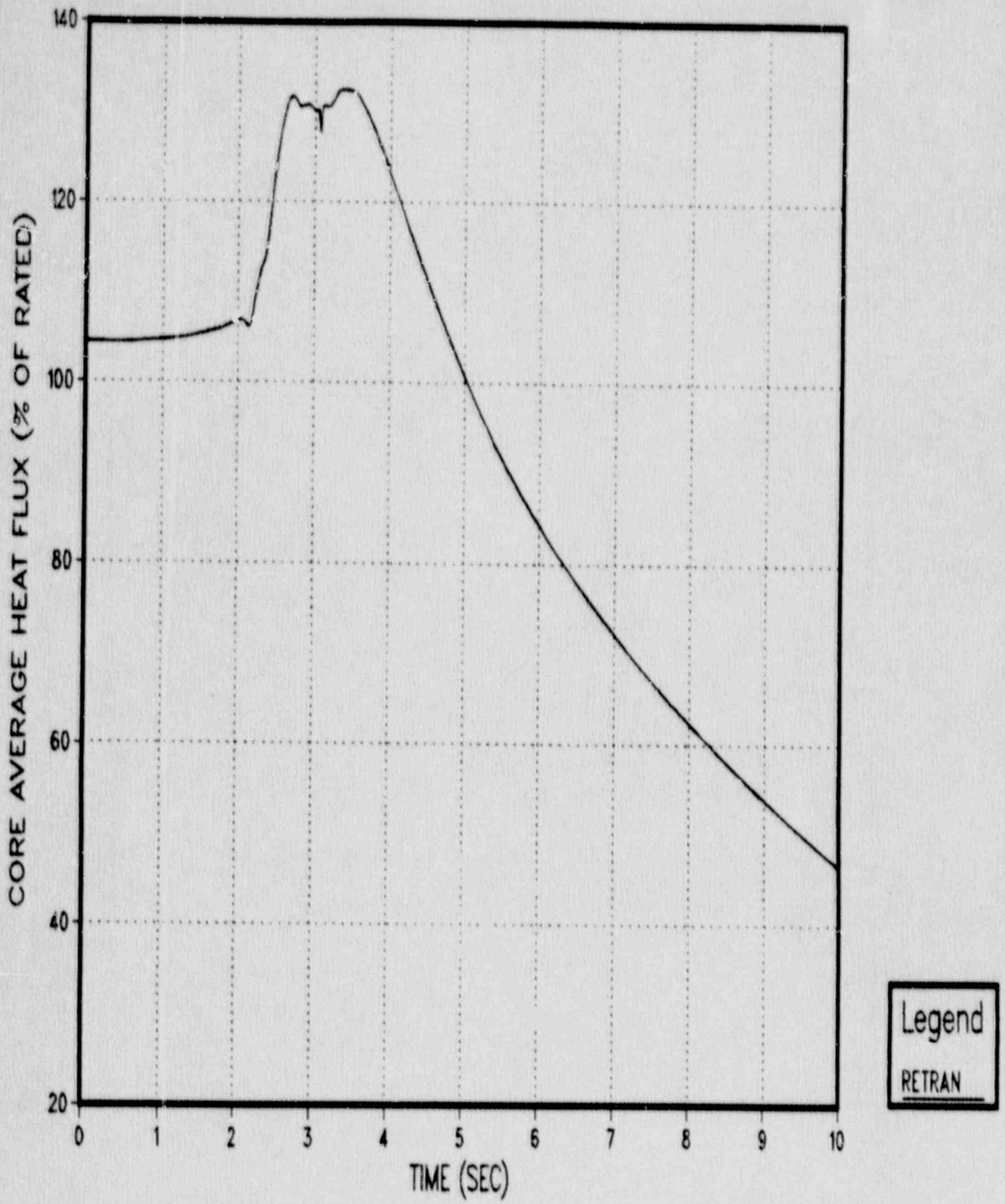

FIGURE 3.5-13 : MSIVC PRESSURE MARGIN

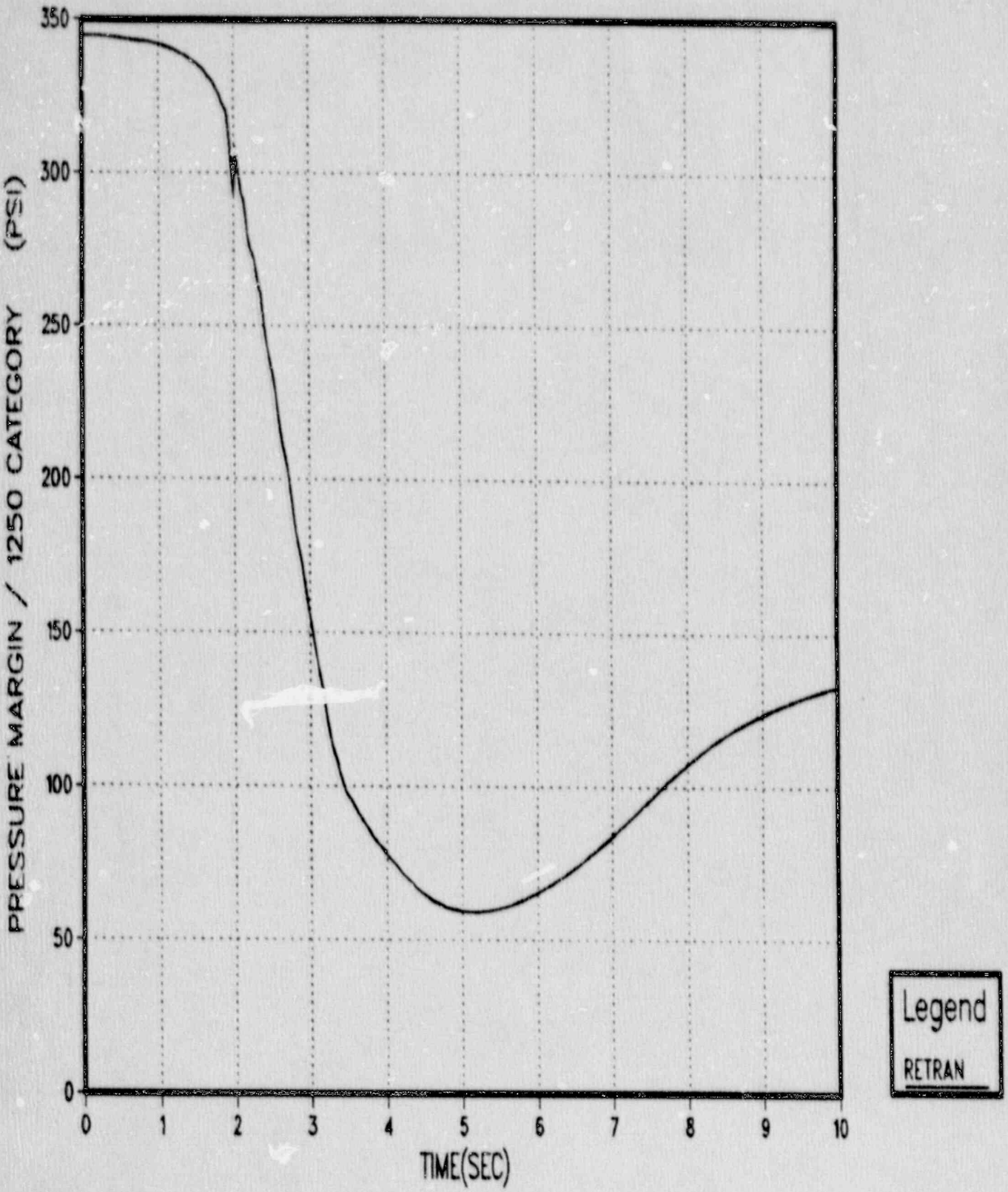

FIGURE 3.5-14 : MSIVC PRESSURE MARGIN

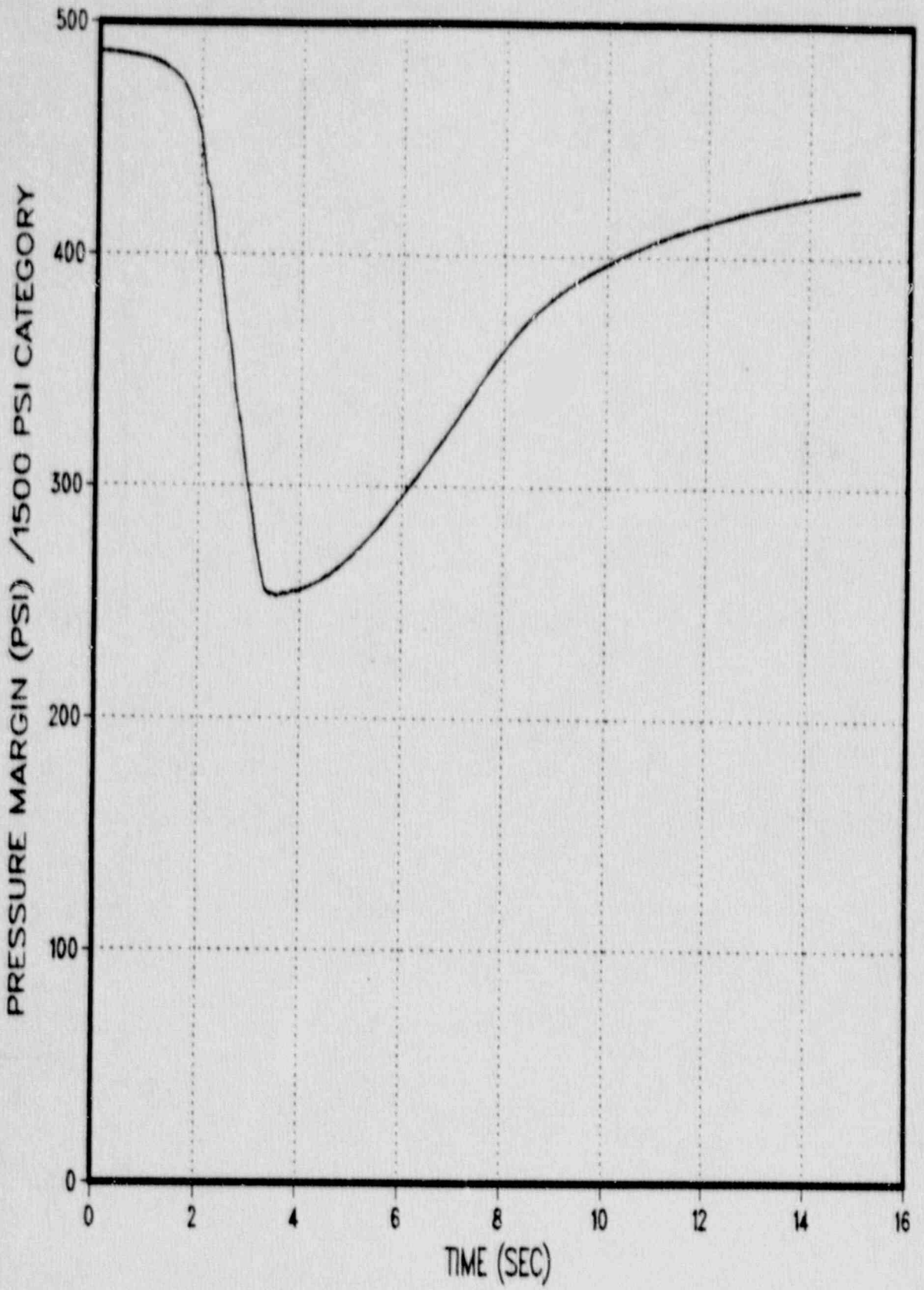

4.0 TECHNICAL SPECIFICATIONS

A function of the Technical Specification limits is to ensure that key assumptions of the safety/licensing analyses are valid. The analysis methodologies described in this report produce results which affect the Technical Specifications. Some of the results represent analyses which will be performed directly by PP&L, while others will be performed with the fuel vendor's methodology using input generated by PP&L. This section describes the manner in which the analysis results would affect the Susquehanna SES Technical Specifications. Clearly, a large number of Technical Specification values are used as input to the reload licensing analyses (e.g., response times, instrument setpoints, number of operable valves required, etc.). The discussions in this section focus on the Technical Specification values which are the result of the PP&L analyses or vendor methodology analyses with PP&L input.

References to specific Susquehanna Technical Specification sections are based on References 15 and 16.

4.1 MCPR Limits

4.1.1 Basic Approach

The safety limit given in Section 2.1.2 will no longer be a single MCPR value. The safety limit will be the condition such that 99.9% of the fuel pins are not expected to experience boiling transition, in conformance with SRP 4.4.

The MCPR operating limits are contained in Section 3.2.3 of the Susquehanna SES Technical Specifications. Section 3.2.3 defines MCPR operating limits for three modes of operation: 1) End of Cycle Recirculation Pump Trip (EOC-RPT) inoperable (mode A), 2) Main turbine bypass inoperable (mode B), and 3) EOC-RPT and main turbine bypass both operable (mode C). The MCPR operating limits as a function of core power, core flow, and operating mode are determined from the results of the transient analyses of the following events:

1) Rod withdrawal error,
2) Fuel loading error,
3) Loss of feedwater heating,
4) Generator load rejection without bypass,
5) Feedwater controller failure,
6) Recirculation flow controller failure (increasing).

The Technical Specification MCPR operating limit is determined for a given core power, core flow, and operating mode as the largest value of required operating limit calculated for the above listed events.

This approach will be maintained when PP&L performs some of the reload analyses previously performed by the fuel vendor. Modifications to the Section 3.2.3 MCPR operating limit Technical Specifications are needed, however, to accommodate the SCU analysis methods for pressurization events

described in Section B.2 of this report. This modification reflects the fact that the MCPR operating limits will be a function of average measured control rod scram insertion speed, in order to be consistent with the analyses. The modifications to Technical Specification 3.2.3 to accommodate the SCU analyses methodology are described in Section 4.1.2.

4.1.2 Scram Speed Dependent MCPR Operating Limits

One of the key inputs that is treated statistically in the SCU method for pressurization events (see Section B.2) is average control rod insertion speed. For these statistical analyses, a control rod insertion versus time curve (hereinafter referred to as a scram curve) is used which is more realistic than the Technical Specification Section 3.1.3.3 scram curve. Thus, a process is required to adjust the MCPR operating limits as a function of the measured scram curve. In other words, the MCPR operating limits (Technical Specification 3.2.3) become functions of measured scram speed. As the measured scram speed decreases (i.e., a slower average control rod insertion), the MCPR operating limit would increase.

Analyses of Susquehanna SES measured scram time data included over 3800 individual rod measurements taken on both units from October 1984 through March 1990. These analyses demonstrate that the average scram speed (ft/second) can be treated as normally distributed using the W test for normality (Reference 25). Thus, statistical analyses of pressurization transients will use the scram speed as the variable of interest along with a conservative time for the start of rod motion. An example of this approach is given in Section 3.1 for the GLRWOB event. The Technical Specification will be written to adjust MCPR operating limits as a function of the measured scram speed.

The statistical analyses will be done assuming a mean scram speed and standard deviation. If the measured mean is such that it would indicate that the transient analyses are potentially non-conservative, the MCPR operating limits would be increased.

In performing the transient analysis of the GLRWOB, or other limiting pressurization events at a given power/flow condition, two separate analyses are performed. A separate required MCPR operating limit is generated by each analysis:

1) A "traditional" conservative analysis using the maximum scram times allowed by Technical Specification 3.1.3.3, and

2) A SCU analysis assuming a more realistic scram curve and using the Appendix B methodology.

These two analyses each produce curves of MCPR operating limit versus core power and core flow. The actual MCPR operating limit to be used will be determined by linear interpolation between points on the curves, using scram speed as the variable of interest.

At the startup of each cycle, a scram time measurement per Specification 4.1.3.2(a) is made for all control rods. Other scram time measurements are required by Specifications 4.1.3.2(b) and (c). If the scram characteristics have changed for the worse (i.e., slower insertion), then an adjustment to the MCPR operating limits using the method described above would be made.

4.2 Other Limits

This section addresses a number of Technical Specification limits, other than the MCPR limits addressed in Section 4.1, which could be affected by the results of the analysis methodologies described in this report. The shutdown margin analysis methodology (Section 2.4) is done to meet the requirements of Specification 3.1.1. The standby liquid control system analysis methodology (Section 2.5) is done to verify, or if necessary, to revise the requirements of Specification 3.1.5. The Loss of Coolant Analysis (LOCA) calculations, performed with certain PP&L inputs (Section 2.7), are done with the fuel vendor's methodology to validate or revise the Average Planar Linear Heat Generation Rate limits given in Specification 3.2.1. The fuel storage criticality analyses (Section 2.11) are performed to demonstrate compliance with Specification 5.6.

5.0 SUMMARY AND CONCLUSIONS

This report describes the methods and assumptions used to apply the PP&L steady state core physics methods (Reference 1) and transient analysis methods (Reference 2) to perform conservative analyses for licensing applications. Analysis methodologies are presented for events to be analyzed by PP&L on a typical reload core licensing application to establish MCPR operating limits (rod withdrawal error, fuel loading error, loss of feedwater heating, generator load rejection, feedwater controller failure, and recirculation flow controller failure). The set of FSAR Chapter 15 events was examined to establish that other transient events are non-limiting for establishing MCPR operating limits. Methodology for the MSIV closure/ASME overpressure analysis is also described. A conservative method of calculating fuel rod gap conductances for the RETRAN system and hot bundle models using the ESCORE code is presented. In addition, Statistical Combination of Uncertainties methods are presented for establishing MCPR operating limits for pressurization transients and for the rod withdrawal error.

Analysis methodologies, using PP&L's steady state core physics methods (Reference 1), are also presented to: 1) verify sufficient shutdown margin, 2) verify the ability of the standby liquid control system to shutdown the reactor, 3) provide lattice physics code (CPM-2) input to the POWERPLEX core monitoring system, and 4) provide input to fuel vendor methodology analyses of LOCA, MCPR safety limit, and the control rod drop accident.

Sample analyses utilizing the methods described in this report are presented for a number of key events. In summary, the codes, models, and methods described in this report and References 1 and 2 will produce conservative results for licensing applications. PP&L plans to utilize the methods described for licensing analyses.

6.0 REFERENCES

1. "Qualification of Steady-State Core Physics Methods for BWR Design and Analysis", PL-NF-87-001-A, Pennsylvania Power & Light, July 1988.

2. "Qualification of Transient Analysis Methods for BWR Design and Analysis", PL-NF-89-005, Pennsylvania Power & Light, December 1989.

3. "Advanced Recycle Methodology Program", EPRI CCM-3, September, 1977.

4. D. B. Jones, "CPM-2 Computer Code User's Manual", Part II, Chapter 6 of EPRI NP-4574-CCM, February, 1987.

5. D. M. VerPlanck, "SIMULATE-E: A Nodal Core Analysis Program for Light Water Reactors", EPRI NP-2792-CCM, March, 1983.

6. M. Edenius, A. Ahlin, "MICBURN: Microscopic Burnup In Gadolinia Fuel Pins", Part II, Chapter 7 of EPRI CCM-3, November, 1975.

7. D. B. Jones and M. J. Anderson, "ARMP-02 Documentation: Part II, Chapter 12-NORGE-B2 Computer Code Manual", EPRI NP-4574-CCM, Part II, Chapter 12, December, 1986.

8. S. W. Jones, et. al., "POWERPLEX Core Monitoring Software System Software Specification for the Susquehanna Steam Electric Station Susquehanna Units 1 and 2", XN-NF-83-35(P), Revision 1, August, 1986.

9. "ARMP-02 Documentation: Part II, Chapter 8 SIMULATE-E (Mod. 3) Computer Code Manual", EPRI NP-4574-CCM, Part II, Chapter 8, September, 1987.

10. "RETRAN 02 - A Program for Transient Thermal-Hydraulic Analysis of Complex Fluid Flow Systems", EPRI-NP-1850-CCM-A, Computer Code Manual, June, 1987.

11. "SIMTRAN-E: A SIMULATE-E to RETRAN-02 Data Link", EPRI NP-5509-CCM, December, 1987.

12. "XN-3 Critical Power Correlation", XN-NF-512-P-A, Revision 1 and Supplement 1, Revision 1, October, 1982.

13. "ESCORE - the EPRI Steady-State Core Reload Evaluator Code: General Description", EPRI-NP-5100, February, 1987.

14. "Susquehanna Steam Electric Station Units 1 & 2, Final Safety Analysis Report", Revision 41, May 1989.

15. "Susquehanna Steam Electric Station Unit 1 Technical Specifications (TS1) Docket No. 50-387, Appendix A to License No. NPF-14", Amendment 94, December 1989.

16. "Susquehanna Steam Electric Station Unit 2 Technical Specifications (TS2) Docket No. 50-388, Appendix A to License No. NPF-22," Amendment 62, January 16, 1990.

17. "Exxon Nuclear Critical Power Methodology for Boiling Water Reactors", XN-NF-524-P-A, Revision 1, November 1983.

18. "Exxon Nuclear Methodology for Boiling Water Reactor, THERMEX: Thermal Limits Methodology Summary Description", XN-NF-80-19-P-A, Volume 3, Revision 2, January 1987.

19. "Standard Review Plan for the Review of Safety Analysis Reports for Nuclear Power Plants", NUREG-0800, July 1981.

20. Code of Federal Regulations 10, Part 50, Appendix A, January 1987.

21. "Safety Evaluation for the General Electric Topical Report Qualification of the One-Dimensional Core Transient Model for BWRs - NEDO-24154 and NEDO-24154-P, Volumes I, II, III," June 1980.

22. "Generic Statistical Uncertainty Analysis Method," XN-NF-81-22-P-A, November 1983.

23. Robert Van Houton, "Fuel Rod Failure as a Consequence of Departure from Nucleate Boiling or Dryout," NUREG-0562, June 1979.

24. ASME Boiler and Pressure Vessel Code, Section III, 1968 Edition, Summer 1970 Addenda.

25. "Assessment of the Assumption of Normality (Employing Individual Observed Values)", ANSI N15.15-1974.

26. "Criticality Safety Analysis Susquehanna New Fuel Vault with Exxon Nuclear Co., Inc. 9x9 Reload Fuel," XN-NF-86-44, Rev. 1, May 1986.

27. "Criticality Safety Analysis Susquehanna Spent Fuel Storage Pool with Exxon Nuclear Co., Inc. 9x9 Reload Fuel," XN-NF-86-45, Rev. 1, May 1986.

28. "Exxon Nuclear Methodology for Boiling Water Reactors: Neutronic Methods for Design and Analysis", XN-NF-80-19(A), Volume 1, and Volume 1 Supplements 1 and 2, March 1983.

29. "Generic Mechanical Design for Exxon Nuclear Jet Pump BWR Reload Fuel", XN-NF-85-67-P-A, Revision 1, September 1986.

30. "Susquehanna LOCA-ECCS Analysis MAPLHGR Results for 9x9 Fuel", XN-NF-86-65, May 1986.

31. "Generic LOCA Break Spectrum Analysis for BWR-3 and 4 with Modified Low Pressure Coolant Injection Logic", XN-NF-84-117-P, December 1984.

32. "Acceptance for Referencing of Licensing Topical Report EPRI-NP-5100, ESCORE - The EPRI Steady-State Core Reload Evaluator Code: General Description", Letter from A. C. Thadani (NRC) to C. R. Lehmann (PP&L), May 23, 1990.

33. "Banked Position Withdrawal Sequence" NEDO-21231, General Electric Company, January 1977.

APPENDIX A

LICENSING BASIS GAP CONDUCTANCE METHODS

A.1 INTRODUCTION

To perform non-LOCA transient analyses, the RETRAN code requires input values of hot bundle and core average gap conductance. The NRC approved ESCORE code (References 13 and 32) is used for this purpose. This Appendix outlines conservative methodologies for calculating gap conductances for use in RETRAN/CPRITER ΔCPR calculations. Separate methods are specified for calculating gap conductances for input to the RETRAN system model and the RETRAN hot bundle model.

Actually, the gap conductance is input to RETRAN as gap conductivity defined as gap conductance times gap width. The gap conductance is a parameter which affects how rapidly a change in rod power will result in a change in surface heat flux. Thus, gap conductance has a significant effect on transients involving a rapid change in power (i.e., a change in power occurring over a time period comparable to the fuel rod time constant).

A.2 DEFINITION OF CONSERVATIVE FOR LICENSING CALCULATIONS

In the RETRAN system model (Reference 2), the gap conductance affects the rate at which a given power change causes a change in heat deposited in the coolant. This, in turn, affects the reactivity feedback due to a change in moderator density and void fraction. Faster heat deposition in the water for an event involving a rapid power increase produces more negative void reactivity feedback, which slows the rate of power increase. Therefore, a low value of gap conductance in the RETRAN system model will cause a larger power increase for a power increasing event.

For those events involving a rapid power increase (i.e., pressurization events), gap conductance will have an impact on the RETRAN system model calculation of core power. All other factors being equal, a larger power increase produces a larger change in Critical Power Ratio (ΔCPR). Events

involving a power decrease are not limiting for ΔCPR. For slow events, the value of gap conductance has little effect on the rate at which heat is deposited in the water. Therefore, a low value of gap conductance in the RETRAN system model is used, because this produces conservative ΔCPR calculations for pressurization transients, and the value of gap conductance has little impact on the calculated ΔCPR for slow events. For the recirculation flow controller failure slow run-up event (Section 3.3), a high value of gap conductance made the calculated ΔCPR slightly higher and will be used for licensing analyses of that event.

The RETRAN hot bundle model (Reference 2) uses the normalized power versus time calculated by the RETRAN system model (i.e., the hot bundle is assumed to have the same normalized power versus time as the core average). Thus, for pressurization events, which involve rapid power increases, a larger hot bundle gap conductance will produce a larger increase in heat flux. The larger heat flux is conservative for ΔCPR calculations.

A.3 USE OF ROD AVERAGE GAP CONDUCTANCE

Physically, gap conductance of a fuel rod varies axially. It is cumbersome, however, to model an axially dependent gap conductance in RETRAN. A RETRAN study was performed to calculate the total heat deposited in the coolant as a function of time for both an axially dependent gap conductance and an axially averaged (axially constant) gap conductance. The study demonstrated that an axially averaged gap conductance produces virtually the same total heat deposited in the coolant as a function of time as the axially variable gap conductance for typical licensing basis pressurization events. Thus, ESCORE calculated values of axially averaged gap conductance will be used in the RETRAN system model.

A similar study was performed to determine the effect of using an axially averaged gap conductance in the RETRAN hot bundle model. Results showed that, for the 14 axial power distributions examined, the axially averaged gap conductance produces equal or higher calculated ΔCPRs than the axially variable gap conductance. Thus, an axially averaged gap conductance will be used for the hot bundle model.

A.4 ESCORE INPUTS

A.4.1 Inputs for System Model Gap Conductance

A large ESCORE parametric study was performed to determine the sensitivity of calculated axial average gap conductance to changes in ESCORE input parameters.

The following describes the basic philosophy used to select input parameters for ESCORE core average/system model calculations. For a given parameter, the rods are expected to have a distribution of values about the nominal value (e.g., cladding outside diameter). Therefore, all parameters will be taken to be at their nominal (best estimate) values, except for axial power distribution (APD) and power history. This is due to the fact that exact values for the APD and power history are not known prior to the cycle of interest. These parameters are conservatively chosen to introduce conservatism into the system model gap conductance calculation. Table A.4-1 summarizes this methodology. The methodology for selecting a conservative power history is presented in Section A.5.

Input parameters which were determined to have negligible effect on gap conductance are listed in Table A.4-2. These parameters are set at their nominal values for calculations of core average gap conductance. Table A.4-3 gives values for the number of axial nodes and time step size. These values were found to produce good results while keeping the computer

run time reasonable and are used for system model core average gap conductance analyses.

A.4.2 Inputs for Hot Bundle Model Gap Conductance

The following describes the basic philosophy used to select input parameters for ESCORE hot bundle gap conductance calculations. Note that the ESCORE model represents a single fuel assembly.

Table A.4-1 lists the ESCORE input parameters which affect calculated gap conductance. These parameters can be grouped into 3 categories: (1) well characterized physical parameters (e.g., yield strength), (2) manufacturing parameters for rods or pellets (e.g., grain size, pellet O.D., cladding I.D., rod pre-pressure), and (3) parameters that are less well known (e.g., change in fuel density, fast flux to LHGR factor, system pressure, resonance escape probability, axial power distribution, and power history). The philosophy for establishing ESCORE inputs to calculate conservative hot bundle gap conductances is:

Category 1: use nominal measured value(s).

Category 2: use nominal values since it is unlikely that all rods or pellets in a bundle will have these parameters biased in the adverse direction.

Category 3: use conservative values for these parameters to bound the way in which a bundle will be operated.

Table A.4-1, describes the selection of input parameters using the above philosophy. The methodology for selecting a conservative power history is presented in Section A.5.

Input parameters which were found to have a negligible effect on gap conductance are listed in Table A.4-2. These parameters are set at their nominal values for calculations of hot bundle gap conductance. Table A.4-3 gives values for the number of axial nodes and the time step size. These values were found to produce good results while keeping the computer run time reasonable and are used for hot bundle gap conductance analyses.

A.5 POWER HISTORY

A.5.1 Effects of Power History

Rod power as a function of time (power history) is one of the major factors affecting gap conductance. As a rod produces power, it undergoes many changes: swelling, cracking, cladding creep, pellet/cladding interaction, fission gas release, etc. All of these changes are affected by power history.

The gap conductance of each rod in the core is different, because each rod has a different power history. It would be theoretically possible to calculate gap conductance for every rod in the core using a combined neutronics/fuel performance code to track the power history of each rod. Such a code is neither practical nor available, however. Therefore, a simplified procedure is required.

Sections A.5.2 and A.5.3 describe the process used to produce simplified power histories for core average and hot bundle gap conductance calculations. As stated previously, a low value of gap conductance is conservative for the core average (RETRAN system model) with the exception of the RFCF event described in Section 3.3, and a high value is conservative for the hot bundle (RETRAN hot bundle model).

A.5.2 Core Average Power History

The core average gap conductance determines how changes in total core power cause changes in heat deposited to the coolant. Thus, high power bundles contribute more to the core thermal response than low power bundles. High power bundles generally have higher gap conductances than low power bundles. Therefore, averaging the gap conductances of all bundles in the core would conservatively underestimate the core average gap conductance.

Rather than calculating a gap conductance for each fuel bundle, it is more convenient to divide the bundles into groups. The most logical grouping is by fuel type and in-core residence time.

The power history used to calculated gap conductance for each group is based on the average power generated during each cycle by that group. In reality, each group would have some bundles operating at powers greater than the average and some bundles operating at powers less than the average. Assuming all bundles have the group average power history will conservatively underestimate the gap conductance. This conclusion is further supported by the shape of the gap conductance versus Local Power Density (LPD) curve. ESCORE analyses demonstrated that the shape of the curve tends to be concave upward (i.e., the slope of gap conductance versus LHGR increases with increasing LHGR). The average power produced per bundle for a given batch is:

$$AP_i = (E_i * W_i) / N_i ,$$

where: AP_i = average power produced per bundle (GWD)

E_i = change in batch average exposure for cycle of interest (GWD/MT)

W_i = total batch fuel weight (MT)

N_i = number of bundles in batch i

At the cycle exposure of interest, the ESCORE power is varied to produce gap conductance as function of core average power. The calculated gap conductances for each fuel type/residence time group (at a given core average power level) are combined into an equivalent gap conductance as described in Section A.6.1.

A.5.3 Hot Bundle Power History

A high value of gap conductance is conservative for RETRAN hot bundle analyses. There are two main phenomena which affect the calculated gap conductance: fuel swelling/cracking and fission gas release. The two phenomena have opposite effects on gap conductance. Increased fuel swelling reduces the gap size and produces a larger gap conductance. Fission gases have a lower thermal conductivity than the helium gas used to initially pressurize the fuel rods. Thus, increased fission gas release decreases the gap gas conductivity and produces a smaller gap conductance. In general, a power history that maximizes swelling (high powers) also maximizes fission gas release.

The power history for generating ESCORE hot bundle gap conductances is given below. The bundle is modelled as a single fuel rod.

1) The rod operates with its peak node at the Maximum Average Planar Linear Heat Generation Rate (MAPLHGR) limit for the first 1,000 MWD/MT of its life. This produces conservative cracking/relocation without significant fission gas release.

2) The rod LHGR is reduced to a value 10% above the fuel type average value and held constant out to the maximum end of cycle bundle exposure.

ESCORE analyses were performed comparing gap conductances produced by the above procedure and those produced by assuming a more realistic power history. The results of these analyses demonstrate that the power history methodology described above produces conservatively high calculated gap conductances.

A.6 GAP CONDUCTANCE METHODOLOGY SUMMARY

A.6.1 Core Average/System Model

The method for calculating a conservative core average gap conductance for use by the RETRAN system model is outlined below:

1) Divide the core into groups by fuel type and residence time.

2) For each group determine a power history as described in Section A.5.2. Group average power levels for each cycle will be obtained from core follow data when available. For predicting conditions where core follow data is not available, SIMULATE-E cycle stepout calculations with expected control rod patterns will be used.

3) Set up ESCORE base decks for each fuel type. Choose appropriate input parameters as discussed previously in Section A.4.1.

4) Perform ESCORE gap conductance calculations for each fuel type/in-core residence time group. The analysis should be performed out to the end of the cycle of interest.

5) Calculate an effective gap conductance at the time in cycle of interest (usually EOC) using the following method. A simplified RETRAN model is set up for each fuel/exposure group using ESCORE calculated gap conductances. The gap conductance of a separate model, set up to represent the fuel type modelled in the RETRAN system model, is adjusted until the heat deposited to the coolant matches the multi-group model for a rapid power increase and decrease. The adjusted value of gap conductance is used in the RETRAN system model.

A.6.2 Hot Bundle

The method for calculating a conservative hot bundle gap conductance for use by the RETRAN hot bundle model is outlined below. These steps are followed for each fuel type/in-core residence time group:

1) Determine the power history as described in Section A.5.3.

2) Set up an ESCORE base deck for the applicable fuel type. Choose appropriate input parameters as discussed in Section A.4.2.

3) Perform ESCORE gap conductance calculations out to the maximum bundle exposure which would exist at end of cycle.

4) Identify the bundle exposure at which the largest calculated gap conductance occurs.

5) Perform a second ESCORE calculation using the same power history out to the exposure identified in Step 4. At this exposure, raise the rod power in a series of small exposure steps.

6) Based on the results of the Step 5 ESCORE calculation, plot axially averaged hot bundle gap conductance as a function of LHGR. The relation between LHGR and gap conductance will be used to select input to the RETRAN hot bundle model.

A.7 SAMPLE RESULTS

The methods described in this Appendix were used to produce sample gap conductances for Susquehanna SES Unit 2 Cycle 2. Results are provided in Tables A.7-1 and A.7-2 for the system and hot bundle models, respectively.

A.8 SUMMARY/CONCLUSIONS

The ESCORE modelling guidelines outlined in this Appendix will result in the calculation of conservative gap conductances for use in licensing basis RETRAN transient analyses. The methods described herein were used to generate gap conductances for the RETRAN analyses described in this report.

TABLE A.4-1

Selection of Conservative Input Values for ESCORE Licensing Basis Gap Conductance Calculation

Parameter (Name)	Units	Value to Use: System Model	Value to Use: Hot Bundle Model	Notes
1. Fast Neutron Flux to LHGR Factor (FQRAT)	$\frac{n/cm^2\ sec}{kw/ft}$	nominal	minimum	1
2. Change in Fuel Density: Final (RHOUT) minus Initial (RHOIN)	% theoretical	nominal	minimum	2
3. Grain Size (GRAIN)	microns	nominal	nominal	9
4. Cladding Yield Strength (SY)	KSI	nominal	nominal	9
5. Pellet O.D.	inches	nominal	nominal	6
6. Cladding I.D.	inches	nominal	nominal	6
7. Rod Pre-Pressure	psig	nominal	nominal	7
8. System Pressure	psia	nominal	nominal	8
9. Resonance Escape Probability (REP)	--	nominal	large	3
10. Axial Power Distribution	--	"flat"	--	4
11. Power History	--	--	--	5

Notes To Table A.4-1

1. These values are obtained from CPM-2 code calculations (Reference 1). A set of CPM-2 runs covering the range of void fractions, exposures, and fuel types is examined.

2. Values currently used are based on vendor re-sinter tests of densification.

3. Conservative value based on ESCORE gap conductance sensitivity analyses is used for the hot bundle analyses.

4. ESCORE analyses demonstrated that an Axial Power Distribution (APD) with a high axial peak produces a slightly larger gap conductance than an APD with a lower axial peak ("flat APD") for a fixed power history. For core average gap conductance calculations, a flat APD should be used.

   ESCORE analyses demonstrated that the hot bundle gap conductance has little sensitivity to APD. This is the case because the high power nodes (which have high gap conductances) and the low power nodes (which have low gap conductances) tend to balance each other. Thus, for example, the full power/full flow EOC core average APD from SIMULATE-E for the cycle being analyzed could be used in the hot bundle analyses.

5. Power History is discussed in Section A.5.

6. It is unlikely that all fuel pellets or cladding in a core or fuel assembly would be at their tolerance limits because they are

fabricated at different times and there are different pellet lots used in each assembly.

7. The rod pre-pressure will have minimal effect on gap conductance since the tolerance is small (on the order of ± 5 psi). It is unlikely that all rod pre-pressures in a bundle or core will be at the tolerance limit. Thus, the nominal value is used for both core average and hot bundle analysis.

8. Since system pressure does not vary greatly throughout the operating cycle, a value of nominal system pressure is used.

9. Although there is some dependence of gap conductance on grain size and cladding yield strength, it is unlikely that all grain sizes in a bundle or core are at their tolerance limits. Thus, nominal values are used.

TABLE A.4-2

ESCORE Input Parameters With Negligible Effect on Gap Conductance
(For Use in Both System & Hot Bundle Analyses)

Parameter	Value	Note
Core Inlet Temperature (°F)	--	Use nominal full power value
Mass Flow Rate (lbm/hr-ft^2 °F)	--	Use nominal full flow bundle average value for the act ve core (assume 10% leakage)
Enrichment	--	Use "bundle type" average value
Cladding Surface Roughness	--	Use value from fuel design drawings
Fuel Pellet Surface Roughness	--	Use value from fuel design drawings
Fast Leakage Factor	.975	Recommend:: by Reference 13
Fraction of Open Porosity	.001	Used for ESCORE benchmarking (Reference 13)
Fraction of Relocation Crack Volume in Porosity Correction Factor	1.0	Used for ESCORE benchmarking (Reference 13)
Burnup at which Densification is Complete (GWD/MT)	5.0	Used for ESCORE benchmarking (Reference 13)
Clad ID Texture Angle	--	Use nominal vendor supplied value

TABLE A.4-3

Noding & Time Step Selection for ESCORE Gap Conductance Calculations (System & Hot Bundle Models)

Parameter	Value	Note
Number of Axial Nodes (System Model)	24*	1 - one foot node at the bottom, plus 23 - six inch nodes
Number of Axial Nodes (Hot Bundle Model)	24*	1 - one foot node at the bottom, plus 23 - six inch nodes
Number of Radial Rings	10	All ESCORE benchmarking was done with 10 rings
Maximum Time Step Size (hrs)	100	Shorter than necessary for accurate results. However, the smaller time step size doesn't significantly affect run time.

*For calculations, this makes the ESCORE power shape virtually identical to a 25 node RETRAN power shape.

TABLE A.7-1

System Model Gap Conductance
Results for Susquehanna SES Unit 2 Cycle 2

Core Power (% rated)	Gap Conductance (BTU/hr ft^{2}F)
104.5	870
100	855
65	760
40	700

TABLE A.7-2

Hot Bundle Model Gap Conductance Results
for Susquehanna SES Unit 2 Cycle 2

Linear Heat Generation Rate (kw/ft)	ANF 9x9 Bundle Gap Conductance (BTU/hr ft^{2}F)
5.7	1291
6.0	1332
6.5	1403
7.0	1483
7.5	1574

APPENDIX B

STATISTICAL COMBINATION OF UNCERTAINTIES

B.1 INTRODUCTION

B.1.1 Background

This Appendix outlines PP&L's method for calculating a licensing basis Minimum Critical Power Ratio (MCPR) operating limit for pressurization events analyzed with RETRAN (e.g., generator load rejection, feedwater controller failure) and for the rod withdrawal error event. The method uses a Statistical Combination of Uncertainties (SCU) approach closely related to other NRC approved methods (References 21 and 22). The main difference between the methodologies described herein and other, NRC approved methods is that the PP&L methods combine the MCPR Safety Limit and transient ΔCPR calculations into a single, unified statistical analysis.

Historically, many licensing basis transient analyses were done assuming all parameters which influence the calculated ΔCPR are biased in the conservative direction. While producing conservative ΔCPR calculations, this approach tends to produce unnecessarily restrictive MCPR operating limits.

The probability that all relevant parameters would simultaneously be at their "worst case" values is exceedingly low. Thus, statistical methods were developed to remove some of this unneeded conservatism. These methods use Monte Carlo techniques to statistically combine the uncertainties of the key parameters, and are referred to as Statistical Combination of Uncertainties methods.

The current NRC approved SCU methods use separate Monte Carlo analyses to calculate a MCPR Safety Limit and a transient ΔCPR. The MCPR operating limit is the sum of the values produced by these separate analyses. The methodology described herein is a logical extension of existing SCU

methods, in that it combines the ΔCPR and Safety Limit analyses into a single Monte Carlo analysis.

B.1.2 Applicable Licensing Requirements

The applicable NRC requirements for establishing a MCPR operating limit can be found in 10CFR50, Appendix A (Reference 20) and are referred to as General Design Criteria (GDC). General Design Criterion 10 requires that Specified Acceptable Fuel Design Limits (SAFDLs) are not violated during normal operation or Anticipated Operational Occurrences (AOOs). The Standard Review Plan (SRP; Reference 19) provides clarification of the NRC criteria given in the GDC. The SRP states that the Generator Load Rejection without Bypass (GLRWOB), Feedwater Controller Failure (FWCF), and Rod Withdrawal Error (RWE) events are subject to GDC 10. Standard Review Plan Sections 4.2 and 4.4 clarify the specified acceptable fuel design limits. Standard Review Plan Section 4.4 states that an acceptable approach to meeting GDC 10 is:

> "For DNBR, CHFR or CPR correlations, the limiting (minimum) value of DNBR, CHFR, or CPR is to be established such that at least 99.9% of the fuel rods in the core would not be expected to experience departure from nucleate boiling or boiling transition during normal operation or anticipated operational occurrences."

Thus, the goal of the SCU method described in this Appendix is to demonstrate that at least 99.9% of the fuel rods in the core would not be expected to experience boiling transition during any portion of the transient.

B.2 PRESSURIZATION EVENTS

This section describes the SCU methodology for calculating MCPR operating limits for pressurization events analyzed with RETRAN (e.g., GLRWOB, FWCF). The methodology consists of three major steps:

1) A Monte Carlo transient analysis using a RETRAN/CPRITER response surface is performed to determine a probability distribution of calculated RCPR.

2) A set of "safety limit type" analyses is performed for a range of MCPR values to generate a set of probability distributions of fraction of the fuel rods in the core in boiling transition.

3) A combined Monte Carlo analysis using the results of steps 1 and 2 is performed to calculate an operating limit such that 99.9% of the pins are not expected to be in boiling transition.

Details of these major steps are provided in the following sections.

B.2.1 Statistical RCPR Calculation

A set of parameters is selected to be treated statistically. Parameters which have significant impact on the ΔCPR (determined by previous analysis) and have significant variation due to uncertainty should be selected. All other parameters are put at conservative "worst case" values. Parameters typically selected for statistical analysis for pressurization events include core power, scram speed, and scram delay. For each parameter to be treated statistically, a Cumulative Probability Distribution Function (CPDF) is generated. The CPDF gives the probability

that a parameter will be less than or equal to a given value as a function of that value.

Since a Monte Carlo procedure requires a large number of trials to produce meaningful results, it is impractical to use the RETRAN/CPRITER methods for each trial. To facilitate the analysis, a set of RETRAN/CPRITER runs are made to define ΔCPR/Initial CPR (referred to as RCPR) as a function of the parameters to be statistically combined. This relation is in the form of a "curve fit" and is referred to as a response surface. The error in the response surface is treated statistically as part of the RCU method. The form of the response surface is:

$$RCPR = A_0 + \sum_{i=1}^{N} A_i X_i + \sum_{i=1}^{N} \sum_{j=i}^{N} A_{ij} X_i X_j$$

where: A_i, A_{ij} = constant coefficients
X_i = the i^{th} parameter in the response surface
N = number of parameters in the response surface

The number of cases to define the response surface increases dramatically with the number of parameters to be treated statistically. Thus, more than 4 variables would be cumbersome to treat statistically.

The Monte Carlo analysis consists of the following steps:

1) Randomly select values of the parameters being treated statistically based on their CPDFs. From these values, calculate a RCPR using the response surface. Randomly select a response surface error based on the response surface uncertainty

(calculated RCPR - response surface predicted RCPR), and add this value to the response surface predicted RCPR.

2) Randomly select a value of the RETRAN code error based on the code uncertainty CPDF. The code uncertainty CPDF was generated in Reference 2 and is in the form of a multiplier on the calculated RCPR from step 1. This produces a calculated RCPR for a given trial:

$$RCPR_j = (RCPR_{RS} + e_{RS})\, e_{RE}$$

where: $RCPR_j$ = calculated value of RCPR for the j^{th} trial
$RCPR_{RS}$ = value of RCPR calculated from the response surface (step 1)
e_{RS} = randomly selected value of response surface error (step 1).
e_{RE} = randomly selected value of code error (step 2)

3) Repeat steps 1 and 2 until the desired number of trials have been run (usually 10,000 - 100,000 can be run due to the speed of the response surface method compared with the speed of RETRAN/CPRITER).

4) The result of steps 1 through 3 is a CPDF of RCPR.

The above procedure is implemented by means of the STATCPR code written for this purpose. Figure B.2-1 illustrates the procedure.

B.2.2 Safety Limit Type Analyses

The Susquehanna SES MCPR safety limit analyses are performed using the fuel vendor's NRC approved methodology (References 17 and 18). The

uncertainties combined statistically in the MCPR safety limit analysis are listed in Table B.2-1.

This step in the procedure requires that a number of "safety limit type" analyses be performed using the ANF methodology for different values of MCPR. Each "safety limit type" analysis produces a CPDF for the fraction of fuel rods in boiling transition (see Figure B.2-2).

Thus, the traditional safety limit analysis which produces a CPDF of fraction of rods in boiling transition, is one of the set of "safety limit type" analyses used in this methodology. A reasonable range of MCPR over which CPDFs would be generated would be 0.96 to 1.16. The CPDFs are adjusted by means of non-parametric statistics to be conservative at the 95% confidence level. The adjusted CPDFs are used in the combined Monte Carlo analysis described in Section B.2.3.

B.2.3 MCPR Operating Limit Determination

This section describes the statistical calculation to combine the results of the analyses described in Sections B.2.1 and B.2.2. The goal of the analysis is to provide a MCPR operating limit that will ensure that 99.9% of the fuel pins are not expected to be in boiling transition for the transient being analyzed at a 95% confidence level. The procedure consists of the following steps (see Figure B.2-3):

1) Select a MCPR operating limit for the transient of interest. The Monte Carlo analysis performed will attempt to validate this limit.

2) Randomly select a transient RCPR from the CPDF previously generated as described in Section B.2.1.

3) Calculate the minimum MCPR for the event based on the assumed MCPR operating limit and the randomly selected RCPR;

$RCPR_i = \Delta CPR_i / ICPR$, and

$MCPR_i = ICPR - \Delta CPR_i$, thus

$MCPR_i = ICPR\ (1-RCPR_i)$,

where: $MCPR_i$ = minimum transient MCPR for the i^{th} trial

ΔCPR_i = maximum change in MCPR for the transient for the i^{th} trial

$RCPR_i$ = transient RCPR for the i^{th} trial

ICPR = initial core MCPR (the MCPR operating limit being tested)

4) Select the CPDF of fraction of rods in boiling transition corresponding to the transient minimum MCPR derived in step 3. Each trial will potentially use a different CPDF, since the minimum MCPR for that trial may be different from the previous trial.

5) Randomly select a fraction of rods in boiling transition from the CPDF selected in Step 4. Store this value.

6) Repeat steps 2 through 5 until the desired number of trials have been made. A large number of trials (e.g., 100,000) is practical since the calculations are rapid. The result of this step is a "final" CPDF for fraction of rods in boiling transition resulting from the transient. To determine the fraction of rods expected to be in boiling transition, select

the 50% probability/95% confidence level. Non-parametric methods are used for this since they require no knowledge of the true population CPDF. This is consistent with the definition of expected used in the fuel vendor's NRC approved safety limit methodology.

7) If the value of fraction of rods expected to be in boiling transition is less than or equal to 0.1% of the core, the trial MCPR operating limit selected in Step 1 is acceptable. If the value is greater than 0.1%, the process is repeated after raising the trial MCPR operating Limit in step 1.

The above procedure implies statistical independence between the transient RCPR analysis and the MCPR "safety limit type" analyses. As part of the PP&L methodology, this assumption is examined. If one of the parameters chosen for statistical analysis is common to both transient and "safety limit type" analyses, then the analyses are not statistically independent calculations. If a variation of the common parameter affects the two analyses in opposite directions (e.g., increased number of rods in boiling transition for the safety limit type analysis and decreased transient RCPR), then assuming that the analyses are statistically independent is conservative since it conservatively increases the variation. If a variation of the common parameter affects the analyses in the same direction (e.g., increased fraction of rods in boiling transition from the safety limit type analysis and increased transient RCPR), then additional conservatism needs to be introduced to compensate. The new methodology combines safety limit and transient analyses into a single analysis to meet the criteria of SRP 4.4

TABLE B.2-1

Uncertainties used to Generate
MCPR Safety Limit

System Uncertainties

Feedwater Flow Rate

Feedwater Temperature

Core Pressure

Core Flow Rate

Core Inlet Temperature

Fuel Related Uncertainties

XN-3 Correlation

Assembly Flow Rate

Radial Bundle Power

Local Power

Axial Power

FIGURE B.2-1
STATISTICAL RCPR ANALYSIS

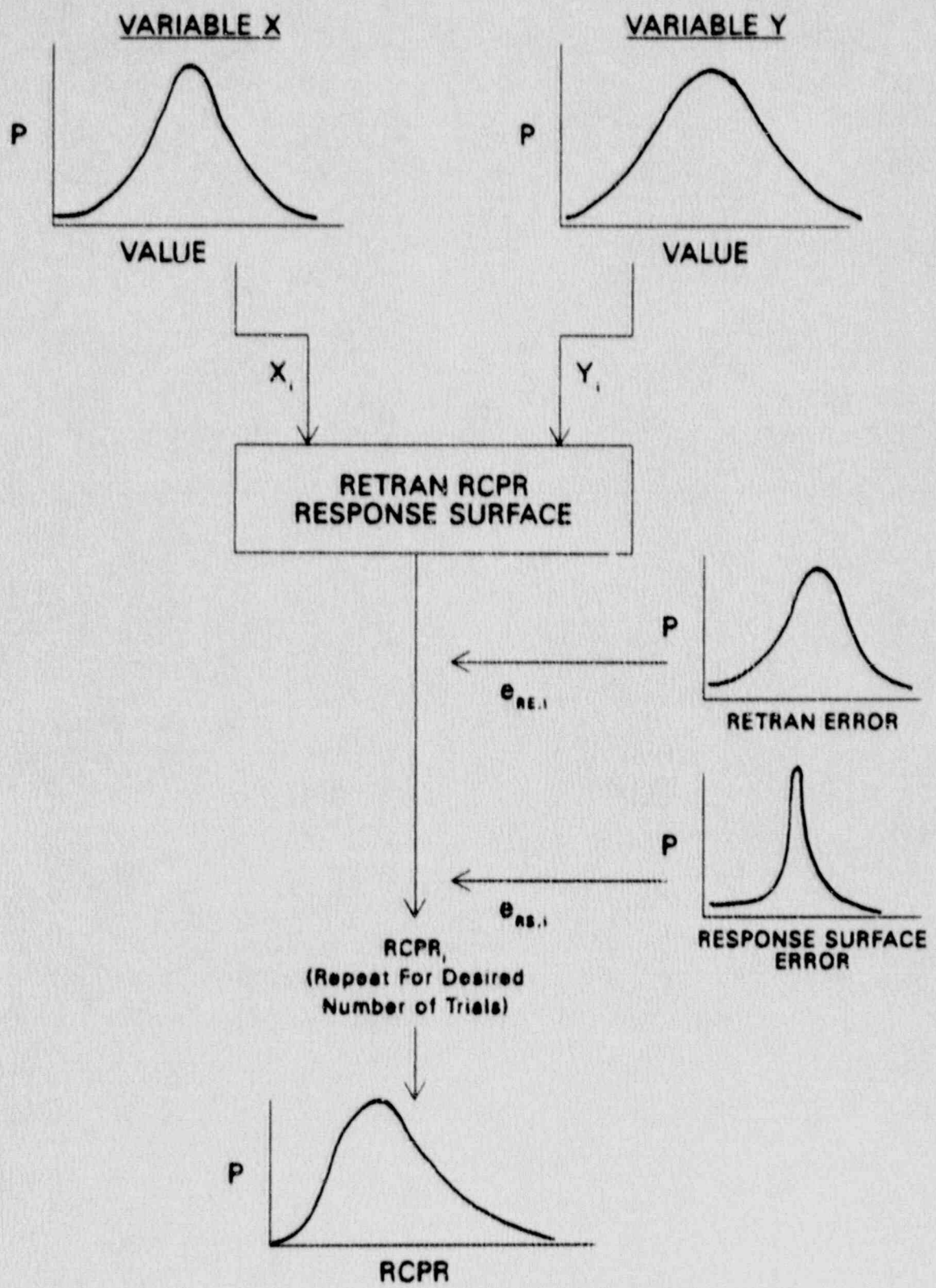

FIGURE B.2-2
SAFETY LIMIT MCPR CALCULATION

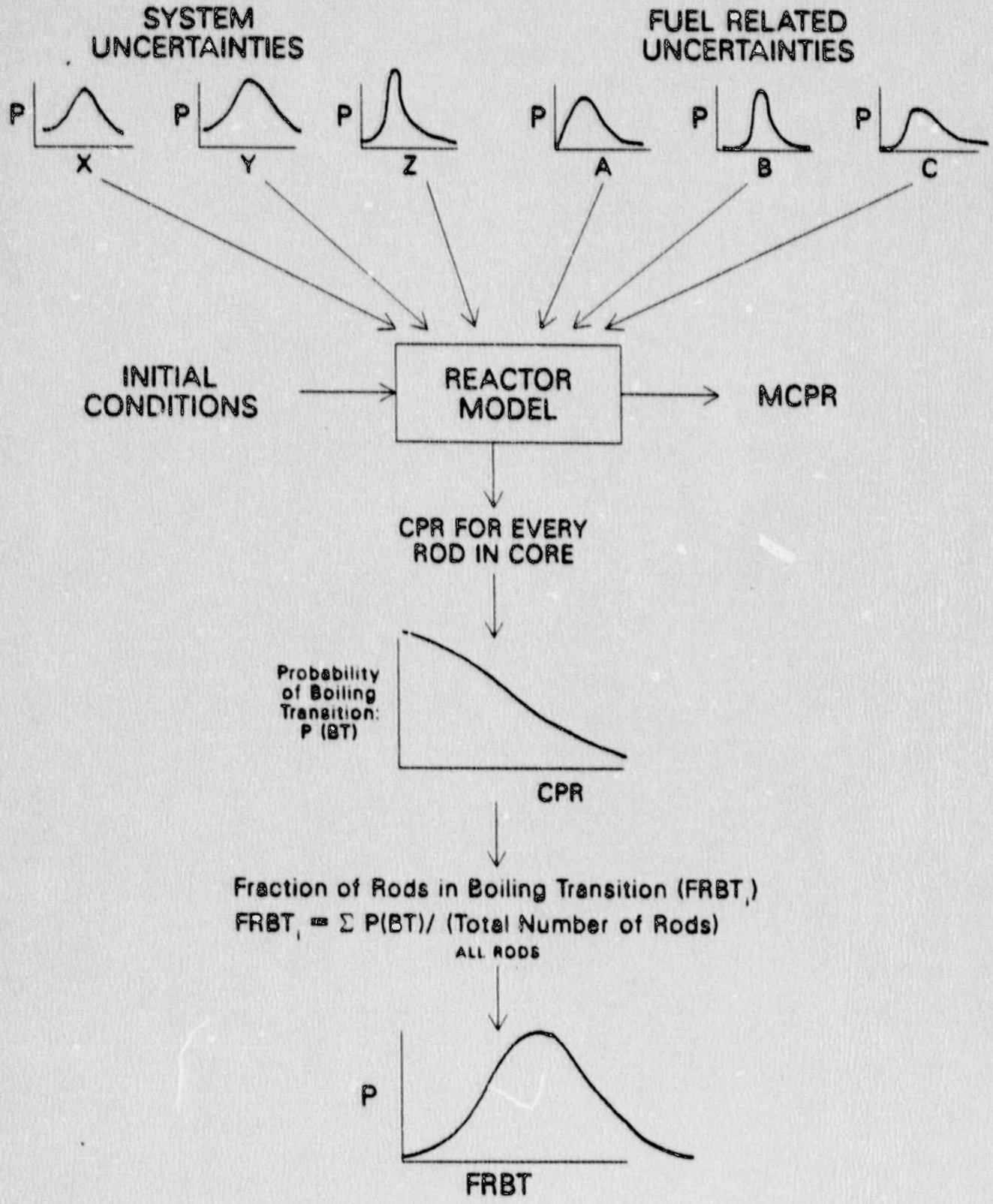

FIGURE B.2-3
STATISTICAL OPERATING LIMIT CALCULATION

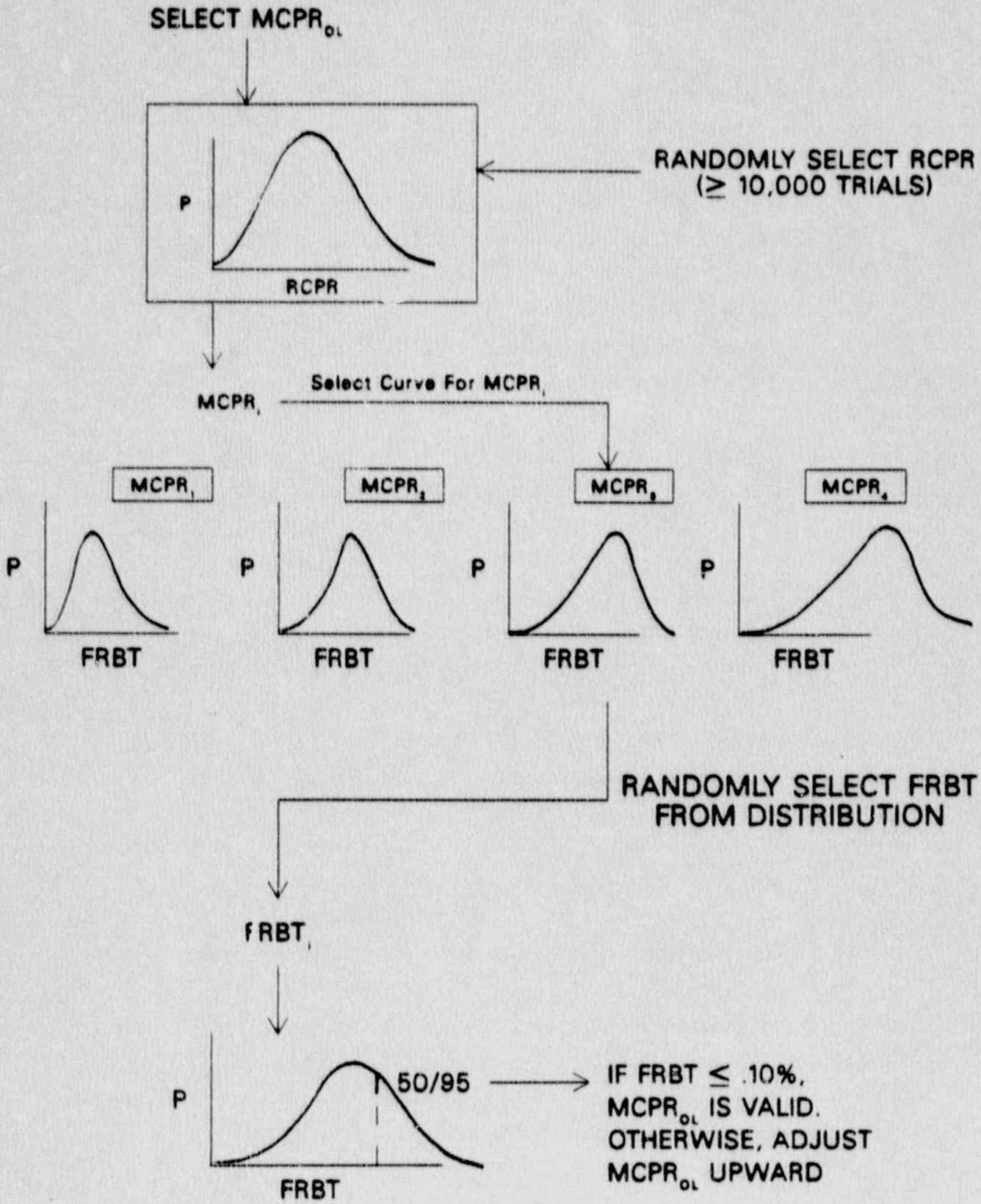

B.3 ROD WITHDRAWAL ERROR

The RWE analysis methods and conservatism are described in Section 2.1. This section describes the SCU methodology for calculating MCPR operating limits for the Rod Withdrawal Error (RWE) event.

As with the SCU method for pressurization events described in Section B.2, the SCU method for the RWE event consists of three major steps:

1) A Monte Carlo analysis using a SIMULATE-E generated RWE response surface is performed to determine the cumulative probability distribution of calculated RCPR.

2) A set of "safety limit type" analyses is performed for a range of MCPR values to generate a set of probability distributions of fraction of the fuel rods in the core in boiling transition.

3) A combined Monte Carlo analysis using the results of steps 1 and 2 is performed to calculate an operating limit such that 99.9% of the pins are not expected to be in boiling transition.

Steps 2 and 3 are identical to those described in Section B.2 for the SCU methods for pressurization transients. Details of the first step of the Monte Carlo analysis are provided below.

B.3.1 Statistical RCPR Calculation

A set of parameters is selected to be treated statistically. Parameters which have a significant impact on the ΔCPR for the RWE and have significant variation due to uncertainty should be selected. The parameters selected for statistical analysis for the RWE are:

1) The uncertainty in the SIMULATE-E calculation of RCPR.

2) The uncertainty in the SIMULATE-E calculation of the response of the Rod Block Monitor.

3) The uncertainty in the Rod Block Monitor (RBM) system response. This uncertainty includes:

   (a) instrument drift
   (b) instrument accuracy
   (c) instrument calibration
   (d) uncertainty in the number of failed Local Power Range Monitor (LPRM) detectors
   (e) uncertainty in the location of the failed LPRM detectors
   (f) uncertainty in which channel of the RBM is operable. The RWE analysis assumes one channel is failed.

The uncertainty in the number of failed LPRMs is handled by selecting a conservative LPRM failure probability. For a given trial in the Monte Carlo process a random number (between 0 and 1) is selected for each LPRM and compared with the LPRM failure probability. For a random number less than the failure probability, that LPRM is assumed to be failed. In this way, the number of failed LPRMs is determined.

The uncertainty in the location of the failed LPRMs is treated by randomly selecting one of the possible failure combinations which have the number of failed LPRMs determined previously. For 0, 1, 2, 3 and 4 LPRM failures, there are 1, 8, 28, 56, and 70 different failure combinations, respectively. In this way, the exact locations with respect to the error rod location of the failed LPRMs are determined for a given trial.

Similarly, a random number is used to determine which RBM channel is operable. One channel is assumed to be operable, with an equal

probability assumed for each of the two channels (i.e., 50% probability of channel A operable, 50% probability of Channel B operable).

As input to the Monte Carlo process, Cumulative Probability Distribution Functions (CPDFs) are determined for the uncertainties described in items 1, 2, 3a, 3b, and 3c.

Since a Monte Carlo procedure requires a large number of trials to produce meaningful results, it is impractical to use SIMULATE-E for each trial. To facilitate the analysis, a set of SIMULATE-E RWE analyses are performed to define RCPR as a function of the parameters to be statistically combined (i.e., RBM setpoint, operable RBM channel, number and location of failed LPRMs). This relation is herein referred to as the SIMULATE-E response surface.

The Monte Carlo Analysis consists of the following steps (See Figures B.3-1 to B.3-3):

1) Based on the assumed LPRM failure probability, randomly determine the number and location of failed LPRMs. The exact number and location of failed LPRMs assumed is characterized as an "LPRM failure combination" (See Figure B.3-2).

2) Randomly determine which RBM channel is operable.

3) Randomly select values of drift, calibration, accuracy, and RBM calculational error. Add these values to the setpoint input to the RBM to obtain the actual RBM "setpoint" at which rod motion will be terminated.

4) Based on the LPRM failure combination, RBM channel operable, and actual RBM setpoint determined in steps 1 through 3, calculate

the RCPR using the relation between these parameters and calculated RCPR (SIMULATE-E response surface).

5) Randomly select a value for the error in the SIMULATE-E calculation of RCPR and add this to the RCPR from Step 4.

6) Repeat Steps 1 through 5 until the desired number of trials has been performed.

7) Using the RCPR values produced by Steps 1 through 5, produce a CPDF of RCPR. This CPDF will be used as input to the combined statistical analysis.

B.3.2 MCPR Operating Limit Determination

The CPDF of RCPR for the rod withdrawal error event is used as input to the combined statistical analysis in exactly the same manner as was described for the pressurization event SCU method (Sections B.2.2 and B.2.3). The result of the combined SCU analysis is a MCPR operating limit that ensures that 99.9% of the fuel pins are not expected to experience boiling transition during a RWE.

A sample analysis using the SCU methodology for the RWE is provided in Section 2.1.4.

FIGURE B.3-1
FLOW PATH FOR COMBINATION OF UNCERTAINTIES IN ROD WITHDRAWAL ERROR ANALYSIS - PART 1

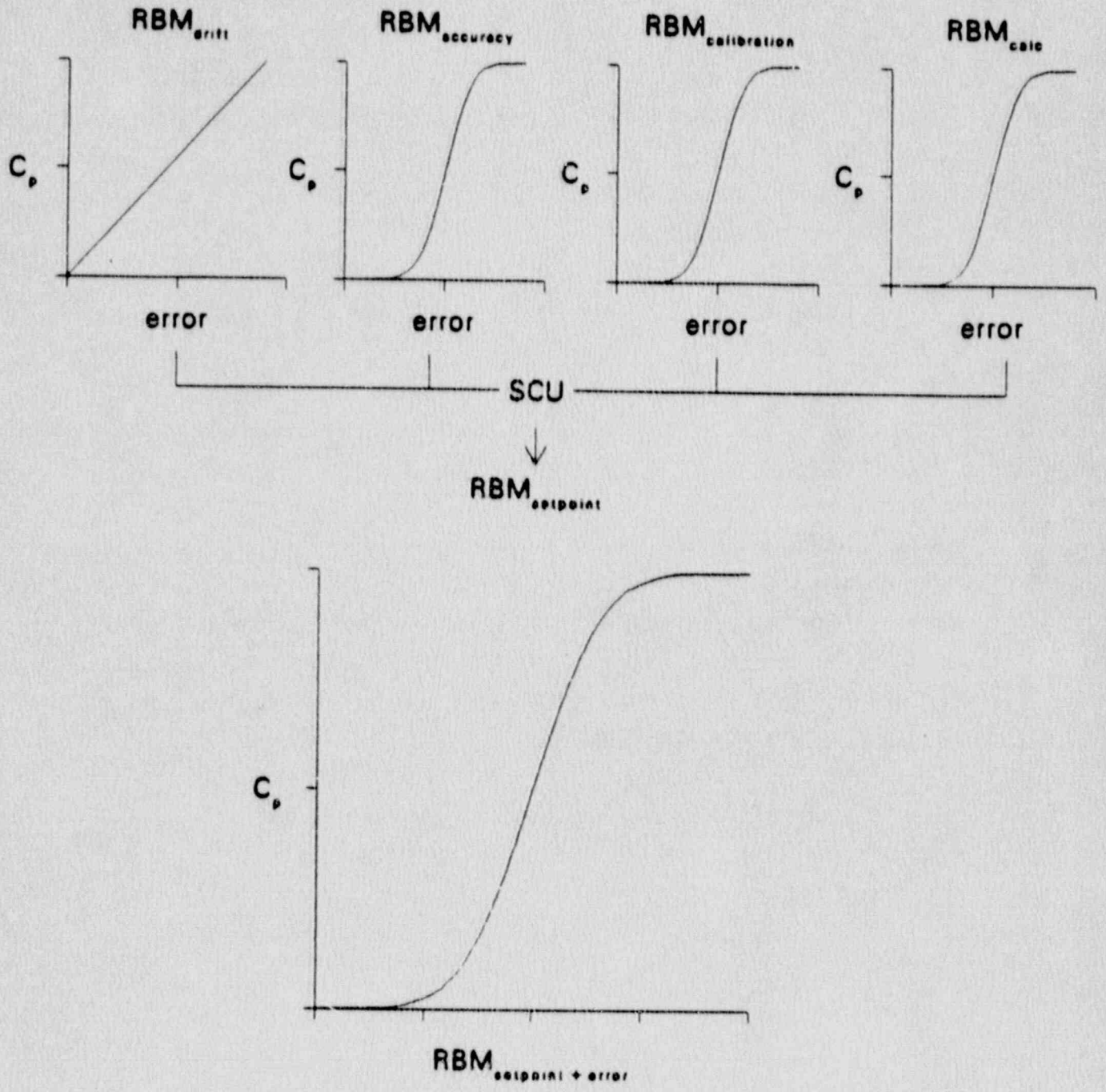

SCU = Statistically combined uncertainties
C_p = Cumulative probability

FIGURE B.3-2
FLOW PATH FOR COMBINATION OF UNCERTAINTIES IN ROD WITHDRAWAL ERROR ANALYSIS - PART 2

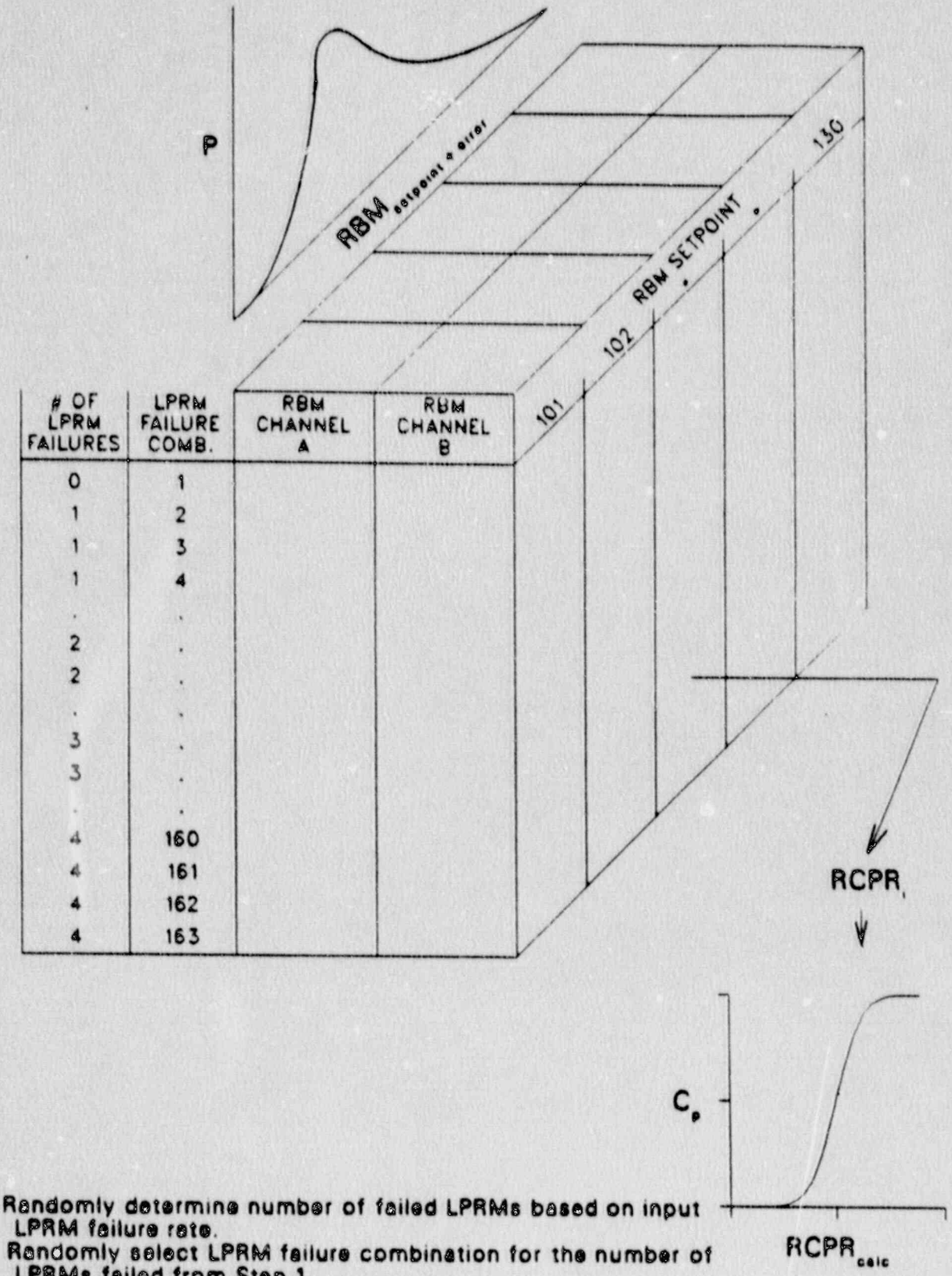

1. Randomly determine number of failed LPRMs based on input LPRM failure rate.
2. Randomly select LPRM failure combination for the number of LPRMs failed from Step 1.
3. Randomly select RBM channel with each channel failure probability set to 50%.

FIGURE B.3-3
FLOW PATH FOR COMBINATION OF UNCERTAINTIES IN ROD WITHDRAWAL ERROR ANALYSIS - PART 3

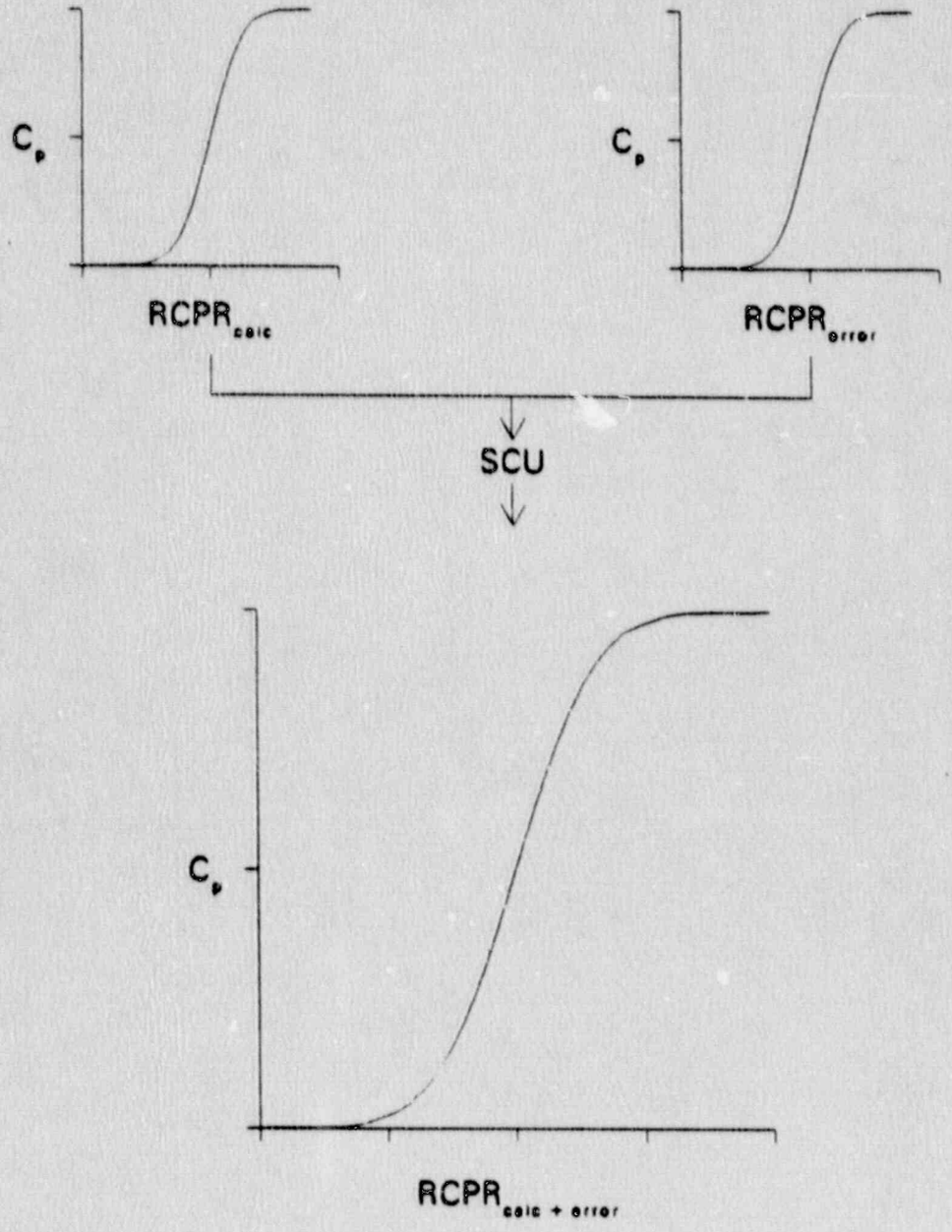

B.4 INTERFACE WITH NON-STATISTICAL ANALYSES

The combination of statistical and non-statistical analyses into a Technical Specification MCPR operating limit is quite simple. The non-statistical analyses for certain events compute MCPR operating limit (MCPROL) from the MCPR safety limit (MCPRSL) and the calculated ΔCPR by:

$$MCPROL = MCPRSL + \Delta CPR$$

The SCU analyses described in this Appendix when applied to certain events will directly generate an operating limit for those events. Currently, MCPR operating limits are defined as a function of core power and core flow. Thus, at a given power/flow point, the maximum operating limit for all events would become the bounding Technical Specification MCPR operating limit.